Mechanistic insights into the hydrocyanation reaction

Please check the document version of this publication:

• A submitted manuscript is the version of the article upon submission and before peer-review. There can be important differences between the submitted version and the official published version of record. People interested in the research are advised to contact the author for the final version of the publication, or visit the DOI to the publisher's website.
• The final author version and the galley proof are versions of the publication after peer review.
• The final published version features the final layout of the paper including the volume, issue and page numbers.

[Link to publication](#)

Mechanistic Insights into the Hydrocyanation Reaction

Laura Bini

Mechanistic Insights into the Hydrocyanation Reaction

PROEFSCHRIFT

ter verkrijging van de graad van doctor aan de
Technische Universiteit Eindhoven, op gezag van de
rector magnificus, prof.dr.ir. C.J. van Duijn, voor een
commissie aangewezen door het College voor
Promoties in het openbaar te verdedigen
op donderdag 10 september 2009 om 16.00 uur

door

Laura Bini

geboren te Lucca, Italië

Dit proefschrift is goedgekeurd door de promotor:

prof.dr. D. Vogt

Copromotor:
dr. C. Müller

Dit proefschrift is goedgekeurd door de manuscriptcommissie:

Prof. Dr. Dieter Vogt (Technische Universiteit Eindhoven)
Dr. Christian Müller (Technische Universiteit Eindhoven)
Prof. Dr. William Jones (University of Rochester)
Prof. Dr. Hans de Vries (Rijksuniversiteit Groningen)
Prof. Dr. Cor Koning (Technische Universiteit Eindhoven)

Contents

Contents

Chapter 6. Hydrocyanation of 1-octene: an open challenge   155

Summary   173

Samenvatting   177

Sommario   181

Chapter **1**

Mechanistic Studies on Hydrocyanation Reactions: a General Introduction.

In this chapter, an overview will be given on the literature dealing with mechanistic studies on the hydrocyanation reaction. Pertinent data on this topic are not easily available, due to the instability of the reactive intermediates and the lack of isolable catalyst species. However, mechanistic considerations are imperative for a detailed understanding of the reaction. Especially a profound knowledge of the delicate structure-performance relation of the catalyst and intermediate species and on the product formation is missing. The major focus of this thesis is to elucidate some of these aspects.
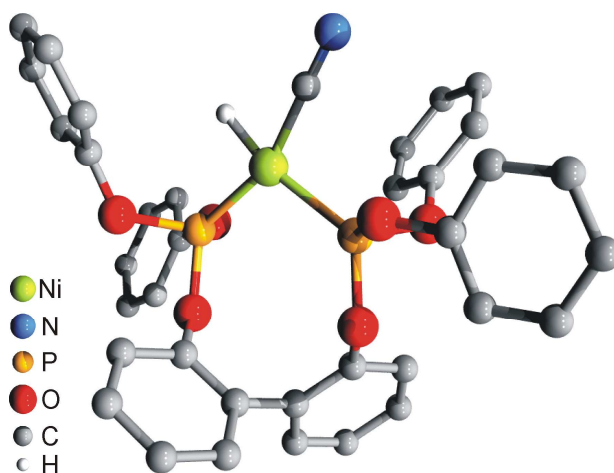
1.1. Introduction

Hydrocyanation is the process in which HCN is added across a double bond of an alkene to form a nitrile (Scheme 1.1).[1] Nitriles are very versatile building blocks that can be used as precursors for amines, isocyanates, amides, carboxylic acids and esters (Scheme 1.2).[2]
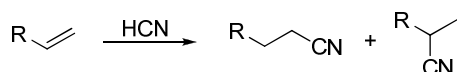
Scheme 1.1. Hydrocyanation of alkenes.
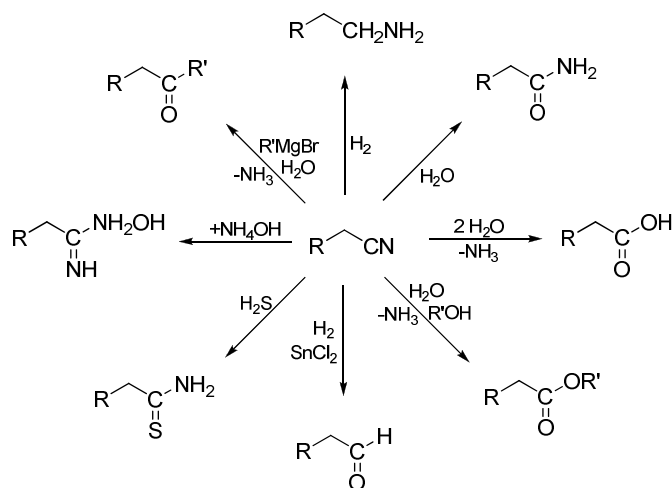
Scheme 1.2. Synthetic versatility of nitriles.

Despite the apparent simplicity of addition reactions to alkenes, it is still an important challenge to control the regioselectivity of such processes.[3] For example, the achiral (linear) anti-Markovnikov products are important intermediates for the chemical industry. Every year linear aliphatic alcohols and amines are produced on a multimillion ton scale as bulk-chemical intermediates. Due to the relatively low price of these products, the corresponding production processes must be highly efficient (product yields > 95%, low catalyst costs, etc.).

On the other hand, the chiral branched products are often intermediates in organic synthesis on a smaller scale and for natural product synthesis. They are also valuable for the fine chemical industry as intermediates for pharmaceuticals and agrochemicals. Apart from the aspect of regioselectivity, the control of stereochemistry is an important issue for these reactions.

In the last decades, more studies have therefore focused on the synthesis of nitriles, based on HCN addition to alkenes or to related systems in the presence of a transition metal catalyst, most commonly based on nickel.[4] This reaction can be considered as an important tool in synthetic chemistry. On the other hand the difficulties in handling the highly toxic, volatile HCN compound is often regarded as a serious drawback. In fact, most of the literature regarding this topic comes from industrial rather than from academic laboratories.

The first report dealing with a homogeneously catalyzed hydrogen cyanide addition to non-functionalized alkenes goes back as far as 1954 and was published by Arthur *et al.*.[5] In this paper several alkenes were transformed to the corresponding nitriles using $Co_2(CO)_8$ as pre-catalyst.

The most outstanding example for the application of hydrocyanation is the DuPont adiponitrile process (Scheme 1.3).[6] Adiponitrile is the precursor of hexamethylene-diamine, one of the building blocks for the synthesis of Nylon 6,6 and is
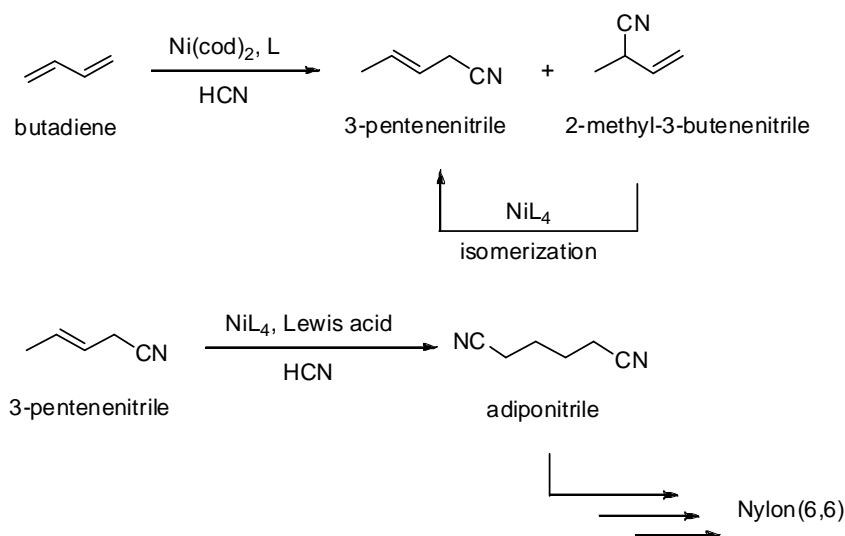
Scheme 1.3. The DuPont adiponitrile process.

obtained by hydrocyanation of butadiene in the presence of nickel(0) phosphite species. This technology for direct addition of HCN to butadiene was unknown until the late 1960's. Since then, the commercial importance of the large-scale adiponitrile synthesis has forced a number of closer investigations in this area.[7] Particular efforts have been made to find an eligible catalyst. Efficient catalyst systems have been developed that show a high degree of product selectivity, suppression of the formation of side products, improved turnover rates of the catalyst, and shorter reaction times.[8] Although a deeper insight into the reaction mechanism would enable the development of tailor-made catalysts for special, well-defined purposes, the homogeneously catalyzed hydrocyanation is still not fully understood.

In this introduction, the chemistry behind the hydrocyanation reaction will be discussed prevalently from a mechanistic point of view, starting with a detailed overview of the DuPont process. The discussion will be extended to other classes of substrates applied in hydrocyanation. Examples focus on nickel-catalyzed reactions while a brief overview on the use of other metals will conclude the chapter.

1.2. The DuPont process: first studies on the reaction mechanism and the hydrocyanation of butadiene

The synthesis of adiponitrile (AdN) based on a nickel-catalyzed double hydrocyanation of butadiene is a major industrial success for homogeneous catalysis (Scheme 1.3).[6] In the first step, hydrocyanation of butadiene leads to a mixture of mononitriles, the desired 3-pentenenitrile (3PN) and the undesired 2-methyl-3-butenenitrile (2M3BN). The branched isomer needs to be isomerized to the linear 3PN. The second hydrocyanation of 3PN produces AdN. This reaction only proceeds with the assistance of a Lewis acid co-catalyst. Extensive mechanistic investigations, in particular by the DuPont group, started to appear more than 30 years ago.

The discovery that monodentate phosphine and phosphite based zero-valent nickel complexes catalyze the hydrocyanation of butadiene led to extensive studies on the formation and reactivity of [NiL$_4$] complexes (Scheme 1.4, 1.5 and 1.6).[9] In particular, a detailed understanding of the solution behavior of tertiary phosphine and phosphite complexes of nickel was developed.[10] Experiments have shown that electronic effects play only a secondary role compared to steric effects in determining the stability of the Ni(0) complexes studied and the strength of the nickel-phosphorus bond. Electronic factors contribute to the substitutional reactivity of [NiL$_4$] complexes and were measured by IR spectroscopy using the change of the carbonyl vibration frequency (ν_{CO}) in [Ni(CO)$_3$L] complexes.[11] For example, the π-acceptor character of the ligand increases the stability of the Ni(0) complexes. Steric factors of a ligand L are defined by the Tolman cone angle.[10a] Complexes with a small ligand cone angle of ~109°, such as [Ni[P(OEt)$_3$]$_4$], do not show dissociation even in dilute solutions. Furthermore, the chelation effect of a bidentate ligand also contributes to the complex stability.

$$NiL_4 \longrightarrow NiL_3 + L$$
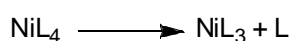
Scheme 1.4. Ligand dissociation of [NiL$_4$] complexes.

The isolation of the 16-electron complex [Ni[P(O-*o*-tolyl)$_3$]][12] containing the bulky monophosphite ($\theta = 141°$)[10] provided a remarkable opportunity to study how various components of the catalytic system interact with nickel. Furthermore, alkene complexes of the formula [Ni(alkene)L$_2$] have been isolated and characterized.[13] The isolable or spectroscopically detectable alkene complexes are generally 16-electron complexes.[14] It appears that substitution occurs through associative pathways. The stability of the alkene complexes seems to be determined by the steric and electronic character of both the phosphorus ligand and the alkene. However, the addition of tri-*o*-tolyl phosphite to a solution of [Ni(ethene)[P(O-*o*-tolyl)$_3$]$_2$] rapidly leads to tris- or tetrakis-Ni(*o*-tolyl-phosphite) complexes (Scheme 1.5). Moreover, the importance of metal to alkene π-electron donation in the alkene complexes was indicated by the quantitative displacement of ethene by acrylonitrile. In this case, the strength of the metal-alkene bond was greatly enhanced by the replacement of one H of ethene by the

15

more electronegative CN. The higher stability of the acrylonitrile complex is clearly an electronic effect since ethene, the smaller alkene of the two, should be sterically preferred.

$$\text{olefin} + \text{NiL}_3 \; \rightleftharpoons \; (\text{olefin})\text{NiL}_2 + \text{L}$$

Scheme 1.5. Alkene coordination to [NiL$_3$] complexes.

The formation and decomposition of nickel hydrides and especially [HNi(CN)L$_3$] was also studied by Tolman.[15] Hydrogen cyanide is a weak acid (pK$_a$ = 9) that, in the presence of a Lewis acid, can become considerably stronger. Addition of HCN to Ni(0) complexes gives the five-coordinated nickel hydride species [HNi(CN)L$_3$], which have been characterized in solution by ^{1}H and ^{31}P NMR as well as by IR spectroscopy for a variety of [NiL$_4$] complexes. The protonation precedes ligand dissociation (Scheme 1.6). Furthermore, ligand dissociation to form the [HNi(CN)L$_2$] species can be observed only for bulky ligands. The addition of an excess of HCN leads to the irreversible formation of [Ni(II)(CN)$_2$L$_2$] complexes.[16] These complexes are not active in the hydrocyanation reaction and their formation is considered as the major reason for catalyst deactivation.

$$\text{NiL}_4 + \text{HCN} \; \rightleftharpoons \; \text{HNiL}_4{}^+\text{CN}^-$$

$$\text{HNiL}_4{}^+\text{CN}^- \; \rightleftharpoons \; \text{HNiL}_3\text{CN} + \text{L}$$
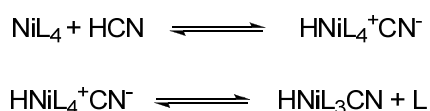
Scheme 1.6. HCN coordination to [NiL$_4$] complexes.

The first mechanistic studies have been published on ethene hydrocyanation (Scheme 1.7).[17, 18] By substituting HCN for DCN, propionitrile is formed in which deuterium is scrambled between the α and β position. This indicates that the nickel hydride addition to ethene is reversible and occurs rapidly with respect to the irreversible reductive elimination of propionitrile.[17] Furthermore, the intermediate [Ni(II)(C$_2$H$_5$)L(CN)(C$_2$H$_4$)] has been characterized by NMR as the most stable intermediate in the ethene hydrocyanation. In the catalytic cycle this intermediate undergoes reductive elimination

16
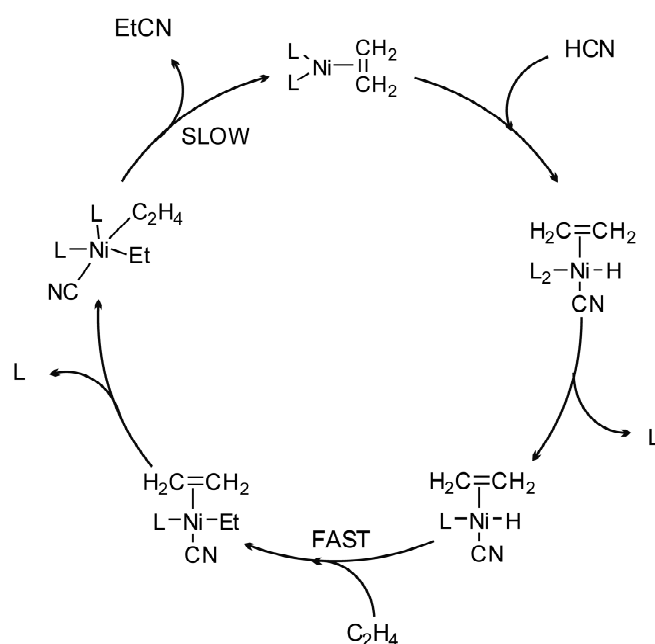
Scheme 1.7. Catalytic cycle for the nickel-catalyzed hydrocyanation of ethene with monodentate ligands proposed by McKinney.[18]

of the nitrile product and regenerates the active Ni(0) catalyst *via* coordination of an additional ligand. The stability of the isolable [Ni(II)(C$_2$H$_5$)L(CN)(C$_2$H$_4$)] complex in combination with a detailed kinetic analysis led to the conclusion that the reductive elimination is the rate determining step of the reaction.[18]

The reaction of butadiene (BD) proceeds through relatively stable π-allyl nickel cyanide intermediates. These 18-electron species have been extensively characterized using IR, UV and NMR spectroscopy.[19] The addition of butadiene and HCN to the NiL$_4$ complex at 25°C leads to the irreversible formation of the π-allyl nickel cyanide species (Figure 1.1).[17] At higher temperature carbon-carbon coupling occurs to form 3PN (coupling of CN with C$_1$, Figure 1.1 and Scheme 1.3) and 2M3BN (coupling of CN with C$_3$, Figure 1.1 and Scheme 1.3) in a 2:1 ratio for Ni complexes with monophosphite ligands. Except for the first and the last 15% of the reaction, the rate is nearly zero order in both [HCN] and [BD], indicating that the consumption of the intermediate, rather than its formation, is rate determining.
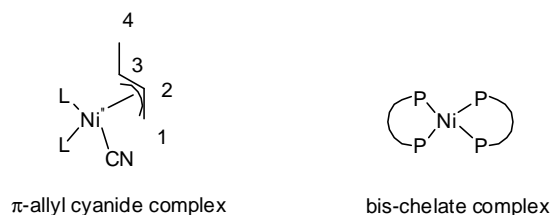
Figure 1.1. π-Allyl nickel cyanide complex and bis-chelate complex.

Keim *et al.*[20] compared the reactivity of conjugated and isolated dienes. The hydrocyanation of conjugated dienes yielded mainly 1,4-adducts. The conversion of the diene decreased in the series butadiene > piperylene > isoprene indicative for the formation of η^3-allyl systems, which show different stabilities. The hydrocyanation of non-conjugated α,ω-dienes, such as 1,4-pentadiene, 1,5-hexadiene, and 1,7-octadiene yielded various nitriles depending on the number of methylene groups separating the two double bonds. The products originating mainly from conjugated dienes are formed by isomerization, followed by hydrocyanation *via* an allyl mechanism.

A pronounced factor in controlling hydrocyanation seemed to be the steric influence of the ligand.[20] Active catalysts based on monodentate ligands have cone angles of 120-130°. In the '90s the monodentate phosphites were replaced by bulky bidentate ligands, which form catalysts superior in terms of activity and efficiency.[8] In particular catalysts based on chelating π-acceptor ligands show high activity in the reaction, although the high affinity for the Ni(0) center can lead to the formation of inactive bis-chelate species (Figure 1.1).[21] In addition, the formation of bis-chelates is disfavored for bulky ligands.

In 1991 Baker et al. reported on the synthesis of a biphenol-based diphosphite Ni(0) complex and its activity in butadiene hydrocyanation (Figure 1.2).[22] The
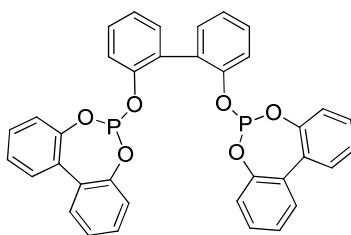
Figure 1.2. Biphenol-based diphosphite ligand used by Baker *et al.*[22]

Ni-catalyst based on the diphosphite ligand, though less selective, showed an increased catalyst turnover of at least four times that of the commercially applied DuPont system [Ni[P(OC$_6$H$_5$Me-p)$_3$]$_4$].

More recently, RajanBabu reported on the first example of a low temperature hydrocyanation of dienes including an asymmetric version.[23] The hydrocyanation of 1,3-dienes was attempted applying various ligands derived from D-glucose (Scheme 1.8). 1-Phenyl-1,3-butadiene depicted in Scheme 1.8 gave 87% yield and 78% *ee* for the 1,2-addition product using bis-3,5-dimethylphenylphosphinite **L3** as ligand. Hydrocyanation of other 1,3-dienes was carried out similarly obtaining moderate to high *ee*'s.

Ligand	Ar
L1	Ph
L2	3,5-(CF$_3$)$_2$-C$_6$H$_3$
L3	3,5-(CH$_3$)$_2$-C$_6$H$_3$
L4	3,5-difluoro-C$_6$H$_3$
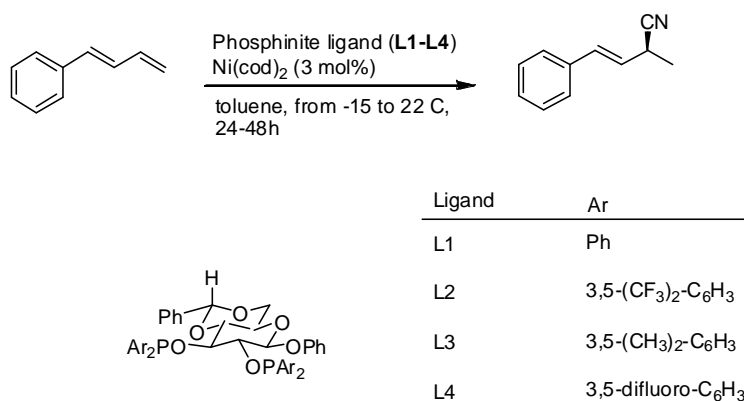
Scheme 1.8. 1,3-Diene hydrocyanation reported by RajanBabu *et al.*[23]

1.3. The DuPont process: isomerization of 2-methyl-3-butenenitrile and C-CN bond activation

In a practical sense, the formation of 2M3BN is undesirable because its direct hydrocyanation cannot give AdN. Nevertheless, 2M3BN can be isomerized to 3PN (Scheme 1.3). The isomerization can be catalyzed by the same Ni(0) catalyst applied in the hydrocyanation reaction. Tolman studied the complexation of different cyanoalkenes to the nickel metal center, using tris-o-tolyl-phosphite as ligand.[24] The complexation is

favored for cyanoalkenes with a terminal alkene double bond and by conjugation of the double bond with the nitrile. Consequently, the terminal alkene 2M3BN will coordinate to the metal center faster than the internal alkene 3PN. Furthermore, a decrease in solvent polarity has been found to generally stabilize nitrile complexes.

The first publications on 2M3BN isomerization reported that the reaction is facilitated by the addition of a Lewis acid, such as $ZnCl_2$.[3, 19] Experiments have been carried out with deuterium-labeled (-CD$_3$ group) 2M3BN in the presence of [Ni[P(O-p-tolyl)$_3$]$_4$] and $ZnCl_2$ at 110°C.[25] The deuterium label was found in both the methyl and methylene groups of the resulting 3PN (Scheme 1.9). It seems that the mechanism involves a dehydrocyanation of the substrate. This result is consistent with the observation of small amounts of butadiene in the reaction mixture.
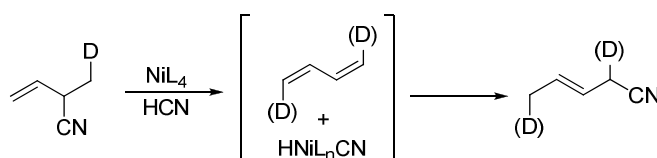
Scheme 1.9. Deuterium scrambling in the isomerization reaction.

In combination with Ni(cod)$_2$, phosphines[26,27,28], phosphinites[8d], phosphonites[8e,27], and phosphites[8b] are reported to catalyze the isomerization reaction without the addition of Lewis acids. The catalysis has also been performed under biphasic conditions (ionic liquid/organic solvent) in the presence of ionic phosphites.[29] The reaction showed sensitivity to the nature of the anions and cations of the ionic liquids. Moreover, partitition experiments showed that the catalyst was immobilized in the ionic phase and recycling of the catalyst was possible, although leading to significant deactivation.

An important contribution to the understanding of the isomerization reaction mechanism comes from the investigation of C-CN bond cleavage reactions mediated by Ni(0) complexes reported by the group of Jones. Reaction of [[(dippe)NiH]$_2$] (dippe = diisopropylphosphinoethane) with a variety of aryl[30,31], heteroaryl[31], and alkyl[32] cyanides have demonstrated the formation of a Ni(0)-η^2-nitrile complex, which undergoes oxidative addition either *via* C-CN or C-H cleavage to form a nickel(II) complex (Scheme 1.10). This electron-rich Ni(0) fragment can cleave the C-CN bonds of aryl

nitriles and heterocyclic nitriles under very mild conditions.[30,31] The C-C bond cleavage proceeds *via* η^2-coordination of the nitriles and is reversible. The same cleavage is observed for alkyl cyanides and is irreversible as well.[32] For the smaller substrate acetonitrile, such activation proceeds both thermally and photochemically. For larger nitriles the process does not proceed thermally but does occur under photochemical conditions. The interaction of acetonitrile with the Ni catalyst was also studied by DFT calculations.[33] The C-CN bond activation was found to be favored over C-H bond activation due to the strong thermodynamic driving force and slightly lower kinetic barrier.
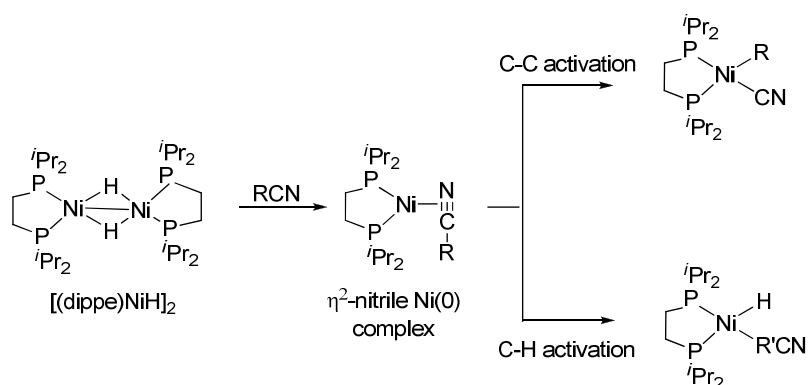
Scheme 1.10. General scheme for the C-C and C-H cleavage of nitriles using [(dippe)NiH]$_2$ as catalyst.

Reaction of [[(dippe)NiH]$_2$] with allyl cyanide at low temperature has also been reported[34] to quantitatively generate the η^2-alkene complex (Scheme 1.11). At ambient temperature or above, the alkene complex is converted to a mixture of C-CN cleavage product and alkene isomerization products, which are formed *via* C-H activation. The latter ones are the exclusive products at longer reaction times; indicating that C-CN cleavage is reversible and the crotonitrile complex is thermodynamically more stable than η^3-allyl species. Addition of the Lewis acid BPh$_3$ to the η^2-alkene complex at low temperature yields exclusively the C-CN activation product [Ni(η^3-allyl)(CNBPh$_3$)(dippe)].[34b] This complex as well as the [Ni(η^3-allyl)(CN)(dippe)] species have been fully characterized by X-ray diffraction studies.[34a] Both complexes show a square pyramidal Ni-center with the CN group in apical position.
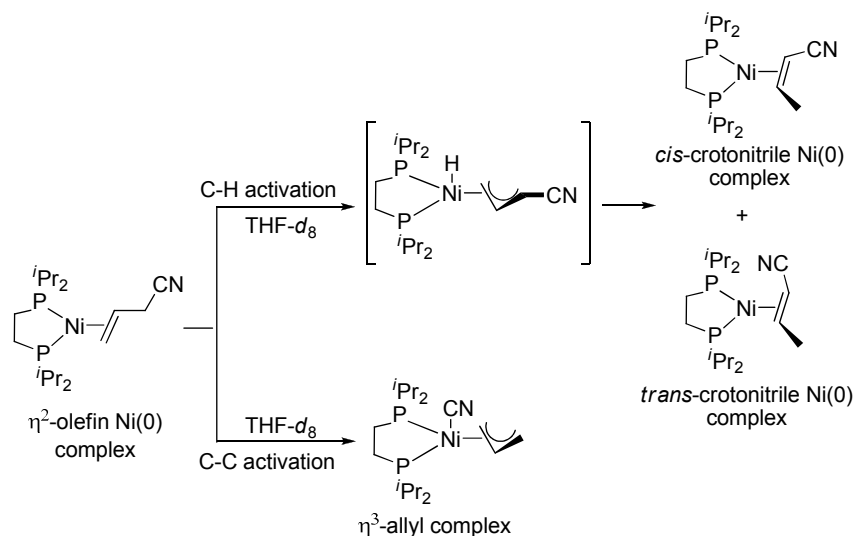
Scheme 1.11. The C-C and C-H cleavage of allyl cyanide using [(dippe)NiH]$_2$ as catalyst proposed by Jones *et al.*[34b]

Sabo-Etienne *et al*. presented a mechanism for the isomerization of 2M3BN to 3PN using the [Ni(PMe$_3$)$_2$] catalyst that was supported by DFT calculations.[28] According to these calculations, there are five steps (Scheme 1.12) involved in the mechanism, beginning with the coordination of the Ni-catalyst to the C=C bond of 2M3BN. The C-CN bond was shown to be cleaved, forming a σ-allylic species that was further isomerized into a π-allylic species. This intermediate rearranged further to a branched σ-allylic species and finally, the C-CN bond was re-formed giving the Ni-3PN complex. However, experimental evidence[33,34,35] would suggest a transition state, in which both the carbon atoms involved in the C-CN bond are coordinated to the metal center, instead of an allylic coordination, as presented by Sabo-Etienne. In this case the σ-alkyl complex B' would be generated after the oxidative addition of 2M3BN and the σ-alkyl complex B would be formed before the reductive elimination of 3PN. Furthermore, the [Ni(η^3-crotyl)(CN)(PPh$_3$)$_2$] has been isolated and characterized by NMR and X-ray spectroscopy, showing a pseudo-tetrahedral Ni-center with the crotyl unit in the apical position.
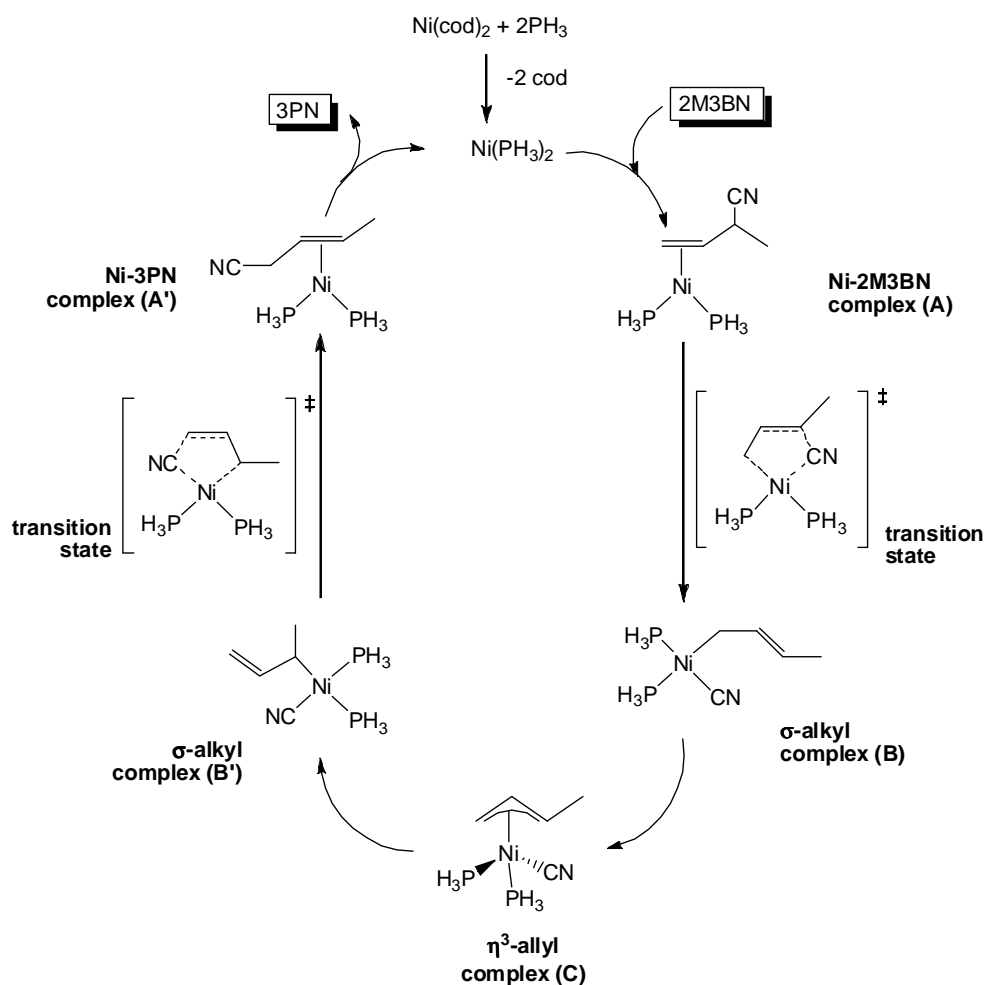
Scheme 1.12. Mechanism for the 2M3BN isomerization proposed by Sabo-Etienne, *et al*[28].

Vogt *et al*. performed spectroscopic studies on the reductive elimination step associated with the 2M3BN isomerization.[35] The activation parameters of this reaction were determined for the [Ni(cod)(DPEphos)] catalyst system (Scheme 1.13), and the individual reaction steps were studied by NMR. The reversibility of the reductive elimination was demonstrated. The catalytic results for the isomerization of 2M3BN to 3PN pointed to zero order kinetics in substrate. Moreover, the C-CN activation product [Ni(η^3-crotyl)(CN*ZnCl$_2$)(DPEphos)][35b] was synthesized independently and characterized by single-crystal X-ray diffraction. The molecular structure is best described as pseudo-tetrahedral around the nickel center.
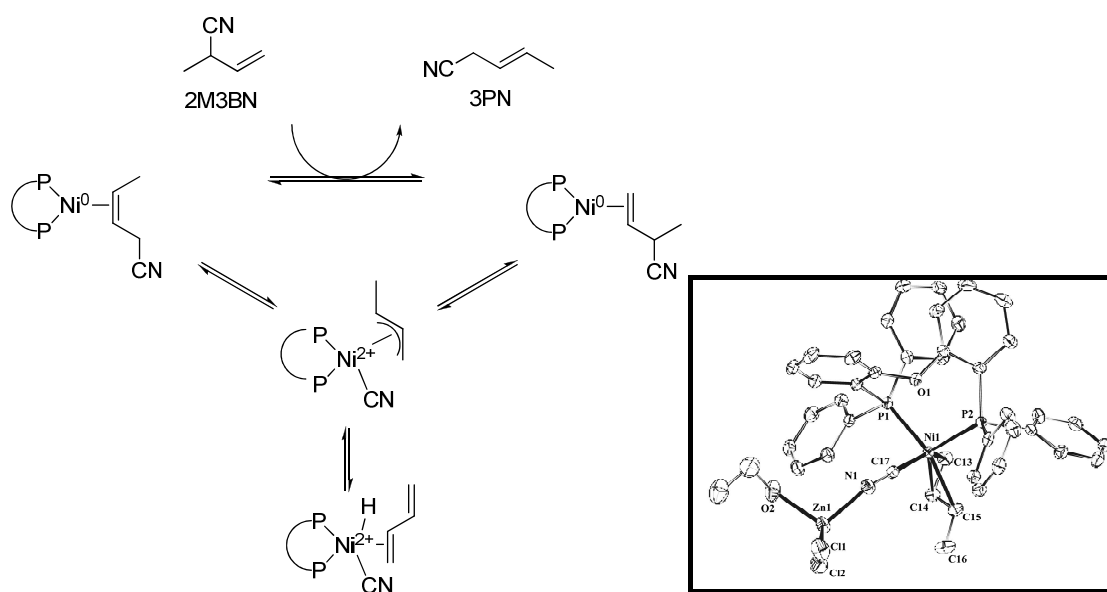
Scheme 1.13. Catalytic cycle for the Ni(0)-catalyzed isomerization proposed by Vogt *et al.* and molecular structure of [Ni(η^3-crotyl)(CN*ZnCl$_2$)(DPEphos)].[36]

Also, stoichiometric and catalytic isomerization reactions of 2M3BN with [[(dippe)NiH]$_2$] in different solvents and at different temperatures have been described in order to further investigate the mechanistic details of this system.[36] The stoichiometric reaction was monitored by NMR and the mechanism shown in Scheme 1.14 was proposed. Two possible pathways for the bond activation resulting in the formation of π-allylic intermediates based on C-CN activation or C-H activation are considered. These intermediates undergo further rearrangement to form either η^2-coordinated, non conjugated 3PN or η^2-coordinated, conjugated 2-methyl-2-butenenitrile (2M2BN). 3PN undergoes C-H cleavage to produce the more stable, conjugated 2-pentenenitrile (2PN). Reactions of 2PN and 2M2BN with [[(dippe)NiH]$_2$] indicated that there is no reverse equilibrium. A series of reactions were run with 2M3BN to determine the molecularity of the system. The resulting data show a first order dependence in 2M3BN. Additionally, a variation of nickel concentration also showed a first order dependence of the initial rate, indicating that the reaction is overall second order. The apparent contradictory results on the order in substrate for the isomerization reaction described by Vogt[35] and Jones[36] might be explained by the difference in activity of the two systems or by the dimeric
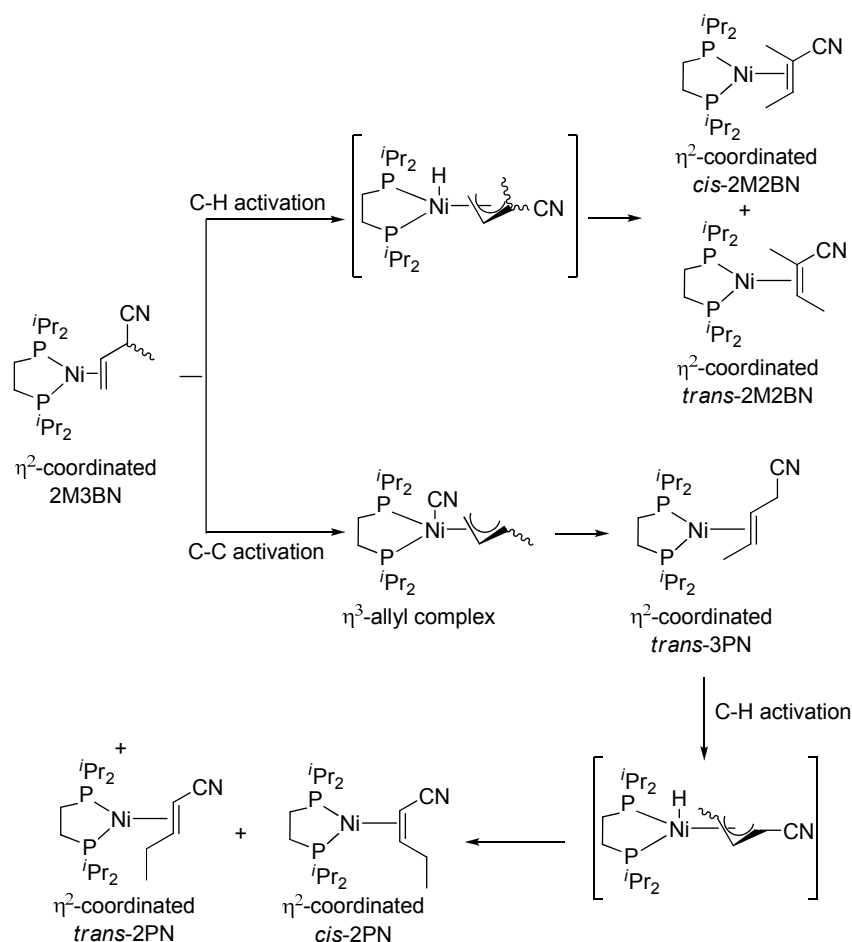
Scheme 1.14. The C-C and C-H cleavage of allyl cyanide using [(dippe)NiH]$_2$ as catalyst proposed by Jones *et al.*[35]

nature of the catalyst precursor applied by Jones. In fact, dippe is a very electron-rich ligand and therefore not comparable in terms of activity and selectivity with the π-acceptor phosphite ligands commonly applied in the 2M3BN isomerization. Furthermore, C-H cleavage appeared to be favored in polar solvents, whereas C-C cleavage is favored in non-polar solvent. This variation was attributed to the different solvation of the transition states.

Several other [NiL$_n$] systems have been investigated by Garcia *et al.*.[38,39,40] The two Ni(0) moieties [Ni(dcype)] and [Ni(dtbpe)] (dcype = 1,2-bis(dicyclohexylphosphino)ethane, dtbpe = 1,2-bis(di-*tert*-butyl-phosphino)ethane; Figure 1.3), convert 2M3BN under catalytic conditions, although the branched *E*-2M2BN

product was preferred.[37] In the case of 2M3BN and 3PN, the π-crotyl metal complex was observed in solution and characterized by NMR spectroscopy. The use of bis-diphenylphosphinoferrocene (dppf) (Figure 1.3) as ligand and Ni(cod)$_2$ as metal precursor gave modest to good yields and selectivities in the isomerization of 2M3BN towards 3PN.[38] A decrease in the catalytic activity of the system was observed when the electronic properties of the phosphorus atom were varied from a σ-donor/π-acceptor ligand (dppf) to a stronger σ-donor such as *t*Buppf (bis-*tert*-butylphenylphosphinoferrocene). Crystals suitable for X-ray diffraction studies of [Ni(η^3-crotyl)(CNBPh$_3$)(dppf)][39a] were obtained, showing a pseudotetrahedral geometry around the Ni center. In addition, the reactivity of [Ni(TRIPHOS)] (TRIPHOS = bis(2-diphenylphosphinoethyl)phenylphosphine, Figure 1.3) with 2M3BN was studied.[39] The C-H activation that promotes the formation of the branched isomers *E*- and *Z*-2M2BN was favored compared to the C-C activation, which enables the formation of 3PN (Scheme 1.14). The low yields for the linear 3PN were attributed to the occurrence of C-P bond cleavage reactions taking place in the TRIPHOS ligand.

The characteristic activity of low-valent nickel complexes toward the oxidative addition of C-CN bonds has been applied in catalysis by Nakao and Hiyama. They reported that the insertion of an alkyne into an aromatic C-CN bond (arylcyanation of alkynes) can be catalyzed by a nickel complex.[40] The choice of the ligand is critical for this type of reaction to occur. The less hindered and electron-rich PMe$_3$ is an efficient ligand in arylcyanation reaction, as was also observed in similar cross-coupling
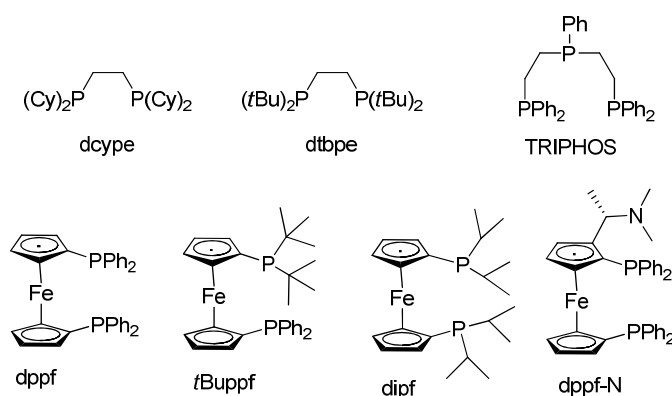
Figure 1.3. Ligands applied in the isomerization of 2M3BN by Garcia *et al.*[38,39,40]
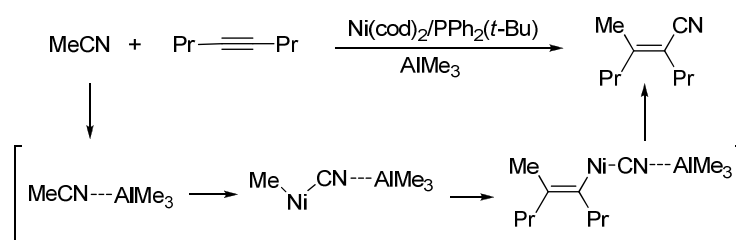
Scheme 1.15. Ni-catalyzed carbocyanation of alkynes in the presence of Lewis acid proposed by Nakao and Hiyama.[44]

reactions.[41] In addition to alkynes, norbornene and norbornadiene can be inserted into C-CN bonds by this reaction.[40] Moreover, C-CN bonds in allyl cyanides can be added to alkynes *via* a π-allyl nickel intermediate.[42] The utilization of C-CN bonds in alkyl cyanides for catalytic reactions represents a difficult task. This is not only due to the thermodynamic stability of the $C(sp^3)$-CN bond but also to the susceptibility of the intermediate, an alkylmetal cyanide complex, to undergo β-hydride elimination.[43] The β-hydride elimination of the alkylmetal cyanide species represents a difficulty also in the hydrocyanation of monoalkenes, as will be explained in Paragraph 1.6. Recently, Nakao and Hiyama reported that the scope of the Ni-catalyzed arylcyanation reaction can be expanded dramatically by the presence of a Lewis acid co-catalyst.[44] Under the improved conditions, the C-CN bond in acetonitrile can be added across an alkyne triple bond (Scheme 1.15). In fact, in stoichiometric systems involving a cyano group, both the oxidative addition[34a] and the reductive elimination[45] are accelerated by the coordination of the cyano group to the Lewis acids.

1.4. The DuPont process: hydrocyanation of 3-pentenenitrile, formation of alkyl intermediates and application of Lewis acids

The isomerization of the internal alkene 3PN to the terminal alkene 4-pentenenitrile (4PN) is the starting point and the critical step in the hydrocyanation of 3PN to AdN. Unfortunately, there is a loss in yield because the undesirable conjugated isomer 2PN is also produced (Scheme 1.16).[19] When a 3PN solution containing [Ni[P(O-*o*-tolyl)$_3$]$_4$] is

treated with trifluoromethylsulfonic acid (1eq/Ni) at 50ºC, rapid isomerization occurs and 4PN and 2PN are produced in a ratio of 70:1.[46] The kinetic preference for the isomerization of an internal alkene to a terminal alkene is in contrast to the strong thermodynamic preference for the conjugated isomer 2PN. The thermodynamic distribution of the pentenenitriles at 50ºC is 78.3:20.1:1.5 (2PN:3PN:4PN). It should be emphasized that the ratio 4PN:3PN never exceeds the equilibrium ratio of about 0.07:1, but arrives at that equilibrium ratio before any significant production of 2PN. The use of acids in the absence of nickel does not cause isomerization. It was proposed that nitrile coordination may direct the nickel hydride addition across the double bond as illustrated in Scheme 1.16.

Scheme 1.17 summarizes the results of the hydrocyanation of 3PN and 4PN to give ethylsuccinonitrile (ESN), methylglutaronitrile (MGN), and adiponitrile (AdN). Lewis acid addition affects both the rate of isomerization of 3PN to 4PN and the relative rates of formation of dinitrile products, as shown in Table 1.1.[17] These results illustrate that the rate of hydrocyanation relative to isomerization is highest with $AlCl_3$ and decreases in the order $AlCl_3 > ZnCl_2 > BPh_3$. Moreover, the selectivity towards adiponitrile is
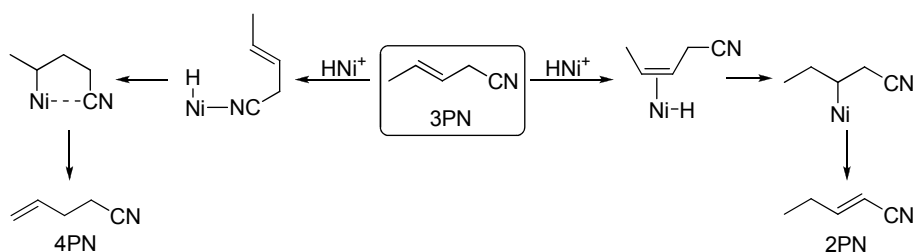
Scheme 1.16. Isomerization of 3PN towards 2PN or 4PN catalyzed by nickel hydride species, proposed by McKinney.[26]
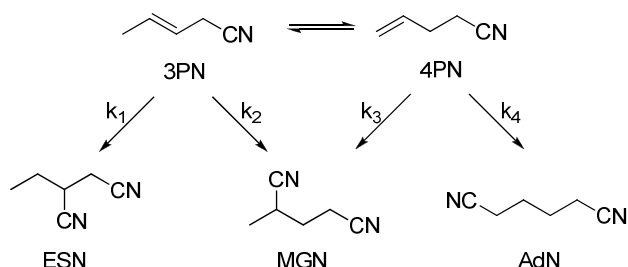
Scheme 1.17. Isomerization of 3PN to 4PN and formation of dinitriles as proposed by Tolman.[17]

Table 1.1. Lewis acid effect on steady-state concentrations and relative hydrocyanation rates of pentenenitriles[a] reported by Tolman.[17]

Lewis acid	$([4PN]/[3PN])_{SS}$[b]	k_1	k_2	k_3	k_4
$AlCl_3$	0.5/99.5	1.0	0.9	365	678
$ZnCl_2$	3.0/97.0	1.0	1.5	220	1470
BPh_3	7.0/93.0	1.0	1.1	39	1260

[a] At 68ºC in neat pentenenitriles with $Ni[P(O-o-tolyl)_3]_4$, $P(O-o-tolyl)_3$, Lewis acid, and PN in the molar ratio of 1:10:2:240. HCN was fed continuously at a rate of 30 mol of HCN/mol of Ni/h. [b] Pentenenitrile ratios at steady state as determined by GC.

different. The reason for the much poorer distribution with $AlCl_3$ (47.7% AdN) compared to $ZnCl_2$ (81.8% AdN) and BPh_3 (90.5% AdN) is partly due to the lower value of $k_4/(k_3 + k_4)$ (Table 1.1) and partly to the very low concentration of 4PN relative to 3PN at steady state.

The role of the Lewis acid in increasing the catalyst lifetime and turnover number is not clear. Isomerization of 3PN to the conjugated 2PN may be negatively influenced compared to the isomerization to 4PN. Furthermore, the steric crowding around the nickel center is increased by the coordination of the Lewis acid to the cyanide nitrogen. This may help in reducing the attack of HCN to nickel cyanide alkyl intermediates with subsequent formation of inactive nickel dicyanide complexes.

Comparable experiments using $H^{13}CN$ and DCN provided additional insight as to which dinitrile formation pathways predominate.[26] Under addition of $H^{13}CN$ it was proven that essentially no MGN is formed *via* hydrocyanation of 2M3BN, using either $ZnCl_2$ or $AlCl_3$ (Scheme 1.18a). Experiments were carried out with DCN (Scheme 1.18b), to distinguish between 3PN and 4PN as precursor of MGN. Experiments with $ZnCl_2$ gave nearly completely regiospecific deuteration in both AdN-*d* and MGN-*d*, both products being derived only from 4PN and not from 3PN. Recovered 3PN contained no significant deuterium. The fact that the deuterium in the AdN-*d* and MGN-*d* was added regiospecifically to 4PN indicates that isomerization of 3PN to 4PN takes place independently of the deuterocyanation step and coordination to the nickel hydride species. In the $AlCl_3$ experiment, deuteration in the ESN-*d* was found only in the –CH_2-group of the ethyl group, indicative of ESN-*d* formation from 3PN but not from 2PN. The deuteration in recovered 3PN using BPh_3 and $AlCl_3$ was observed at C4, as well as at C3

29

and C5. The result is consistent with alkene double-bond isomerization catalyzed by addition and elimination of nickel hydride species[20].

A series of tin compounds [(C$_6$H$_5$)$_3$SnX] with X = SbF$_6$, CF$_3$SO$_3$, or CF$_3$CO$_2$ has been synthesized and their steric and electronic effects on the selectivity in the nickel-catalyzed pentenenitriles hydrocyanation has been explored.[47] The nucleophilicity of X in [R$_3$SnX] may be expected to affect the electronic nature, for example the acidity of the tin center. A second way to analyze electronic effects was to vary the aryl substituents using the Hammett relation. Results were obtained from a set of tin compounds [(4-Y-C$_6$H$_4$)$_3$SnO$_3$SCF$_3$] with Y = F, H, CH$_3$, or CH$_3$O. In an attempt to probe steric effects, a series of [(alkyl)$_3$SnSbF$_6$] compounds (alkyl = CH$_3$, C$_2$H$_5$, i-C$_3$H$_7$, t-C$_4$H$_9$) were evaluated. The selectivity towards the formation of AdN was found to be insensitive to electronic changes of the co-catalyst, but sensitive to the size of the Lewis acid with the paths leading to AdN being favored by greater steric bulk. In fact, with increased steric
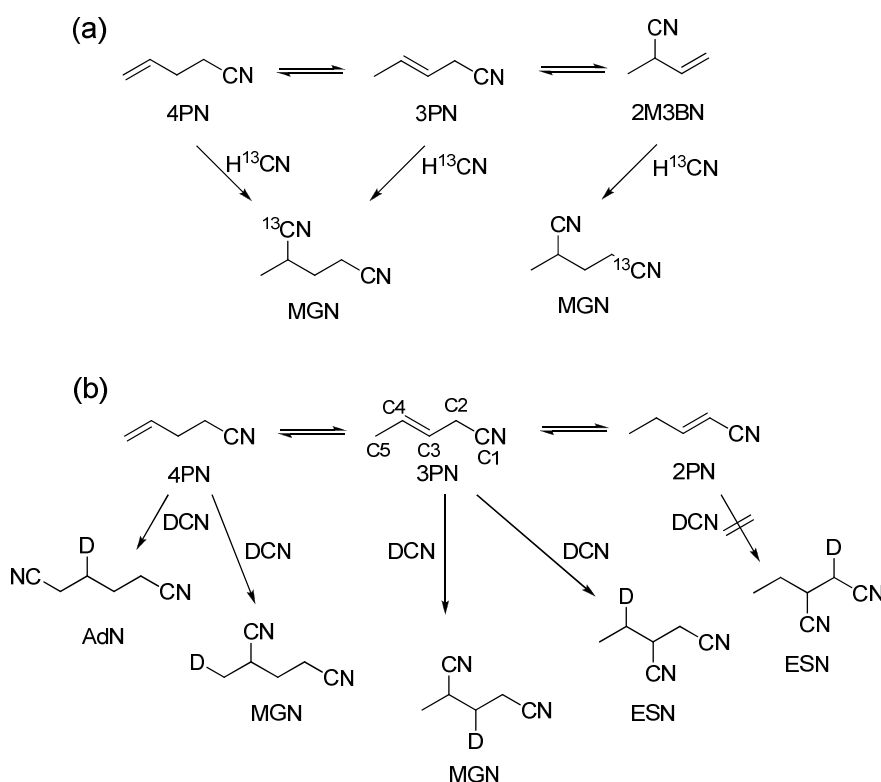
Scheme 1.18. Reaction pathways for dinitrile formation using H^{13}CN (a) or DCN (b) as reactant, proposed by Druliner.[26]

bulk around the nickel center, coordination of an α-olefin like 4PN should be preferred over a sterically more demanding internal alkene, such as 3PN.

The hydrocyanation of 3PN to AdN was also investigated using ionic phosphites in ionic liquids (Figure 1.4).[48] Varying the $ZnCl_2$/Ni ratio and the ligand/nickel ratio caused large variations of more than 80% of yield. A low ratio of L:Ni (2 equivalents) and an excess of Lewis acid (3-5 equivalents) are necessary to obtain high yields. Furthermore, it has been proven that there was no significant interaction between the two factors. The catalytic performance was similar to commonly used systems for hydrocyanation reactions (conversion 3PN ~ 40%, yield of dinitriles ~ 40%, and linearity > 70%). The cationic phosphite-based system might provide the supplementary advantage of the immobilization of the catalyst and the Lewis acid in the ionic phase when the reaction is run under biphasic condition.

The use of bidentate ligands to increase the activity of the nickel catalyst in the hydrocyanation of 3PN has been introduced in the patent literature.[49] Lower L:Ni ratios could be applied in the reaction and higher conversions were achieved.
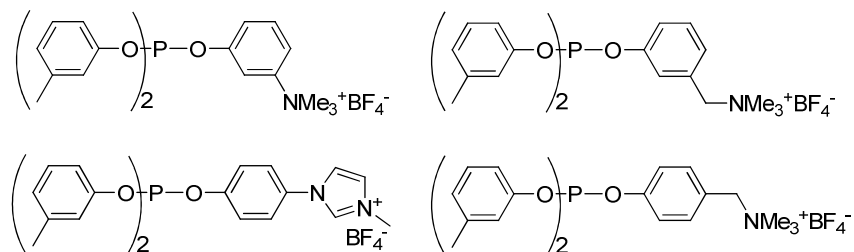
Figure 1.4. Ionic phosphite ligands applied in the hydrocyanation of 3PN carried out in ionic liquids by Galland *et al.*[48]

1.5. Asymmetric hydrocyanation: use of chiral ligands and prochiral substrates

Practical industrial application of asymmetric C-C bond formation reactions are rare. In the case of the hydrocyanation reaction they became particularly interesting, because

the resulting nitrile products are easily transformed into amines, aldehydes, acids and a variety of other valuable intermediates.

[Pd(+)-(diop)$_2$] and [Ni(+)-(diop)$_2$] complexes have been prepared and used as catalysts in the asymmetric addition of hydrogen cyanide to norbornene (Scheme 1.19).[50] Lower yields and enantioselectivities were obtained with the nickel based compound. Moreover, the addition of a small amount of a Lewis acid, zinc chloride, was not beneficial. Pd and Ni complexes containing monodentate phosphine and phosphite ligands were found to be much less effective than the diop-based catalyst systems. Only when much greater quantities of metal compound and free ligand were used, did the reaction give appreciable yields. The hydrocyanation of norbornene in the presence of [Pd(+)-(diop)$_2$] shows a significant predominance for the formation of the (1*S*,2*S*,4*R*) enantiomer, while the use of the Ni catalyst leads to a predominance of the (1*S*,2*R*,4*S*) enantiomer. An explanation for this effect is not reported.

The Ni(0) catalyst based on the diphosphine ligand BINAP (Scheme 1.19) was also tested as hydrocyanation catalyst in the reaction of norbornene in the presence of acetonecyanohydrine (ACH) as HCN precursor.[51] The reported chemical yields were up to 70% and the optical yields up to 38%. The addition of BPh$_3$ increased the
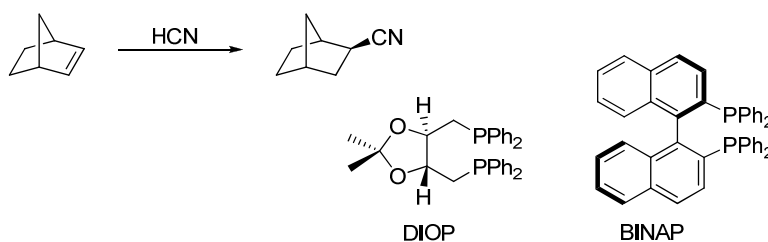
Scheme 1.19. Hydrocyanation of norbornene in the presence of DIOP[50] or BINAP[51] as ligand.
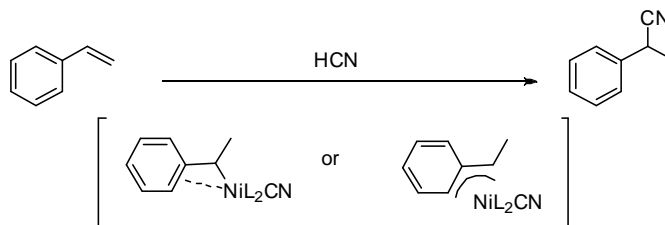
Scheme 1.20. Hydrocyanation of styrene proposed by Tolman.[19]

hydrocyanation rate and allowed the use of lower temperatures.

Tolman *et al.* were the first to report on the hydrocyanation of styrene using [Ni(P(O-*o*-tolyl)$_3$)$_3$] as catalyst.[19] The favored product was the branched nitrile (Scheme 1.20), the yield of the linear nitrile was only 10%. The different regioselectivity compared to other dienes or monoalkenes (BN and 3PN) was attributed either to the stabilization of the branched alkylnickel cyanide intermediate by interaction of the nickel center with the aromatic ring or by formation of an η^3-benzyl intermediate. The addition of BPh$_3$ as Lewis acid gave higher yield of the linear product (33%), though product formation was considerably slower. These findings were explained with an increased steric bulk around the nickel metal center due to the Lewis acid coordination to the nitrile group and a consequent increase of the strain energy associated with larger alkenes.

Other vinylarenes were investigated by Nugent and McKinney[52] as precursors for the two anti-inflammatory drugs ibuprofen® and naproxen® (Scheme 1.21). The hydrocyanation was carried out in the presence of [Ni(P(O-*p*-tolyl)$_3$)$_3$] as catalyst, leading regiospecifically to the branched nitrile product. The addition of a limited amount of the Lewis acid ZnCl$_2$ seemed to increase the rate of the hydrocyanation compared to the competing oligomerization reaction of the vinylarenes.

The addition of HCN to 6-methoxy-2-vinylnaphthalene (MVN) in the presence of catalytic amounts of Ni(cod)$_2$ and carbohydrate-derived diphosphinites was investigated by RajanBabu *et al.*.[53,54] The enantioselectivity of the catalyst increased dramatically when the glucose-based ligands contained electron-withdrawing P-aryl substituents (Scheme 1.22).[53] The substrate and the solvent also strongly influenced the
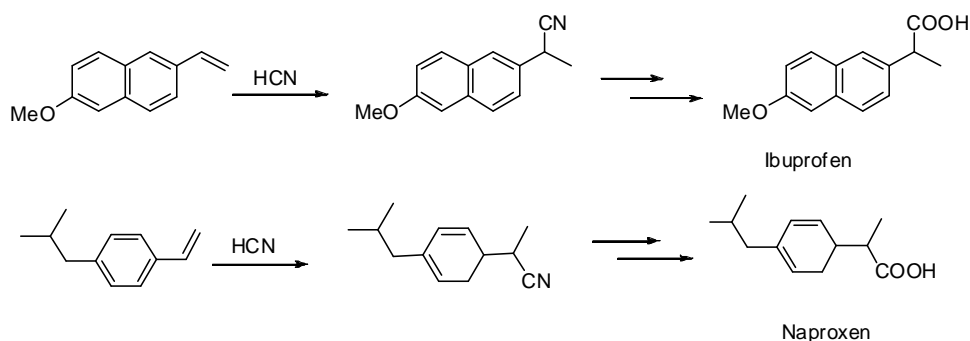
Scheme 1.21. Synthesis of ibuprofen® and naproxen® according to McKinney *et al.*[52]

enantioselectivity, and the highest *ee*'s (85-91%) for the hydrocyanation of MVN were obtained in a non polar solvent such as hexane. The enantioselectivities were independent from MVN conversion, catalyst loading, and L:Ni ratio. The branched nitrile was formed irreversibly in the final reductive elimination step. This conclusion was based on the fact that the enantioselectivity did not change with reaction time or substrate conversion, along with the observation that the optical activity of the enriched nitrile was unchanged when it was stirred with the catalyst and HCN. During deuterocyanation experiments, the deuterium incorporation proceeded exclusively in the β-methyl position, but to different extent. Therefore, it seems that after MVN coordination only the η³-benzyl intermediate (Scheme 1.20) is formed, but the formation of this species is reversible.

In combination with nickel, electronically asymmetrical bis-3,4-diarylphosphinite ligands derived from a α-D-fructofuranoside (Figure 1.5) were described to achieve the highest enantioselectivity ever reported (up to 97.5%) for the asymmetric hydrocyanation of MVN.[54] As illustrated in Table 1.2, electron-donating substituents on the phosphorus aryl groups of the ligand formed the Ni-catalysts, which gave the lowest ee's (Table 1.2, Entries 1, 5, and 8). Electron-deficient phosphinite based catalysts increase the selectivity to some extent (Table 1.2, Entries 2, and 10). However, the most dramatic increase
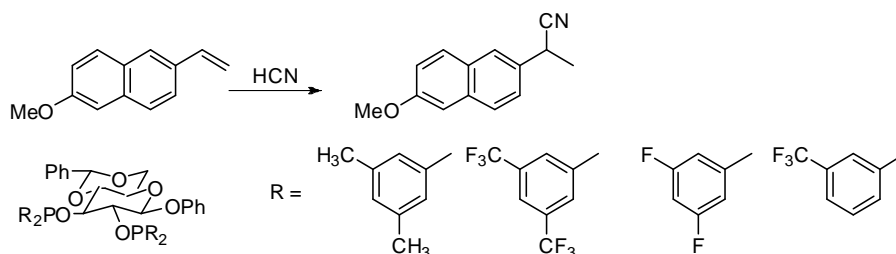
Scheme 1.22. Ni-catalyzed hydrocyanation of MVN using glucose-based diphosphinite ligands proposed by RajanBabu *et al.*[53]
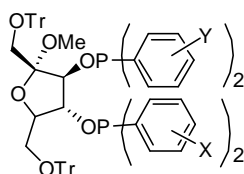
Figure 1.5. Fructofuranoside-based phosphinite ligands reported by RajanBabu *et al.*[54]

Table 1.2. Substituent effects of asymmetrically substituted fructofuranoside-based phosphinites on MVN hydrocyanation reported by RajanBabu et al.[54]

Entry/Ligand	X	Y	% ee
1	H	H	43
2	$3,5-(CF_3)_2$	$3,5-(CF_3)_2$	56
3	H	$3,5-(CF_3)_2$	58
4	**$3,5-(CF_3)_2$**	**H**	**89 (95 at 0 °C)**
5	$4-CH_3O$	$4-CH_3O$	25
6	$3,5-(CF_3)_2$	$4-CH_3O$	84
7	$3,5-(CF_3)_2$	4-F	88
8	$3,5-(CF_3)_2$	$3,5-(CH_3)_2$	40
9	$3,5-(CF_3)_2$	$3,5-(CH_3)_2$	78
10	$3,5-F_2$	$3,5-F_2$	45
11	H	$3,5-F_2$	40
12	$3,5-F_2$	H	63
13	$3,5-F_2$	$3,5-(CF_3)_2$	42
14	$3,5-(CF_3)_2$	$3,5-F_2$	78

(Table 1.2, Entry 4) was noticed when ligands with one electron-rich (Ph_2P) and one electron-deficient ($[3,5-(CF_3)_2C_6H_3)]_2P$) phosphinite were applied

Chelating phoshorus ligands with a rigid backbone and a large natural bite angle were applied in the hydrocyanation of styrene by Vogt et al..[16] The *para* substituents in the diphenylphosphanyl moiety of the 4,6-bis-(diphenylphosphanyl)-2,8-dimethylphenoxanthine (Thixantphos) ligands were varied (Figure 1.6) and their electronic effect on the activity and selectivity of the catalytic experiments were investigated. The activity of the nickel complexes decreased when basic phosphorus ligands, bearing electron-donating substituents, were applied, while electron-withdrawing

P-P	R
La	Me_2N
Lb	MeO
Lc	Me
Ld	H
Le	F
Lf	Cl
Lg	CF_3
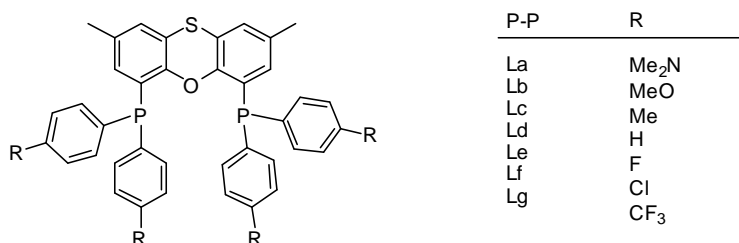
Figure 1.6. Thixantphos-type phosphine ligands reported by Vogt et al.[54]

substituents led to higher activities. For the catalytic hydrocyanation it was proposed that ligands with fixed large bite angles would disfavor inactive square planar nickel(II) dicyano species and stabilize active tetrahedral nickel(0) complexes.

Enantiopure xantphos and thixantphos diphosphonite ligands bearing binaphthoxy substituents (Figure 1.7) have also been applied by the group of Vogt in the nickel-catalyzed hydrocyanation of styrene and other vinylarynes.[21] Enantioselectivities of up to 63% were obtained for 4-isobutylstyrene. In the hydrocyanation of MVN in the presence of xantphos ligands toluene and hexane were applied as solvents. In contrast to the results reported by RajanBabu[52], the *ee* value dropped from 31% (toluene) to 10% (hexane), using a less polar solvent. This led to the conclusion that a solvent effect may be attributed at least partially to the different solubility of the diastereomeric catalyst-substrate complexes formed during the reaction. Furthermore, it has been observed that the strongly coordinating diphosphite ligands tend to form very stable and catalytically inactive bis-chelate complexes. Introduction of steric encumbering substituents in the 3,3′-position of the binaphthyl moieties prevented the formation of bis-chelates.

Chiral aryl diphosphite ligands derived from binaphthol (Figure 1.8) were found to be effective in the nickel-catalyzed hydrocyanation of a variety of alkenes.[55] Enantioselective hydrocyanation of styrene, 4-substituted styrenes, and norbornene was achieved with excellent regioselectivity and moderate enantioselectivity. The hydrocyanation of vinyl acetate gave the product with 72.9% *ee*. The catalytic activity and the enantioselectivity of the [Ni(0)-diphosphite] complexes were found to be highly dependent on the structure of the ligands.

Xant(*S*,*S*)Bino, X=CMe$_2$, R=R'=H

Xant(*R*,*R*)Bino, X=CMe$_2$, R=R'=H

Thix(*S*,*S*)Bino, X=S, R=$_{Me}$, R'=H

Thix(*S*,*S*)BinoMe, X=S, R=R'=Me
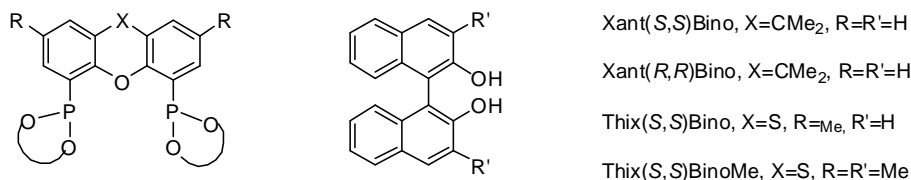
Figure 1.7. Xantphos and Thixantphos diphosphonite ligands reported by Vogt *et al.*[21]
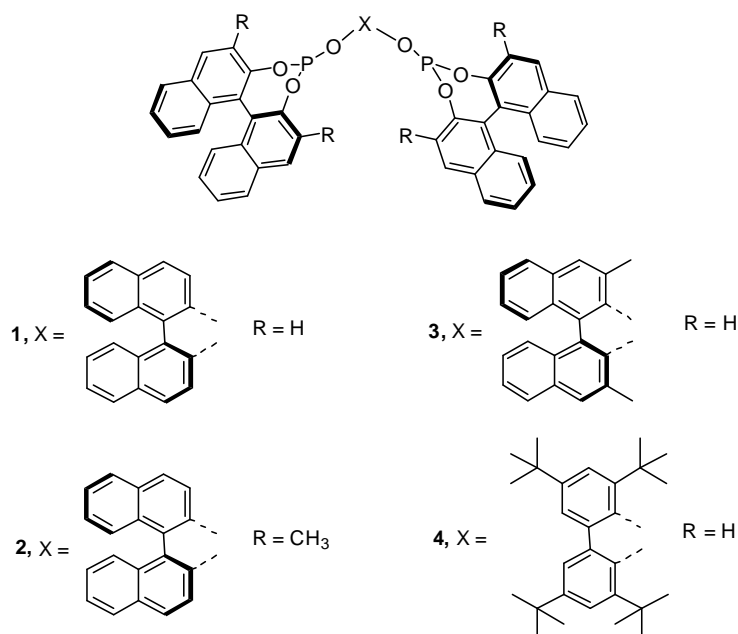
Figure 1.8. Binaphthol-based diphosphonite ligands reported by Chan *et al.*[55]
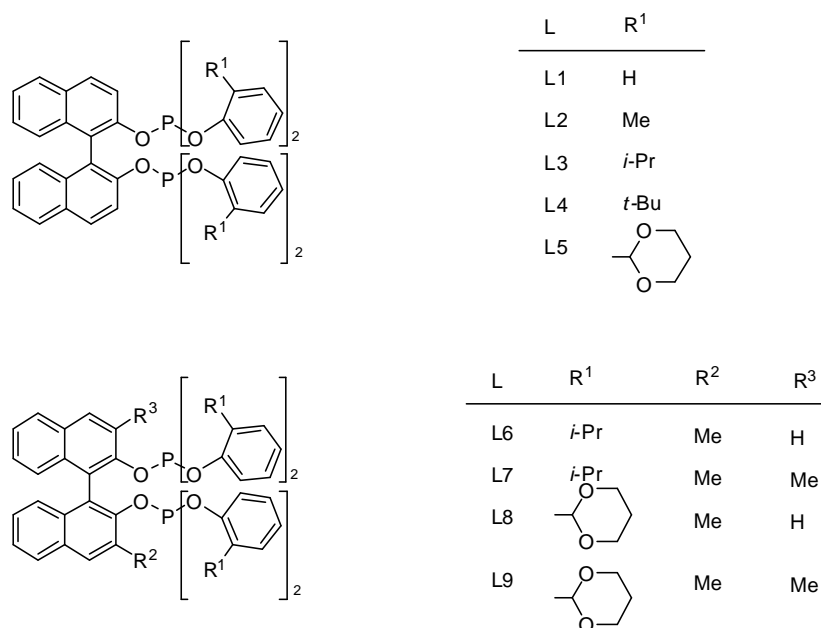
Figure 1.9. Binaphthol-based diphosphonite ligands reported by Vogt *et al.*[56]

A series of chiral (R)-binaphthol-based diphosphite ligands with different substituents (Figure 1.9) was prepared and applied in the asymmetric nickel-catalyzed hydrocyanation of styrene and 1,3-cyclohexadiene by Vogt *et al.*.[56] The optimum steric properties of the

ligands for the application in the hydrocyanation reaction lie within a narrow window. By controlling the steric properties, the ligand can be tuned not to form bis-chelates, while the corresponding metal complexes remain active in the hydrocyanation of vinylarenes and (cyclic)-1,3-dienes. Moderate enantioselectivities were found for styrene (53%) and 4-methylstyrene (54%). The hydrocyanation of 1,3-cyclohexadiene proved to be selective to 2-cyclohexene-1-carbonitrile with 86% *ee*.[56]

Diphosphonite ligands containing (bi)cycloalkyl spacers were synthesized covering a range of different steric properties at the spacer and at the phosphacycle (Figure 1.10).[57] Their complexation behavior with Ni(cod)$_2$ was investigated by NMR spectroscopy.
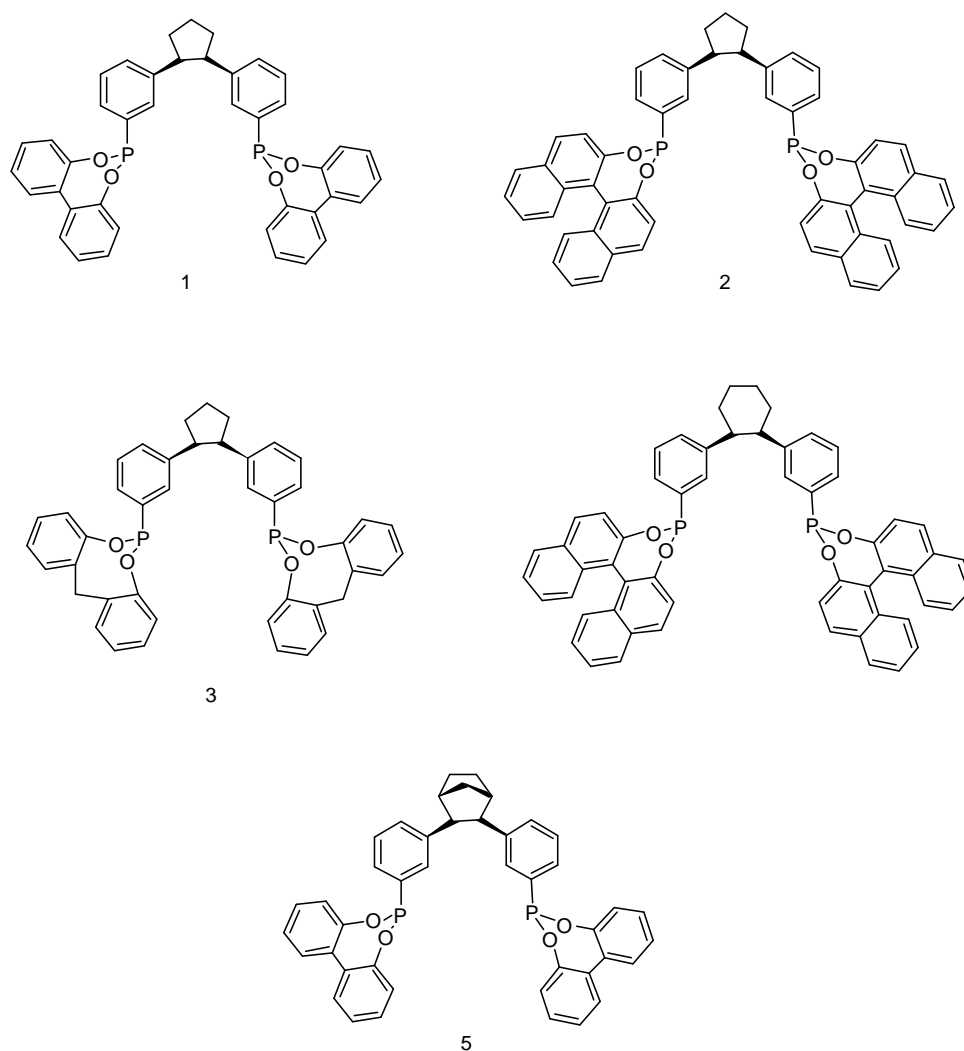
Figure 1.10. Diphosphonite ligands with (bi)cycloalkyl spacers reported by Hofmann *et al.*[57]

[Ni(cod)(monochelate)] complexes were formed in all cases. No bischelate complexes were observed. In the hydrocyanation of styrene, these catalysts were highly active (93% conversion) and highly regioselective (99.9% branched product) at a moderately high catalyst concentration (1 mol%). They also proved to be very active in the hydrocyanation of butadiene and efficiently catalyzed the isomerization of 2M3BN to the linear 3PN.[57]

Addition of HCN to 1,3-cyclohexadiene resulted in the formation of 2-cyclohexene-1-carbonitrile. Both 1,2- and 1,4-addition led to identical products. However, by using DCN instead of HCN, one could distinguish between the 1,2- and 1,4-addition products by NMR spectroscopy. These deuterium labeling experiments, reported by Vogt *et al.*,[58] were performed in the presence of a chiral diphosphite[56] ligand (Scheme 1.23). From GC-MS measurements, it could be proven that the product had incorporated only one deuterium atom and that the substrate had no detectable deuterium incorporation. If the insertion of the alkene into the metal hydride was the enantioselective step, 1,3-cyclohexadiene would insert in a specific way leading to only one regioisomer (either from 1,2- or 1,4-addition). The reductive elimination of the product was established to be the enantioselective step in the nickel-catalyzed hydrocyanation of 1,3-cyclohexadiene, on the basis of equal 1,2-/1,4-product distribution.
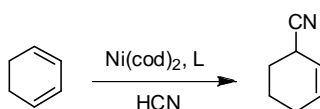
Scheme 1.23. Hydrocyanation of 1,3-cyclohexadiene.

1.6. The hydrocyanation of non-activated monoalkenes: the role of the Lewis acid

The hydrocyanation of 1-hexene to a mixture of heptanenitrile and 2-methylhexanenitrile, using Ni(0) phosphite complexes in combination with Lewis

acids, has been studied by Taylor and Swift.[59] Analysis of the reaction mixture showed that the isomerization of 1-hexene to the equilibrium mixture of isomers was a very rapid reaction compared to hydrocyanation. The Lewis acid, in addition to significantly enhancing the reaction rate, has an effect on the ratio of heptanenitrile: 2-methylhexanenitrile. Although it is possible to see how the Lewis acid can cause changes in this ratio, it is not easy to correlate the changes with any particular property of the series of Lewis acids studied. Using $AlCl_3$ as the promoter, approximately 85% of the 2-methyl-hexanenitrile produced resulted from direct hydrocyanation of 2-hexene, and only 15% from "Markovnikov" addition to 1-hexene. Steric hindrance in the substrate had a marked effect in directing the –CN addition to the terminal rather than to the internal position. Propene gave only 60% of the terminal addition product, whereas isobutene gave >99%. Phenolic solvents were found to have a promoting effect on the reaction rate compared to aromatic and nitrile solvents and also improved the selectivity to terminal addition products.

Keim *et al.*[60] investigated the hydrocyanation of 1-octene using a 15-fold excess of monophosphites as ligands and different Lewis acids (Scheme 2.24). The reactions, in which BPh_3, $ZnCl_2$, and $AlCl_3$ were added as co-catalyst showed very low conversions. Only by applying $AlEtCl_2$ a good activity was achieved. Furthermore, using *n*-octenes as starting material it was found that the anti-Markovnikov product 1-cyanooctane was formed with 80% regioselectivity, irrespective of the position of the double bond. The double bond of the unsaturated substrate is isomerized *via* an intermediate σ-alkyl species, reaching an equilibrium between internal and terminal alkenes. The isomerization and β-(H)-elimination rate (k_2) was found to be much higher than the hydrocyanation rate (k_1) (Scheme 1.25).
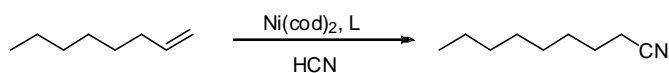
Scheme 1.24. Hydrocyanation of 1-octene.
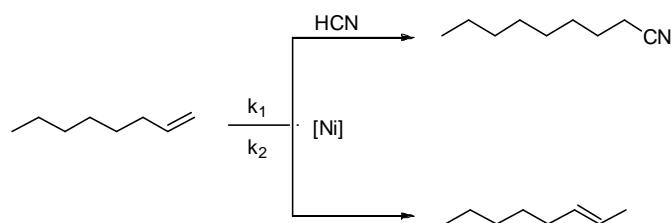
Scheme 1.25. Competition between isomerization and hydrocyanation of monoalkenes reported by Keim *et al.*[60]

Hydrocyanation of 1-alkenes and ω-unsaturated fatty acid esters was accomplished by Vogt *et al.*,[61] applying chelating diphosphines with a L:Ni ratio of only 1.05 (Scheme 1.24 and 1.26). The use of diphosphines with large bite angles induced yields that are comparable to the commercial *ortho*-tolylphosphite system in the hydrocyanation of 1-octene. For methyl-dec-9-enoate the obtained yields and selectivities were similar to the non-functionalized alkenes. The presence of the ester group did not inhibit the catalytic reaction. The Xantphos type diphosphines have almost identical electronic properties but different bite angles. Moreover, the S-bridge in the backbone of DPEphos is missing, which makes the ligand rather flexible. These characteristics influence the regioselectivity towards the nitrile products. It was suggested that the more rigid ligand backbones disfavor conformational changes in the corresponding metal complexes.

Nickel-catalyzed addition of deuterium cyanide to (*E*)-1-deuterio-3,3-dimethylbut-1-ene and subsequent analysis of the bis-deuterated nitrile to establish the stereochemistry of the hydrocyanation have been reported in 1991 by Bäckvall.[62] Estimation of the ratio of *erythro-* to *threo*-product by ^{1}H NMR spectroscopy
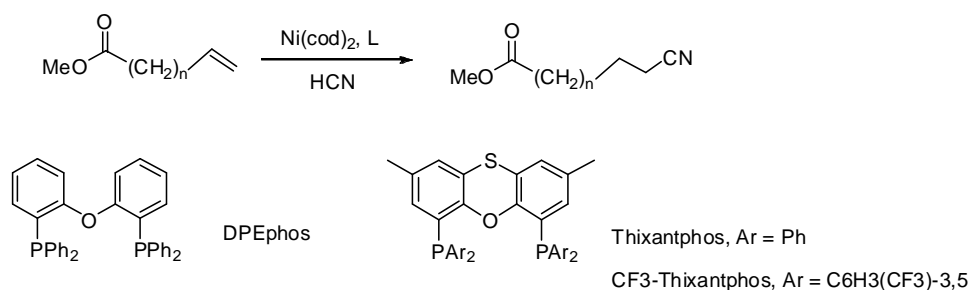
Scheme 1.26. Hydrocyanation of methyl-dec-9-enoate in the presence of diphosphine ligands reported by Vogt *et al.*[61]

indicated that the addition had occurred >90% *cis*. The remaining traces of unchanged alkene have been isolated, in order to find the source of the small fraction of *threo*-product formed in the addition of DCN. NMR analysis of the recovered alkene showed that no *E-Z*-isomerization had occurred (>98% *E*) and therefore, alkene isomerization cannot account for the slight loss of stereoselectivity. The proposed mechanism for the reaction is depicted in Scheme 1.27. Coordination of the alkene to the metal followed by hydride addition would give a nickel σ-complex, which on reductive elimination would yield the organic nitrile. Since transition metal hydride additions are known[63] to proceed *cis*, the observed stereochemistry requires the reductive elimination to occur with retention of configuration at the carbon.
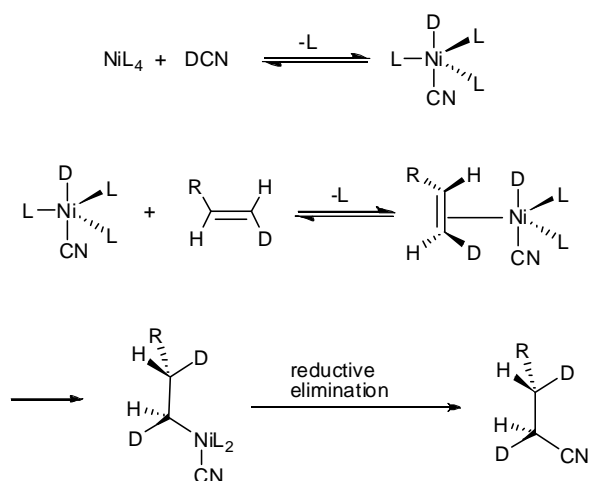
Scheme 1.27. Stereochemistry of the nickel-catalyzed hydrocyanation of alkenes reported by Bäckvall *et al.*[62]

1.7. The hydrocyanation reaction applying different metals

1.7.1. Cobalt-catalyzed hydrocyanation

The first example of homogeneously catalyzed alkene hydrocyanation was reported by Arthur *et al.* in 1954.[5] Unactivated monoalkenes, as well as conjugated dienes, were hydrocyanated in the presence of $Co_2(CO)_8$. Hydrocyanation of monoalkenes appeared to become more difficult as the chain length of the alkene increased. For example, ethene,

propene, and 1-butene gave more than 65% conversion to nitriles under similar conditions whereas 1-octene gave only 13% conversion. Styrene gave 50% conversion to 2-phenylpropionitrile. 2-Butene, having an internal double bond, gave only 9% conversion to 2-methylbutyronitrile. Under these conditions, only branched nitriles were accessible. The addition of HCN to conjugated alkenes such as butadiene and isoprene gave primarily 1,4-addition products. However, this early stage of research was marked by its empirical character and a lack of mechanistic insight.

A conceptually new hydrocyanation reaction of non-activated alkenes giving access to secondary and tertiary nitriles has been recently documented.[64] The cobalt-catalyzed HCN addition is one of the few procedures to allow the selective synthesis of branched nitriles (Scheme 1.28). The salient features of this process are the broad functional-group tolerance, mild reaction conditions (room temperature, EtOH as solvent), readily available starting materials (TsCN, PhSiH$_3$, alkenes), and ease of execution.
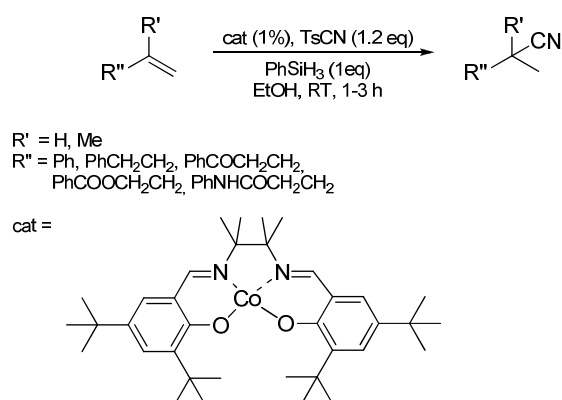
Scheme 1.28. Cobalt-catalyzed hydrocyanation reported by Carreira.[64]

1.7.2. Copper-catalyzed hydrocyanation

Few patents[65] have reported on the advantages of copper compared to nickel complexes as catalyst for the hydrocyanation of butadiene: low price, stability, and high selectivity for the addition reaction. Copper catalysis appears to be a very convenient and efficient method for realizing the monohydrocyanation of butadiene, as the yields are good (>90%) and the reaction leads selectively to substituted 2-butenes (>95% of 1,4-addition). Moreover, the catalyst is practically insensitive to traces of water or

oxygen. However, as the copper-catalyzed hydrocyanation of butadiene has to date been limited to the monoaddition of HCN, this reaction has not been applied on an industrial scale for the preparation of Nylon 6,6. A decrease in nitrile yield was observed for substituted conjugated dienes and is mainly due to the competition of cationic side-reactions. Oligomerization, telomerization, and polymerization are enhanced by the presence of electron-donating methyl substituents on the diene.

In comparison with nickel catalysts, copper-based systems have been rarely studied from a mechanistic point of view.[66,67,68] The copper-catalyzed hydrocyanation of butadiene leads essentially to the 1,4-monoaddition product (unsaturated nitrile) with the addition of a second molecule of HCN being undetected under standard hydrocyanation conditions. The activity of CuBr and CuBr$_2$ as catalysts seems to be linked to the facile formation of intermediates by initial protonation of the alkene (Scheme 1.29). The role of the bromide anion can be explained by the increased acidity given to the [H(CuBrCN)] complex. The reaction would then proceed through activation of HCN by preferential coordination to copper. The very acidic [H(CuBrCN)] species leads to the formation of the allyl moiety, which remains to some extent controlled by the copper center. However, the synthesis of *trans*-3-pentenenitrile from butadiene strongly supports the hypothesis of a nucleophilic attack of a non-coordinated CN$^-$ to a π–allyl Cu$^+$ species.[66] The copper-allyl intermediates have not been detected, but the formation of such species as transient intermediates is considered to provide the best explanation for the results.
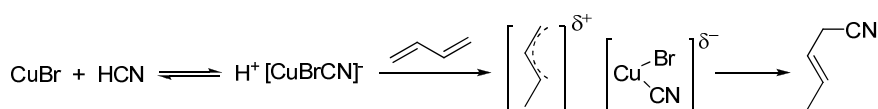
Scheme 1.29. Copper-catalyzed hydrocyanation reported by Waddan.[65]

1.7.3. Palladium-catalyzed hydrocyanation

The hydrocyanation reaction has been investigated by Jackson *et al.*,[69] using the catalyst system [Pd(diop)$_2$]. Reactions of both terminal and cyclic alkenes have been shown to occur in a stereospecifically *cis-* manner *via* deuterium cyanide addition (Scheme 1.30). The conditions chosen for the hydrocyanation were deliberately mild to

minimize the chance of isotope exchange reactions and the yield of nitriles was restricted to ~10%. The stereochemistry of the deuterium incorporation was established by ^{1}H and ^{2}H NMR spectroscopic analysis of the products. When the catalyst system based on [Ni[P(OPh)$_3$]$_4$] and ZnCl$_2$ was applied, both intramolecular and intermolecular scrambling of the deuterium label occurred.

Similar *cis*-addition of DCN to norbornene and norbornadiene was also observed by Jackson using [Pd(DIOP)$_2$] as catalyst system. Furthermore, an enantiomeric excess of 28% was reported for the hydrocyanation of norbornene and 17% for norbornadiene.[70] Addition of a Lewis acid, for example ZnCl$_2$, did not lead to any improvement in yield or enantioselectivity.

The asymmetric hydrocyanation of norbornene catalyzed by chiral palladium diphosphine complexes has been investigated by Hodgson and Parker[71] (Scheme 1.19). The lowest *ee*'s (13%) were obtained with [Pd(diop)$_2$], while [Pd(binap)$_2$] gave 40% *ee*, but with an inferior isolated chemical yield. The mechanism has been studied using [Pd(C$_2$H$_4$)(diop)$_2$] as convenient precursor complex, whose crystal structure is reported. Stereoselective complexation of norbornene to the palladium(0) center *via* the *exo* face was observed. The reaction intermediates [Pd(norbornene)(diop)] and [Pd(II)hydrido(cyanide)] have been characterized by NMR spectroscopy. The oxidative addition of hydrogen cyanide to the Pd(0) center seems to precede the alkene binding and β-*cis* hydride transfer. The weakness of the palladium alkene bond, manifested by the structural analysis of the ethene complex suggests that the alkene binding is rate limiting.
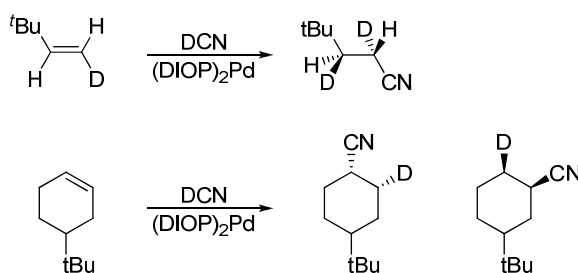
Scheme 1.30. Palladium-catalyzed deuterocyanation reported by Jackson *et al.*[69]

The palladium complex bearing the phosphine-phosphite ligand (*R,S*)-Binaphos (Figure 1.11) has been applied in the asymmetric hydrocyanation of norbornene by

Nozaki,[72] giving the corresponding *exo*-nitrile. Enantioselectivities of up to 48% *ee* have been obtained, which is the highest *ee* ever reported using norbornene as substrate. The palladium-catalyzed reaction was greatly inhibited by an excess of ligand.
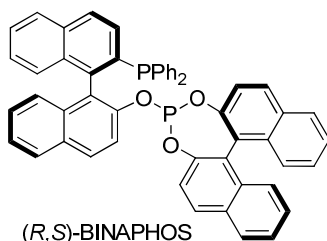
(*R*,*S*)-BINAPHOS

Figure 1.11. (*R*,*S*)-BINAPHOS.

Vinyl and allyl silanes have been tested in the addition of HCN, catalyzed by [palladium(0)tetrakis(thiphenylphosphite)], obtaining yields in the range of 30-80%.[73] The linear cyano-silane isomer was always the major addition product.

Furthermore, the rate of the reductive elimination of the complex $[Pd(CH_2R)(CN)(L)]$ has been studied by Marcone and Moloy (Scheme 1.31).[45] It was shown that relatively minor changes in the chelate bite angle induce a significant effect (ca. 10^4 fold) on the rate of reductive elimination. Variation of the alkene structure can also cause the elimination rate to vary. Moreover, the reductive elimination can be significantly enhanced adding Lewis acids. This represents a third parameter that governs reductive elimination rates of nitriles. The coordination of Lewis acids, for example BEt_3 or $AlEt_3$, to metal cyanides is known to induce positive charge formation at the nitrogen and

LA = BEt_3, $AlEt_3$, BPh_3, $B(C_6F_5)_3$, $AlPh_3$
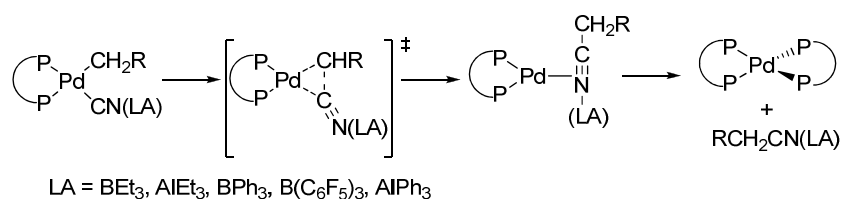
Scheme 1.31. Reductive elimination in the Pd-catalyzed hydrocyanation reported by Marcone and Moloy.[45]

carbon, with concomitant negative charge formation at the boron or aluminium. The nitrile carbon is consequently rendered more susceptible to nucleophilic attack by the alkyl group, thus explaining the rate acceleration in the Lewis acid adduct.

1.7.4. Platinum-catalyzed hydrocyanation

Although the study of the kinetically more inert platinum analogues of reactive palladium complexes has been often advocated, there are not many examples of platinum-catalyzed hydrocyanation reactions.[74]

Details on the reaction mechanism of the catalytic cycle for the hydrocyanation of ethene catalyzed by bis(hydrido-bridged)diplatinum complexes were obtained by DFT calculation of the relevant intermediates and transition state structures (Scheme 1.32). The catalytically active species was identified as a 16e$^-$ coordinatively unsaturated [Pt(CN)(H)(PH$_3$)(η^2C$_2$H$_4$)] species, formed upon addition of ethene on the monomeric [Pt(CN)(H)(PH$_3$)] precursor. The following three steps were found to be critical for the
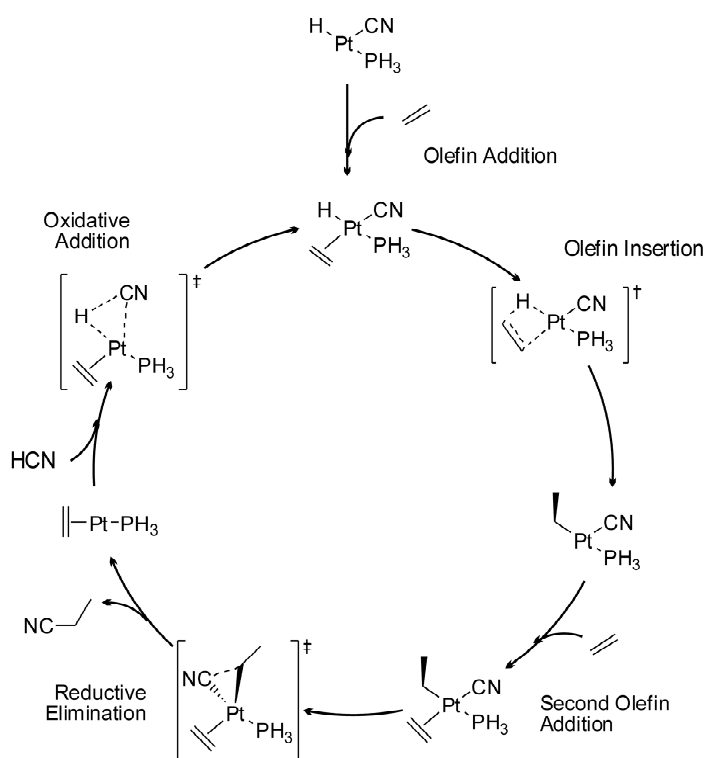
Scheme 1.32. Catalytic cycle for the hydrocyanation of ethene proposed by Kefalidis.[74]

catalytic reaction: the migration of the hydride to the acceptor C atom of the coordinated ethene substrate, the reductive elimination of the final product and the oxidative addition process that regenerates the catalyst. The rate determining step seems to be the reductive elimination and the overall catalytic process is exergonic.

1.8. Conclusions and Outlook

Most of the investigations on the hydrocyanation reaction are regarding dienes or vinylarenes as substrates. The formation of intermediate π-allyl or η^3-benzyl species allows better activity and higher stability of the nickel catalysts. Several ligands have been applied in these reactions and their influence on activity, regio- and enantioselectivity has been considered. Furthermore, the effect of electronic and steric parameters of the ligands, as well as the influence of the substrate and solvent, have been elucidated.

Nevertheless, a comprehensive study of the nickel catalyst deactivation pathways is still missing. A deeper understanding of these processes would allow improvements on the catalyst stability.

Very few examples for the nickel-catalyzed hydrocyanation of monoalkenes have been reported. In fact, this reaction presents several difficulties, such as the low reactivity of the substrates, the easy deactivation of the metal-alkyl intermediate species to dicyano complexes, and the unclear role of the Lewis acid. Cobalt-catalyzed hydrocyanation, although hardly explored, seems to offer a valid alternative to convert monoalkenes to nitriles, although the two reactions present complementary regioselectivity. In the cobalt-catalyzed hydrocyanation prevalence of branched nitriles is obtained while nickel catalysts favor linear products. So far, the hydrocyanation of monoalkenes represents one of the major open challenges in this field.

1.9. Scope of the thesis

The performance of existing catalysts for the Ni-catalyzed hydrocyanation can be improved in terms of activity, stability and selectivity. In this thesis, the development and application of new catalytic systems and the addition of co-catalysts in the hydrocyanation of different alkenes is described. The results obtained are analyzed in view of a better understanding of the reaction mechanism.

The preparation and application of a triptycene-based diphosphine ligand in the hydrocyanation of butadiene has been reported in Chapter 2. High activities and excellent selectivities of up to 98% towards 3-pentenenitrile (3PN) were achieved. The catalytic activity and the mechanism of this system are extensively discussed.

Contributions on the isomerization of 2-methyl-3-butenenitrile (2M3BN) towards 3PN by means of IR spectroscopy in *operando* modus are discussed in Chapter 3. The kinetics of the reaction are analyzed using chemometrics.

The development and application of new tetraphenol-based diphosphite ligands in the hydrocyanation of 3PN is described in Chapter 4. The coordination of the substrate and of $ZnCl_2$ as Lewis acid co-catalyst to the corrisponding $[NiL_n]$ catalyst is investigated by means of IR and NMR spectroscopy.

In Chapter 5 of this thesis a study on the regioselectivity of the hydrocyanation of styrene is described. The application of Lewis acids to control the branched/linear product distribution is deeply investigated.

In Chapter 6 the hydrocyanation of terminal monoalkenes, in particular 1-octene, is investigated. For the first time diphosphite ligands were applied in this reaction, obtaining the best conversion ever reported.

1.10. References and Notes

1. (a) Huthmacher, K.; Krill, S. in *Applied Homogeneous Catalysis with Organometallic Compounds,* 2nd ed.; Cornils, B., Hermann, W. A., Eds.; Wiley-VCH: Weinheim, **2002**; Vol. 1 pp 465; (b) Tolman, C. A. *Chem. Rev.* **1977**, *77*, 313-348.

2. Pollak, P.; Romeder, G.; Hagedorn, F.; Gelbke, H. in *Nitriles. Ullman's encyclopedia of industrial chemistry, 5th copl. Rev. ed., Vol. A17*, Wiley-VCH, Weinheim, **1985**, pp. 363-376.

3. Keim, W. *Angew. Chem.* **1990**, *102*, 251.

4. Beller, M.; Seayad, J.; Tillack, A.; Jiao, H. *Angew. Chem Int. Ed..* **2004**, *43*, 3368.

5. Arthur, P., Jr., England, D.C., Pratt, B.C., and Whitman, G. M. *J. Am. Chem. Soc.* **1954**, *76*, 5364-536.

6. van Leeuwen, P. W. N. M. in *Homogeneous Catalysis: Understanding of the Art*; Kluwer Academic Publishers: Dordrecht, The Netherlands, **2004**; pp 229-233.

7. Tolman, C. A. *J. Chem. Educ.* **1986**, *3*, 199.

8. (a) Foo, T.; Garner, J. M.; Tam, W., WO 99/06357, **1999**. *Chem. Abstr.* **1999***, 130*, 169815; (b) Ahlers, W.; Paciello, R.; Vogt, D.; Hofmann, P., WO02/083695, **2002**. *Chem. Abstr.* **2002***, 137*, 311033; (c) Bartsch, M.; Baumann, R.; Kunsmann-Keitel, D. P.; Harderlein, G.; Jungkamp, T.; Altmayer, M.; Seigel, W. and Molnar, F., DE 10150286, **203**. *Chem. Abstr.* **2005***, 138*, 304408; (d) Lenges, C. P.; WO 03/076394, **2003**. *Chem. Abstr.* **2006***, 139*, 262467.

9. Drinkard, W. C.; Lindsey, R. W. Jr. US 3496215, **1970**.

10. (a) Tolman, C. A. *J. Am. Chem. Soc.*, **1970**, *92,* 2953; (b) Giering, W. P.; Prock, A.; Eriks, K.; Rahaman, M. N:; Liu, H.-Y. *Organometallics* **1989**, *8*, 1.

11. Gosser, L. W.; Tolman, C. A. *Inorg. Chem.,* **1970**, *9,* 2956.

12. Tolman, C. A. *J. Am. Chem. Soc.*, **1970**, *92,* 2956.

13. Seidel, W. C.; Tolman, C. A. *Inorg. Chem.,* **1970**, *9,* 2354.

14. Tolman, C. A. *Chem. Soc. Rev.*, **1972**, *1,* 337.

15. (a) Tolman, C. A. *J. Am. Chem. Soc.*, **1970**, *92,* 4217; (b) Druliner, J. D.; English, A. D.; Jesson, J. P.; Meakin, P. Tolman, C. A. *J. Am. Chem. Soc.*, **1976**, *98,* 2156.

16. Goertz, W.; Keim, W.; Vogt, D.; Englert, U.; Boele, M. D. K.; van de Veen, L. A.; Kamer, P. C. J.; van Leeuwen, P. W. N. M. *J. Chem. Soc., Dalton Trans.,* **1998**, 2981.

17. Tolman, C. A.; Seidel, W. C.; Druliner, J. D.; Domaille, P. J. *Organometallics* **1984**, *3*, 33.

18. McKinney, R. J. and Roe, D. C. *J. Am. Chem. Soc.*, **1985**, *107*, 261.

19. Tolman, C. A.; McKinney, R. J.; Seidel, W. C.; Druliner, J. D.; Stevens, W. R. *Adv. Catal.* **1985**, *33*, 1.

20. Keim, W; Behr, A.; Lühr, H.-O.; Weisser, J. *J. Catal.*, **1982**, *78*, 209.

21. Goertz, W.; Kamer, P. C. J.; van Leeuwen, P. W. N. M.; Vogt, D. *Chem. Eur. J.*, **2001**, *7,* 1614.

22. Baker, M. J.; Harrison, K. N.; Orpen, A. G.; Pringle, P. G. and Show, G *J. Am. Chem. Soc., Chem. Comm.* **1991**, *12*, 803.

23. Saha, B., RajanBabu, T. V. *Org. Lett.* **2006**, *8*, 4657.

24. Tolman, C. A. *Organometallics* **1983**, *2,* 614.

25. Druliner, J. D. *Organometallics* **1984**, *3*, 205.

26. Bini, L.; Müller, C.; Wilting, J.; von Chrzanowski, L.; Spek, A. L.; Vogt, D. *J. Am. Chem. Soc.* **2006**, *128,* 11374.

27. van der Vlugt, J. I.; Hewat, A. C.; Neto, S.; Sablong, R.; Mills, A. M.; Lutz, M.; Spek, A. L.; Müller, C.; Vogt, D. *Adv. Synth. Catal.* **2004**, *346*, 993.

28. Chaumonnot, A.; Lamy, F.; Sabo-Etienne, S.; Donnadieu, B.; Chaudret, B.; Barthelat, J. C. and Galland, J. C. *Organometallics* **2004**, *23* (14), 3363.

29. Valee, C.; Valerio, C.; Chauvin, Y.; Niccolai, G. P.; Basset, J.-M.; Santini, C. C.; Galland, J.-C.; Didillon, B. *J. Mol. Catal.A* **2004**, *214*, 71.

30. (a) Garcia, J. J.; Jones, W. D. *Organometallics* **2000**, *19,* 5544; (b) Atesin, T. A.; Li, T.; Lachaize, S.; Garcia, J. J.; Jones, W. D. *Organometallics* **2008**, *27,* 3811.

31. Garcia, J. J.; Brukan, N. M.; Jones, W. D. *J. Am. Chem.Soc.* **2002**, *124,* 9547.

32. Garcia, J. J.; Arevalo, A.; Brunkan, N. M.; Jones, W. D. *Organometallics* **2004**, *23,* 3997.

33. Atesin, T. A.; Li, T.; Lachaize, S.; Brennessel, W. W.; Garcia, J. J.; Jones, W. D. *J. Am. Chem.Soc.* **2007**, *129,* 7562.

34. (a) Brukan, N. M.; Jones, W. D. *J. Organomet. Chem.* **2003**, *683,* 77; (b) Brukan, N. M.; Brestensky, D. M.; Jones, W. D. *J. Am. Chem.Soc.* **2004**, *126,* 3627.

35. Wilting, J.; Müller, C.; Hewat, A. C.; Ellis, D. D.; Tooke, D. M.; Spek, A. L.; Vogt, D. *Organometallics* **2005**, *24*, 13.

36. Swartz, B. D.; Reinartz, N. M.; Brennessel, W. W.; Garcia J. J., Jones, W. D. *J. Am. Chem.Soc.* **2008**, *130,* 8548.

37. Acosta-Ramirez, A.; Flores-Gaspar, A.; Muñoz-Hernandez, M.; Arevalo, A.; Jones, W. D.; Garcia, J. J. *Organometallics* **2007**, *26*, 1712.

38. (a) Acosta-Ramirez, A.; Munoz-Hernandez, M.; Jones, W. D.; Garcia, J. J. *J. Organomet. Chem.* **2006**, *691*, 3895; (b) Acosta-Ramirez, A.; Munoz-Hernandez, M.; Jones, W. D.; Garcia, J. J. *Organometallics* **2007**, *26*, 5766.

39. Acosta-Ramirez, A.; Flores-Alamo, M.; Jones, W. D.; Garcia, J. J. *Organometallics* **2008**, *27*, 1834.

40. Nakao, Y.; Oda, S.; Hiyama, T. *J. Am. Chem.Soc.* **2004**, *126,* 13904.

41. Miller, J. A.; Dankwardt, J. W. *Tetrahedron Lett.* **2007**, *129*, 2428.

42. Nakao, Y.; Yukawa, T.; Hirata, Y.; Oda, S.; Satoh, J.; Hiyama, T. *J. Am. Chem.Soc.* **2006**, *128,* 7116.

43. Tobisu, M.; Chatani, N. *Chem. Soc. Rev.* **2008**, *37,* 300.

44. Nakao, Y.; Yada, A.; Ebata, S.; Hiyama, T. *J. Am. Chem.Soc.* **2007**, *129,* 2428.

45. (a) Marcone, J. E. and Moloy, K. G. *J. Am. Chem.Soc.* **1998**, *120,* 8527; (b) Huang, J.; Haar, C. M.; Nolan, S. P.; Marcone, J. E.; Moloy, K. G. *Organometallics* **1999**, *18*, 297.

46. McKinney, R. J. *Organometallics* **1985**, *4*, 1142.

47. McKinney, R, J.; Nugent, W. A. *Organometallics* **1989**, *8*, 2871.

48. Vallee, C.; Chauvin, Y.; Basset, J.-M.; Santini, C. C.; Galland, J.-C. *Adv. Synth. Catal.* **2005**, *347*, 1835.

49. a) Kreutzer, K. A.; Tam, W. Hydrocyanation process and multidentate phosphite and nickel catalyst composition therefore. WO 96/11182, **1996.** *Chem. Abstr.* **1996**, *125*, 114851. b) Brunel, E. E.; Kenneth, C. Process for the hydrocyanation of alkenes using bidentate phosphite ligands and zero-valent nickel catalyst system which enable facile nitrile product and catalyst separation. US 5847191 A, **1998.** *Chem. Abstr.* **1998**, *130*, 26464; c) Lenges, C. P.; Lu, H. S. M.; Ritter, J. C. Phosphonite ligands and their use in hydrocyanation. WO 03/076394, **2003.** *Chem. Abstr.* **2003**, *139*, 262467.

50. Elmes, P. S.; Jackson, W. R. *Aust. J. Chem.*, **1982**, *35*, 2041.

51. Baker, M. J.; Pringle, P. G. *J. Am. Chem. Soc., Chem. Comm.*, **1991**, 1292.

52. Nugent, W. A.; McKinney, R. J. *J. Org. Chem.*, **1985**, *50*, 5370.

53. Casalnuovo, A. L.; RajanBabu, T. V.; Ayers, T. A.; Warren, T. H. *J. Am. Chem. Soc.*, **1994**, *116,* 9869.

54. Casalnuovo, A. L.; RajanBabu *J. Am. Chem. Soc.*, **1996**, *118,* 6325.

55. Yan, M.; Xu, Q.-Y.; Chan, A. S. C. *Tetrahedron: Asymmetry* **2000**, *11,* 845.

56. Wilting, J.; Janssen, M.; Müller, C.; Lutz, M.; Spek, A. L.; Vogt, D. *Adv. Synth. Catal.* **2006**, *349*, 350.

57. Göthlich, A. P. V.; Tensfeldt, M.; Rothfuss, H.; Tauchert, M. E.; Haap, D.; Rominger, F.; Hofmann, P. *Organometallics* **2008**, *27*, 2189.

58. Wilting, J.; Janssen, M.; Müller, C.; Vogt, D. *J. Am. Chem. Soc.* **2006**, *128,* 11374.

59. Taylor, B. W.; Swift, H. E. *J. Catal.* **1972**, *26*, 254.

60. Keim, W., Behr, J. P.; Weisser, J. *Erdöl Kohle, Erdgas, Petrolchrm.* **1982**, *35* (9), 436.

61. Goertz, W.; Kamer, P. C. J.; van Leeuwen, P. W. N. M.; Vogt, D. *Chem. Comm.* **1997**, 1521.

62. Bäckvall, J.-E.; Andell, O. S.*J. Am. Chem. Soc., Chem. Comm.*, **1981**, 1098.

63. Kochi, J. K. in *Organometallic Mechanism and Catalysis*; Academic Press, New York, **1978**, pp 312.

64. Gaspar, B.; Carreira, E. M. *Angew. Chem.* **2007**, *46*, 4519.

65. (a) Waddan, D. Y.; Benzie, R. J.; Robert, J. *Ger. Offen.,* 1497276, **1976**; (b) Waddan, D. Y.; Benzie, R. J.; Robert, J. *Ger. Offen.,* 2812156, **1978**; (c) Waddan, D. Y. *Brit. Pat.,* 2624449, **1978**

66. Puentes, E.; Mamalis, I.; Noels, A. F.; Hubert, A. J.; Teyssie, P.; Waddan, D. Y. *J. Catal.* **1983**, *82*, 365.

67. Puentes, E.; Noels, A. F.; Warin, R.; Hubert, A. J.; Teyssie, P.; Waddan, D. Y. *J. Mol. Catal.* **1985**, *31*, 183.

68. Mamalis, I.; Noels, A. F.; Puentes, E.; Warin, R.; Teyssie, P.; Hubert, A. J.; Gandjean, J.; Hubin, R.; Waddan, D. Y. *J. Catal.* **1986**, *102*, 357.

69. (a) Jackson, W. R.; Lovel, C. G. *Tetrahedron Lett.* **1982**, *23,* 1621; Jackson, W. R. and Lovel, C. G. *Aust. J. Chem.* **1982**, *35,* 2053.

70. Elmes, P.; Jackson, W. R. *J. Am. Chem.Soc.* **1979**, *20,* 6129.

71. (a) Hodgson, M.; Parker, D. *J. Organomet. Chem.* **1987**, *325*, C27; (b) Hodgson, M.; Parker, D.; Taylor, R. J.; Ferguson, G. *Organometallics* **1988**, *7*, 1761.

72. Horiuchi, T.; Shirakawa, E.; Nozaki, K.; Takaya, H. *Tetrahedron Lett.* **1987**, *8,* 57.

73. Brown, E. S.; Rick, E. A.; Mendicino, F. D. *J. Organomet. Chem.* **1972**, *38*, 37.

74. Tsipis, C. A.; Kefalidis, C. E. *Organometallics* **2006**, *25*, 1696.

Chapter **2**

Highly Selective Hydrocyanation of Butadiene towards 3-Pentenenitrile

In this chapter, a new route for the synthesis of the triptycene-based diphosphine ligand Tript(PPh₂)₂ is described giving the desired compound in good yield. The corresponding Pt(II)- and Ni(0)-complexes are characterized. In butadiene hydrocyanation the [Ni(cod)(tript-PPh₂)₂] pre-catalyst leads to exceptionally high selectivities for the linear product 3-pentenenitrile, combining high activity for both, hydrocyanation and isomerization. This enables reduction of the synthesis to a one-step procedure and could be the key towards process intensification in the future.
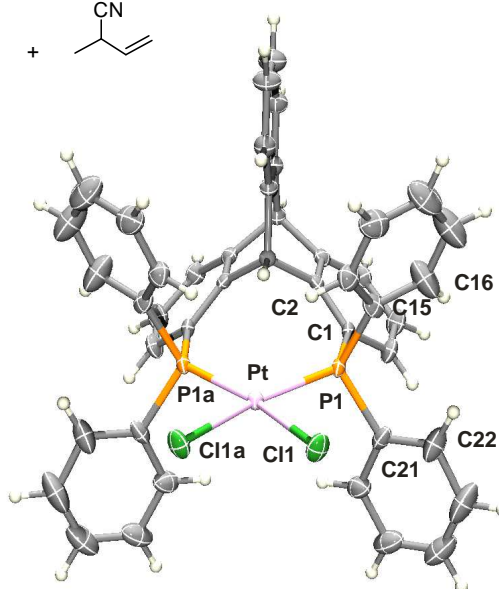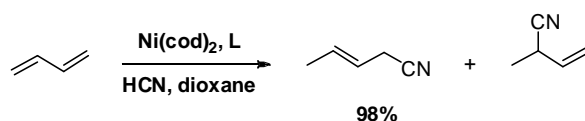
2.1. Introduction

In 1971 Du Pont started the production of adiponitrile (AdN) as an intermediate in the manufacture of Nylon(6,6).[1,2] This process is so far the only example of a large scale industrial application of an alkene hydrocyanation. Originally it was developed using a monodentate phosphite-based zerovalent nickel catalyst.[3] The process consists of three steps (Scheme 2.1). The first step concerns the hydrocyanation of butadiene to a mixture of 2-methyl-3-butenenitrile (2M3BN) and 3-pentenenitrile (3PN), obtained in varying ratio depending on the ligand employed. In a second step, the branched 2M3BN is isomerized to the desired linear 3PN. The last step is the hydrocyanation of 3PN to AdN, which requires an additional Lewis acid co-catalyst such as $AlCl_3$, $ZnCl_2$, or BPh_3.

Many efforts have been made to improve the performance of the nickel catalysts. An important step was the replacement of monodentate ligands by bidentate π-acceptor ligands that lead to higher conversion in butadiene hydrocyanation and selectivities for 3PN up to a reported maximum of 70%.[4] A higher selectivity has been claimed only in a patent for bis(diphenyl-phosphino)ferrocene (DPPF) as ligand used in large excess.[5] Large bite angle ligands, based on a rigid xanthene backbone (e.g. xantphos or thixantphos) were proven to enhance the Ni(0)-catalyst performance in hydrocyanation.[6] It was proposed that these ligands improve the reductive elimination of the product and
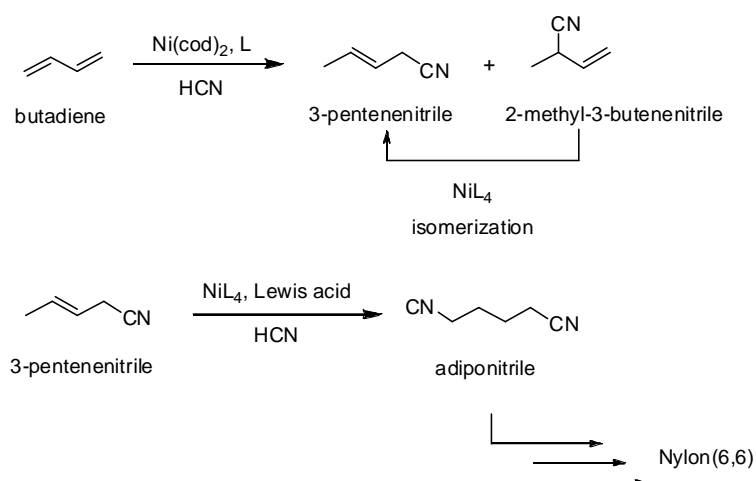
Scheme 2.1. DuPont Adiponitrile process.

stabilize the active Ni-species while suppressing the formation of inactive dicyano Ni(II)-complexes during the catalytic cycle.

Triptycene-based bidentate phosphorus ligands, first described by Hofmann *et al.*,[7] possess both a very rigid backbone and a large bite angle. So far, these systems have been only described in the patent literature with examples of rhodium-catalyzed hydroformylation reactions.[7, 8] In more recent publications different mono- and dinuclear metal complexes with a variety of different bite angles and geometries were investigated for these ligands.[9]

The application of a triptycene-based diphosphine ligand in the hydrocyanation of butadiene is described in this chapter. A new route towards the ligand Tript(PPh$_2$)$_2$ (**5**) (Scheme 2.2) has been designed, giving considerably higher yields than the previously reported method.[7, 8] The coordination chemistry of **5** towards Pt(II) and Ni(0) was investigated. Application in the Ni-catalyzed hydrocyanation of butadiene gave unprecedented high selectivities of up to 98% of the linear product 3PN.

2.2. Synthesis of the ligand

According to Scheme 2.2, 1,8-dichloroanthraquinone (**1**) was converted into the difluoro compound (**2**) and subsequently reduced to 1,8-difluoroanthracene (**3**) with Zn dust.[10, 11] The triptycene moiety (**4**) was obtained by reaction of the corresponding anthracene with benzyne, generated *in situ* from anthranilic acid. The last step, leading to the formation of the ligand (**5**), was performed by a nucleophilic substitution of the fluoro groups with potassium diphenylphosphide in 20% overall yield. The ligand Trip(PPh$_2$)$_2$ (**5**) was obtained as a white powder. After recrystallization from methanol the compound was characterized by NMR spectroscopy and elemental analysis. The ^{31}P NMR shows a single resonance at δ = -14.95 ppm. The ligand and all intermediates in the synthesis are stable to air and moisture.
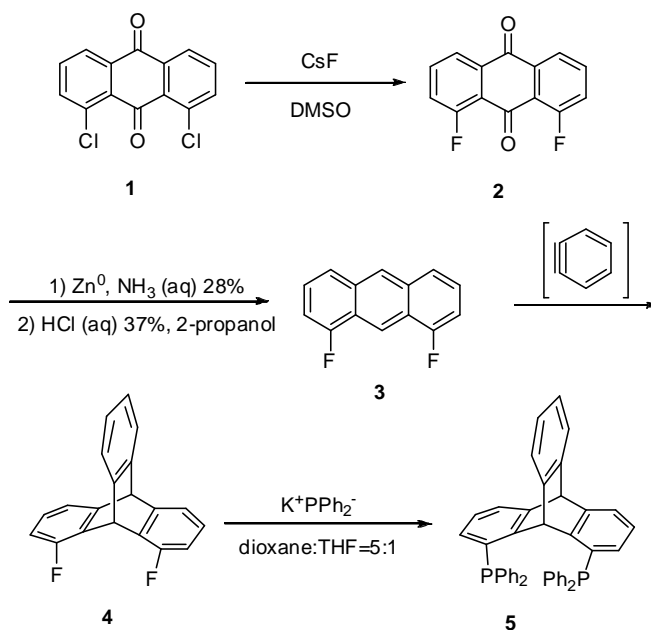
Scheme 2.2. Synthesis of the triptycene-based ligand **5**.

2.3. Synthesis of Pt(II) and Ni(0) complexes

The coordination behavior of (**5**) towards transition metal centers with potential relevance for homogeneous catalytic reactions was investigated. Reactions of (**5**) with Pt(cod)Cl$_2$ and Ni(cod)$_2$, respectively, led to the corresponding complexes [PtCl$_2$(**5**)] (**6**) and [Ni(cod)(**5**)] (**7**), shown in Figure 2.1.
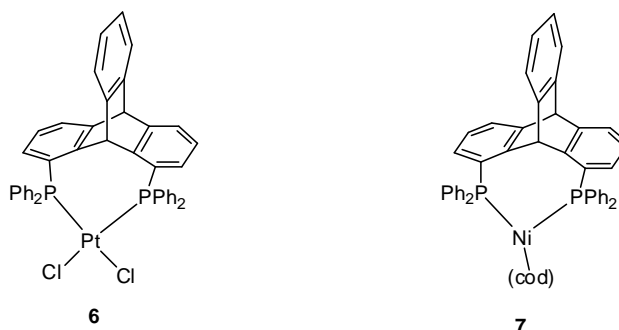
Figure 2.1. Complexes [PtCl$_2$(**5**)] (**6**) and [Ni(cod)(**5**)] (**7**).

2.3.1. The coordination towards platinum

The pale-yellow compound **6** was obtained in 74% yield and was handled as an air and moisture sensitive solid. The complex was characterized by means of ^{1}H, ^{13}C and ^{31}P NMR spectroscopy as well as by elemental analysis. In the ^{31}P NMR spectrum of **6** a singlet at δ = 0.42 ppm with platinum satellites ($^1J_{Pt-P}$ = 3761 Hz) was observed, suggesting that the ligand is coordinated in a *cis* fashion towards the metal centre (Figure 2.2).

Crystals of the Pt(II) complex suitable for X-ray diffraction were obtained by slow diffusion of diethyl ether into a dichloromethane solution of the compound. The molecular structure of **6** is depicted in Figure 2.3 along with selected bond lengths and angles. The molecule exhibits crystallographic mirror symmetry, with the mirror plane passing through C7 to C14 and Pt1. The coordination environment of the central Pt(II) atom, defined by the two P donors and the two Cl^{-} ligands, is strongly distorted square planar. The sum of all angles in the plane is 360°, with the largest deviation from the ideal value of 90° of 27.53(5)° for P1-Pt1-P1a. The *trans* angle Cl1(a)-Pt1-P1 deviates by 12.52(5)° from the ideal value of 180°. This strongly distorted coordination geometry was also observed for the similar di-*i*-propylphosphino-triptycene Pt(II) complex reported by Gelman *et al.*[9c] The largest deviation of the *cis* angles in this compound of 29° is even higher [P-Pt-P = 109.27(2)°]. Pt-Cl [2.3553(6) and 2.3661(6) Å] bond distances agree well with that found in (**6**), while the Pt-P [2.3208(6) and 2.3285(6) Å] distances are
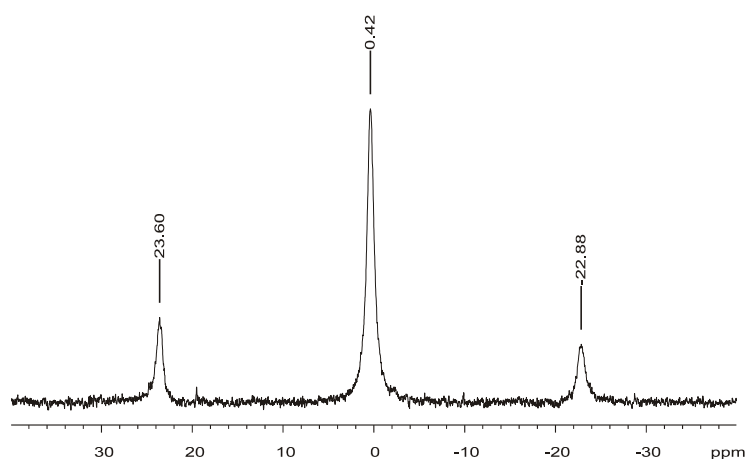
Figure 2.2. ^{31}P {^{1}H} NMR (CD$_2$Cl$_2$) of the complex [PtCl$_2$(**5**)] (**6**).

significantly longer. This difference is probably due to the steric effects of the *iso*-propyl groups in the compound obtained by Gelman in comparison with the phenyl rings in (**6**) and is also expressed by a shorter non bonding P⋯P distance of 3.6124(16) Å, compared to the 3.79 Å in the previously reported Pt(II) complex.[9c]
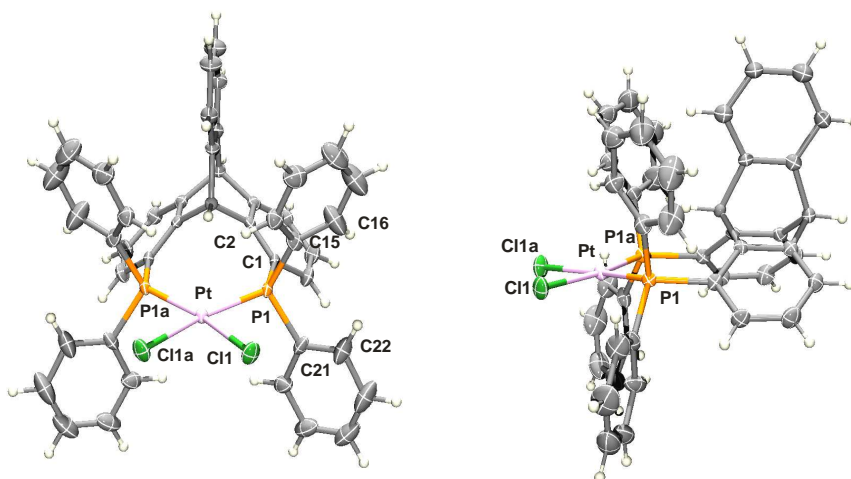
Figure 2.3. The molecular structure of [PtCl$_2$(**5**)] (**6**) in the crystal (front view left and side view right). All hydrogen atoms and the CH$_2$Cl$_2$ solvate molecules have been omitted for clarity. Displacement ellipsoids are drawn at the 50% probability level. Selected bond lengths [Å]: Pt1-Cl1 = 2.3338(14), Pt1-P1 = 2.2392(12), P1-C1 = 1.858(5), P1-C15 = 1.832(6), P1-C21 = 1.830(5). Selected bond angles [°]: Cl1-Pt1-P1 = 167.48(5), Cl1-Pt1-Cl1a 82.69(5), Cl1-Pt1-P1a = 84.87(5), P1-Pt1-P1a = 107.53(5).

2.3.2. The coordination towards nickel

[Ni(cod)(**5**)] **7** complex was synthesized *in situ* and displayed a singlet at δ = 25.82 ppm in the ^{31}P NMR spectrum. The formation of the complex was also confirmed by the clear signals in the ^{1}H NMR spectrum for the 1,5-cyclooctadiene ligand (cod) coordinated to the nickel atom. No formation of bischelate complexes[6, 12] was detected by NMR spectroscopy even in the case of an excess of the ligand added to the [Ni(cod)(**5**)] solution. The formation of bischelates, which are often catalytically inactive, is strongly related to the steric bulk of the ligand; the triptycene backbone apparently provides a rigid and bulky structure with mono-chelation to the Ni(cod)$_2$ metal precursor.

2.4. Hydrocyanation of butadiene

The complex **7** [Ni(cod)(**5**)] was applied in the hydrocyanation of butadiene (Scheme 2.3). The reaction with acetonecyanohydrine (ACH) as HCN source was carried out in toluene and in dioxane as solvent. The reaction in toluene was slow (Table 2.1, Entry 1), giving 49% conversion and 65% selectivity to the linear product 3PN in 5 hours. The selectivity was comparable to the results obtained with the best performing diphosphite ligands described for this process.[4]
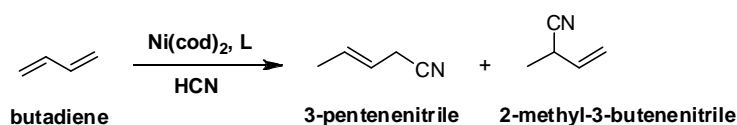
Scheme 2.3. Hydrocyanation of butadiene.

Most strikingly, the hydrocyanation of butadiene with ACH in the polar solvent dioxane gave excellent selectivities towards 3PN (98%) and a conversion of up to 85% (Table 2.1, Entries 2 and 3), attributed to the higher solubility of gaseous butadiene in polar solvents.[13a] The dielectric constants for butadiene, toluene and dioxane confirm this solubility trend ($\varepsilon_{butadiene} = 2.050$, $\varepsilon_{toluene} = 2.408$, $\varepsilon_{dioxane} = 2.1$).[13b] Solvent effects in the hydrocyanation reaction have been reported earlier, especially in asymmetric catalysis, where higher *ee*'s were obtained in apolar solvents for MVN

Table 2.1. Butadiene hydrocyanation in dioxane with ACH as HCN source.

Entry	Ratio S/Ni	Ratio (5)/Ni	Ratio ACH/BN	Conversion (%)	3PN (%)	Time (h)
1[a]	125	1	1.2	48	65.0	5
2	125	1	1.2	59	97.6	3
3	125	1	1.2	85	94.8	5
4	125	2	1.2	62	92.0	5
5	125	1	3.0	21	70.5	5
6	600	1	1.2	20	90.0	3

Conditions: 0.018 mmol Ni(cod)$_2$, acetonecyanohydrine (ACH) as HCN source, 90°C, 2m L dioxane. [a)]Reaction performed in toluene (2 mL).
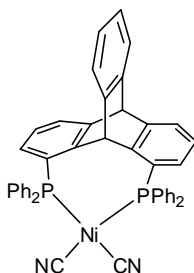
Figure 2.4. Dicyano Ni(II) species.

(6-methoxy-2-vinyl-naphthalene)[14] as substrate. Addition of an excess of ligand slowed down the reaction but still led to high product linearity (Table 2.1, Entry 4). An excess of ACH led to a decrease in conversion and to lower product linearity (Table 2.1, Entry 5). The high concentration of ACH probably deactivated the catalyst by formation of dicyano Ni(II)-species (Figure 2.4). At low catalyst loading, the conversion to nitriles decreased as expected, but 3PN was still formed in 90% selectivity (Table 2.1, Entry 6).

Subsequently, the reaction was performed by slow addition of free HCN dissolved in dioxane *via* a syringe pump. Full conversion of butadiene to nitriles could be achieved at lower catalyst loading and the selectivity towards the linear products (3PN and 4PN) was still very high (Table 2.2, Entry 1). Traces (<2%) of the product isomers 2M2BN and 2PN were detected in case of full conversion of butadiene to nitriles (Table 2.2, Entry 1 and 2).

In order to gain detailed insight in the origin of the high selectivity towards 3PN, an additional hydrocyanation reaction under different HCN concentration was performed (Table 2.2, Entry 3). As anticipated from the results shown in Table 1, high HCN concentrations led to both low conversion and moderate selectivity. As mentioned above, the low conversion can most likely be attributed to the formation of catalytically inactive [Ni(CN)$_2$(**5**)] species. Indeed, direct addition of an excess of HCN deactivated the catalyst and only low selectivities towards 3PN were observed (Table 2.2, Entry 3). The formation of the dicyano complex was confirmed by isolation of red crystals from the reaction mixture of the experiment in Table 2.2, Entry 3. Unfortunately, the crystals were not suitable for X-ray analysis. However, the compound was characterized by IR spectroscopy as a Ni(dicyano) species (Figure 2.4).[6, 15]

Table 2.2. Butadiene hydrocyanation in dioxane with HCN dosation and direct addition.

Entry	Ratio S/Ni	Ratio (5)/Ni	Conversion (%)	2M3BN (%)	3PN (%)	Time (h)
1[a]	1:125	1	>99.0	2.4	93.3	5
2[a]	1:300	1	>99.0	25.6	73.3	5
3[b]	1:125	1	9.3	58.5	41.5	0.5

Conditions: 0.018 mmol Ni(cod)$_2$, excess HCN, T = 90℃, 2 mL dioxane. [a)]*Slow HCN dosation (excess) as dioxane solution (13μmol/min).* [b)]*Direct addition of excess HCN.*

2.5. Mechanistic explanation

These results indicate that two independent processes are responsible for the high linearity observed with this catalyst system: (i) the hydrocyanation of butadiene giving the usual mixture of branched (2M3BN) and linear (3PN) product, and (ii) the isomerization of 2M3BN towards 3PN (Scheme 2.3).[16] In fact, the selectivity towards
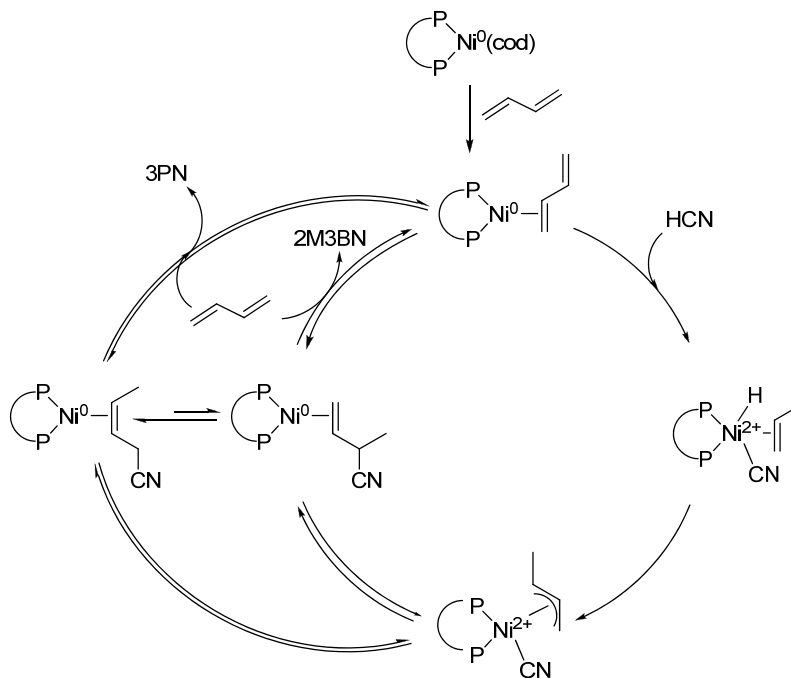
Scheme 2.4. Proposed cycle for the concurrent butadiene hydrocyanation and 2M3BN isomerization.

3PN is low in the presence of an excess of HCN (Table 2.2, Entry 3), which causes a high rate of catalyst degradation. On the other hand, the hydrocyanation of butadiene using ACH as HCN source showed a very high selectivity after 3 and 5 h, respectively, and only the conversion increases in time (Table 2.1, Entries 2 and 3). This means that [Ni(cod)(**5**)] must also be an efficient isomerization catalyst. Under conditions of HCN starvation (use of ACH or HCN dosation) the isomerization reaction plays a dominant role: 2M3BN undergoes oxidative addition to the Ni(0) species, leading to a high selectivity of 3PN after reductive elimination. On the other hand, with an excess or fast addition of HCN, oxidative addition of HCN dominates resulting in the hydrocyanation of butadiene and giving rise to the usual linear to branched mixture and ultimately deactivating the catalyst after complete conversion of butadiene.

2.6. Isomerization of 2M3BN towards 3PN

In order to test this hypothesis, the isomerization of 2M3BN towards 3PN in the absence of HCN was performed, using [Ni(cod)(**5**)] (Scheme 2.5). The formation of 3PN at different catalyst loadings was followed in time as depicted in Figure 2.5. The concentration of 3PN was measured *via* GC-analysis, taking samples of the reaction mixture every 10 minutes. The complex [Ni(cod)(**5**)] was able to isomerize 2M3BN to 3PN very efficiently, giving selectivities of up to 97% within 30 minutes, at a substrate to catalyst ratio of 100. A higher substrate to catalyst ratio led to a lower isomerization of the branched nitrile to the linear one. A conversion of up to 97% was obtained after 70 minutes with a substrate to catalyst ratio of 200 and the conversion was still 78% after 100 minutes with a ratio of 300.
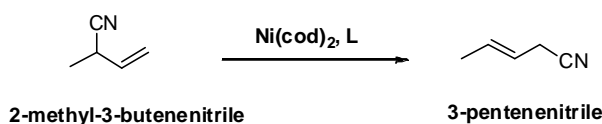
Scheme 2.5. Isomerization of 2-methyl-3-butenenitrile towards 3-pentenenitrile.
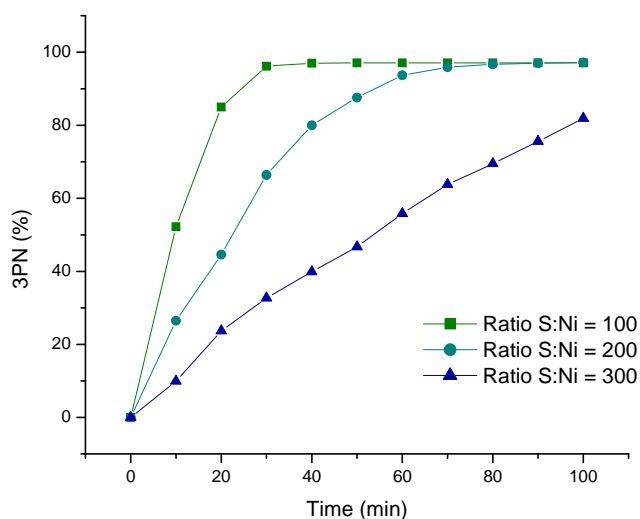
Figure 2.5. Isomerization of 2M3BN in dioxane. Conditions: 0.018 mmol Ni(cod)$_2$, 90℃, 2 mL dioxane.

2.7. Comparison with other ligands

The high regioselectivity of the [NiTript(PPh$_2$)$_2$] catalyst in butadiene hydrocyanation can be explained with the ability of the system to catalyze concurrently hydrocyanation and isomerization under low HCN concentration conditions. The polar solvent dioxane seems to facilitate this double activity. Other ligands were applied under identical conditions in the hydrocyanation and isomerization reactions with the aim to verify whether the high isomerization activity of [Ni(0)Tript(PPh$_2$)$_2$], which causes the high selectivity towards 3-pentenenitrile during the hydrocyanation process, is due to the reaction conditions or to the application of the new catalyst developed. For comparison three bidentate phosphite and phosphine ligands depicted in Figure 2.6 were chosen, which are typically applied in these reactions. The diphosphine Sixantphos (**8**), structurally closely related to the Tript(PPh$_2$)$_2$ ligand shows good activity in styrene hydrocyanation, due to the large bite angle.[6] The diphosphite (**9**) is, according to patent literature, one of the best performing ligands for hydrocyanation of butadiene and for the

65

Sixantphos (**8**)

[1,1]-Binaphthenyl-2,2'-bis
[di-(2-isopropylphenyl)-phosphite (**9**)
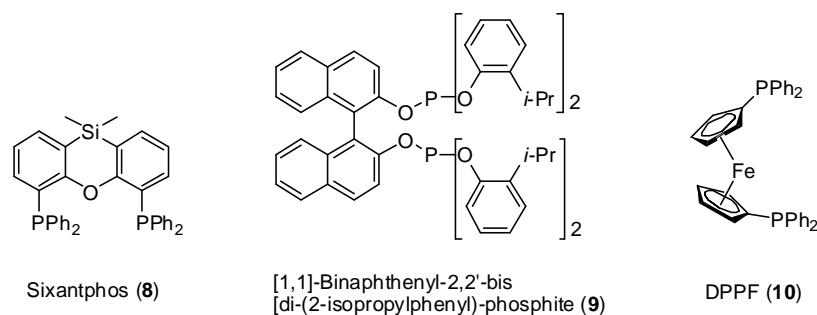
DPPF (**10**)

Figure 2.6. Diphosphite and diphosphine ligands applied in hydrocyanation and isomerization as comparison.

isomerization of 2M3BN[4]. DPPF (**10**) is reported in patent literature as well, to give high selectivity towards 3PN in the hydrocyanation of butadiene.[5]

In the hydrocyanation experiments, the Sixantphos (**8**)-based catalyst gave 62% conversion and very low selectivity of 28% towards 3PN (Table 2.3, Entry 1). The Diphosphite [Ni(**9**)] catalyst showed higher activity and selectivity to 3PN of respectively 78% and 63% (Table 2.3, Entry 2). Applying DPPF-based [Ni(**10**)] catalyst a conversion up to 80% was obtained, but the selectivity to 3PN was only 53% (Table 2.3, Entry 3). Under the same conditions the Tript(PPh$_2$)$_2$-based [Ni(**5**)] catalyst was performing with total conversion and 93% selectivity towards 3PN (Table 2.2, Entry 1).

The isomerization experiments are illustrated in Figure 2.7, in which the conversion of 3PN, determined by GC, is plotted as a function of time. The results obtained with the [Ni(**5**)] system are also reported for clarity; after only 30 minutes 97% of 3PN was obtained. Applying the [Ni(**10**)] catalyst 97% conversion of 2M3BN to 3PN was achieved after 70 minutes. After 100 minutes the conversions with catalyst [Ni(**8**)] and [Ni(**9**)] were still 73% and 32%, respectively.

Table 2.3. Hydrocyanation of butadiene in dioxane with HCN dosation using different ligands.

Entry	Ligand	Conversion (%)	3PN (%)	2M3BN (%)	Other nitriles
1	Sixantphos (**8**)	62.1	28	64.3	7.7
2	Diphosphite (**9**)	78.3	63.2	34.1	2.7
3	DPPF (**10**)	80.2	53.1	41.5	5.4

Conditions: 0.018 mmol Ni(cod)$_2$, Ni :L :S=1 :1 :100, 90℃, 2 ml dioxane.

Figure 2.7. Isomerization of 2M3BN with different ligands. Conditions: 0.018 mmol Ni(cod)$_2$, Ni :L :S=1 :1 :100, 90°C, 2 ml dioxane.

In general, these systems showed a lower activity in the isomerization of 2M3BN to 3PN and a lower selectivity in the hydrocyanation experiments (Table 2.3 and Figure 2.6), compared to the Tript(PPh$_2$)$_2$-based catalyst system.

2.8. Conclusions

An improved synthetic procedure for the preparation of a bidentate diphosphine based on a triptycene backbone was developed. The ligand was obtained in 4 synthetic steps with good yields.

The coordination behavior of this ligand towards Pt(II) and Ni(0) was investigated by ^{1}H, ^{13}C and ^{31}P NMR spectroscopy and the molecular structure of the complex [*cis*-PtCl$_2$(**5**)] was determined by X-ray crystal structure analysis.

The [Ni(cod)(**5**)] complex was applied in the hydrocyanation of butadiene, showing excellent selectivities of up to 98% towards the linear product 3PN. Low HCN concentrations achieved by controlled dosation guarantee both high conversion and high

selectivity, avoiding catalyst deactivation in this one-step procedure. A mechanistic explanation for this excellent catalytic result was proposed. The [NiTript(PPh$_2$)$_2$] catalyst also shows very high activity in the isomerization of 2M3BN to 3PN. The isomerization must be active during the hydrocyanation reaction. The hydrocyanation step determines the prevalent formation of 2M3BN, but concurrently the [NiTript(PPh$_2$)$_2$] catalyst isomerizes 2M3BN to 3PN, which is in the end the major product. Therefore, a low HCN concentration allows also the oxidative addition of 2M3BN to a Ni(0) species and consequently the formation of 3PN after isomerization, which is crucial to obtain high selectivity. Thus, this robust hydrocyanation catalyst system [NiTript(PPh$_2$)$_2$] with additional isomerization activity could be the key towards future process intensification developments.

2.9. Experimental Section

General considerations

Chemicals were purchased from Aldrich, Acros, or Merck and used as received. 1,4-dioxane and THF were distilled over CaH_2 prior to use. 1,3-Butadiene was dried over molecular sieves (4 Å) and stored at -30°C. 2M3BN was provided in high purity by Degussa and distilled prior to use. All preparations were carried out under argon atmosphere using standard Schlenk techniques. 1,8-Difluoroanthrachinone (**2**),[11] 1,8-difluoroanthracene (**3**),[12] Ni(cod)$_2$,[17] PtCl$_2$(cod),[18] and HCN[19] were synthesized according to literature procedures. NMR spectra were recorded on a Mercury 400 and a Varian Mercury 200 spectrometer (^{1}H, ^{13}C{^{1}H}, ^{31}P{^{1}H}, ^{19}F{^{1}H}). Elemental analyses were performed by Kolbe Mikroanalytisches Laboratorium, Mülheim an der Ruhr, Germany. IR spectra were recorded on an Avatar 360 FT-IR instrument in ATR mode.

Caution! HCN is a highly toxic, volatile liquid (bp 27°C) that is also susceptible to explosive polymerization in the presence of base catalysts. It should be handled only in a well-ventilated fume hood by teams of at least two technically qualified persons who have received appropriate medical training for treating HCN poisoning. Sensible precautions include having available proper first aid equipment as well as HCN monitors. Inhibitor-free HCN should be stored at a temperature lower than its melting point (- 13°C). Excess of HCN may be disposed by addition to aqueous sodium hypochlorite, which converts the cyanide to cyanate.

Synthesis of 1,8-difuorotriptycene (4)

1,8-Difluoroanthracene (18.69 mmol, 4.00 g) was suspended in dichloroethane (80 mL) and the mixture was heated to reflux. *N*-butylnitrite (21.5 mmol, 1.37 g) was added to the yellow solution, followed by anthranilic acid (121.3 mmol, 1.70 g) in 2-ethoxyethyl ether (13 mL). The latter was added dropwise over a period of 20-30 minutes. After half an hour the solvent was removed *in vacuo* from the dark red solution. A solution of maleic anhydride (9.1 mmol, 895 mg) in *p*-xylene (20 mL) was added and the mixture was refluxed for 1 hour. The same solution was cooled by means of an ice bath until precipitation of a brown solid occurred. After filtration, the solid was washed

with a cold solution of KOH in methanol/H_2O (4g in 33 / 17 mL). The crude material was purified by filtration through alumina and further recrystallization from hexane. Yield: 3.49 g (13.08 mmol, 70%). ^{19}F NMR (CDCl$_3$): δ -123.04 (s). ^1H NMR (CDCl$_3$): δ 7.50-7.40 (m, 2H), 7.20 (d, J = 7 Hz, 2H), 7.07-6.93 (m, 4H), 7.77 (td, J = 8.8 Hz, J = 1.2 Hz, 2H), 6.23 (s, 1H), 5.51 (t, J = 2 Hz, 1H). ^{13}C NMR (CDCl$_3$): δ 160.22, 155.31, 148.66, 145.17, 143.45, 126.82, 126.67, 125.57, 124.19, 123.92, 119.43, 113.07, 112.63, 53.68, 39.31. Anal. Calcd. for $C_{20}H_{12}F_2$: C, 82.8, H, 4.2. Found: C, 82.9, H, 4.2.

Synthesis of 1,8-diphenylphosphinotriptycene (5)

An excess of potassium (25.63 mmol, 1.00 g) was suspended in dioxane (20 mL) and ClPPh$_2$ (6.81 mmol, 1.5 g) was slowly added. The solution was heated to reflux for 2.5 h and cooled afterwards by means of an ice bath. The unreacted potassium was removed and a solution of **4** (2.64 mmol, 760 mg) in THF (5 mL) was added to the red solution. The reaction was left under reflux overnight. The mixture was then quenched with H_2O and extracted with CH_2Cl_2. The product was obtained pure by recrystallization from MeOH. Yield: 940 mg (1.51 mmol, 57.2%). ^1H NMR (CDCl$_3$): δ 7.34-7.18 (m, 22H), 6.87 (t, J = 7.4 Hz, 4H), 6.59-6.56 (m, 2H), 6.49-6.46 (m, 2H), 5.86 (d, J = 7.8 Hz, 1H), 5.40 (s, 1H). ^{13}C NMR (CDCl$_3$): δ 149.05 (t, J = 14.5), 145.55 (t, J = 3.1 Hz), 145.40, 143.46, 136.99 (t, J = 5.6 Hz), 136.51 (t, J = 5.4 Hz), 134.25 (td, J = 10.3, 2.8 Hz) 132.89 (t, J = 6.9 Hz), 129.03, 128.50, 128.42, 128.36, 128.30, 125.14, 124.67, 124.49 (d, J = 4.2 Hz), 123.90, 122.78. ^{31}P NMR (CDCl$_3$): δ -14.95. Anal. Calcd. for $C_{44}H_{32}P_2*C_4H_8O_2$: C, 81.1, H, 5.7. Found: C, 81.1, H, 5.6.

Synthesis of (5)PtCl$_2$ (6)

Pt(cod)Cl$_2$ (40 mg, 10.69 μmol) and **5** (70.65 mg, 11.36 μmol) in CH_2Cl_2 (8 mL) were stirred for 1h at room temperature. Crystals suitable for X-ray analysis were obtained by slow diffusion of Et$_2$O into the CH_2Cl_2 solution. Yield: 95 mg (7.88 μmol, 73.7%). ^1H NMR (CD$_2$Cl$_2$): δ 8.13 (bs, 4H), 7.62-7.38 (m, 18H), 7.05-6.68 (bs, 6H), 6.28 (bs, 2H), 5.68 (bs, 1H), 5.51 (s, 1H). ^{13}C NMR (CD$_2$Cl$_2$): δ 167.53, 150.36, 147.59, 141.84, 137.65, 136.67, 133.17, 133.13, 132.99, 132.46, 132.27, 131.45, 130.87, 130.13, 128.69, 128.54, 128.32, 128.07, 127.95, 127.84, 126.37, 126.38, 126.36, 125.41, 67.96,

53.78. ^{31}P NMR (CD$_2$Cl$_2$): δ 0.42 (s, with Pt-satellites, $^1J_{\text{Pt-P}}$= 3761 Hz). Anal. Calcd. for C$_{44}$H$_{32}$Cl$_2$P$_2$Pt: C, 59.5, H, 3.6. Found: C, 59.6, H, 3.8.

Synthesis of (5)Ni(cod) (7)

Ni(cod)$_2$ (5 mg, 0.018 mmol) and **5** (11.5 mg, 0.018 mmol) were dissolved in 1 mL of dioxane. The solution was stirred for 30 minutes and all volatiles removed under vacuum. The remaining red-brown powder was dissolved in deuterated benzene. ^{1}H NMR (C$_6$D$_6$): δ 8.23 (s, 1H), 7.94 (bs, 3H), 7.82-6.45 (m, 26H), 5.85-5.78 (m, 1H), 5.21 (s, 1H), 5.14 (bs, 2H), 4.67 (bs, 2H), 2.11-1.99 (m, 6H), 1.73 (s, 2H). ^{31}P NMR (C$_6$D$_6$): δ 25.31 (s).

Synthesis of (5)Ni(CN)$_2$ (8)

Red crystals were isolated from the catalytic reaction mixture (Table 2.2, Entry 3). Due to the fact that they were not suitable for X-ray analysis, the compound was analyzed *via* IR spectroscopy.[6, 15] IR (cm^{-1}) ṽ : 2169 (CN).

General procedure for the hydrocyanation experiments

A solution of ligand **5** (11.5 mg, 0.018 mmol) in 2 mL of solvent was added to Ni(cod)$_2$ (5.0 mg, 0.018 mmol). Cooled liquid butadiene (200 μL, 125 equiv.) was added by an Eppendorf pipette, followed by 50 μL of *n*-decane as internal standard. The solution was transferred into a 15 mL Schlenk tube equipped with a Teflon coated stirring bar.

Method A: Acetonecyanohydrine (250 μL, 150 equiv.) was added via Eppendorf pipette and the Schlenk tube was warmed up to 90°C in an oil bath. The mixture was stirred for 3-5 h.

Method B: An excess of HCN was added via Eppendorf pipette and the Schlenk tube was warmed to 90°C in an oil bath. The mixture was stirred for 5h.

Method C: A round-bottom Schlenk flask was filled with 1 mL of dioxane and an excess of HCN (13 μmol/min), which was taken up in a 5 mL syringe and was added to the reaction mixture by syringe pump during 3 h (closed system). The mixture was stirred for another 2 h. The reaction product was cooled to 0°C and flushed with a gentle stream of argon for 1 minute to remove traces of HCN. Samples were analyzed by GC, using

n-decane as internal standard. All the reactions were carried out in duplicate, showing variability for conversion and selectivity of ±2 % and ±1 %, respectively.

General procedure for the isomerization experiments

A solution of ligand **5** (11.5 mg, 0.018 mmol) in 2 mL of dioxane was added to Ni(cod)$_2$ (5.0 mg, 0.018 mmol) in a Schlenk tube and stirred for 5 minutes. 2M3BN (200 μL, 100 equiv.) was added with an Eppendorf pipette, followed by 50 μL of *n*-decane as internal standard. The Schlenk tube was placed in an oil bath at 90°C and samples for GC analysis were taken over time. The selectivity is defined as 3PN/(Σ nitriles).

X-ray Crystal Structure Determination of (6)

C$_{44}$H$_{32}$Cl$_2$P$_2$Pt·2(CH$_2$Cl$_2$), fw 1058.48 g/mol, colorless block, 0.30 x 0.30 x 0.18 mm^3, orthorhombic, C*mc*2$_1$ (no. 36), a = 16.14097(18) Å, b = 16.8563(3) Å, c = 15.2270(4) Å, V = 4142.93(14) Å^3, Z = 4, D$_x$ = 1.697 g/cm^3, μ = 3.885 mm^{-1}. 18 011 Reflections were measured on a Nonius Kappa CCD diffractometer with a rotating anode (graphite monochromator, λ = 0.71073 Å) at a temperature of 150 K. Data reduction was performed by the program EVALCCD.[20] An absorption correction based on multiple measured reflections was applied with the program SADABS[21] (T$_{min}$ = 0.28, T$_{max}$ = 0.51). 3802 Reflections were unique (R$_{int}$ = 0.0231) of which 3734 with I >2σ(I). The structure was solved with Direct Methods using the program SIR-97[22] and refined with SHELXL-97[23] against F^2 of all reflections. Non-hydrogen atoms were refined with anisotropic displacement parameters; carbon atoms C2-C4, C10-C12, C16-C20 and C22-C26 were restrained to an approximate isotropic behavior. All hydrogen atoms were calculated in idealized positions and refined with a riding model. 250 Parameters were refined with 103 restraints. R$_1$/wR$_2$ [I>2σ(I)] = 0.0268/0.0700; R$_1$/wR$_2$ [all refl.] = 0.0272/0.0702; S = 1.037. One of the two CH$_2$Cl$_2$ molecules of crystallization was found to be disordered over a mirror plane. Its contribution to the structure factors was taken into account with the SQUEEZE routine as implemented in the PLATON[24] program package. Residual electron density excursions between -4.118 (2.62 Å from H27B) and 1.128 e/Å^3 (0.83 Å from Pt1). Geometric calculations and checking for higher symmetry were also performed with the PLATON[24] program.

2.5 References and Notes

1. Huthmacher, K.; Krill, S. in *Applied Homogeneous Catalysis with Organometallic Compounds,* 2nd ed.; Cornils, B., Hermann, W. A., Eds.; Wiley-VCH: Weinheim, **2002**; Vol. 1 pp 465; (b) Tolman, C. A. *Chem. Rev.* **1977**, *77*, 313-348.

2. Tolman, C. A.; McKinney, R. J.; Seidel, W. C.; Druliner, J. D.; Stevens, W. R. *Adv. Catal.* **1985**, *33*, 1.

3. Tolman, C. A. *J. Chem. Educ.* **1986**, *3*, 199.

4. Foo, T.; Garner, J. M.; Tam, WO 99/06357, **1999**. *Chem. Abstr.* **1999***, 130*, 169815.

5. Fischer, J.; Siegel, W., DE 19733682 A1, **1999**. *Chem. Abstr.* **1999***, 130*, 169818.

6. Goertz, W.; Keim, W.; Vogt, D.; Englert, U.; Boele, M. D. K.; van de Veen, L. A.; Kamer, P. C. J.; van Leeuwen, P. W. N. M. *J. Chem. Soc., Dalton Trans.,* **1998**, 2981.

7. Ahlers, W.; Roeper, M.l; Hofmann, P.; Warth, D. C. M.; Paciello, R., CA 02399431, **2001**. *Chem. Abstr.* 2001*, 130*, 169815.

8. Ahlers, W.; Paciello, R.; Vogt, D.; Hofmann, P., WO02/083695, **2002**. *Chem. Abstr.* **2002***, 137*, 311033.

9. (a) Grossman, O.; Azerraf, C.; Gelman, D. *Organometallics* **2006**, *25*, 375.(b) Azerraf, C.; Cohen, S.; Gelman, D. *Inorg. Chem.*, **2006**, *45*, 7010; (c) Azerraf, C.; Grossman, O.; Gelman, D. *J. Organomet. Chem.* **2007**, *692*, 761.

10. Echegoyen, L.; Hafez, Y. ; Lawson, R. C.; de Mendoza, J. ; Tores, T. *J. Org. Chem.* **1993**, *58*, 2009.

11. House, H. O.; Ghali, N. I.; Haack, J. L.; VanDerveer, D. *J. Org. Chem.* **1980**, *45*, 1807.

12. (a) Baker, M. J.; Harrison, K. N.; Orpen, A. G.; Pringle, P. G. *J. Chem. Soc., Chem. Comm.* **1991**, 803; (b) Baker, M. J.; Pringle, P. G., *J. Chem. Soc., Chem. Comm,* **1991**, 1292; (c) Rajanbabu, T. V.; Casalnuovo, A. L. *J. Am. Chem. Soc,* **1996**, *118, 6325.

13. (a) Ogura, S.; Soumai, M., US 4556461, **1983**. *Chem. Abstr.,***1983***, 99*, 176431; (b) *Handbook of Chemistry and Physics, 80th edition*, David R. Lide Ed., CRC Press, **1999-2000**.

14. Casalnuovo, A. L.; RajanBabu, T. V.; Ayers, T. A.; Warren, T. H. *J. Am. Chem. Soc,* **1994**, *116, 9869.

15. Nakamoto, K., Infrared and raman spectra of inorganic and coordination compounds, Wiley, 3rd Edition, 1978.

16. (a) Chaumonnot, A.; Lamy, F.; Sabo-Etienne, S.; Donnadieu, B.; Chaudret, B.; Barthelat, J. C. and Galland, J. C. *Organometallics* **2004**, *23* (14), 3363; (b) van der Vlugt, J. I.; Hewat, A. C.; Neto, S.; Sablong, R.; Mills, A. M.; Lutz, M.; Spek, A. L.; Müller, C.; Vogt, D. *Adv. Synth. Catal.* **2004**, *346*, 993; (c) Wilting, J.; Müller, C.; Hewat, A. C.; Ellis, D. D.; Tooke, D. M.; Spek, A. L.; Vogt, D. *Organometallics* **2005**, *24*, 13; (d) Acosta-Ramirez, A.; Muñoz-Hernandez, M.; Jones, W. D.; Garcia, J. J. *J. Organomet. Chem.* **2006**, *691*, 3895; (e) Acosta-Ramirez, A.; Flores-Gaspar, A.; Muñoz-Hernandez, M.; Arevalo, A.; Jones, W. D.; Garcia, J. J. *Organometallics* **2007**, *26*, 1712; (f) Swartz,

B. D.; Reinartz, N. M.; Brennessel, W. W.; Garcia J. J., Jones, W. D. *J. Am. Chem.Soc.* **2008**, *130,* 8548.

17. Schunn, R. A. *Inorg. Synth.* **1974**, *15*, 5.

18. Clark, H. C.; Manzer, L. E. *J. Organometal. Chem.* **1973**, *59*, 411.

19. Slotta, K. H. *Ber. Dtsch. Chem. Ges.*, **1934**, *67B*, 1028.

20. Duisenberg, A. J. M.; Kroon-Batenburg, L. M. J.; Schreurs, A. M. M. *J. Appl. Crystallogr.* **2003**, *36*, 220-229.

21. Sheldrick, G. M. SADABS. Program for data scaling and absorption correction; University of Göttingen: Germany, 2002.

22. Altomare, A.; Burla, M. C.; Camalli, M.; Cascarano, G. L.; Giacovazzo, C.; Guagliardi, A.; Moliterni, A. G. G.; Polidori, G.; Spagna, R. *J. Appl. Crystallogr.* **1999**, *32*, 115.

23. Sheldrick, G. M. SHELXL-97. Program for crystal structure refinement; University of Göttingen: Germany, 1997.

24. Speck, A. L. *J. Appl. Crystallogr.* **2003**, *36*, 7.

Chapter 3

Nickel-Catalyzed Isomerization of 2-Methyl-3-Butenenitrile to 3-Pentenenitrile. A Kinetic Study Using *in situ* FTIR-ATR Spectroscopy

The isomerization of 2-methyl-3-butenenitrile to 3-pentenenitrile was followed using in situ FTIR spectroscopy. The spectrum was analyzed comprehensively to obtain kinetic profiles from the different band dynamics. Calculated spectra of the substrate and the products support the peak assignment. An average profile was calculated applying a quasi-multivariate analysis technique.
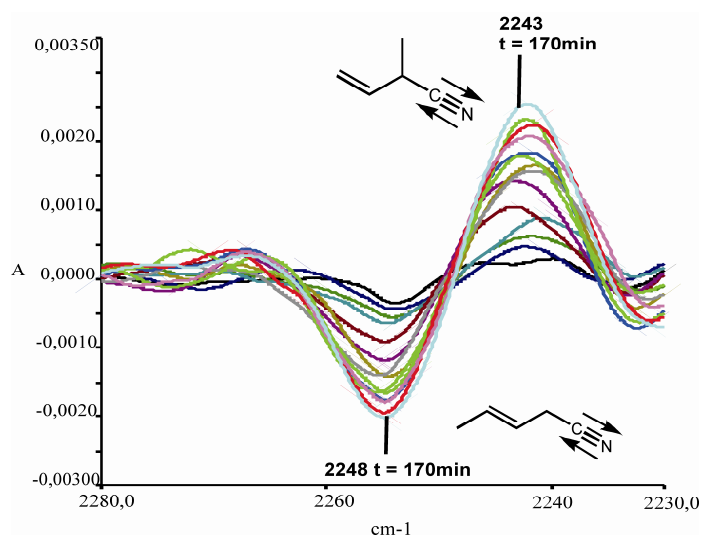
3.1. Introduction

The DuPont adiponitrile process is so far the only example of an industrial application of the Ni-catalyzed alkene hydrocyanation.[1] Adiponitrile (AdN) is produced from butadiene *via* hydrocyanation and isomerization reactions. The addition of HCN to butadiene leads to both the desirable linear isomer 3-pentenenitrile (3PN) and the undesirable branched isomer 2-methyl-3-butenenitrile (2M3BN) in a variable ratio.[1] In the second step of the process, 2M3BN is isomerized to 3PN in the presence of the same nickel catalyst used for the hydrocyanation, through a C-CN bond breaking/forming reaction involving a [Ni(II)allyl(cyanide)] complex (Scheme 3.1).[2]

In the hydrocyanation reaction, the Ni(II) intermediate is formed *via* HCN addition to the metal complex. As one of the first steps in the catalytic cycle of the isomerization, the Ni(0) species is oxidized to Ni(II) upon 2M3BN addition. The reductive elimination of nitriles that is believed to be the rate-determining step in catalytic hydrocyanation reactions takes place as last step of the cycle in both processes (see Chapter 2, Scheme 1.2). The two reactions are closely related. However, in the presence of HCN excess, the Ni-catalyst is rapidly deactivated, due to the formation of [Ni(CN)$_2$L$_n$] species.[3] On the other hand, during the Ni-catalyzed isomerization of 2M3BN (Scheme 4.1) HCN is not
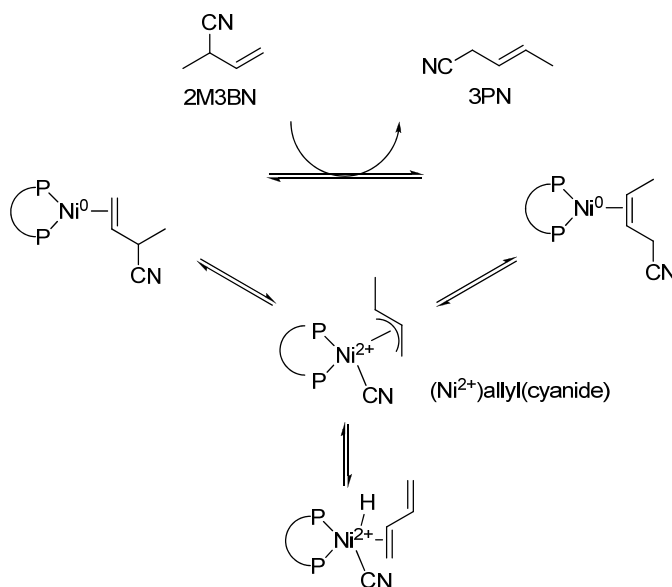
Scheme 3.1. Isomerization of 2M3BN.

present.[4] Therefore, the isomerization can be considered as a model reaction for *in situ* studies of the mechanism and the kinetics of the rate-limiting step in the hydrocyanation.

The first challenge is to find a suitable technique for the *in situ* experiments. So far, the investigations have been limited to a few papers reporting on the characterization of the isomerization reaction intermediates by NMR spectroscopy, using phosphine ligands.[5] In combination with $Ni(cod)_2$, all classes of bidentate phosphorus ligands, such as phosphines, phosphinites, phosphonites, and phosphites catalyze the isomerization.[6] The influence of the ligand parameters on the catalyst activity for this reaction still remains unknown. However, *in situ* NMR studies of this reaction are difficult. In fact, the tetrahedral coordination geometry of the Ni(II) intermediates causes the presence of paramagnetic species.[7]

Tolman[8] and Druliner[9] have already reported on the characterization of Ni complexes by IR spectroscopy. In their work, the interaction of zero-valent nickel phosphite complexes with various independent components of the catalytic system, such as HCN and different olefins, has been investigated aiming for a better understanding of the mechanism. In this study the isomerization of 2M3BN was performed and for the first time the reaction was followed by *operando* FTIR spectroscopy. A kinetic profile was obtained by analyzing the dynamics of the peaks in the IR spectra. DFT calculations were used to confirm the peak assignment.

3.2. *In situ* FTIR-ATR spectroscopy applied to the analysis of the 2M3BN isomerization reaction

An FTIR-ATR (Fourier Transform Infrared in Attenuated Total Reflection mode) spectroscopic technique[10] was used to monitor in real time the isomerization of 2M3BN. Using FTIR spectroscopy the detection would not be negatively influenced by the presence of paramagnetic species. The reaction was performed in dioxane at 60°C for 4 hours using a triptycene-based diphosphine ligand[11] (Scheme 3.1 and Figure 3.1) and $Ni(cod)_2$ as the metal precursor. An IR spectrum was recorded every 10 minutes using a

diamond ATR probe connected to an FTIR instrument with a flexible light guide or deep immersion probe (Scheme 3.2).

The IR beam that exits the Michelson interferometer is converged by a hollow mirror and directed into a flexible light guide. The light guide is coupled to a stainless steel deep immersion probe equipped with a diamond ATR crystal. The sample solution in the Schlenk flask is in intimate contact with the ATR crystal. Due to the cone-like crystal geometry and high refractive index, the IR beam double reflects from the internal surfaces of the crystal and creates an evanescent wave, which projects orthogonally into the sample solution (Scheme 3.2, ATR effect). Some of the energy of this beam is absorbed by the sample and the reflected radiation is returned to the detector *via* a second light guide also coupled to the probe.

However, the choice of this analytical method presented some drawbacks. The light transmission efficiency of this set-up is less than 20% and consequently the sensitivity was relatively low. High concentrated samples and long collection times (up to 7 min.) were required, implying that fast reactions cannot be monitored with this specific setup.
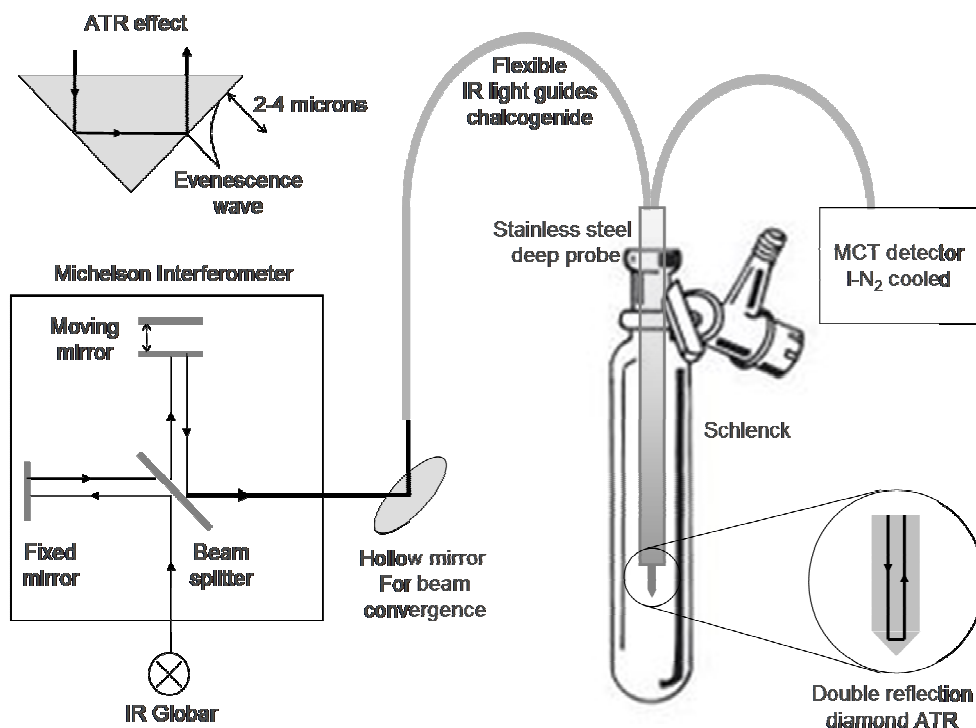
Scheme 3.2. Schematic representation of the FTIR-ATR setup.
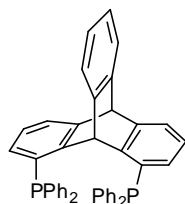
Figure 3.1. Triptycene-based phosphine ligand

The experiment was also performed using a ZnSe ATR probe. The diamond crystal shows absorbance in the region 2200-1900 cm^{-1}, which is also the typical region for the peaks of the nitrile group. To avoid a high noise to peak ratio the ZnSe crystal would be a better choice. Unfortunately, the nitriles in the reaction mixture can coordinate to the Zn on the crystal surface, resulting in broadening of the peaks in the IR spectra. Moreover, the coordinated species are not reacting further, creating an artefact in the detected spectrum.

3.3. IR spectra: interpretation and kinetic profiles

3.3.1. In situ or operando technique

True fundamental understanding of the structure-activity/selectivity relationship requires molecular level characterization of catalytic species under realistic catalytic operation conditions. The molecular characterization is generally obtained *via in situ* spectroscopy. *Operando* spectroscopic methodology was just recently introduced into the catalysis literature to express a methodology that combines simultaneously *in situ* spectroscopy and kinetic measurements on the same sample. *Operando* is borrowed from Latin, which means "working" or "operating" since the recorded spectra are obtained from an "operating" catalytic system.[12] Applying an *operando* spectroscopic technique, different regions in the spectra recorded during the 2M3BN isomerization were analyzed.

3.3.2. The nitrile region

In the isomerization reaction, the branched nitrile alkene 2M3BN is converted *via* C-CN bond cleavage to the linear nitrile alkene, 3PN (Scheme 3.1). Therefore, the nitrile bands are most characteristic for this reaction. The vibration involved is the stretching of the triple bond, which occurs at 2260-2240 cm^{-1} in aliphatic nitriles[13] (Figure 3.2). Since this region of the spectrum is relatively free of other signals, even weak bands can be distinctive and reliable.
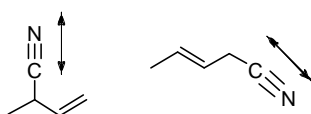
Figure 3.2. The triple bond stretching for 2M3BN and 3PN.

The isomerization reaction was monitored for 4 hours, recording a spectrum every 10 minutes. The overlaying of the spectra showed no further dynamics of the bands after 170 minutes. Consequently, the reaction was complete after the first 3 hours and only these spectra will be discussed. The band at 2243 cm^{-1} is assigned to the nitrile stretch vibration of 2M3BN. This band showed a decrease in intensity and peak broadening, while the formation of 3PN was confirmed by the appearance of a nitrile absorption at 2248 cm^{-1}. The two bands are not well resolved (Figure 3.3).

Therefore, second derivative spectroscopy was applied for the interpretation of these spectra. This technique consists in recording the second derivative of the spectrum with respect to the wavelength (or frequency).[14] According to Beer's law, the second derivative of the absorbance spectrum is linear in concentration:

$$A(\nu) = \ln(\frac{I}{I_0}) = [C]l\alpha(\nu) \tag{1}$$

$$\frac{d^2A}{d\nu^2} = l[C]\frac{d^2\alpha}{d\nu} \tag{2}$$

A = absorbance

ν = frequency

I = intensity

[C] = concentration

l = path length

α = absorption coefficient

After recording an infrared spectrum, the second derivative is easily derived by numerical differentiation. In the second derivative spectra well-resolved peaks are observed, which can be associated to the formation of 3PN and the consumption of 2M3BN (Figure 3.3). Furthermore, a total conversion of 87% in this experiment was determined after 4 h by GC-analysis. The dynamics in the spectra were calculated by integration methods and normalized to the final conversion. Nitrile isomers, other than 2M3BN and 3PN, were detected only in traces. A kinetic profile for the formation of 3PN was obtained,[15] as shown in Figure 3.4. It must be mentioned that the use of a deep immersion probe does not allow a fast temperature change. In other words, the probe needs a slow equilibration to have the best detection conditions. Therefore, the temperature was slowly increased from room temperature to 60°C over 20 minutes. During this period, the reaction does not lead to 3PN formation.
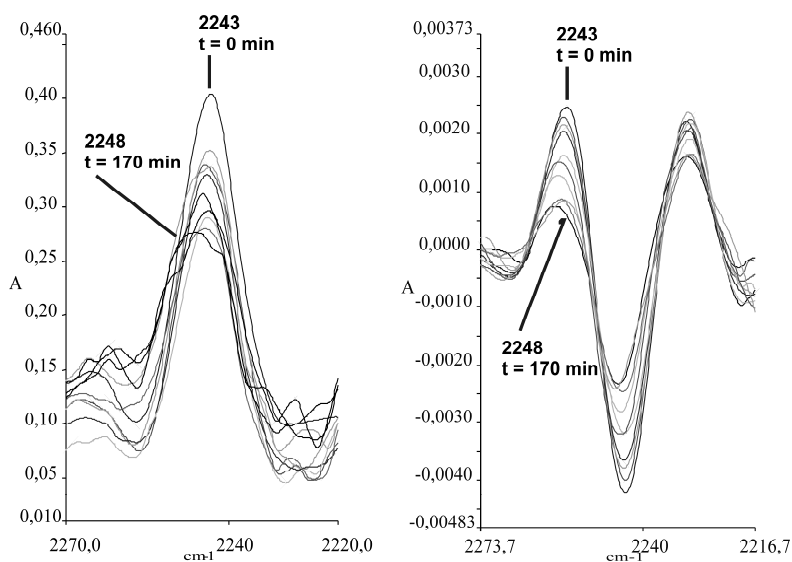
Figure 3.3. Absorbance spectra (left) and 2nd derivative spectra (right) of the -CN region.
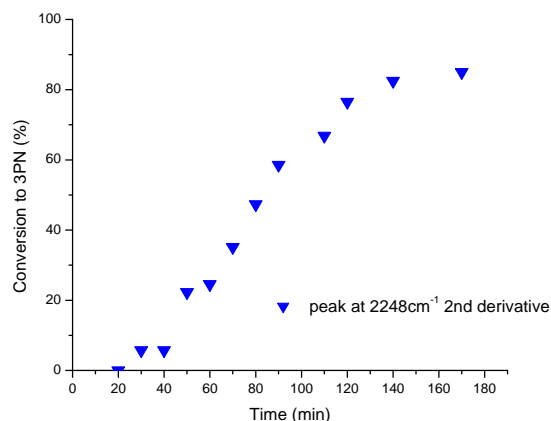
Figure 3.4. Kinetic profile obtained from the CN band of 3PN at 2248 cm^{-1}.
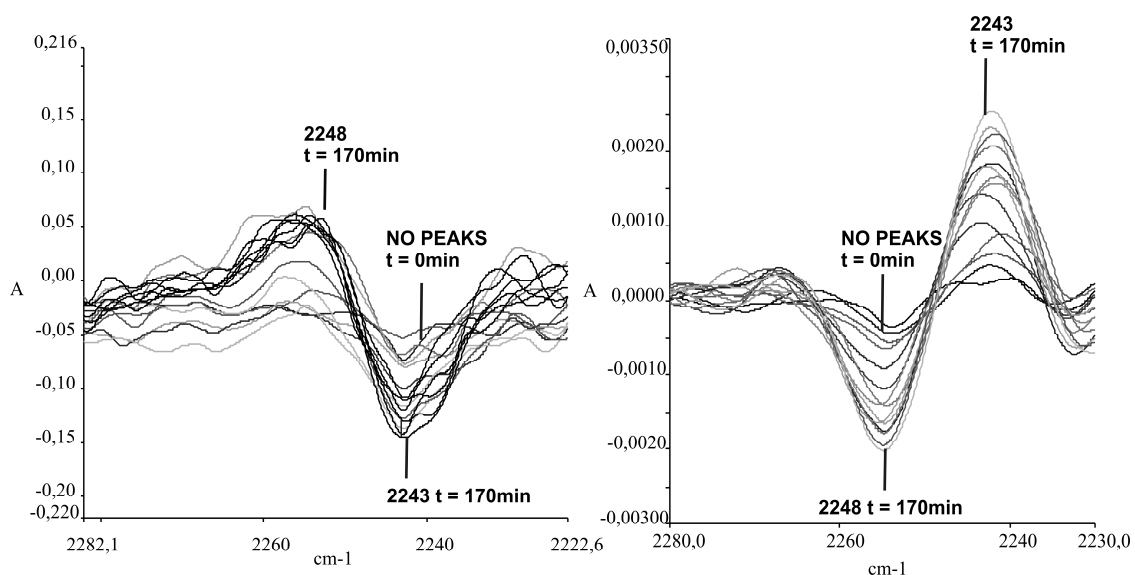
Figure 3.5. Absorbance spectra (left) and 2nd derivative spectra (right) of the -CN region after subtraction of the spectrum recorded at the initial time (only 2M3BN).

The initial IR spectrum recorded at the start of the reaction, when only 2M3BN is present in the reaction mixture, was taken as background spectrum and subtracted from the spectra recorded during the isomerization experiment (Figure 3.5). Consequently, the initial difference spectrum does not show any bands in the nitrile region. The following difference spectra show the formation of a new band at 2248 cm^{-1} related to 3PN and a

negative band at 2243 cm^{-1} related to the consumption of 2M3BN. The 2nd derivative was again calculated in order to reduce the peak to noise ratio.

3.3.3. The C-H deformation band region

Stretching and deformation vibrations characterize methyl and methylene groups. In aliphatic compounds, the asymmetric out-of-phase -CH_3 deformation (Figure 3.6) occurs near 1465 cm^{-1}, although the methyl wave numbers show some sensitivity to the electronegativity of the attached atoms.[16] The -CH_2- deformation bands (Figure 3.6),[17] which are located near 1463 cm^{-1} in alkenes, is lowered to about 1440 cm^{-1} when the -CH_2- group is next to a double or a triple bond. A carbonyl, nitrile, or nitro group each lowers the frequency of the adjacent -CH_2- group to about 1425 cm^{-1} and increases its intensity.[18] The –CH- deformation absorbs weakly at 1350-1315 cm^{-1}.[19]

The C-H deformation band region was analyzed in the dynamic IR spectra of the isomerization. A band originating from the solvent was present at 1365 cm^{-1} (dioxane C-H twisting band)[20] and used to normalize the IR spectra. The other bands clearly showed dynamic transformations, although there is extensive overlapping of the peaks. The peak intensities of the bands at 1478 and 1434 cm^{-1} evolve during the reaction. The two bands are assigned respectively to the methyl and the methylene group C-H deformation of 3PN (Figure 3.7).

The second derivative allowed again having a clearer pattern for the peak intensity, especially for the band at 1478 cm^{-1}. The kinetic profiles obtained for these dynamics were similar to the one for the nitrile group (Figure 3.8).
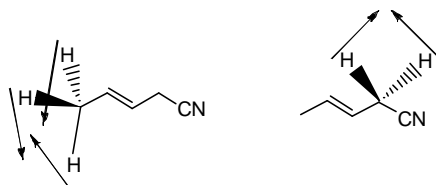
Figure 3.6. The methyl and the methylene C-H deformation for 3PN.
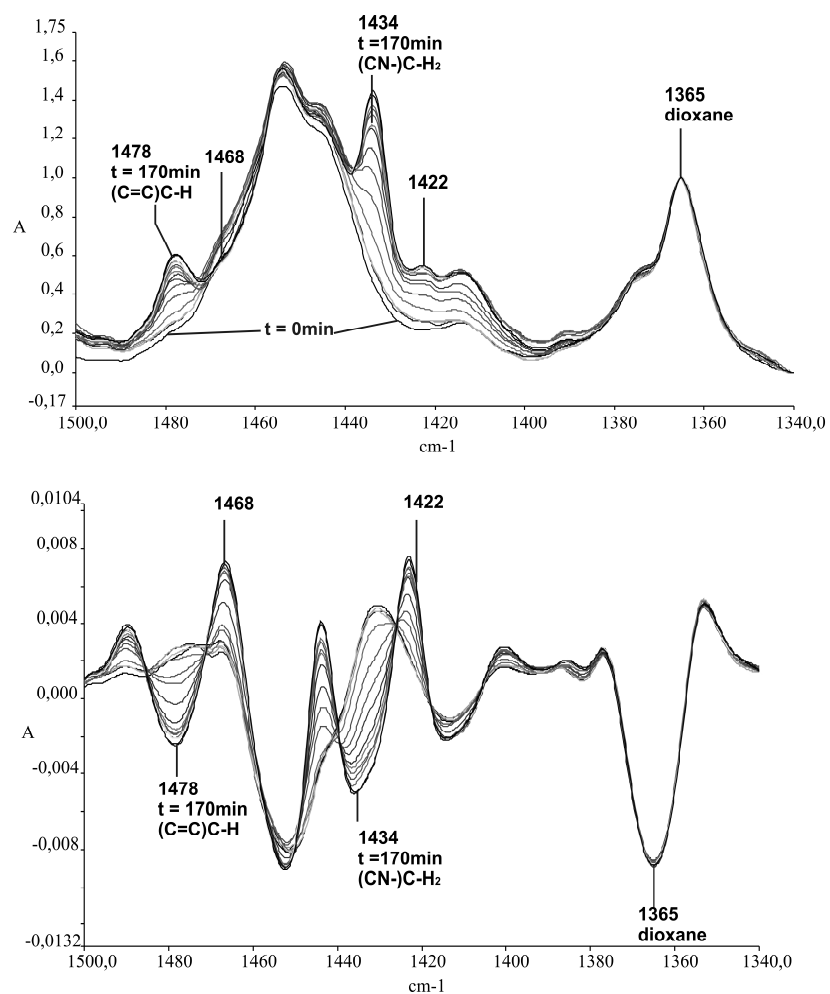
Figure 3.7. Absorbance spectra (upper) and 2nd derivative spectra (lower) for the C-H band region.
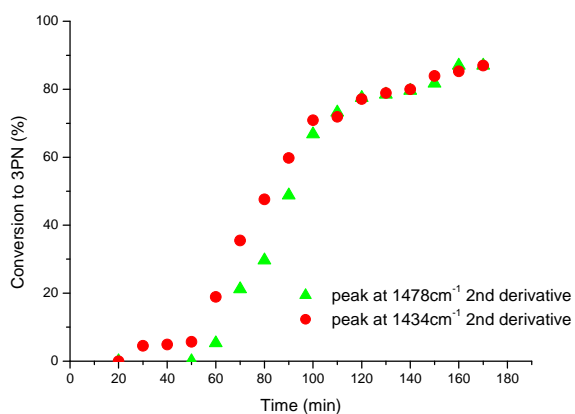
Figure 3.8. Kinetic profile obtained from the -CH_3 and -CH_2- deformation bands of 3PN at 1478 cm^{-1} and 1434 cm^{-1}, respectively.

3.3.4. The (C=)C-H stretching band region

Olefinic =CH- stretching occurs at 3130-2980 cm^{-1}. In particular, the out-of-phase =CH$_2$ stretch vibrations of vinyl compounds (Figure 3.10.) (monosubstituted ethylenes) give rise to a band in the region 3100-3070 cm^{-1} in hydrocarbons.[21] This band is well separated from other =CH- stretching bands below 3000 cm^{-1}.

2M3BN contains a vinyl group. Therefore, also the (C=)C-H stretch band region was taken into consideration. The peak intensity at 3055 cm^{-1} decreases during the reaction. The 2nd derivative of the spectra allows an improved calculation of the kinetic profile (Figure 3.12). The calculation was made considering the 2M3BN consumption during the
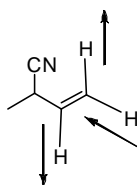
Figure 3.10. The (C=)C-H stretching for 2M3BN.
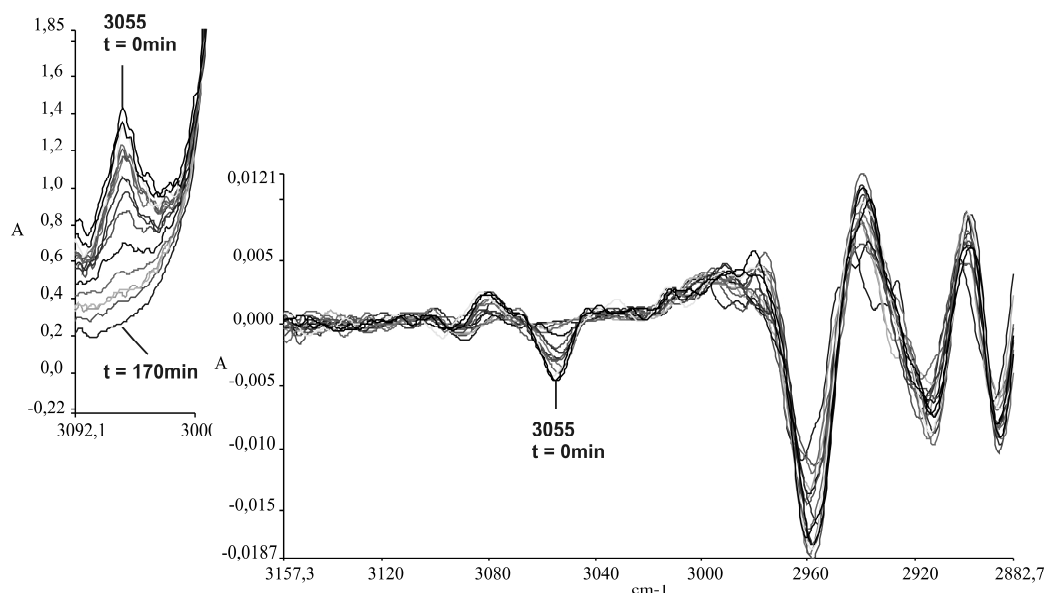
Figure 3.11. Absorbance spectra (left) and 2nd derivative spectra (right) for the (C=)C-H stretching band.

85
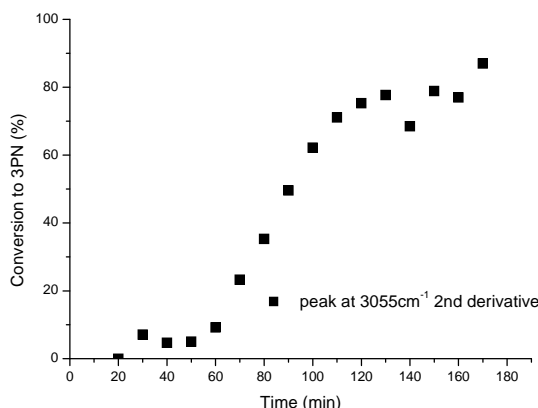
Figure 3.12. Kinetic profile obtained from the $=CH_2$ stretching band at 3055 cm^{-1}, relative to 2M3BN consumption. The conversion is calculated as 3PN(%) = 100 − 2M3BN(%).

formation of 3PN: 3PN(%) = 100 − 2M3BN(%). The obtained graph shows a kinetic curve similar to the three previous ones, calculated from the nitrile, methyl and methylene 3PN bands.

3.4. DFT calculations and peak assignment

The simplest description of a vibration is a harmonic oscillator. Applying this concept, it is possible to use computational methods to gain insights into the vibrational motion of molecules. There are a number of computational methods available with varying degrees of accuracy.[23] Frequencies computed with a quantum harmonic oscillator approximation tend to be 10% higher than the experimental value, due to the approximation itself and the lack of electron correlation. Most studies are done using *ab initio* methods. The overall systematic error is less with DFT calculations.[24]

Another related issue is the computation of the intensities of the peaks in the spectrum. Peak intensities depend on the probability that a particular wavelength photon will be absorbed and are obtained by computing the transition dipole moments as relative peak intensities, since the calculation does not include the density of the substance.

CN
iso = 2M3BN

CN
cis = *cis*-3PN

CN
trans = *trans*-3PN
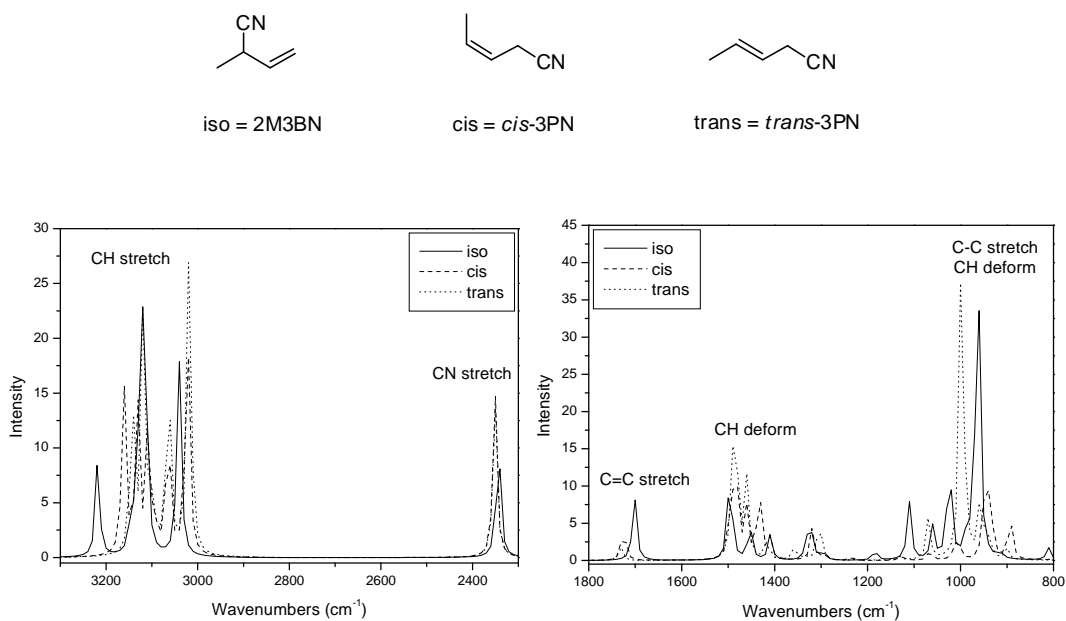
Figure 3.13. Overlaid spectra of 2M3BN, *cis*- and *trans*-3PN. The spectra are obtained from DFT calculations.

The DFT calculations were used to confirm the peak assignment in the spectra obtained from the reaction mixture and to study the formation of *trans*- and *cis*-3PN separately. Calculations for 2M3BN, as well as for *trans*- and *cis*-3PN were performed and the spectra were superimposed as shown in Figure 3.13. The frequency values showed a shift to higher wave numbers compared to the experimental results, but the general trend is confirmed. The nitrile bands for the products (*trans*- and *cis*-3PN) have higher wave numbers than the band for the substrate (2M3BN). The C-H deformation bands are in a very narrow spectral region and not completely resolved. The same overlapping is observed in the C-H stretching region, except for the vinyl (C=)C-H band. Unfortunately, isolated peaks of *cis*- or *trans*-3PN were identified only in the finger print region (900-1000 cm^{-1}). The IR light guide used during the experiment, limited the spectral range in the low wave number region giving very low signal to noise ratio. Consequently, the formation of these two products could not be investigated separately.

Figure 3.14 and 3.15 show the spectra of 3PN and 2M3BN and, in particular, the vibrations identified in the experimental spectra. The methyl and methylene groups were

detected at 1478 and 1434 cm^{-1}, respectively and the calculations showed that these vibrations occur at 1490 and 1461 cm^{-1}. For the vinyl C-H stretching band, a shift was observed from 3055 cm^{-1} in the experimental to 3218 cm^{-1} in the calculated spectrum. The shift increases at higher wave numbers, because the error in the calculations becomes bigger for larger motions of the harmonic oscillator. However, the peak positions maintain the same trend. It can be concluded that DFT calculations confirm the peak identification that we proposed for the experimental spectra.
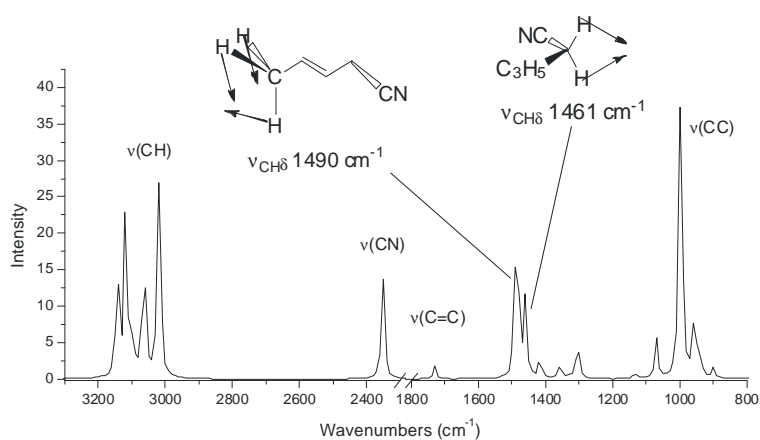
Figure 3.14. DFT calculation of the 3PN IR spectrum, assignment of the deformation bands for the methyl and methylene groups.
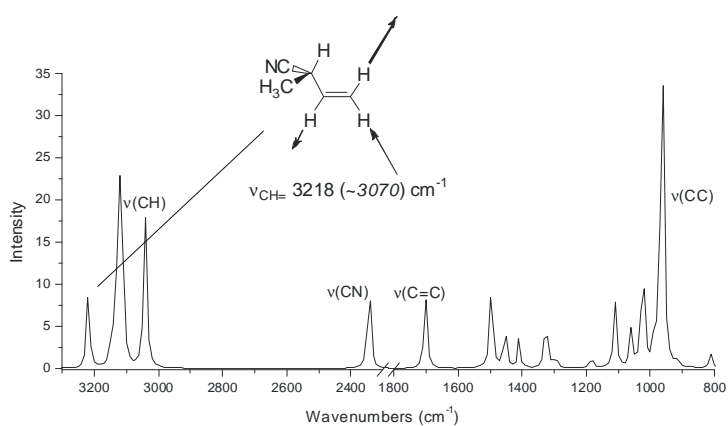
Figure 3.15. DFT calculation of the 2M3BN IR spectrum, assignment of the stretching band for the vinyl group.

3.5. "*Quasi*-multivariate" analysis

The profiles calculated from the different IR bands presented similar dynamics, but show also a considerable error range (Figure 3.16). This error is due to the low peak to noise ratio in the IR spectra recorded during the isomerization experiment. There are two main reasons for the low peak to noise ratio. The low light transmission through the ATR probe has a negative effect on the noise level of the whole spectrum. On the other hand, low signal to noise ratio was detected mainly in the high frequency range (>1500 cm^{-1}). The path length through the reaction mixture and subsequently the absorbance (peak intensity) are inversely related to the frequency. In other words, the depth of penetration (d_p) is directly related to the wave length (λ), as it is shown in the formula below:

$$ d_p = \frac{\lambda}{2\pi n_1 \sqrt{\sin^2\theta - \left(\dfrac{n_2}{n_1}\right)}} \tag{1} $$

d_p = depth of penetration

λ = wave length

$\theta = 45°$ angle of penetration

n_1 = refractive index of the crystal

n_2 = refractive index of the solvent (dioxane)

Furthermore, a systematic error was introduced *via* the integration method that involves the arbitrary choice of the base line points and the peak maxima.

Due to such complexity of the samples, more sophisticated methods of data analysis are now being used, such as the multivariate analysis technique[25]. As the name indicates, multivariate analysis comprises a set of techniques dedicated to the analysis of data sets with more than one variable. In the IR spectra each frequency can be regarded as one variable. Several of these techniques were developed in the last twenty years, because they require the computational capabilities of modern computers.
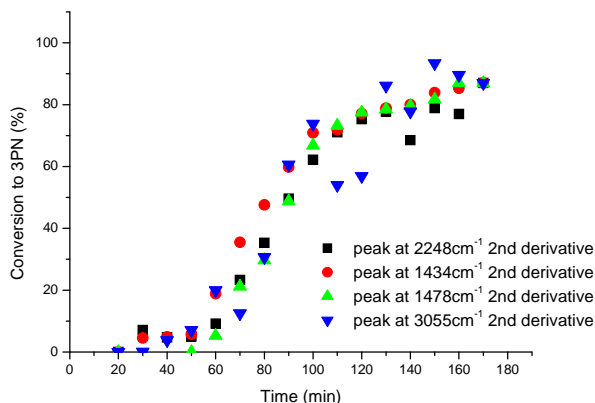
Figure 3.16. Kinetic profiles obtained from the -CN stretching, the -CH$_3$ and -CH$_2$- deformation and the =CH$_2$ stretching bands, for the formation of 3PN and the consumption of 2M3BN.
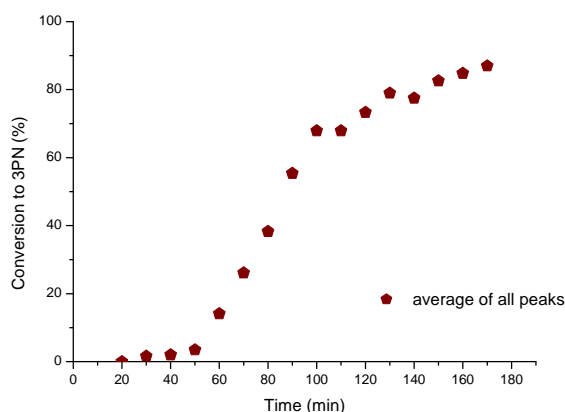
Figure 3.17. Kinetic profile obtained as average of the four kinetic profiles of different IR bands.

A "*quasi*-multivariate" (QMV) analysis was applied to the spectra recorded for the isomerization of 2M3BN. Each band dynamic in the spectra was considered as a different variable and an average kinetic profile was calculated (Figure 3.17). The profile was obtained by averaging the conversions for each recording time. The aim was to minimize the error in the average profile compared to the single band dynamic one. This method is an easy approach to make use of the correlation between different band dynamics, in order to increase the accuracy of the kinetic profile. In fact, the formation of 3PN and the

consumption of 2M3BN are taken into consideration simultaneously, being directly correlated in the reaction and, consequently, showing the same kinetics.

3.6. Multivariate analysis

The IR data were further analyzed by chemometrics, which is the application of mathematical or statistical methods to chemical data. The method used was the multivariate curve resolution (MCR).[25b] With this method the spectrum of a multicomponent system, D, is considered as the sum of individual spectra of its components:

$$D = \sum_{k=1}^{p} S_k C_k \tag{1}$$

where p is the number of components that contribute to the observed spectral intensities in D. S_k and C_k is the spectrum of component k and its concentration, respectively. The entire spectroscopic data set of n spectra can be expressed in a matrix, D, of dimension m by n, namely:

$$D_{ij} = \sum_{k=1}^{p} S_{ik} C_{kj} \text{ for } i = 1, 2, \ldots, m \text{ and } j = 1, 2, \ldots, n \tag{2}$$

The objective of the analysis is to solve the above equation for S and C. There may be other factors representing the spectral baseline and other fixed pattern errors from the measurement of the spectra. Therefore, the observed data matrix, D, can be approximated by the matrix product S and C with the first q components and a residue matrix, E, representing experimental errors:

$$D_{m \times n} = S_{m \times q} C_{q \times n} + E_{m \times n} \tag{3}$$

Alternating least squares regression methods are used to refine the C and S matrices to real spectra and concentration profiles of pure chemical species. This is an iterative process by minimizing the residue matrix, E, while applying some physically meaningful constraints such as a maximum amount of components.
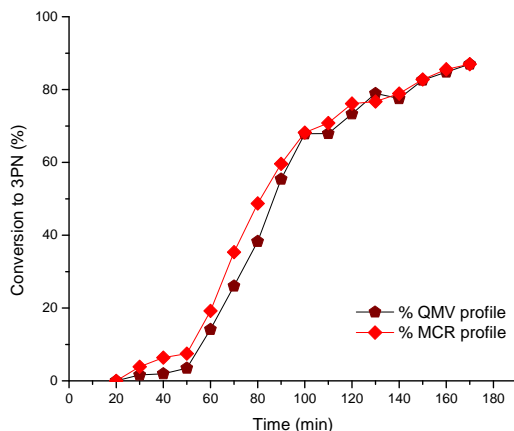
Figure 3.18. Superimposed QMV and MCR kinetic profiles.

The –CH- deformation region of the IR spectra was chosen for the multivariate analysis. In fact, this region presents a lower peak to noise ratio, leading to a lower residue matrix and consequently more accurate chemometric calculation. The kinetic profile calculated from the multivariate analysis is depicted below (Figure 3.18). The profile obtained *via* a *quasi*-multivariate analysis is superimposed in Figure 3.18. The two profiles show a very good agreement, which validates the results obtained with the first more accessible method for analyzing the data (QMV).

Due to the limitations of the setup, a series of experiments carried out at different concentrations and temperatures could not be performed, in order to analyze the kinetics of the reaction. However, the profile for the isomerization of 2M3BN at 60°C and in the presence of the [NiTripty(PPh$_2$)$_2$] catalyst suggests zero-order for the 2M3BN consumption and the 3PN formation.[5b] The first 3% of conversion are neglected, since the temperature of the reaction mixture needed to be equilibrated slowly. The last 20% of conversion are also not taken into account because of catalyst deactivation. The profiles obtained with the QMV and the MCR methods both show a good linear fitting, while a logarithmic fitting, which would indicate a first order, does not apply (Figure 3.19).
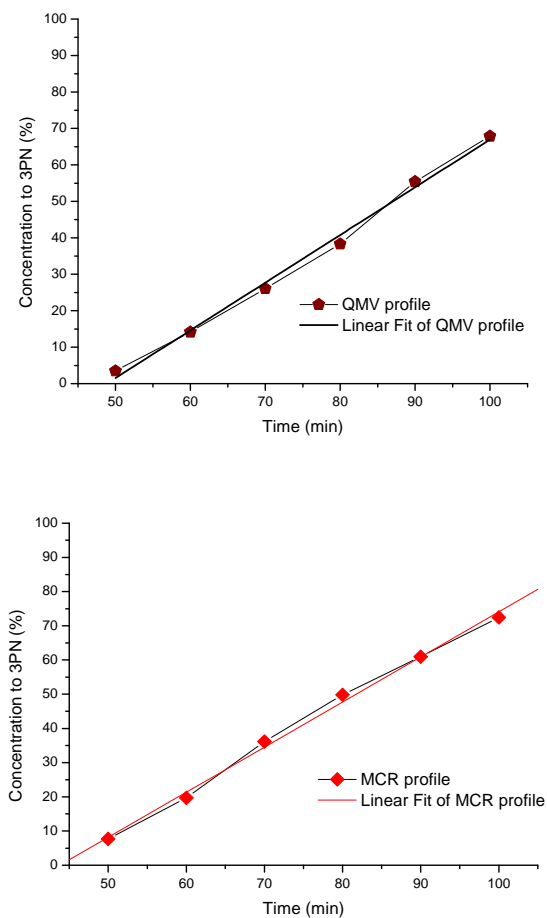
Figure 3.19. Linear fitting for the QMV and MCR kinetic profile.

3.7. Limitations of the IR analysis technique and outlook

Next, the investigation of the Ni-catalyzed hydrocyanation reaction by means of IR spectroscopy was considered (Scheme 3.3). In Chapter 2 the application of the triptycene-based ligand in the butadiene hydrocyanation and the double activity of the [NiTrip(PPh$_2$)$_2$] catalyst in promoting hydrocyanation and isomerization at the same time
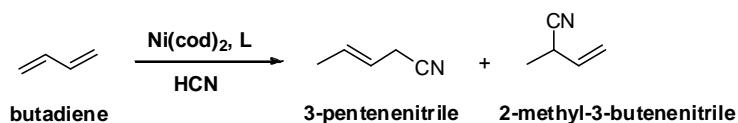
Scheme 3.3. Hydrocyanation of butadiene.

Table 3.1. Butadiene hydrocyanation in dioxane with ACH as HCN source.

Entry	Temperature (°C)	Conversion (%)	3PN (%)
1	60	12	89
2	80	75	92
3	90	87	95

Conditions: 0.036 mmol Ni(cod)$_2$, acetonecyanohydrine (ACH) as HCN source,
Ni:L:S:ACH=1:1:125:excess, T = 90°C, 4h, 2 mL dioxane.

were reported. An extensive study of this reaction would be of great interest. The experiments with the IR-probe were carried out at a maximum of 60°C, due to the limited temperature resistance of the probe. Unfortunately, the hydrocyanation of butadiene did not work efficiently at that temperature (Table 3.1, Entry 1). The best conditions for both hydrocyanation and a slow isomerization reaction (slow enough to be detected *via* IR spectroscopy using this specific setup) were at 80°C (Table 3.1, Entry 2).

A second limitation of this setup is the lack of sensitivity. A possible solution, together with a better IR setup, would be a more sensitive analytical technique such as Raman spectroscopy, which shows better sensitivity for groups with high polarizability, e.g. the nitriles.

3.8. Conclusions

The isomerization of 2M3BN was performed in dioxane at 60°C for 4 hours using a triptycene-based diphosphine ligand in combination with Ni(cod)$_2$. A final conversion of 87% was determined by GC-analysis. An IR spectrum was recorded every 10 minutes using an ATR probe connected to a FTIR instrument with a flexible light guide.

Different regions in the spectra were analyzed. The peak in the -CN stretch region at 2243 cm^{-1} gradually decreased and a second peak at 2248 cm^{-1} arose, while the 2M3BN is converted into 3PN. Also the CH deformation and the (C=)CH stretch regions showed transformations in time. Several spectral regions have been transformed to their second derivative. The dynamics in the spectra were calculated and normalized to the final conversion determined by GC. Similar kinetic profiles were obtained from the dynamics of different bands. Furthermore, DFT calculations have been performed to obtain calculated IR spectra of 2M3BN, *trans-* and *cis-* 3PN, in order to assign the corresponding bands in the spectra of the mixture. An average kinetic profile was obtained from the dynamics of four different peaks in the spectra applying a "*quasi-multivariate*" analysis (QMV), taking into consideration the correlated formation of 3PN and consumption of 2M3BN.

A chemometric analysis of the CH deformation region generated a profile similar to the one obtained *via* QMV. The latter method was, therefore, validated as a more accessible approach to make use of the correlation between different band dynamics of the significant spectral regions.

For the first time IR spectroscopy was applied to monitor the kinetics of the 2M3BN isomerization reaction. Using a more suitable FTIR setup or applying Raman spectroscopy, such a spectroscopic method would be very useful to study also the hydrocyanation reaction.

3.9. Experimental Section

General considerations

Chemicals were purchased from Aldrich, Acros or Merck and used as received. 1,4-Dioxane was distilled over CaH_2 prior to use. All preparations were carried out under an argon atmosphere using standard Schlenk techniques. 1,8-(Bis-diphenylphosphino)triptycene[11] and $Ni(cod)_2$[27] were synthesized according to literature procedures. IR spectra were recorded on a Nicolet Avatar 360 FT-IR instrument connected to a Remspec IR Fiber-Optic Immersion Probe. The spectra were recorded and elaborated using the Omnic E.S.P. 5.2a program.

General procedure for the isomerization experiments

A solution of ligand (23.0 mg, 0.036 mmol) in 2 mL of dioxane was added to $Ni(cod)_2$ (10.0 mg, 0.036 mmol) in a Schlenk tube and stirred for 5 minutes. 2M3BN (400 μL, 200 equiv.) was added with an Eppendorf pipette, followed by 100 μL of *n*-decane as internal standard. A diamond ATR deep immersion probe connected to a FTIR instrument with a flexible light guide was immersed in the reaction mixture. The Schlenk tube was placed in an oil bath and heated to 60°C. IR spectra were recorded every 10 minutes. A sample for GC analysis was taken after 4h. The selectivity is defined as 3PN/(Σ nitriles).

IR spectra

Number Scans: 700
Resolution: 4 cm^{-1}
Data Spacing: 1.929 cm^{-1}
Gain: 4
Velocity: 1.8988 cm/s
Spectral Range: $4000\text{-}900 \text{ cm}^{-1}$

IR data treatment

The FTIR spectra were transformed into the absorbance mode. Further data treatment was performed using the Perkin Elmer software Spectrum v5.0.1. All spectra were normalized using the C-H deformation vibrational band originating from the dioxane solvent. The peak maximum at 1365 cm^{-1} was set at ordinate 1.0 with a one sided base

point at 1340 cm^{-1}. The second derivative spectra were calculated applying 13 points. In both the absorbance spectra as well as the second derivative spectra the peak heights are linear with the concentration as given by the Lambert-Beer law. The peak heights were determined at 3055, 2248, 1478 and 1434 cm^{-1} using fixed base points in the nearest maxima at both sides using the t = 170 min spectrum. The data for the band at 1478 cm^{-1} are reported as example.

Time (min)	Peak height 2nd derivative at 1478 cm^{-1}(A)	Normalized value (%)
170	-0,008	87
160	-0,008	87
150	-0,0075	82
140	-0,0073	80
130	-0,0072	79
120	-0,0071	77
110	-0,0067	73
100	-0,0061	67
90	-0,0044	49
80	-0,0026	30
70	-0,0018	21
60	-0,0003	5.0
50	0,0002	0
40	0,0006	0
30	0,0006	0
20	0,0002	0

Multi-variate analysis

The multi variate calculations were performed in MATLAB R2006B (The Mathworks, Inc.) using the PLS toolbox version 4.2 (Eigenvector Research, Inc.). Multi Curve Resolution (MCR) was applied to the set of spectra in the interval 1500 - 1400 cm^{-1} with the constraints that the output must contain only non-negative pure spectra and non-negative concentrations. The calculation of the first two components captured > 98 % of the variation in the spectra. The resulting profile was normalized to the end conversion of 87 % determined by GC.

General procedure for the hydrocyanation experiments

A solution of ligand (23.0 mg, 0.036 mmol) in 2 mL of dioxane was added to $Ni(cod)_2$ (10.0 mg, 0.036 mmol) in a Schlenk tube and stirred for 5 minutes. Butadiene (400 μL, 200 equiv.) was added with an Eppendorf pipette, followed by 100 μL of *n*-decane as internal standard. The Schlenk tube was placed in an oil bath and heated to 60°C. A sample for GC analysis was taken after 4h. The selectivity is defined as 3PN/(Σ nitriles).

Computational Details

Quantum chemical calculations were carried out in the framework of density functional theory using the Gaussian 03 program[28]. The hybrid B3LYP functional was used in a combination with the 6-311+G(d,p) basis set in all computations. No symmetry restrictions were imposed during the geometry optimization. The nature of the calculated structures was evaluated from the analytically computed harmonic normal modes. All of the optimized structures showed no imaginary frequencies and thus were assumed to correspond to the local minima.

3.10. References and Notes

1. Huthmacher, K.; Krill, S. in *Applied Homogeneous Catalysis with Organometallic Compounds,* 2nd ed.; Cornils, B., Hermann, W. A., Eds.; Wiley-VCH: Weinheim, **2002**; Vol. 1 pp 465; (b) Tolman, C. A. *Chem. Rev.* **1977**, *77*, 313.

2. Chaumonnot, A.; Lamy, F.; Sabo-Etienne, S.; Donnadieu, B.; Chaudret, B.; Barthelat, J. C.; Galland, J. C. *Organometallics* **2004**, *23* (14), 3363.

3. (a) Goertz, W.; Keim, W.; Vogt, D.; Englert, U.; Boele, M. D. K.; van de Veen, L. A.; Kamer, P. C. J.; van Leeuwen, P. W. N. M. *J. Chem. Soc., Dalton Trans.,* **1998**, 2981; b) Nakamoto, K., Infrared and raman spectra of inorganic and coordination compounds, Wiley, 3rd Edition, 1978.

4. (a) van der Vlugt, J. I.; Hewat, A. C.; Neto, S.; Sablong, R.; Mills, A. M.; Lutz, M.; Spek, A. L.; Müller, C.; Vogt, D. *Adv. Synth. Catal.* **2004**, *346*, 993; (b) Acosta-Ramirez, A.; Munoz-Hernandez, M.; Jones, W. D.; Garcia, J. J. *J. Organomet. Chem.* **2006**, *691*, 3895; (c) Acosta-Ramirez, A.; Munoz-Hernandez, M.; Jones, W. D.; Garcia, J. J. *Organometallics* **2007**, *26*, 5766.

5. (a) Brukan, N. M.; Brestensky, D. M.; Jones, W. D. *J. Am. Chem.Soc.* **2004**, *126,* 3627; (b) Wilting, J.; Müller, C.; Hewat, A. C.; Ellis, D. D.; Tooke, D. M.; Spek, A. L.; Vogt, D. *Organometallics* **2005**, *24*, 13; (c) Acosta-Ramirez, A.; Flores-Gaspar, A.; Muñoz-Hernandez, M.; Arevalo, A.; Jones, W. D.; Garcia, J. J. *Organometallics* **2007**, *26*, 1712; (d) Swartz, B. D.; Reinartz, N. M.; Brennessel, W. W.; Garcia J. J., Jones, W. D. *J. Am. Chem.Soc.* **2008**, *130,* 8548.

6. (a) Foo, T.; Garner, J. M.; Tam, WO 99/06357, **1999**. *Chem. Abstr.* **1999***, 130*, 169815; (b) Bartsch, M.; Baumann, R.; Kunsmann-Keitel, D. P.; Haderlein, G.; Jungkamp, T.; Altmayer, M.; Siegel, W.; Molnar, F., DE 10150286, **2003**. *Chem. Abstr.* **2005***, 138*, 304408; (c) Lenges, C. P., WO 03/076394, **2003**. *Chem. Abstr.* **2006***, 139*, 262467.

7. Maki, G. *J. Chem. Phys.* **1958**, *15,* 5.

8. Tolman, C. A.; Seidel, W. C.; Druliner, J. D.; Domaille, P. J. *Organometallics* **1984**, *3*, 33.

9. Druliner, J. D. *Organometallics,* **1984**, *3,* 205.

10. (a) Harrick, N. J., Internal Reflection Spectroscopy, Wiley, New York, **1967**; (b) Griffiths, P. R. and de Haseth, J. A., Fourier Transform Infrared Spectroscopy, Wiley, New York, **1986**.

11. Bini, L.; Müller, C.; Wilting, J.; von Chrzanowski, L.; Spek, A. L.; Vogt, D. *J. Am. Chem.Soc.* **2006**, *128,* 11374.

12. (a) Weckhuysen, B. M. *Chem. Commun.* **2002**, 97; (b) Guerrero-Perez, M. O.; Banarez, M. A. *Chem. Commun.* **2002**, 1292.

13. Kitson, E.; Griffith, N. E. *Anal. Chem.* **1952**, *24*, 334.

14. Whitbeck, M. R. *Appl. Spectr.* **1981**, *35*, 93.

15. Susi, H.; Byler, D. M. *Biochem. Biophys. Res. Comm.* **1983**, *115*, 391.

16. Sheppard, N. *Trans. Faraday Soc.* **1955**, *51*, 1465.

17. Sheppard, N.; Simpson, D. M. *Quart. Rev. Chem. Soc.* **1953**, *7*, 19.

18. Bellamy, L. J.; Williams, R. L. *J. Chem. Soc, London* **1956**, 2753.

19. Fox, J. J.; Martin, A. E. *Proc. Roy. Soc., Ser. A* **1938**, *167*, 257.

20. Malherbe, F. E.; Berustein, H. J. *J. Am. Chem.Soc.* **1952**, *17,* 4408.

21. McMurry, H. L.; Thornton, *Anal. Chem.* **1952**, *24*, 318.

22. Wilson, E. B. Jr.; Decius, J. C.; Cross, P. C., Molecular Vibrations: The Theory of Infrared and Raman Vibrational Spectra, Dover, New York, **1980**.

23. Young, D. C., Computational Chemistry: A Practical Guide for Applying Techniques to Real-World Problems, Wiley, New York, **2001**.

24. Meier, R. J. *Vib. Spectrosc.* **2007**, *43,* 26.

25. (a) Martens, H.; Naes, T., Multivariate Calibration, Wiley, New York, 1989; (b) Tummers, P. H. G.; Houben, E. J. E. ; Jansen, J. F. G. A. ; Wienke, D. *Vib. Spectrosc.* **2007**, *43,* 116.

26. K. L. A. Chan ; S. G. Kazarin *Appl. Spectr.* **2007**, *61*, 48.

27. Schunn, R. A. *Inorg. Synth.* **1974**, *15*, 5.

28. Frisch, M. J.; Trucks, G. W.; Schlegel, H. B.; Scuseria, G. E.; Robb, M. A.; Cheeseman, J. R.; Montgomery, J. A., Jr.; Vreven, T.; Kudin, K. N.; Burant, J. C.; Millam, J. M.; Iyengar, S. S.; Tomasi, J.; Barone, V.; Mennucci, B.; Cossi, M.; Scalmani, G.; Rega, N.; Petersson, G. A.; Nakatsuji, H.; Hada, M.; Ehara, M.; Toyota, K.; Fukuda, R.; Hasegawa, J.; Ishida, M.; Nakajima, T.; Honda, Y.; Kitao, O.; Nakai, H.; Klene, M.; Li, X.; Knox, J. E.; Hratchian, H. P.; Cross, J. B.; Bakken, V.; Adamo, C.; Jaramillo, J.; Gomperts, R.; Stratmann, R. E.; Yazyev, O.; Austin, A. J.; Cammi, R.; Pomelli, C.; Ochterski, J. W.; Ayala, P. Y.; Morokuma, K.; Voth, G. A.; Salvador, P.; Dannenberg, J. J.; Zakrzewski, V. G.; Dapprich, S.; Daniels, A. D.; Strain, M. C.; Farkas, O.; Malick, D. K.; Rabuck, A. D.; Raghavachari, K.; Foresman, J. B.; Ortiz, J. V.; Cui, Q.; Baboul, A. G.; Clifford, S.; Cioslowski, J.; Stefanov, B. B.; Liu, G.; Liashenko, A.; Piskorz, P.; Komaromi, I.; Martin, R. L.; Fox, D. J.; Keith, T.; Al-Laham, M. A.; Peng, C. Y.; Nanayakkara, A.; Challacombe, M.; Gill, P. M. W.; Johnson, B.; Chen, W.; Wong, M. W.; Gonzalez, C.; Pople, J. A. Gaussian 03, revision B.05; Gaussian, Inc.: Pittsburgh PA, **2003**.

Chapter **4**

Hydrocyanation of 3-Pentenenitrile with Tetraphenol-Based Diphosphite Ligands: Formation of π-Allyl and σ-Alkyl Intermediates

New tetraphenol-based diphosphite ligands (TP) were applied in the alkene hydrocyanation reaction. Very high activities were observed in the conversion of 3-pentenenitrile. Surprisingly, these systems are neither active in the hydrocyanation of butadiene nor do they show any isomerization of 2M3BN. This peculiar behavior was investigated by means of NMR and IR spectroscopy, considering the formation of π-allyl and σ-alkyl intermediates. Moreover, the coordination of ZnCl2 to the complex [Ni(2M3BN)(TP2)] was studied by IR spectroscopy.
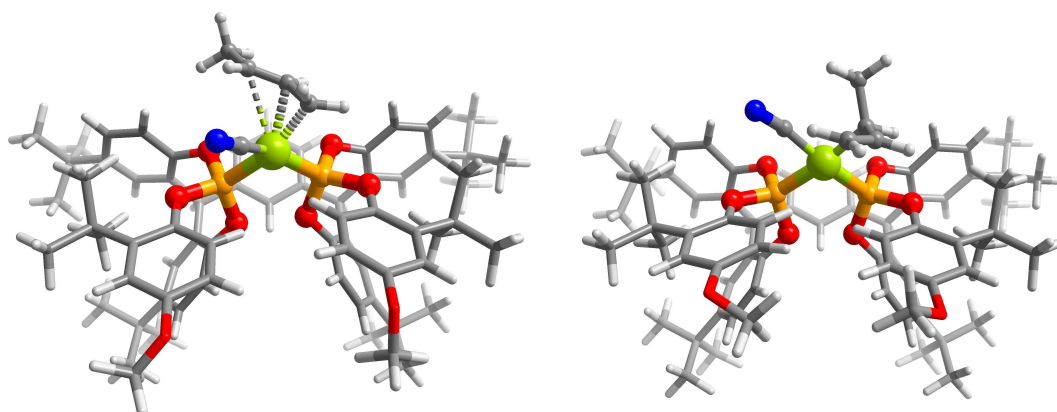
4.1. Introduction

Recently, our group reported on the synthesis of tetraphenol-based diphosphite ligands (TP) (Figure 4.1) and their application in the hydroformylation of octenes.[1] In combination with Ni(cod)$_2$, bulky phosphites with a rigid backbone are known to give the most active catalysts in alkene hydrocyanation.[2] Therefore, the application of these new diphosphite ligands in the DuPont adiponitrile process, in which adiponitrile (AdN) is obtained *via* hydrocyanation of butadiene in three steps, was investigated.

The hydrocyanation of 3-pentenenitrile (3PN) is the most difficult step of the process (Scheme 4.1). In general, monoalkenes[3,4] are less active substrates than dienes[3,5] or vinylarenes.[3,6] So far only patent literature reported on the 3PN hydrocyanation in terms of catalyst activity.[7] Many ligands have been screened, but only few catalysts based on bulky phosphites and phosphinites perform with good conversion and selectivity towards adiponitrile.[8] Tolman *et al.*[9] investigated the kinetics and the influence of different Lewis acids on the selectivity of the 3PN hydrocyanation with catalysts based on monodentate phosphites. Deuterium labeling studies applying DCN in the 3PN hydrocyanation have been reported by Druliner.[10] The reaction has also been performed in ionic liquids, using phosphites modified with ionic groups.[11]
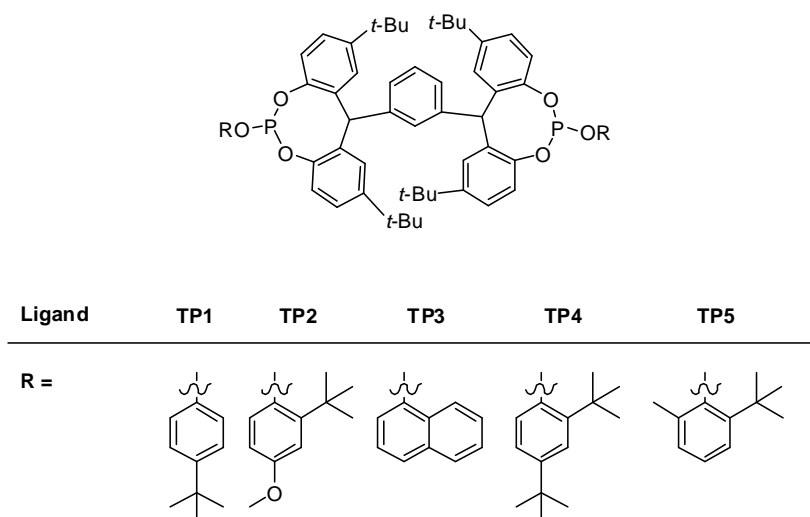
Figure 4.1. Tetraphenol-based ligands TP1-TP5.
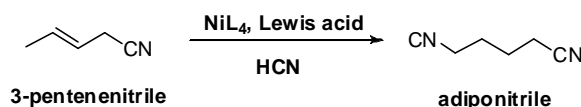
Scheme 4.1. Hydrocyanation of 3-pentenenitrile.

4.2. Hydrocyanation of 3-pentenenitrile

The tetraphenol backbone was used for the synthesis of five ligands (TP1-TP5, Figure 4.1), which have been reported and characterized previously.[1] Butadiene hydrocyanation and 2M3BN isomerization were performed in toluene at 90°C for 4h. Curiously, no conversion was observed in either reactions. The hydrocyanation of 3PN was also carried out in toluene at 90°C for 4h, applying ACH (acetonecyanohydrine) as HCN precursor and $ZnCl_2$ as Lewis acid. In this case, a conversion of up to 39% was obtained (Table 4.1, Entry 2).

The catalyst based on ligand TP2 was the best performing system (Table 4.1, Entry 2) with a conversion of 39% and a selectivity of 96% towards AdN. A conversion and selectivity to AdN of 24% and 83% respectively were obtained using the catalyst based on ligand TP1 (Table 4.1, Entry 1). The other systems based on TP3 and TP4 gave lower conversions (~15%) and selectivities (Table 4.1, Entries 3-5).

To optimize the reaction conditions with the [Ni(TP2)] catalyst, THF was used as solvent. The more polar medium allowed variation of the amount of Lewis acid (Table 4.2, Entries 1-4), since $ZnCl_2$ is soluble in THF but not in toluene. The addition of three

Table 4.1. Hydrocyanation of 3PN with tetraphenol ligands TP1-TP5.

Entry	Ligand	Conversion[a]%	2PN[b]%	4PN[b]%	Yield DN[c]%	ADN/MGD
1	TP1	24	10	/	14	83/17
2	TP2	39	0	19	20	96/4
3	TP3	15	1	7	7	75/25
4	TP4	14	1	1	12	59/41
5	TP5	15	1	8	6	68/32

Conditions: 0.018 mmol Ni(cod)₂, Ni:L:Zn:S:ACH=1:1:1:170:excess, acetonecyanohydrine (ACH) as HCN source, T = 90°C, 2 mL toluene, t = 4h. [a] Conversions are based on the amount of substrate left [mmol] and calculated using GC data and n-decane as internal standard. [b] Yield of 2PN and 4PN. [c] Yield of DN (adiponitrile + methylglutaronitrile).

equivalents of $ZnCl_2$ resulted in an increase of conversion up to 53% with a selectivity of 85% towards the linear adiponitrile (AdN) (Table 4.2, Entry 4). The reaction was repeated with a reaction time of 7 h, but the conversion did not increase. Consequently, the catalyst is completely deactivated during the first 4 h of reaction. The facile deactivation is most likely due to the reaction conditions, in which HCN (ACH) is added at once in large excess. In fact, the Ni(0) catalyst is generally prone to the double addition of HCN leading to the formation of catalytically inactive Ni(II) dicyanide species. A higher temperature of 110°C lowered the conversion, although the selectivity towards adiponitrile remained at 87% (Table 4.2, Entry 5). Using $AlCl_3$ as Lewis acid, the activity towards AdN decreased dramatically (Table 4.2, Entry 6).

By addition of DCN to pentenenitriles, Druliner studied the reaction mechanism in the presence of $AlCl_3$ and $ZnCl_2$, using a mixture of *para-* and *ortho*-tolyl phosphite as ligands.[10] It was proven that 4PN is the predominant substrate for the formation of dinitriles. 3PN is first isomerized to 4PN, which is converted to AdN *via* hydrocyanation (Scheme 4.2). Furthermore, it has been concluded that the double bond isomerization is catalyzed by addition and elimination of a Ni hydride species in the presence of $AlCl_3$. Using $ZnCl_2$, the isomerization of 3PN to 4PN occurs independently from the hydrocyanation step without coordination to the nickel. The catalyst [Ni(TP2)*(AlCl_3)] showed neither activity in the isomerization of 3PN to 4PN, nor in the hydrocyanation reaction.

Table 4.2. Hydrocyanation of 3PN with tetraphenol ligand TP2.

Entry	Lewis acid (eq)	Conversion[a]%	Other nitriles[b] (%) [2PN-4PN-2M2BN]	Yield DN[c] (%) [ADN/MGD]
1	$ZnCl_2$ (1eq)	41	[4-5-0]	32 [88/12]
2	$ZnCl_2$ (2eq)	40	[4-2-0]	34 [88/12]
3	$ZnCl_2$ (5eq)	14	[1-1-0]	12 [85/15]
4	$ZnCl_2$ (3eq)	53	[3-11-0]	38 [85/15]
5[d]	$ZnCl_2$ (3eq)	29	[3-9-0]	20 [87/13]
6	$AlCl_3$ (1eq)	1	[0.2-0.4-0]	0.1 [100/0]
7[e]	$ZnCl_2$ (3eq)	43	[3-17-1]	22 [82/18]

Conditions: 0.018 mmol Ni(cod)₂, Ni:L:Zn:S:ACH=1:1:1:170:excess, acetonecyanohydrine (ACH) as HCN source, T = 90°C, 2 mL THF, t = 4h, TP2 as ligand. [a] Conversions are based on the amount of substrate left [mmol] and calculated using GC data and n-decane as internal standard. [b] Yield of 2PN, 4PN and 2M2BN. [c] Yield of DN (ADN + MGD). [d] T = 110°C. [e] BIPPP as ligand.
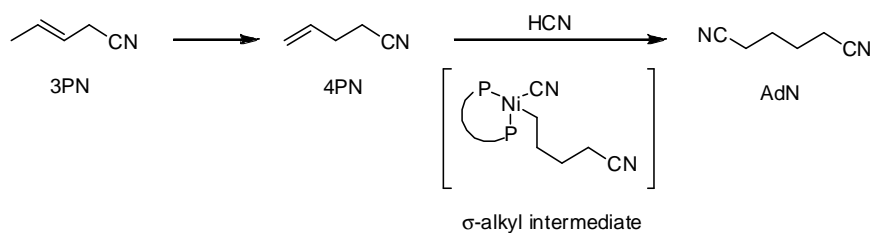
Scheme 4.2. Hydrocyanation of 3PN, σ-alkyl intermediate.

To facilitate the formation of AdN, the hydrocyanation of 4PN with [Ni(TP2)] was performed under the best conditions established for the hydrocyanation of 3PN. The substrate largely isomerized to 3PN (53%), but the yield of dinitriles and the selectivity to adiponitrile were 42% and 89%, respectively, and thus higher compared to the reaction using 3PN as substrate. Only C-C double bond isomerization within the pentenenitrile skeleton was observed (2PN, 3%).

It is remarkable that during the 3PN hydrocyanation with catalysts based on TP ligands and in the presence of $ZnCl_2$ the double bond isomerization only occurs to other linear nitriles (2PN and 4PN). The isomerization of linear to branched mononononitriles could not be detected by GC analysis in the unreacted starting material mixture. This isomerization to branched isomers would have to involve oxidative addition of a C-CN bond to Ni(0) with the formation of π-allyl intermediates and subsequent reductive elimination of 2M3BN (Scheme 4.3). Apparently, the reactions that proceed *via* the formation of π-allyl intermediates do not take place using the TP ligand systems (isomerization of 3PN towards 2M3BN and *vice versa*, but also hydrocyanation of butadiene). Such behavior for the Ni-catalysts based on tetraphenol ligands is different compared to other diphosphite-based catalyst, which normally give better results in the hydrocyanation of butadiene and isomerization of 2M3BN than in the hydrocyanation of
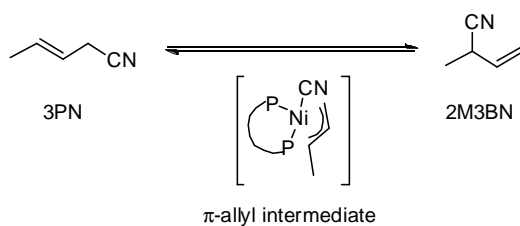
Scheme 4.3. Isomerization of 3PN to 2M3BN, π-allyl intermediate.

3PN. Conversion is observed only in the reaction that proceeds *via* the formation of a σ-alkyl intermediate (3PN hydrocyanation, Scheme 4.2) and double bond isomerization was only detected to other linear products. Therefore, it can be proposed that either the TP ligands disfavor the formation of π-allyl intermediates in the corresponding Ni-complexes, or π-allyl species are generated, but they are too stable to undergo reductive elimination.

4.3. Comparison with the diphosphite ligand BIPPP

The binaphthol-based diphosphite BIPPP (Figure 4.2) was reported in the patent literature as one of the best performing ligands in the Ni-catalyzed hydrocyanation of 3PN.[8a] The reaction was usually carried out in the absence of solvent with a stream of HCN, obtaining conversions of up to 90%. Due to safety regulations, it is difficult to reproduce such experiments in our laboratory, as they require manipulation of large amounts of gaseous HCN and a precise regulation of its flow. In fact, the conversion of 3PN to dinitriles seems to be very sensitive to the rate of HCN addition. Therefore, 3PN hydrocyanation using BIPPP as ligand was performed under the same optimized reaction conditions applied for TP2, in order to compare the two ligands (Table 4.2, Entry 7). Conversion and selectivity towards adiponitrile were higher for the [Ni(TP2)] catalyst, which makes this system a very promising candidate for the industrial process. The presence of a small amount of branched nitrile (2M2BN) was detected in the reaction mixture, using BIPPP as ligand.
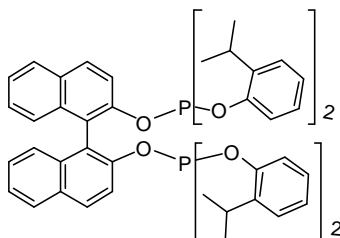
Figure 4.2. Binaphthyl diphosphite ligand (BIPPP).

4.4. NMR studies

Sabo-Etienne *et al.* presented a mechanism for the isomerization of 2M3BN to 3PN based on DFT calculations using [Ni(PH$_3$)$_2$] as catalyst (Figure 4.3).[12] According to these calculations, there are five steps involved in the mechanism beginning with the coordination of the 2M3BN double bond to the Ni-catalyst (A). The C-CN bond is cleaved, forming a σ-allyl species (B) that is further converted to a π-allylic species (C). This intermediate rearranges further to a branched σ-allyl species (B´) and finally, a new C-CN bond is formed by reductive elimination giving the [Ni-3PN] complex (A´). The complexes of the type A, B, and C are expected to be present in the reaction mixture,
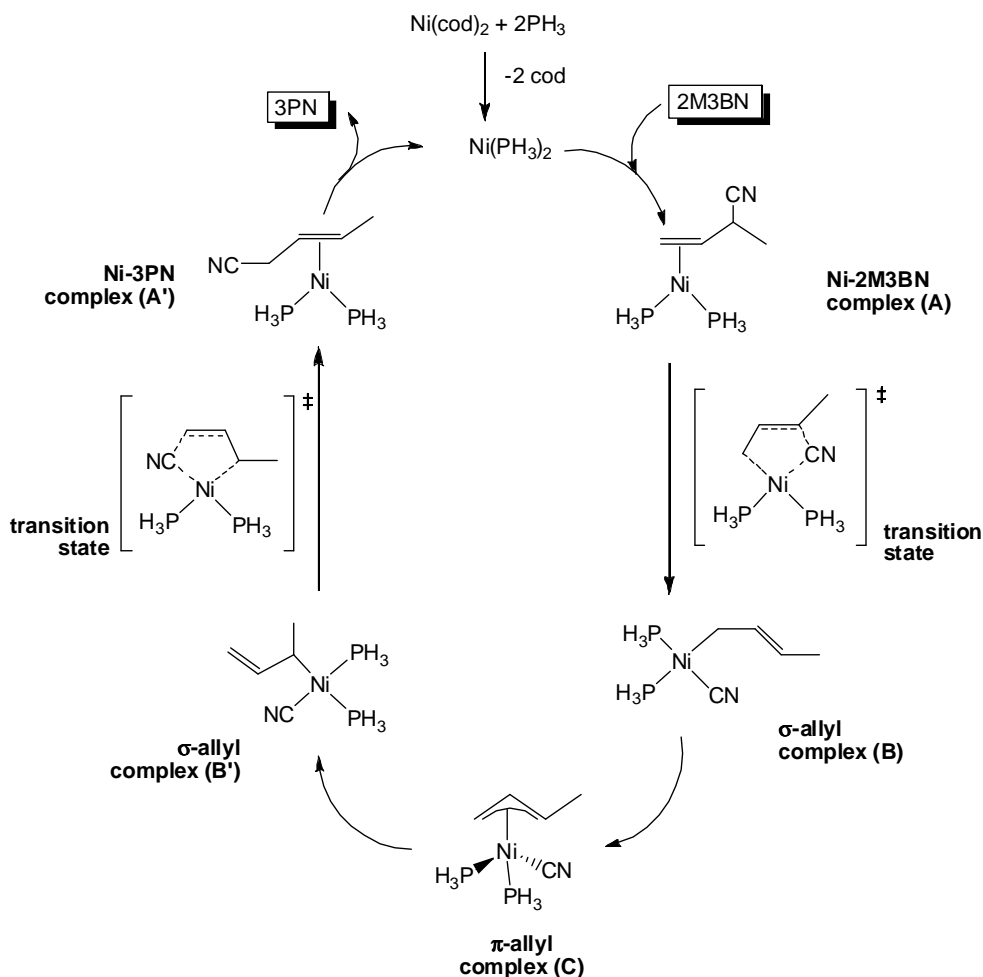
Figure 4.3. Mechanism for the 2M3BN isomerization proposed by Sabo-Etienne *et al.*[12]

when 2M3BN is added to a [Ni(0)(L)] complex. The isomerization takes place in the absence of HCN.

The formation of the π-allyl complex and its stability using the TP2 ligand was investigated by NMR spectroscopy. One equivalent of 2M3BN was added to the [Ni(cod)(TP2)] complex in an NMR tube. The ^{1}H NMR spectrum of the complex before and after the addition showed differences in the signals of the alkyl proton resonances. This indicates coordination of the 2M3BN to the complex (Figure 4.4). However, the allyl complex as well as the signals of free 2M3BN or 3PN could not be detected. A second NMR experiment was performed using the phosphite ligand BIPPP, which is active in 2M3BN isomerization (Figure 4.5). The π-allyl complex could not be detected at room temperature, but all the 2M3BN was consumed and the 3PN resonances were
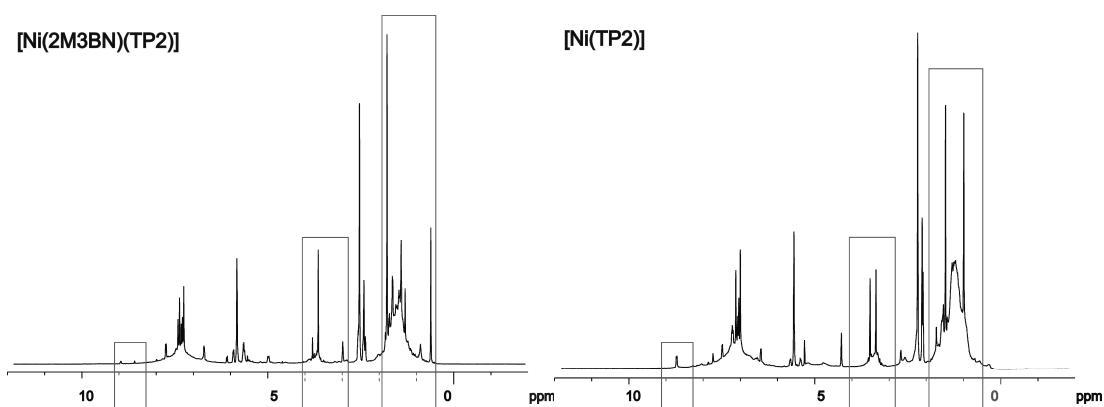
Figure 4.4. ^{1}H NMR spectrum of the complex [Ni(2M3BN)(TP2)] (left) and the [Ni(cod)(TP2)] complex (right) (toluene-d_8).
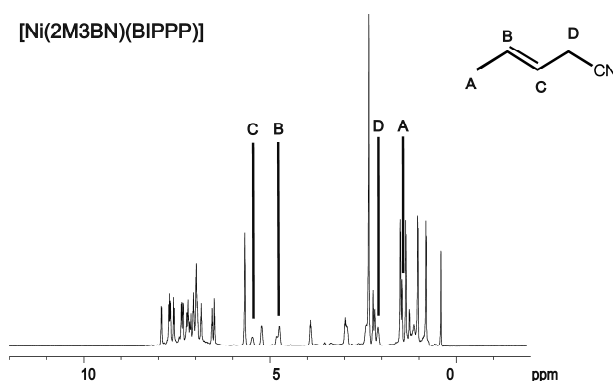
Figure 4.5. ^{1}H NMR spectrum of the [Ni(2M3BN)BIPPP] complex (toluene-d_8).

clearly identified.

VT ^{1}H and ^{31}P NMR experiments were performed with TP3 as ligand, in order to slow down the reaction and to be able to identify the π-allyl species. Three different substrates were tested in the formation of the allyl intermediate. 2M3BN, 3PN and allyl bromide were added to the [Ni(cod)(TP3)] solution in the NMR tube at -80°C and the temperature was slowly increased to 90°C. ^{1}H and ^{31}P NMR spectra were recorded with time intervals related to steps of 20°C. During the three experiments, the resonances of the complex disappear approximately at room temperature and the double bond resonances of the substrate shifted and broadened slightly. Therefore, the coordination of the substrate is considered to be complete only at 20°C. Resonances related to the allyl complex could not be detected. Furthermore, the isomerization of 2M3BN to 3PN and *vice versa* was not observed, even at 90°C.

4.5. IR studies

The coordination of 2M3BN to [Ni(TP2)] and [Ni(BIPPP)] was further investigated by IR spectroscopy. The two spectra were compared with the ones of 3PN and 2M3BN (Figure 4.6 and 4.7). The most interesting bands were observed in the -C≡N stretching region. The two IR spectra showed a very similar pattern of bands and several species were present in the mixture.

Only few papers have been published on the IR characterization of such species.[9,10] Tolman reported on IR frequencies for different [Ni-C≡N] complexes, containing P(O-*o*-tolyl)$_3$ as ligand.[13] In the IR spectra of these complexes the electronic parameters of the ligand play a crucial role, but the steric properties are less determining. Therefore, the IR values will probably not differ significantly between mono- and diphosphites. This effect was also supported by the IR data of the [Ni(CO)$_2$L] species. The IR frequencies of the A$_1$ and B$_1$ CO vibrations were the same for the two bulky bidentate phosphite ligands and very similar to those of the monodentate ligand (Table 4.3). Therefore, the frequency

values reported by Tolman were used as a reference to identify the species obtained by coordination of 2M3BN to [Ni(TP2)] and [Ni(BIPPP)].

Table 4.3. IR frequencies of the A_1 and B_1 vibrations of CO in $Ni(CO)_2$(**L**).

Ligand	A_1 (cm^{-1})	B_1 (cm^{-1})
$P(OPh)_3$ [a]	2045	1996
TP2 [b]	2040	1987
BIPPP [c]	2041	1987

Literature values a) [14], b) [5], c) [9c].

The complexes [Ni(2M3BN)(L)] and [Ni(3PN)(L)] (Figure 4.3) contain an organic nitrile group and their IR frequencies should be very close to the values of 3PN and 2M3BN. The major difference is the partial loss of double bond character after the coordination to the Ni atom. A shift of the peak maxima toward higher frequencies is expected without the vicinity of a double bond[15] along with a more rigid structure.[16]
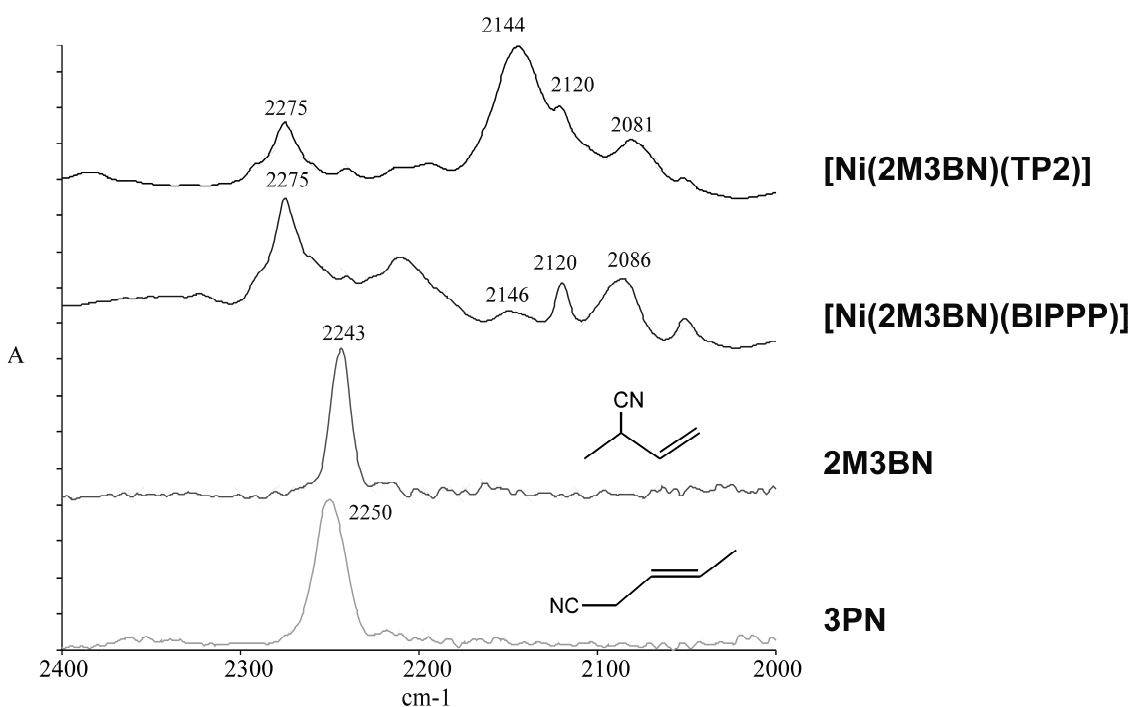
Figure 4.6. IR spectra f the [Ni(2M3BN)(TP2)], the [Ni(2M3BN)(BIPPP)] complexes, 3PN and 2M3BN (nitrile region).

Therefore, the bands at 2275 cm^{-1} could be assigned to the [Ni(2M3BN)(L)] and [Ni(3PN)(L)] species, in the spectrum containing TP2 as well as in the spectrum with BIPPP.

Tolman reported on the π-allyl complex (Figure 4.3) with intense bands at 2110 and 2090 cm^{-1}. Similar bands were detected during both experiments, but they were predominant only in the species containing BIPPP as ligand at 2120 and 2081 cm^{-1}.

σ-Alkyl intermediates were detected during hydrocyanation of cyano-alkenes and reported by Tolman with a Ni-C≡N stretching band at ~2144 cm^{-1}. These complexes are very similar to the σ-allyl intermediate formed during the isomerization reaction (Figure 4.3). Bands at 2144 cm^{-1} were also present in the spectra of [Ni(TP2)] and [Ni(BIPPP)] coordinated to 2M3BN and they have been assigned to σ-allyl species. In this case the band was predominant for the TP2 complex. Minor peaks in the spectra (~2210 cm^{-1}) could not be assigned referring to the literature.

It seems that the π-allyl and σ-allyl complexes were formed in the presence of both ligands and the bands related to the two species are present in both spectra. The π-allyl species is predominant in the BIPPP-containing complexes, while the σ-allyl complexes
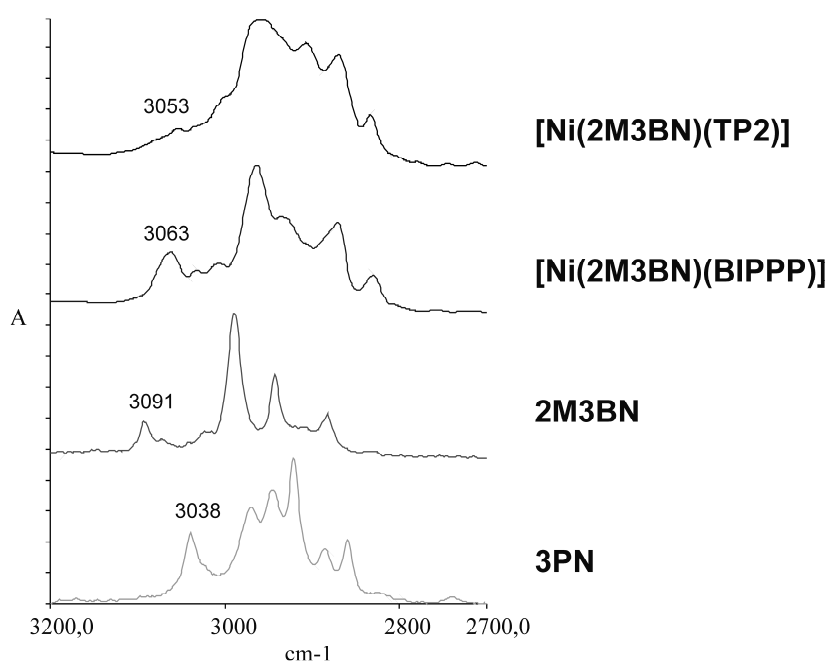
Figure 4.7. IR spectra of the complexes [Ni(2M3BN)(TP2)] and [Ni(2M3BN)(BIPPP)], 3PN and 2M3BN (C=(C-H) stretch vibrations in the double bond region).

apparently occur mainly in the TP2-based ones. Since the hydrocyanation of 3PN proceeds *via* σ-alkyl intermediates and the hydrocyanation of butadiene and the isomerization of 2M3BN *via* π –allyl species, these results could provide an explanation for the observed catalytic activity.

The double bond regions in the IR spectra were also analyzed. Olefinic CH stretching vibrations occur at 3130-2980 cm^{-1}.[17] These bands are normally well separated from other CH stretching bands below 3000 cm^{-1}. Therefore, the frequencies related to the double bond were easy to identify (Figure 4.7). The spectra showed double bond signals at different wave numbers compared to free 2M3BN and 3PN. Consequently, these peaks have been assigned to the σ-allyl complexes, which together with the substrate and product are the only species containing a double bond (Figure 4.3).

4.6. Coordination of ZnCl$_2$ to the [(TP2)Ni(2M3BN)] complex

Molecular structures of [Ni(2M3BN)(diphosphine)] complexes have been reported in the presence of the Lewis acids BPh$_3$ and ZnCl$_2$.[18] The [Ni(2M3BN)(TP2)] and [Ni(2M3BN)(BIPPP)] complexes were also investigated after addition of ZnCl$_2$, which is the Lewis acid used in the 3PN hydrocyanation. ^{31}P and ^{1}H NMR spectra of these species showed broad resonances, confirming the presence of Ni(II) species. In fact, the Ni(0) is oxidized to Ni(II) *via* 2M3BN oxidative addition and the tetrahedral configuration of these intermediates causes the formation of paramagnetic species.[19]

In the case of [Ni(2M3BN)(TP2)*ZnCl$_2$] and [Ni(2M3BN)(BIPPP)*ZnCl$_2$] only one signal was observed by IR spectroscopy in the metal-cyanide region at 2150 cm^{-1} (Figure 4.8). This result suggests that ZnCl$_2$ stabilizes one of the intermediates formed before the Lewis acid addition (Figures 4.6 and 4.7), which becomes obviously the only species present. A signal for the double bond vibration at 3061 cm^{-1} was also detected. The presence of a Ni(II) species (NMR), a Ni-C≡N as well as a double bond band (IR) in the adduct confirm the formation of σ-allyl complexes (Figure 4.9).
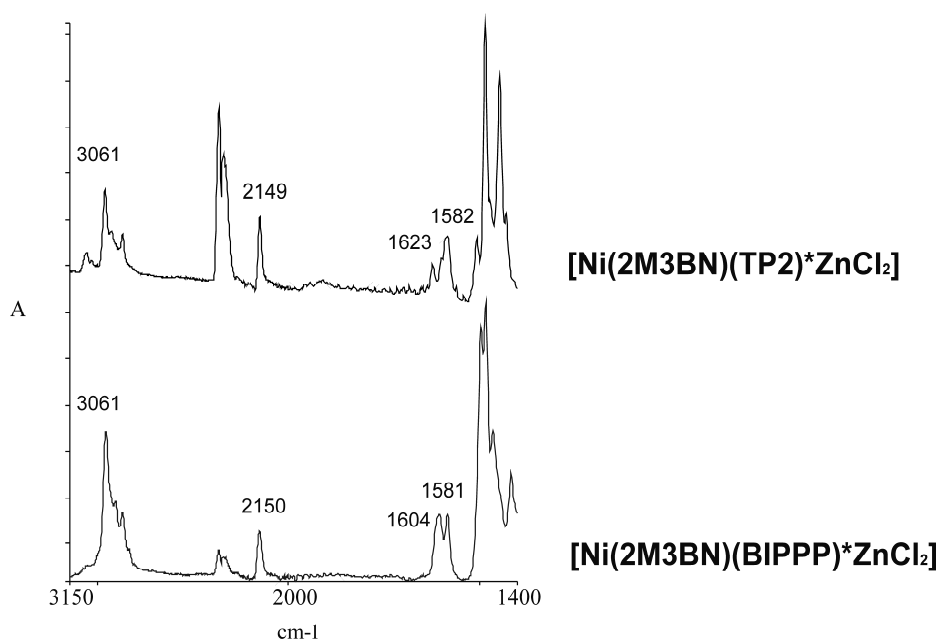
Figure 4.8. IR spectra of the complexes [Ni(2M3BN)(TP2)*ZnCl₂] and [Ni(2M3BN)(BIPPP)*ZnCl₂] (nitrile region).
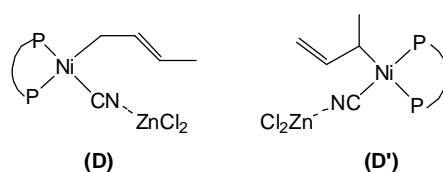
Figure 4.9. σ-Alkyl complexes D and D´.

Furthermore, the 2M3BN isomerization was performed at 90°C using [Ni(2M3BN)(TP2)*ZnCl₂] and [Ni(2M3BN)(BIPPP)*ZnCl₂] as catalysts and at a 2M3BN/Ni ratio of 100:1. After 1.5 h the conversion to 3PN was only 10-13% in both experiments, indicative that the two complexes showed very similar activity. In the absence of Lewis acid the [Ni(cod)(TP2)] could not isomerize 2M3BN to 3PN, while the [Ni(cod)(BIPPP)] led to 40% of conversion after 1.5 h. The Lewis acid addition seems to slow down the reaction in the case of [Ni(BIPPP)] and is promoting the activity of the [Ni(TP2)] catalyst.

4.7. Conclusions

In conclusion, tetraphenol-based ligands were applied in the three Ni-catalyzed steps of the DuPont adiponitrile process. High activities were observed in the hydrocyanation of 3-pentenenitrile, compared to the reaction performed using the [Ni(BIPPP)] systems, one of the best catalysts reported in patent literature. The coordination of 2M3BN to the Ni metal center in the presence of TP2 and BIPPP as ligands was investigated by NMR and IR spectroscopy. Using IR spectroscopy it was observed that the σ-allyl complexes are favored using TP2 as ligand, while the π-allyl complexes are favored using BIPPP. The addition of $ZnCl_2$ to the catalyst led to the formation of identical species for both ligands, which showed a very low activity in the 2M3BN isomerization reaction.

4.8. Experimental Section

General considerations

Chemicals were purchased from Aldrich, Acros, and Merck and used as received. All preparations were carried out under argon atmosphere using standard Schlenk techniques. Ni(cod)$_2$[20] was synthesized according to literature procedures. NMR spectra were recorded on a Varian Mercury 400 and a Mercury 200 spectrometer (^{1}H, ^{13}C{^{1}H}, ^{31}P{^{1}H}). IR spectra were recorded on an Nicolet Avatar 360 FT-IR instrument in ATR mode.

Caution! HCN is a highly toxic, volatile liquid (bp 27°C) that is also susceptible to explosive polymerization in the presence of base catalysts. It should be handled only in a well-ventilated fume hood by teams of at least two technically qualified persons who have received appropriate medical training for treating HCN poisoning. Sensible precautions include having proper first aid equipment available as well as HCN monitors. Inhibitor-free HCN should be stored at a temperature lower than its melting point (- 13°C). Excess of HCN may be disposed by addition to aqueous sodium hypochlorite, which converts the cyanide to cyanate.

General procedure for the hydrocyanation experiments

A solution of ligand (0.018 mmol) in 2 mL of solvent was added to Ni(cod)$_2$ (5.0 mg, 0.018 mmol). 3-Pentenenitrile (300 µL, 170 equiv.) was added by an Eppendorf pipette, followed by 50 µL of *n*-decane as internal standard and the Lewis acid (1 equiv.). The solution was transferred into a 15 mL Schlenk tube equipped with a Teflon coated stirring bar. Acetonecyanohydrine (400 µL, 250 equiv.) was added via Eppendorf pipette and the Schlenk tube was warmed to 90°C in an oil bath. The mixture was stirred for 4 h. The reaction product was cooled to 0°C and flushed with a gentle stream of argon for one minute to remove traces of HCN. Samples were analyzed by GC, using *n*-decane as internal standard. All the reactions were carried out in duplo, showing variability for conversion and selectivity of ±2 % and ±1 %, respectively.

General procedure for the isomerization experiments

A solution of ligand (0.018 mmol) in 2 mL of solvent was added to Ni(cod)$_2$ (5.0 mg, 0.018 mmol) in a Schlenk tube and stirred for 5 minutes. 2M3BN (200 μL, 100 equiv.) was added with an Eppendorf pipette, followed by 50 μL of *n*-decane as internal standard and ZnCl$_2$ as Lewis acid (5.0 mg, 1 equiv.). The Schlenk tube was placed in an oil bath at 90°C and samples for GC analysis were taken over time. The selectivity is defined as 3PN/(Σ nitriles).

Synthesis of [Ni(cod)(TP2)]

A solution of TP2 (22.0 mg, 0.018 mmol) in 1 mL of benzene-*d$_6$* was added to Ni(cod)$_2$ (5.0 mg, 0.018 mmol) in a Schlenk tube and stirred for 30 minutes. ^{1}H NMR (500 MHz, C$_6$D$_6$) δ (ppm): 8.75 (d, J = 8.5 Hz), 7.75 (s), 7.48 (d, J = 8.5 Hz), 7.23-7.19 (m), 7.12 (s), 7.07 (s), 7.03 (s), 6.99 (s), 6.44 (d, J = 8.5 Hz), 5.56 (s), 5.27 (s), 3.51 (s), 3.35 (s), 2.11 (s), 1.69 (s), 1.58-1.54 (m), 1.48 (s), 1.42-1.04 (m), 0.99 (s). ^{31}P NMR (202 MHz, CDCl$_3$) δ (ppm): 124.6 (s).

Synthesis of [Ni(cod)(BIPPP)]

A solution of BIPPP (14.0 mg, 0.018 mmol) in 1 mL of benzene-*d$_6$* was added to Ni(cod)$_2$ (5.0 mg, 0.018 mmol) in a Schlenk tube and stirred for 30 minutes. ^{1}H NMR (400 MHz, C$_6$D$_6$) δ (ppm): 7.83 (d, ^3J = 8.06 Hz, 2H), 7.63 (d, ^3J = 8.79 Hz, 2H), 7.54 (d, ^3J = 8.05 Hz, 2H), 7.46 (d, ^3J = 8.78 Hz, 2H), 7.31 (d, ^3J = 8.42 Hz, 2H), 7.20 (dd, ^3J = 7.69, ^4J = 1.84 Hz, 2H), 7.05 (dt, ^3J = 7.51 Hz, ^4J = 0.74 Hz, 2H), 6.94-6.83 (m, 6H), 6.80 (dt, ^3J = 7.88 Hz, ^4J = 1.83 Hz, 2H), 6.74 (dt, ^3J = 7.32 Hz, ^4J = 1.10 Hz, 2H), 6.47 (dt, ^3J = 7.51 Hz, ^4J = 1.47 Hz, 2H), 6.41 (d, ^3J = 7.33 Hz, 2H), 5.15 (br s, 2H), 4.67 (br s, 2H), 3.79 (sept, ^3J = 6.96 Hz, 2H), 2.91 (sept, ^3J = 6.96 Hz, 2H), 2.80 (br s, 2H), 2.32 (br s, 2H), 2.20 (br s, 2H), 1.99 (br s, 2H), 1.35 (d, ^3J = 6.59 Hz, 6H), 1.21 (d, ^3J = 6.59 Hz, 6H), 0.91 (d, ^3J = 6.96 Hz, 6H), 0.70 (d, ^3J = 7.81 Hz, 6H). ^{31}P NMR (162 MHz, C$_6$D$_6$) δ (ppm): 147.8 (s).

Synthesis of [Ni(2M3BN)(TP2)]

A solution of TP2 (89.0 mg, 0.079 mmol) in 3 mL of toluene-d_8 was added to Ni(cod)$_2$ (22.0 mg, 0.079 mmol) in a Schlenk tube and stirred for 5 minutes. 2M3BN (10 µL, 1 equiv.) was added with an Eppendorf pipette and the solution was stirred for 30 minutes. A sample (800 µL) was taken for NMR analysis and the remaining solution was dried under vacuum. The red-orange powder was analyzed by IR spectroscopy. IR (cm^{-1}) ṽ : 3053 [C=(C-H)]; 2275, 2144, 2120, 2081 (CN). Due to the presence of a mixture of species, the signals detected by NMR spectroscopy could not be assigned unambiguously.

Synthesis of [Ni(2M3BN)(BIPPP])

A solution of BIPPP (70.0 mg, 0.079 mmol) in 3 mL of toluene-d_8 was added to Ni(cod)$_2$ (22.0 mg, 0.079 mmol) in a Schlenk tube and stirred for 5 minutes. 2M3BN (10 µL, 1 equiv.) was added with an Eppendorf pipette and the solution was stirred for 30 minutes. A sample (800 µL) was taken for NMR analysis and the residue solution was dried under vacuum. The red-orange powder was analyzed by IR spectroscopy. IR (cm^{-1}) ṽ : 3063 [C=(C-H)]; 2275, 2146, 2120, 2086 (CN). Due to the presence of a mixture of species, the signals detected by NMR spectroscopy could not be assigned unambiguously.

*Synthesis of [Ni(2M3BN)(TP2)*ZnCl$_2$]*

A solution of TP2 (89.0 mg, 0.079 mmol) in 3 mL of toluene-d8 was added to Ni(cod)$_2$ (22.0 mg, 0.079 mmol) in a Schlenk tube and stirred for 5 minutes. 2M3BN (10 µL, 1 equiv.) was added with an Eppendorf pipette, followed by ZnCl$_2$ as Lewis acid (22.0 mg, 1 equiv.) and the solution was stirred for 30 minutes. A sample (800 µL) was taken for NMR analysis and the remaining solution was dried under vacuum. The red-orange powder was analyzed by IR spectroscopy. IR (cm^{-1}) ṽ : 3061 [C=(C-H)]; 2150 (CN). ^{1}H NMR (400 MHz, C$_6$D$_6$) δ (ppm): 8.26 (br s), 7.59-6.94 (m), 6.47 (d, J = 8.4 Hz), 6.21-6.10 (m), 5.08 (m), 4.78 (br s), 4.42 (br s), 4.16 (br s), 3.95 (br s), 3.83 (br s), 3.64 (br s), 3.44-3.40 (m), 3.37 (s), 3.36 (d, J = 2 Hz), 3.34-3.30 (m), 3.30 (d, J = 3 Hz), 3.28 (s), 2.92 (br s), 2.62 (br s), 1.59-0.82 (m), 0.64 (d, J = 6.8 Hz), 0.25 (s). ^{13}C NMR

(100.6 MHz, C_6D_6) δ (ppm): 156.46, 153.72, 148.49, 148.27, 146.70, 137.10, 129.15, 128.88, 126.55, 125.29, 124.12, 116.64, 115.94, 114.02, 110.54, 70.49, 69.44, 66.56, 55.71, 54.87, 35.54, 34.26, 33.94, 30.95, 29.95, 29.82, 29.31, 28.91, 27.98, 14.94, 1.01. ^{31}P NMR (400 MHz, C_6D_6) δ (ppm): 124.6 (bs). Maldi-Tof:1114.39 (TP2), 1172.36 [Ni(TP2)], 1227.40 [Ni(TP2)(2M3BN)-CN].

*Synthesis of [Ni(2M3BN)(BIPPP)*ZnCl₂]*

A solution of BIPPP (70.0 mg, 0.079 mmol) in 3 mL of toluene-d_8 was added to Ni(cod)₂ (22.0 mg, 0.079 mmol) in a Schlenk tube and stirred for 5 minutes. 2M3BN (10 μL, 1 equiv.) was added with an Eppendorf pipette, followed by $ZnCl_2$ as Lewis acid (22.0 mg, 1 equiv.) and the solution was stirred for 30 minutes. A sample (800 μL) was taken for NMR analysis and the remaining solution was dried under vacuum. The red-orange powder was analyzed by IR spectroscopy. IR (cm^{-1}) $\tilde{v}$: 3061 [C=(C-H)]; 2149 (CN). Maldi-Tof: 944.18 [Ni(BIPPP)], 999.23 [Ni(BIPPP)(2M3BN)-CN], 1025.18 [Ni(BIPPP)(2M3BN)], 1095.23 [Ni(BIPPP)(2M3BN)Zn]. ^{31}P NMR (400 MHz, C_6D_6) δ (ppm): 131.1 (bs). The NMR spectroscopic data are not reported, due to the presence of paramagnetic species in the sample.

4.9. References and Notes

1. Janssen, M.; Bini, L.; Hamers, B.; Müller, C.; Vogt, D. *submitted for publication*

2. Goertz, W.; Keim, W.; Vogt, D.; Englert, U.; Boele, M. D. K.; van de Veen, L. A.; Kamer, P. C. J.; van Leeuwen, P. W. N. M. *J. Chem. Soc., Dalton Trans.,* **1998**, 2981.

3. Huthmacher, K.; Krill, S. in *Applied Homogeneous Catalysis with Organometallic Compounds,* 2nd ed.; Cornils, B., Hermann, W. A., Eds.; Wiley-VCH: Weinheim, **2002**; Vol. 1 pp 465.

4. a) Taylor, B. W., and Swift, H. E. *J. Catal.* **1972,** *26* (2), 254; b) Goerz, W., Kamer, P. C. J., van Leeuwen, P. W. N. M., Vogt, D., *Chem. Commun.,* **1997**, 1521.

5. a) Keim, W.; Behr, A.; Lühr, H.-O.; and Weisser, J. *J. Catal.* **1982**, *78*, 209; b) Bini, L.; Müller, C.; Wilting, J.; von Chrzanowski, L.; Spek, A. L.; and Vogt, D. *J. Am. Chem. Soc.,* **2007**, *129(42)*, 12622.

6. a) Casalnuovo, A. L.; RajanBabu, T. V.; Ayers, T. A.; Warren, T. H. *J. Am. Chem. Soc,* **1994**, *116,* 9869; b) RajanBabu, T. V; Casalnuovo, A. L *J. Am. Chem. Soc,* **1996**, *118,* 6325; c) Wilting, J.; Janssen, M.; Müller, C.; Lutz, M.; Spek, A. L.; Vogt, D. *Adv. Synth. Catal.* **2006**, *349*, 350; d) Göthlich, A. P. V.; Tensfeldt, M.; Rothfuss, H.; Tauchert, M. E.; Haap, D.; Rominger, F.; Hofmann, P. *Organometallics,* **2008**, *27(10*), 2189.

7. Foo, T.; Garner, J. M.; Tam, W. Hydrocyanation of diolefins and isomerization of nonconjugated 2-alkyl-3-monoalkenenitriles. WO 99/06357, **1999.** *Chem. Abstr.* **1999**, *130*, 169815.

8. a) Kreutzer, K. A.; Tam, W. Hydrocyanation process and multidentate phosphite and nickel catalyst composition therefore. WO 96/11182, **1996.** *Chem. Abstr.* **1996**, *125*, 114851. b) Brunel, E. E.; Kenneth, C. Process for the hydrocyanation of olefin using bidentate phosphite ligands and zero-valent nickel catalyst system which enable facile nitrile product and catalyst separation. US 5847191 A, **1998.** *Chem. Abstr.* **1998**, *130*, 26464; c) Lenges, C. P.; Lu, H. S. M.; Ritter, J. C. Phosphonite ligands and their use in hydrocyanation. WO 03/076394, **2003.** *Chem. Abstr.* **2003**, *139*, 262467.

9. Tolman, C. A.; Seidel, W. C.; Druliner, J. D.; Domaille, P. J. *Organometallics* **1984**, *3*, 33.

10. Druliner, J. D. *Organometallics,* **1984**, *3,* 205.

11. Vallée, C.; Chauvin, Y.; Basset, J.-M.; Santini, C. C., Galland, J.-C. *Adv. Synth. Catal.* **2005**, *347*, 1835.

12. Chaumonnot, A.; Lamy, F.; Sabo-Etienne, S.; Donnadieu, B.; Chaudret, B.; Barthelat, J.-C.; and Galland, J.-C. *Organometallics* **2004**, *23*, 3363.

13. Tolman, C. A.; McKinney, R. J.; Seidel, W. C.; Druliner, J. D.; Stevens, W. R. *Adv. Catal.* **1985**, *33*, 1.

14. van Hecke, G. R.; Horrocks, W.D. *Inorg. Chem.* **1966**, *5*, 1960.

15. Bernstein, M. P.; Sandford, S. A.; and Allamandola, L. J. *Astrophys. J.,* **1997**, *476*, 932.

16. Nakamoto, K., Infrared and Raman spectra of inorganic and coordination compounds, Wiley, 3rd Edition, 1978.

17. a) McMurry, H. L. and Thornton, *Anal. Chem.* **1952**, *24*, 318; b) Kitson, R. E., and Griffith, N. E. *Anal. Chem.* **1952**, *24*, 334.

18. a) Brunkan, N. M.; Brestensky, D. M.; Jones, W. D. *J. Am. Chem. Soc,* **2004**, *126,* 3627; b) Wilting, J.; Müller, C.; Hewat, A. C.; Ellis, D. D.; Tooke, D. M.; Spek, A. L.; and Vogt, D. *Organometallics* **2005**, *24*, 13; c) Acosta-Ramirez, A.; Munõz-Hernandez, M.; Jones, W. D.; Garcia, J. J. *J. Organomet. Chem.,* **2006**, *691*, 3895; d) Acosta-Ramirez, A.; Flores-Gaspar, A.; Munõz-Hernandez, M.; Arvalo, A.; Jones, W. D.; Garcia, J. J. *Organometallics,* **2008**, *26*, 1712.

19. Maki, G. *J. Chem. Phys.* **1958**, *29*, 162.

20. Schunn, R. A. *Inorg. Synth.* **1974**, *15*, 5.

120

Chapter **5**

Lewis Acid-Controlled Regioselectivity in Styrene Hydrocyanation

According to present knowledge, the Ni-catalyzed hydrocyanation of styrene leads predominantly to the branched product 2-phenylpropionitrile (98%). A dramatic inversion of the regioselectivity upon addition of a Lewis acid was observed. Up to 83% of the linear product 3-phenylpropionitrile was obtained applying phosphite ligands in the presence of AlCl₃. The mechanism of the Ni-catalyzed reaction and the influence of additional Lewis acids have been elucidated by means of deuterium labeling experiments, NMR studies, and DFT calculations. Furthermore, the behaviour of different Lewis acids, such as CuCN, could be predicted via DFT calculations.
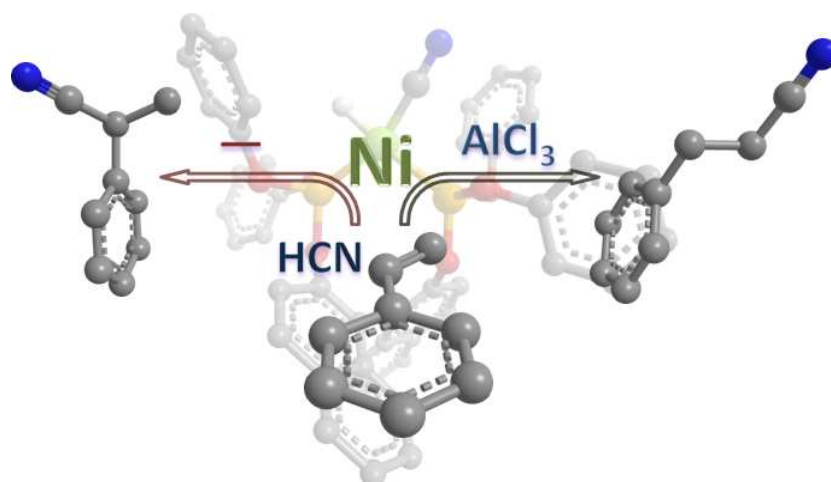
5.1 Introduction

During the past decade, the asymmetric hydrocyanation of norbornene and vinylarenes has attracted new interest as a potentially versatile route to chiral nitriles, amines, and acids.[1] The most successful ligand systems employed in these reactions are based on binaphthyl-,[2] sugar-,[3] xanthene-[4] or triptycene-[5] derived backbones. Very recently self-assembled bidentate phosphine ligands have been applied in the Ni-catalyzed hydrocyanation of styrene.[6] However, still open questions remain on how to improve the performance of the catalyst, and particularly on the role of the Lewis acid co-catalyst[7] that generally has to be applied in the hydrocyanation of non-conjugated alkenes. The promotional effect on the reactivity and the influence on the regioselectivity have been investigated mainly for monoalkenes using several Lewis acids,[8] such as $ZnCl_2$, $AlCl_3$, and BPh_3. Nevertheless, it still remains unclear how exactly the co-catalyst is involved in the reaction and how it enhances the reactivity.

So far, hardly any studies have addressed the application of Lewis acids in the hydrocyanation of vinylarenes. Tolman *et al.*[7] reported on the hydrocyanation of styrene with boron-based Lewis acids and P(O-*o*-tolyl)$_3$ as ligand, leading to the linear nitrile product 3-phenylpropionitrile in up to 33% yield, rather than to the branched product 2-phenylpropionitrile. While the latter is usually obtained as the major product in the hydrocyanation of styrene, this observation was explained with the increase of steric crowding around the nickel centre introduced by the Lewis acid and the bulky phosphite ligand.

The effect of different Lewis acids in the Ni-catalyzed hydrocyanation of styrene is addressed in this chapter (Scheme 5.1). Deuterium labeling experiments and DFT calculations were applied in order to get a better insight into the role of the co-catalyst, especially its influence on the regioselectivity and reactivity.
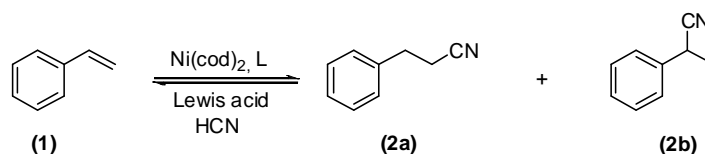
Scheme 5.1. Hydrocyanation of styrene.

5.2. Hydrocyanation of styrene

Diphosphines of the xantphos family, DPEphos, the monodentate phosphite P(OPh)$_3$, and the bulky binaphthyl-isopropylphenyl-diphosphite (BIPPP) (Figure 5.1) were applied in the Ni-catalyzed hydrocyanation of styrene **1** (Scheme 5.1). According to the literature[2, 4] these are among the most efficient ligands for this reaction.

Catalysis experiments were performed at 90°C in toluene with a high catalyst loading of 5 mol%, applying a slight excess of HCN. The influence of AlCl$_3$ as Lewis acid co-catalyst on the activity and on the regioselectivity was investigated for all catalyst systems and the results are listed in Table 5.1. Oligomerization and polymerization of styrene occurred in parallel with the hydrocyanation reaction, lowering the selectivity towards nitrile products.
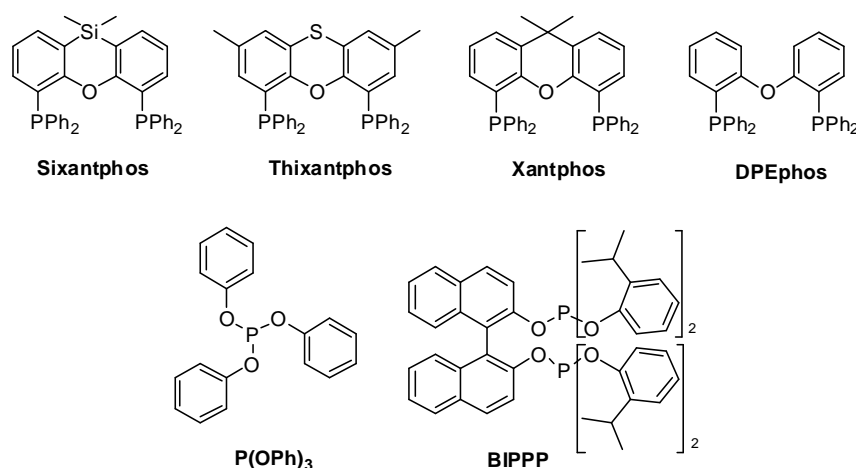
Figure 5.1. Phosphorus ligands applied in hydrocyanation catalysis.

Table 5.1. Hydrocyanation of styrene (neat HCN added in one portion).

Entry	Ligand	Lewis acid	Conversion (%)[a]	Selectivity (%)[b]	l/b[d]
1	Sixantphos	/	90	78	<1/99
2	Sixantphos	$AlCl_3$	77	92	48/52
3	Thixantphos	/	92	58	<1/99
4	Thixantphos	$AlCl_3$	84	77	19/81
5	Xantphos	/	74	85	<1/99
6	Xantphos	$AlCl_3$	97	64	6/94
7	DPEphos	/	53	40	<1/99
8	DPEphos	$AlCl_3$	71	47	23/77
9[c]	$P(OPh)_3$	/	62	63	8/92
10[c]	$P(OPh)_3$	$AlCl_3$	96	81	83/17
11	BIPPP	/	100	86	9/91
12	BIPPP	$AlCl_3$	100	51	74/26

Conditions: 0.033 mmol Ni(cod)$_2$, Ni:Lewis acid:L:S:HCN=1:1.05:1.2:20:25, T = 90℃, 16 h, 1 mL toluene. [a] Conversions are based on the substrate and were determined by GC using n-decane as internal standard. [b] Selectivity= yield of nitriles/conversion. Styrene oligomers are identified as by-products. [c] Ligand to nickel ratio=5. [d] Linear/ Branched ratio.

In the absence of $AlCl_3$ the phosphine-based catalysts produced exclusively the branched product 2-phenylpropionitrile **2b** (Table 5.1; Entry 1, 3, 5, 7). Likewise, styrene was converted predominantly into the branched product using the mono- and di-phosphites $P(OPh)_3$ and BIPPP, respectively (Table 5.1; Entry 9 and 11). However, a small amount of the linear product 3-phenylpropionitrile **2a** was also obtained (<10%), while at lower temperature (60°C) the branched product was again formed selectively.[2] This observation is in accordance with several literature examples in which high regioselectivities towards the branched product (>98%) were reported for this particular reaction. The regioselectivity was attributed to the preferred formation of η^3-benzylic nickel intermediates.[2-4]

Interestingly, this trend in product distribution was dramatically reversed upon addition of the Lewis acid $AlCl_3$: up to 83% of the linear product **2a** was obtained with

Scheme 5.2. Isomerization of 2-phenylpropionitrile to 3-phenylpropionitrile under catalytic conditions.

the system [Ni/P(OPh)$_3$], while this catalyst produces 92% of **2b** in the absence of AlCl$_3$ (Table 5.1; Entry 9, 10). Moreover, the presence of AlCl$_3$ in this particular system also influenced both conversion (96% versus 62%) and selectivity (81% versus 63%) towards nitriles (Table 5.1; Entry 9, 10). In general it turned out that the observed effect on the regioselectivity was more pronounced for the more active phosphite-based catalysts than for the phosphine-based ones (Table 5.1; Entries 9-12).[2, 4] In fact, the Ni-catalysts based on the phosphine ligands DPEphos, Thixantphos and Xantphos did not show such remarkable inversion of the selectivity. Only 10-20 % of the linear product was detected in the final mixture (Table 5.1; Entries 4, 6 and 8), while Sixantphos gave almost a 1:1 mixture of linear and branched nitriles (Table 5.1; Entry 2).

In order to exclude any Ni-catalyzed isomerization of 2-phenylpropionitrile towards 3-phenylpropionitrile and *vice versa* as a possible reason for these unexpected results, commercially available **2b** was heated to 90°C in the presence of the most active Ni-complex based on Ni(cod)$_2$, AlCl$_3$, and BIPPP. In fact, this mechanism is known for the Ni-catalyzed hydrocyanation of butadiene: the two major products 3-pentenenitrile and 3-methyl-2-butenenitrile can interconvert after the hydrocyanation step, with a C-C activation step involved in this process.[5] However, such a reaction does not occur in the hydrocyanation of styrene, since no conversion to 3-phenylpropionitrile was observed. Thus, the production of the linear nitrile **2a** can only proceed *via* the formation of a σ-alkyl intermediate (Figure 5.2). Interestingly, such species has never been reported before for the hydrocyanation of vinylarenes.

5.3. Deuterium labeling experiments

To verify whether the formation of a Ni-alkyl intermediate could occur in the presence of AlCl$_3$, hydrocyanation experiments of deuterated styrene (styrene-d_8) were performed. Deuterium labeling studies have been reported for various hydrocyanation reactions before, especially for mechanistic investigations.[3a, 7, 9] In particular, Casalnuovo and Rajanbabu[3a] reported on experiments with MVN (6-methoxy-2-vinyl-naphthalene) and 4-substituted styrenes. Branched nitriles were the only products observed and the deuterium incorporation proceeded exclusively in the β-methyl-position. Moreover, η^3-allyl complexes (Figure 5.2) have also been described as intermediates in the hydrocyanation of dienes,[7,10] vinylarenes[3a,7] and in the isomerization of 2-methyl-3-butenenitrile to 3-pentenenitrile.[11] The η^3-benzyl-intermediate was generally assumed to be the preferred intermediate formed after insertion of a vinylarene into the Ni-H bond, rather than the linear σ-alkyl intermediate (Figure 5.2).

The Ni-catalyzed hydrocyanation of styrene-d_8 was carried out both in the presence and in the absence of AlCl$_3$, using P(OPh)$_3$ as ligand. The conversion reached approximately 40% in both cases, thus lower than with non-deuterated styrene as substrate. In the presence of AlCl$_3$ a linear/branched ratio of 73/27 was observed, while the linear product was only obtained in traces (detected by GC) in the absence of Lewis acid. The lower conversion and selectivity might be due to the different purification procedure applied for styrene and styrene-d_8. The latter was degassed and filtered, while
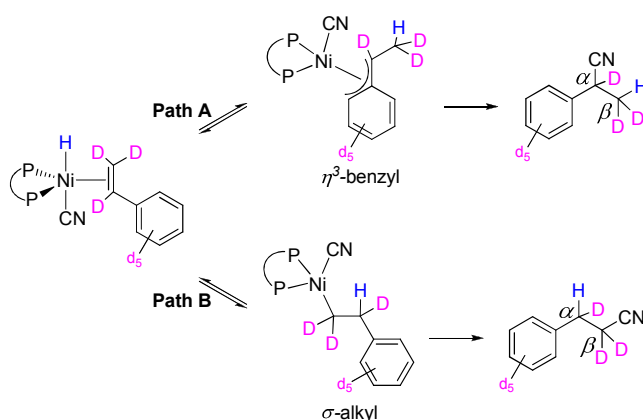
Figure 5.2. Proposed catalytic pathways for hydride incorporation.
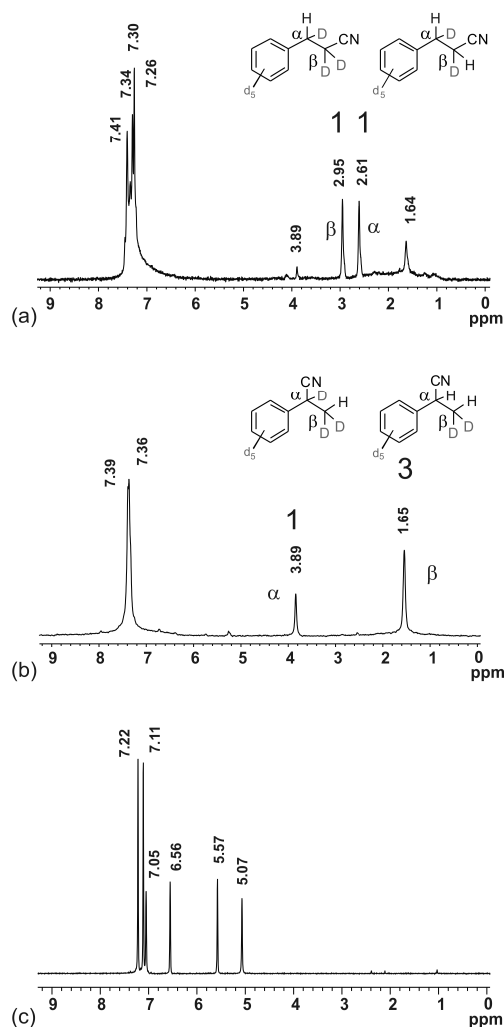
Figure 5.3. ^{2}H NMR spectra of the reaction mixture after hydrocyanation of deuterated styrene in the presence of AlCl$_3$ (a) and in the absence of Lewis acid co-catalyst (b). The ^{2}H NMR spectrum of styrene-d_8 is also added as reference (c).

styrene was also distilled. The formation of a η^3-benzyl Ni-species (Path A; Figure 5.2) during the hydrocyanation of styrene-d_8 implies the addition of the hydride (generated from oxidative addition of HCN to Ni(0)) in β-position of the phenyl group in **2a**. In contrast, the formation of a Ni-alkyl species (Path B; Figure 5.2) implies the addition of the hydride in α-position of the phenyl group in **2b**. ^{1}H and ^{2}H NMR spectroscopic investigations on the hydrocyanation reaction mixtures showed, however, an unexpected deuterium distribution (Figure 5.3).

In the ^{2}H NMR spectrum the ratios between the deuterium atoms in α and β position of the two propionitrile products differ from the expected values (Figure 5.3 (a) and (b)). One deuterium atom in α and two in β position to the phenyl group were expected for the

127

linear nitrile, but the ratio calculated *via* the integrals in the NMR spectrum was 1:1. One deuterium atom in α and two in β position to the phenyl group were expected also for the branched nitrile, the observed ratio was 1:3. The experimental data suggest that proton incorporation is not selective. Moreover, the ^{1}H NMR shows the presence of protons in α and in β positions (Figure 5.4 (a) and (b)) and, consequently, the hydride was added in both positions in the linear and in the branched products. Both the η^3-benzyl and σ-alkyl intermediates must therefore be formed, since the incorporation of a hydride in the α position of the branched product can only be explained by the presence of an alkyl-intermediate in equilibrium with the η^3-benzyl species.

(a)

(b)
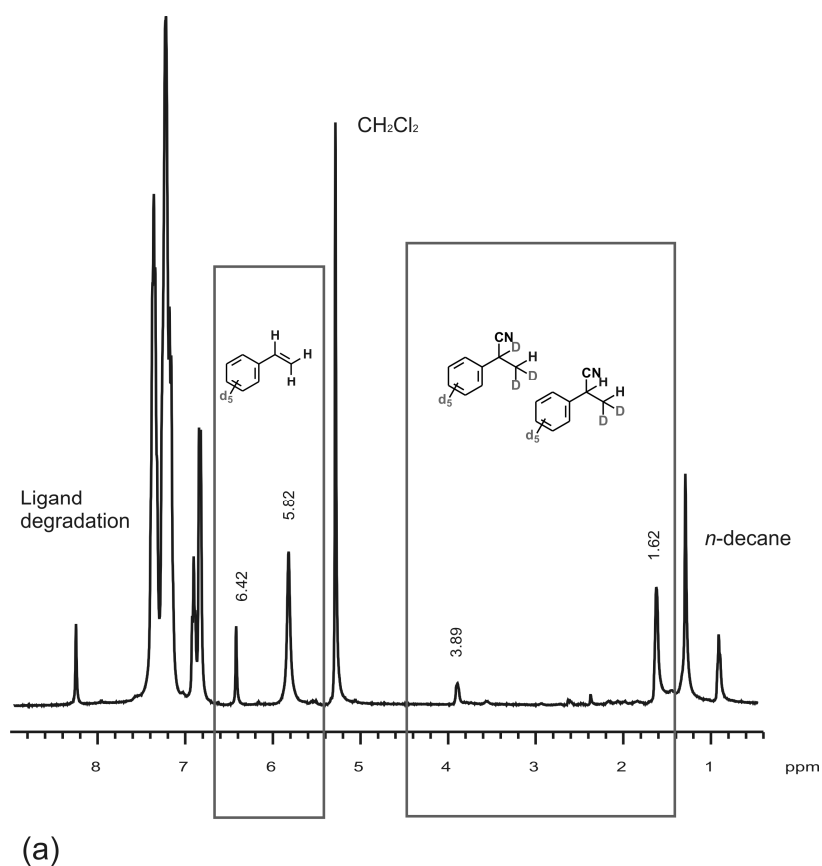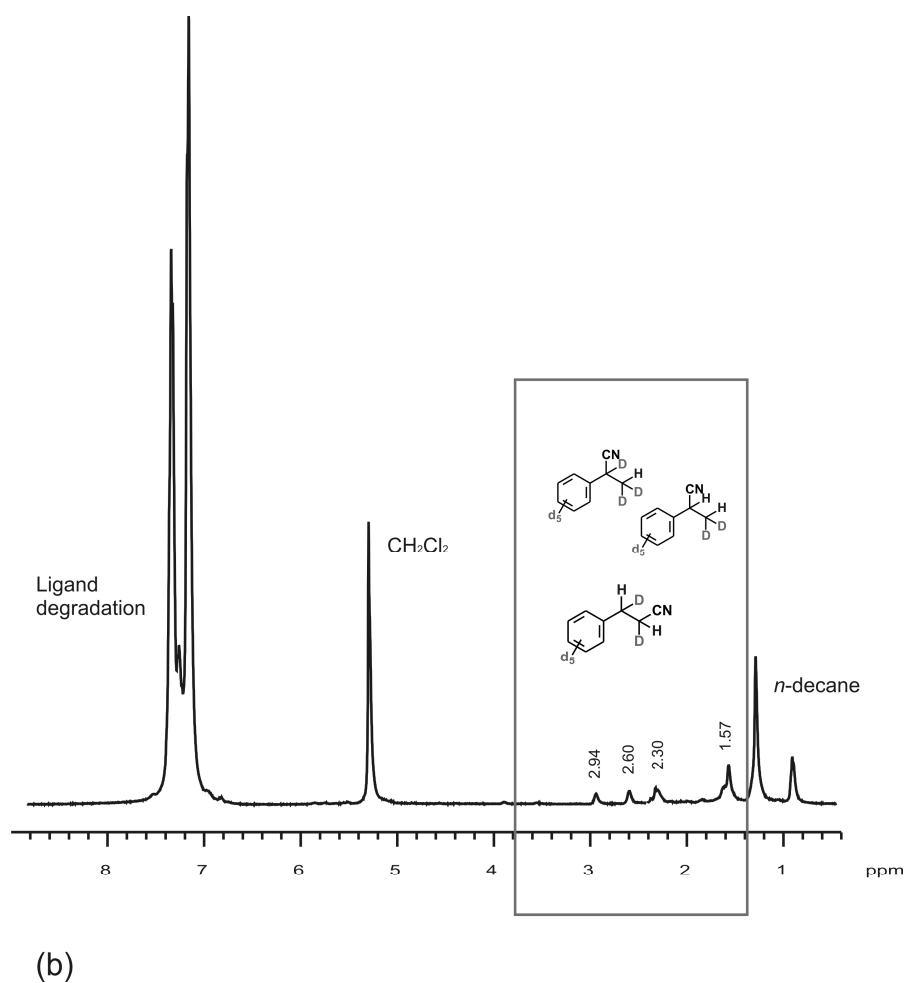
Figure 5.4. ^{1}H NMR spectrum of the crude mixture for the styrene–d_8 hydrocyanation in the absence of AlCl$_3$ (in benzene-d_6). Protons are detected in α and in β position to the nitrile of the branched product (**2b**). Peaks of the unreacted styrene are also present (a). ^{1}H NMR spectrum of the crude mixture for the styrene–d_8 hydrocyanation in the presence of AlCl$_3$ (in benzene-d_6). Protons are detected in α and in β position to the nitrile of the linear (**2a**) and the branched product (**2b**) (b).

Similar considerations can be made for the linear product: the hydride in β-position implies the formation of a η^3-benzyl intermediate as well as a σ-alkyl intermediate, responsible for the presence of the nitrile in terminal position.

Nevertheless, AlCl$_3$ seems to be crucial for the reductive elimination of the linear nitrile-product, which is obtained in significant amount only in the presence of the Lewis acid. The hydride incorporation and the deuterium scrambling were also detected for the unreacted styrene in the reaction mixture. Therefore, it was concluded that the two Ni-species are in equilibrium with the free styrene.

5.4. Lewis acid effect on the reaction rate: hydrocyanation versus polymerization

The hydrocyanation reaction at lower catalyst loading and under slow HCN addition *via* a syringe pump was further investigated. The results are reported in Table 5.2.[12] The diphosphite ligand (BIPPP) gave high conversion and high selectivity with S/Ni ratios of 100 and 300 (Table 5.2; Entries 3 and 6). The Lewis acid effect was still present using $P(OPh)_3$ as ligand, but the reaction showed low conversion and low selectivity to nitriles (Table 5.2; Entry 2). The other experiments performed with the diphosphite ligand BIPPP and $AlCl_3$ led to very poor selectivity towards the nitrile products. On increasing the concentration of Lewis acid, the selectivity drops dramatically (Table 5.2; Entry 5).

The lower nitrile selectivity observed for lower catalyst loading, especially in the presence of $AlCl_3$, is likely caused by a Lewis acid-catalyzed oligomerization/polymerization of styrene.[13] Upon heating of styrene to 90°C in the presence of the complex [(BIPPP)Ni(cod)] for 4 h, no polymerization was detected. However, the addition of $AlCl_3$ led to total conversion of the substrate to polymeric material. Similar results were also obtained in a control experiment after addition of

Table 5.2. Hydrocyanation of styrene with slow HCN addition.

Entry	Ligand	Lewis acid	Conversion (%)[a]	Selectivity (%)[b]	l/b[d]
1[c]	$P(OPh)_3$	/	17	87	<1/99
2[c]	$P(OPh)_3$	$AlCl_3$	27	11	44/66
3	BIPPP	/	99	100	7/93
4	BIPPP	$AlCl_3$	22	30	<1/99
5[e]	BIPPP	$AlCl_3$	100	2	<1/99
6[f]	BIPPP	/	97	68	1/99

Conditions: 0.00925 mmol $Ni(cod)_2$, Ni: Lewis acid : L :S :HCN = 1: 1.05: 1.2: 100: excess, 90°C, 4 h, 1 mL toluene. [a] Conversions are based on the substrate and were determined by GC using n-decane as internal standard. [b] Selectivity = yield of nitriles/conversion. Styrene oligomers are identified as by-products. [c] Ligand to nickel ratio = 5. [d] Linear/Branched ratio. [e] $AlCl_3$ to nickel ratio=20 [f] Substrate to nickel ratio=300.

AlCl$_3$ and AlCl$_3$/HCN to styrene in the absence of the Ni-catalyst. A white powder was isolated from the reaction mixture and analyzed by IR spectroscopy (Figure 5.5), confirming the formation of polystyrene. GC-analysis of the solution showed total conversion of the styrene. Consequently, the addition of an excess of HCN in the presence of the Ni-catalyst seems to be crucial for trapping aluminium species and preventing the polymerization reaction.
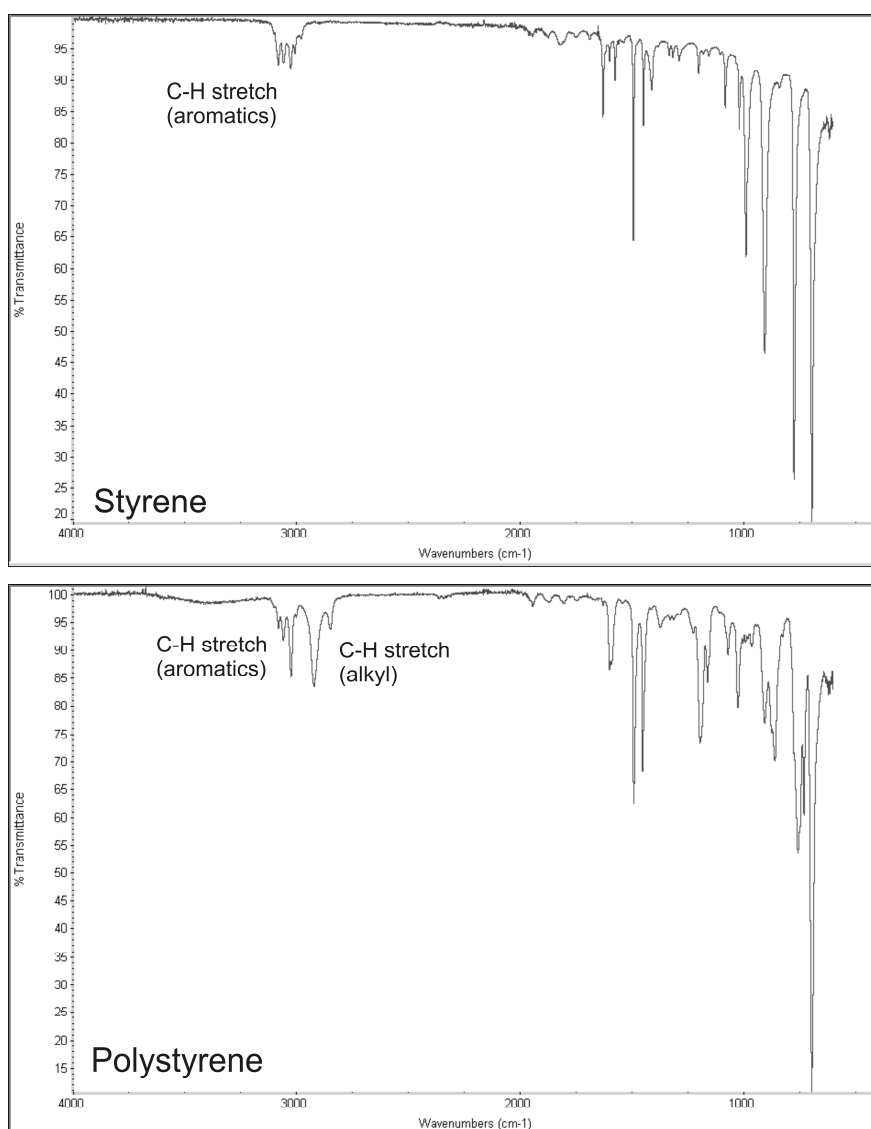
Figure 5.5. IR spectra of styrene and polystyrene, obtained after stirring styrene in the presence of [(**BIPPP**)Ni(cod)]*(AlCl$_3$).

5.5. DFT calculations and NMR spectroscopy

5.5.1. DFT calculations and NMR experiments on AlCl₃ coordination

The coordination behavior of $AlCl_3$ was investigated by means of DFT calculations as well as by ^{1}H and ^{31}P NMR spectroscopy in order to understand the role of the Lewis acid in the hydrocyanation reaction. The interaction of the Lewis acid $AlCl_3$ with the substrates styrene and HCN and with the phosphite ligand, the Ni(0) catalyst precursor, and one Ni(II) intermediate were examined. The computed energies for the formation of the corresponding species are summarized in Figure 5.6.

The interaction of $AlCl_3$ with the π-system of the arene moiety of styrene (**1**) was first considered (Figure 5.6). This type of interaction might prevent the formation of a (η³-benzyl)Ni-species, which is generally considered to be responsible for the exclusive formation of the branched product for this type of substrates.[3a] However, DFT calculations indicate that the formation of complexes **(1a-c)$_{Al}$** is rather unfavorable
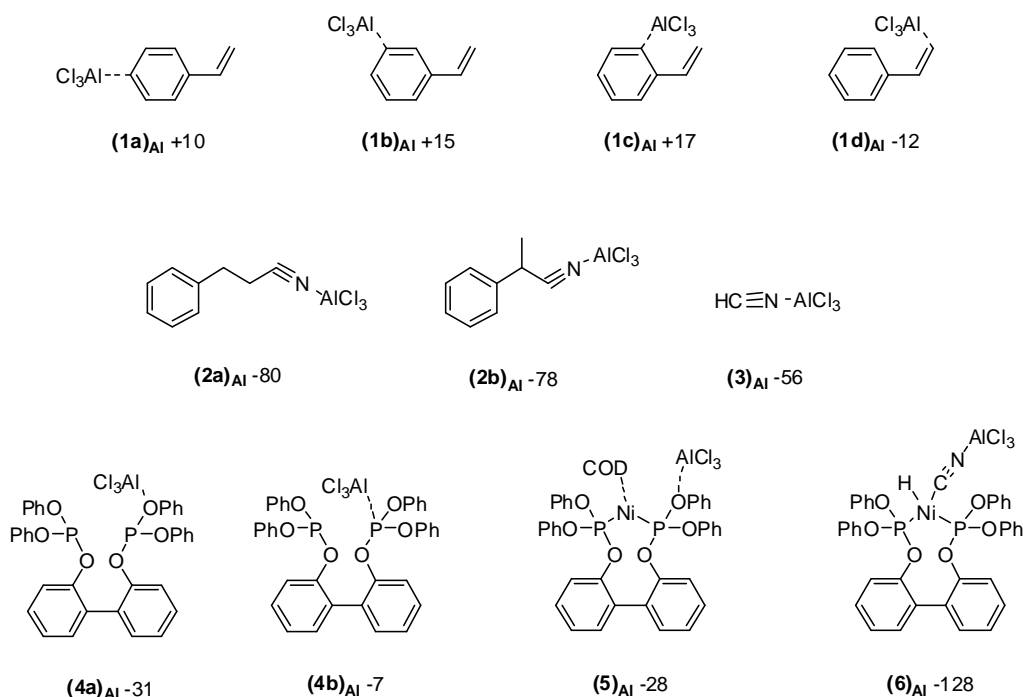
Figure 5.6. Coordination modes for $AlCl_3$ Lewis acid to various substrates (S) present in the reaction mixture and their relative stabilities defined as the corresponding DFT computed free energy changes (ΔG^{solv}, kJ mol^{-1}) in toluene for the reaction $S + \frac{1}{2} Al_2Cl_6 \rightarrow S\cdots AlCl_3$ (ΔG^{solv} for the reaction $Al_2Cl_6 \rightarrow 2\ AlCl_3$ in toluene equals +80 kJ mol^{-1}).

(Figure 5.6). The energy difference for the binding of the Lewis acid to various positions of the phenyl ring does not exceed 7 kJ/mol and, hence, a substituent-effect does not seem to play a significant role. On the other hand, coordination of $AlCl_3$ to the vinyl group of styrene (**(1d)$_{Al}$**) is favorable and the corresponding complex is by 22−29 kJ/mol more stable than those involving coordination to the phenyl group. Independent of the coordination site, $AlCl_3$ binds to only one carbon atom of styrene resulting in a

Figure 5.7. ^{1}H NMR spectra of styrene and styrene($AlCl_3$) (in $CDCl_3$). The shift of the vinylic proton resonances upon addition of $AlCl_3$ shows Lewis acid coordination to the vinyl group.

tetrahedral coordination of the Al^{3+} ion. The calculated higher stability for complex **(1d)$_{Al}$** is in agreement with the ^1H and ^{13}C NMR data of styrene, that show a shift of the vinylic proton- and carbon-resonances to lower field upon addition of $AlCl_3$ (Figure 5.7). Furthermore, this species is the prevalent one detected at room temperature by NMR spectroscopy.

Possible competing interactions of $AlCl_3$ with the Lewis-basic oxygen or phosphorus atoms of the BIPPP ligand and with the corresponding Ni-complexes were further considered. DFT calculations show that the coordination of the Lewis acid to the ligand is preferred over coordination to the styrene substrate. To perform the model DFT calculations the BIPPP ligand was replaced by the simplified phosphite ligand (**4**). Coordination of $AlCl_3$ to one of the oxygen atom results in the formation of the rather
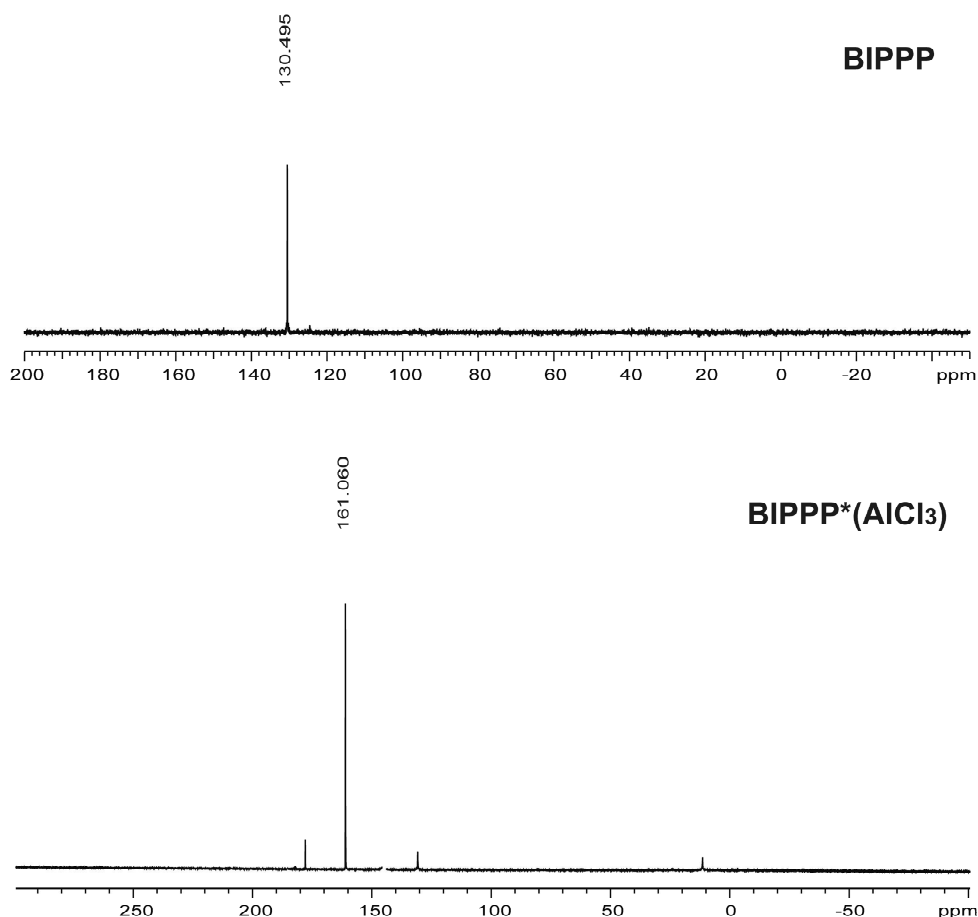
Figure 5.8. ^{31}P NMR spectra of the phosphite ligand BIPPP and BIPPP*($AlCl_3$) (in benzene-d_6).

stable complexes **(4a)$_{Al}$** and **(5)$_{Al}$**. Although the interaction with the phosphorus atom in **(4b)$_{Al}$** is thermodynamically slightly favored, the resulting energy gain is substantially lower as compared to that in the cases of the O-bound complexes. The theoretical calculations were supported by NMR spectroscopic investigations. In fact, the ^{31}P NMR spectrum of an equimolar mixture of BIPPP and AlCl$_3$ in benzene-d_6 clearly shows a shift of the phosphorus resonance from 130 to 160 ppm (Figure 5.8).[14] In the case of the corresponding complex [(BIPPP)Ni(cod)]*(AlCl$_3$) a shift of the signal to higher field could be detected (δ(ppm) = 140 vs. 126) (Figure 5.9). The preference for the formation
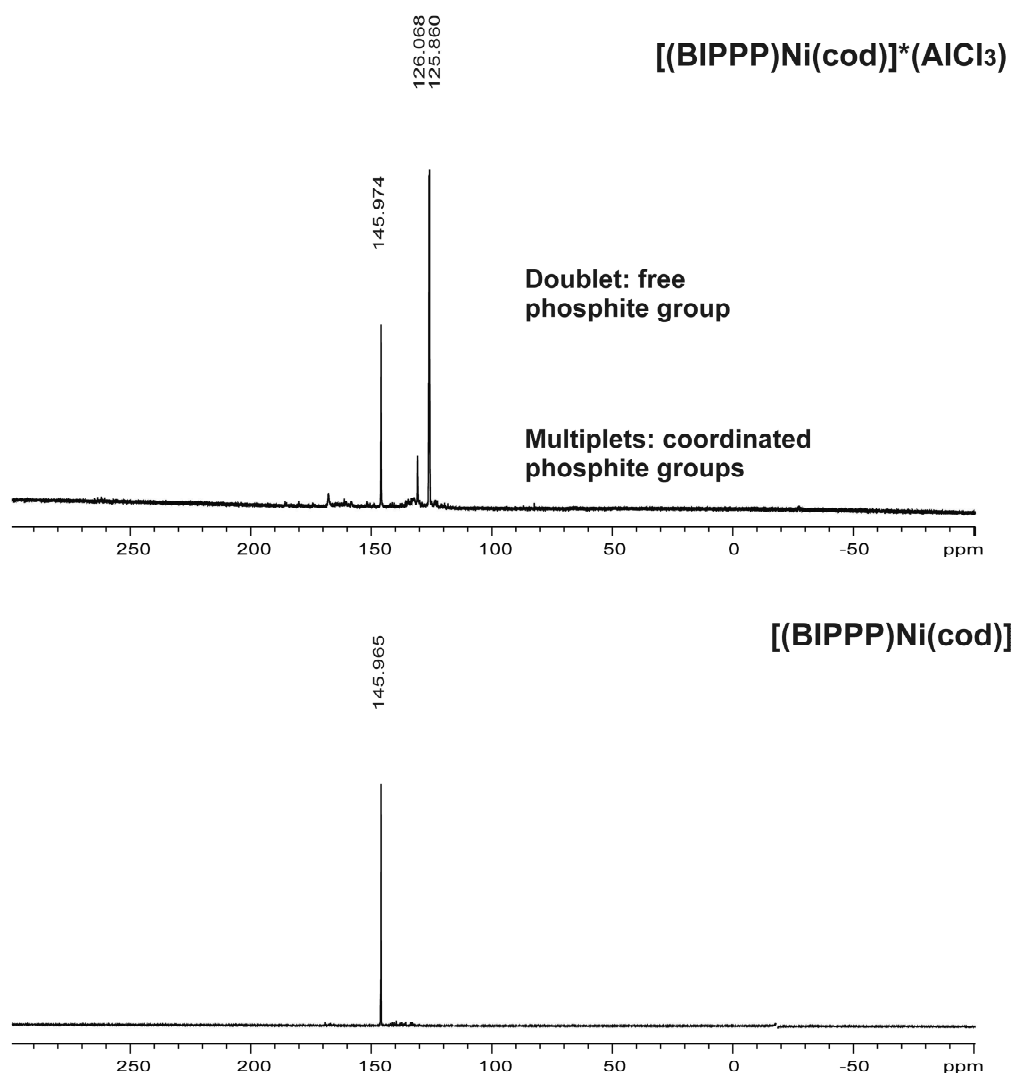
Figure 5.9. ^{31}P NMR spectra of the [(BIPPP)Ni(cod)] and [(BIPPP)Ni(cod)]*(AlCl$_3$) complexes (in benzene-d_6).

of the Al···O interaction over the Al···P interaction is probably due to the fact that the Lewis acid AlCl$_3$ binds stronger to the "hard" oxygen atom rather than to the "softer" phosphorus atom.[15] In agreement with the DFT computed free energy changes, the ^{31}P NMR spectroscopy indicates that the addition of styrene to [(BIPPP)Ni(cod)]*(AlCl$_3$) does not displace the AlCl$_3$ from the oxygen atom.

Due to the higher basicity of the nitrogen atom in the CN group among the species considered, the strongest binding of the Lewis acid was found for the CN-containing compounds. Even the least basic free HCN molecule binds the AlCl$_3$ co-catalyst ((**3**)$_{Al}$) somewhat stronger than the phosphite ligand ((**4**)$_{Al}$) and the Ni-catalyst precursor ((**5**)$_{Al}$). These results confirm the trapping of AlCl$_3$ by HCN, which prevented the Al-catalyzed polymerization of styrene.

The strongest interaction is predicted for the adduct (**6**)$_{Al}$, that is formed via oxidative addition of HCN to the Ni(0) catalyst. This is due to the higher basicity of the anionic CN group in the [L$_2$Ni(H)CN] species compared to that in the covalently bound free HCN and nitrile species. The result is in line with the computed NBO charges on the N-atom in the corresponding species (**2a**: −0.34 e⁻, **2b**: −0.34 e⁻, **3**: −0.31 e⁻, **6**: −0.49 e⁻). Indeed, the oxidative addition of HCN to the Ni(0) species and the resulting significant polarization of the CN-moiety substantially enhance the basicity of the nitrogen atom in **6**. Although a fast equilibrium is expected between the complexes with HCN and the hydrocyanation products, the much higher free energy of formation of complex (**6**)$_{Al}$ indicate, that as soon as the initial oxidative addition of HCN takes place, the Lewis acid is bound to the active Ni-containing complex.

5.5.2. DFT calculations based on the hydrocyanation catalytic cycle

To provide a molecular-level insight into the actual role of the Lewis acid co-catalyst in the hydrocyanation reaction, the energetics of the elementary reaction steps involved and of the full catalytic cycles both in the presence and in the absence of the Lewis acid co-catalyst AlCl$_3$ were analyzed by means of DFT calculations.

The catalytic cycle[2-4,7] corresponding to the hypothetical situation, when the Lewis acid co-catalyst remains attached to the active Ni-complex during the hydrocyanation reaction (Figure 5.10(a)) was first considered. The Lewis acid does not leave the

Ni-complex simultaneously with the products of the reaction during the active site regeneration step (step **8a,b** → **6** + **2a,b**, Figure 5.10(a)). In principle, this would correspond to the thermodynamically most favorable situation. Although this cycle does not fully represent the mechanistic details of the hydrocyanation reaction, its
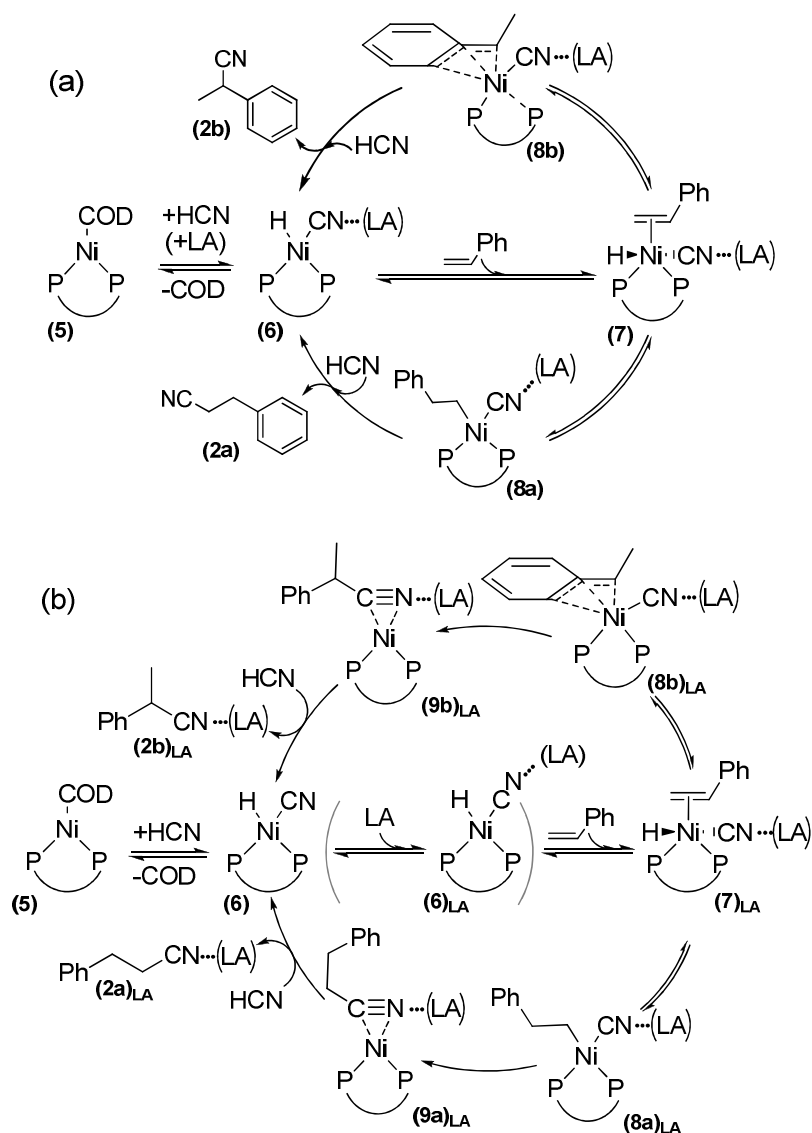
Figure 5.10. Simplified catalytic cycles considered in DFT calculations for styrene hydrocyanation with a model Ni-catalyst (5). Part (a) depicts the generally accepted thermodynamic cycle[2–4, 7] based on the preferential mode of coordination of the AlCl₃ Lewis acid, whereas part (b) shows a more complex reaction scheme reflecting the mechanistic details of the catalytic reaction. In both cases, LA indicates a Lewis acid depending on whether the reaction takes place in the presence or in the absence of the co-catalyst, respectively.

consideration allows the determination of the reaction steps, whose thermodynamics are mostly affected by the presence of the Lewis acid co-catalyst. The corresponding free energy changes along the reaction coordinates (Figure 5.10(a)) are summarized in Figure 5.11(a). The catalytic cycle both in the presence and in the absence of the Lewis acid co-catalyst is initiated by oxidative addition of HCN to the Ni(0)–center with simultaneous elimination of the COD ligand. Within the postulated thermodynamic cycle it is considered that the introduction of the $AlCl_3$ species takes place at this step.

In the absence of $AlCl_3$, the initial step (**5**→**6**, Figure 5.10(a)) proceeds with a very slight energy change (Figure 5.11(a)). Subsequent coordination of the styrene molecule to compound **6** is slightly unfavorable. Taking into account the exothermic nature of this reaction ($\Delta E^{ZPE} = -4$ kJ mol^{-1}) the positive value of the computed reaction free energy is due to the significant entropy loss upon formation of adduct **7**. In agreement with the above presented deuterium labeling experiments, which indicated the formation of η^3–benzyl and σ–alkyl Ni complexes during the reaction, the DFT calculated free energies for the formation of (**8a**) and (**8b**) from **7** are equal to –35 and –33 kJ mol^{-1}, respectively. Thus, although the higher stability of the η^3–benzyl complex is anticipated[7], in this particular case there is no apparent preference for the formation of either of the complexes. This relatively small energy difference is most likely due to the bulkiness of the bidentate phosphite ligand **4** that destabilizes complex **8b**. The closure of the catalytic cycle proceeds *via* the reductive elimination of products **2a** or **2b** followed by the oxidative addition of the next HCN molecule (**8a**→**6**+**2a** and **8b**→**6**+**2b**, Figures 5.10(a) and 5.11(a)). According to the DFT computed associated free energy changes (ΔG^{solv}, Figure 5.11(a)) these reactions are thermodynamically strongly favored. At this step for the first time within the thermodynamic cycle considered, the preference for the formation of a particular isomer is observed. However, in contrast to the experimental observations, the energetics presented suggest the preference for the formation of the linear product **2a**.
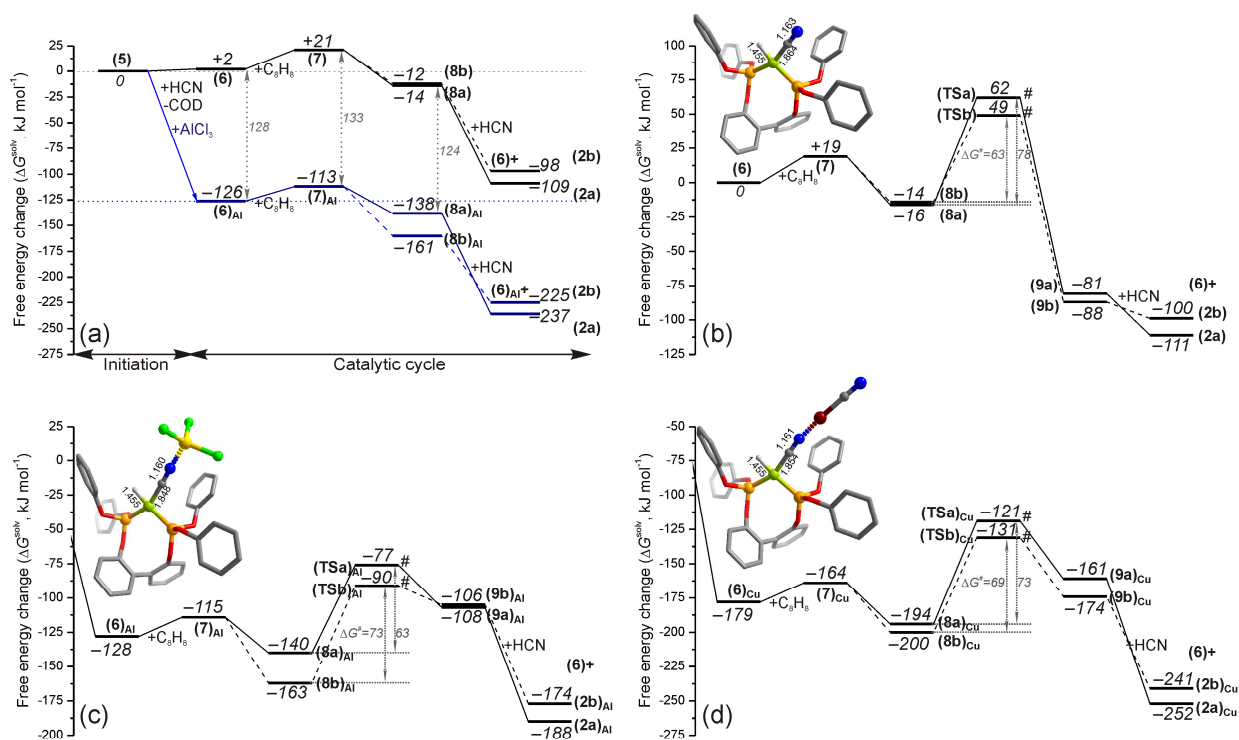
Figure 5.11. DFT computed reaction free energy diagrams (ΔG^{solv}, kJ mol^{-1}) for catalytic hydrocyanation reactions with Ni-(4) model complex: part (a) represents the thermodynamic cycle constructed under the assumption that the Lewis acid is always attached to the Ni-complex (as illustrated in Figure 5.11(a)). The free energy changes corresponding to the catalytic cycle that follows the mechanistic paths (according to the reaction scheme in Figure 5.10(b)) in the absence and in the presence of the AlCl$_3$ and CuCN co-catalysts are shown in parts (b), (c) and (d), respectively. Complex 6 is chosen as the zero-level for the free energy diagrams (b)-(c). Dashed lines in all diagrams correspond to the reaction path leading to the formation of branched product (2b), whereas the solid lines correspond to the formation of the linear product (2a). Corresponding molecular structures of the active DFT optimized complexes (6)$_X$ and selected bond lengths (Å) are shown for comparison.

As depicted in the diagram shown in Figure 5.11(a), the addition of AlCl$_3$ apparently causes a shift of the relative energies by ~130 kJ/mol compared to the Lewis-acid free situation. This value corresponds to the binding energy of the AlCl$_3$ species to complex **6**. Thus, the most notable effect of the Lewis acid is observed for the initial step of the hydrocyanation reaction with the formation of intermediate **6**. In the absence of AlCl$_3$, oxidative addition of HCN to the Ni precursor **5** is endothermic ($\Delta E^{ZPE} = 25$ kJ mol^{-1}). The complex **5** and the active species **6** are in equilibrium ($\Delta G^{solv} = +2$ kJ mol^{-1}). On the other hand, when the AlCl$_3$ co-catalyst is present in the reaction mixture, this initial step

is highly exothermic (ΔE^{ZPE} = –124 kJ mol^{-1}) and the equilibrium is completely shifted towards formation of the product of HCN oxidative addition (**6**)$_{Al}$ (ΔG^{solv} = –128 kJ mol^{-1}). The relative energies of most of the subsequent intermediates of the catalytic cycle are apparently not affected by the presence of the co-catalyst, as their energy separation remains essentially constant during the course of the reaction. This suggests only a minor variation of the basicity of the N-center of the CN moiety with respect to other ligands in the square-planar (**6** and **8a**) and "trigonal-bipyramidal" (**7**) Ni complexes. Indeed, the deviation in the NBO computed charges on the N-atom in the respective complexes does not exceed 0.02 e$^-$. The only substantial effect of the Lewis acid co-catalyst within the effective catalytic cycle is observed for the relative stability of the η^3–benzyl Ni complexes (**8b**) and (**8b**)$_{Al}$ (Figure 5.10(a)). In fact, interaction with AlCl$_3$ stabilizes the branched adduct **8b** by 149 kJ mol^{-1}, which is substantially larger than the stabilization energies computed for other reaction intermediates (Figure 5.11(a)). As a result and in contrast to the situation when no co-catalyst is present in the reaction mixture, there is a clear thermodynamic preference for the formation of the branched complex (**8b**)$_{Al}$. The stronger interaction of AlCl$_3$ with **8b** is due to the specific coordination environment of the Ni–center. Complex **8b** contains a bulky η^3–benzyl moiety as compared to the linear intermediate **8a** (Figure 5.12) that is accompanied with the strong displacement of the cyanide group. The distorted coordination in **8b** results in an elongation and an increase in ionic character of the Ni–CN bond (Figure 5.12) as compared to the situation in **8a**. The NBO-summed charge on the CN moiety increases by more than 0.1 e$^-$, while Ni is stronger positively charged by 0.2 e$^-$ in **8b**. These perturbations enhance the basicity of the N atom (the corresponding NBO charge increases by 0.04 e$^-$) in the Ni–CN moiety resulting in a higher affinity towards AlCl$_3$ binding and a substantial additional stabilization (by ~50 kJ mol^{-1}) of the respective complex (**8b**)$_{Al}$.

5.5.3. Addition of mechanistic details to the catalytic cycle

Nevertheless, the thermodynamic data computed for the hydrocyanation catalytic cycle[2-4] (Figure 5.11(a)) cannot explain the selectivity patterns observed experimentally both in the presence and in the absence of the Lewis acid co-catalyst (Table 5.1). This is

ΔG^{solv} = −65 and $\Delta G^{\#,solv}$ = 78

ΔG^{solv} = −74 and $\Delta G^{\#,solv}$ = 63

ΔG^{solv} = 34 and $\Delta G^{\#,solv}$ = 63

ΔG^{solv} = 57 and $\Delta G^{\#,solv}$ = 73
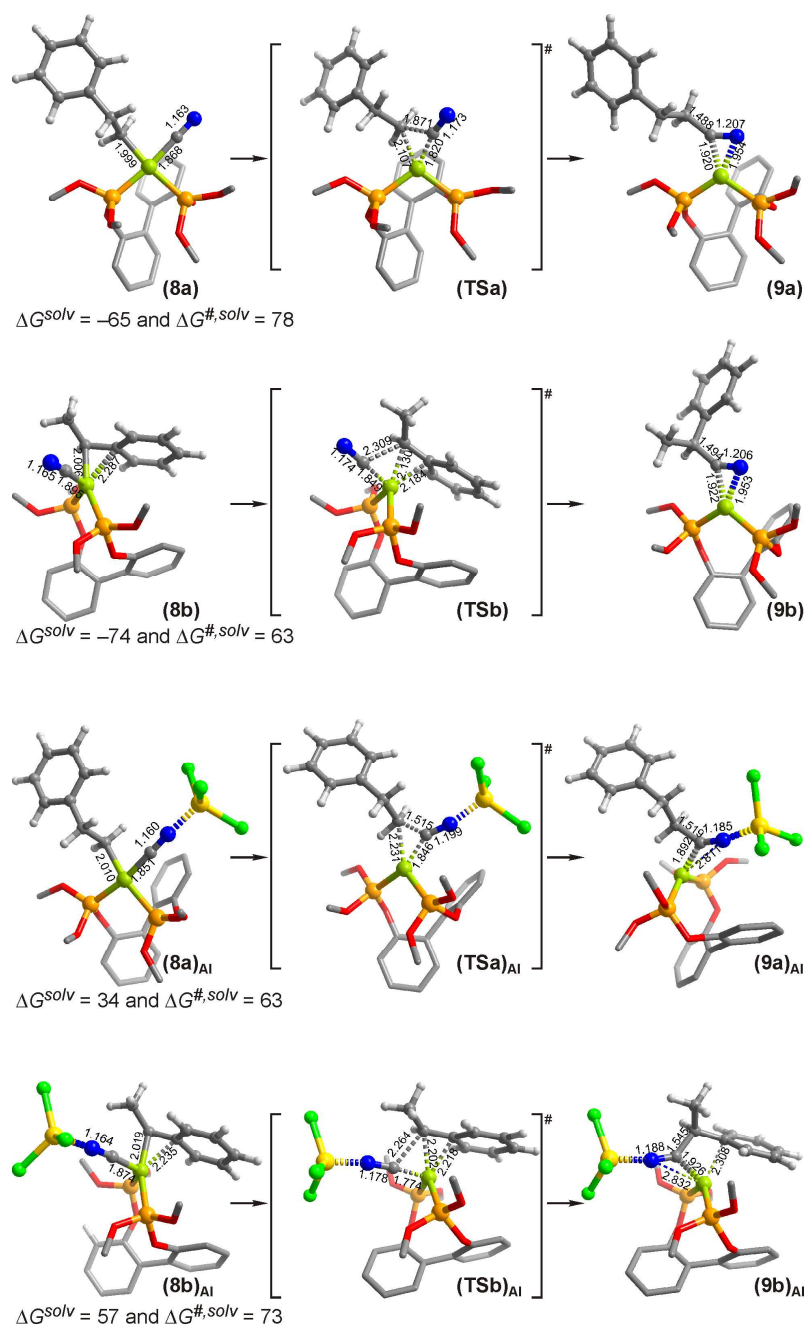
Figure 5.12. DFT optimized structures involved in the reductive elimination elementary step of the catalytic hydrocyanation of styrene to Ni-(4) catalyst in the presence and in the absence of the AlCl$_3$ Lewis acid co-catalyst (Ni: yellow−green, N: blue, C: dark grey, H: light grey, P: orange, O: red, Al: yellow, Cl: green). The corresponding DFT computed activation ($\Delta G^{\#,solv}$, kJ mol^{-1}) and reaction (ΔG^{solv}, kJ mol^{-1}) free energies in toluene (ΔG^{solv}) for the reductive elimination step of catalytic hydrocyanation of styrene to Ni-(4) model catalyst are given in italic. Selected optimized bond lengths are shown in Å. Molecular details of the L2 ligand (hydrogen atoms and phenyl substituents) are omitted for clarity.

due either to a lack of mechanistic details in the cycle considered or to the effects on the variation of the kinetic parameters (activation energies) upon Lewis acid coordination along the reaction coordinate. In particular, the reductive elimination of the hydrocyanation products **2** and the regeneration of the active species **6** should take place as two consecutive elementary steps. As a result, the Lewis acid would leave the catalytic cycle as part of the product of reductive elimination ((2)$_{Al}$). This would initially result in the formation of a molecular coordination complex between the coordinatively unsaturated Ni-(**4**) complex and the nitrile product. In the next step, an additional HCN molecule that rapidly undergoes oxidative addition, leading to the regeneration of the active complex **6**, replaces the nitrile product. The corresponding catalytic cycles towards formation of linear and branched products both in the presence and in the absence of Lewis acid are schematically illustrated in Figure 5.10(b).

It is important to point out again the differences in the interaction energies between AlCl$_3$ and the CN group bound to the Ni center and the same interaction of AlCl$_3$ with the nitrile products (Figure 5.6). Corresponding stabilization effects are expected for the reaction intermediates by the Lewis acid co-catalyst within the catalytic cycle. The implication of the above-mentioned additional mechanistic details may have changed the thermodynamic picture of the hydrocyanation cycle substantially. Therefore, the effect of AlCl$_3$ on the thermodynamics of the corresponding catalytic cycles (Figure 5.11(b)) was analyzed by means of DFT calculations. In addition, and in order to better understand the possible kinetic effects due to the presence of the co-catalyst, the activation free energies ($\Delta G^{\#,solv}$) for the rate-limiting[16] reductive elimination steps were computed. Optimized structures of the reaction intermediates and the transition states involved in the reductive elimination steps are shown in Figure 5.12. The DFT-computed free energy diagrams in the absence and in the presence of the AlCl$_3$ co-catalyst are depicted in Figure 5.11 parts (b) and (c), respectively.

The major change in the qualitative thermodynamic picture due to the implication of the more realistic catalytic cycle (Figure 5.10(b)) was observed in the relative stabilities of the direct products of the reductive elimination **9a** and **9b** (Figure 5.11(b)). The formation of the branched nitrile coordinated to the Ni–complex (**8b** → **9b**) in toluene is thermodynamically more favored (ΔG^{solv}, Figure 5.12) over the formation of the linear

isomer (**8a** → **9a**). Furthermore, the computed activation free energy ($\Delta G^{\#,solv}$) for the former elementary reaction step is 15 kJ mol^{-1} lower than that of the latter one. This is most probably due to the fact that the corresponding transition state **TSb** is substantially stabilized by rather strong interactions between the Ni center and the π–system of the η^3–benzyl moiety, as is evident from the shortened interatomic Ni···C contacts between the respective moieties (**TSb**, Figure 5.12). Such stabilizing interactions are obviously missing in the transition state **TSa** for the formation of the linear product (Figure 5.12). The reverse reaction in both cases is very difficult. The associated activation free energy barriers exceed 135 kJ mol^{-1}. Thus, despite the change of the relative stabilities of the linear and branched isomeric products upon the regeneration of the active complex **6** (**9a,b** → **6** + **2a,b**), the selectivity of the hydrocyanation catalytic cycle is controlled by the energetics of the reductive elimination step. Therefore, it was concluded that in the absence of the Lewis acid co-catalyst, formation of the branched nitrile product **2b** is both thermodynamically and kinetically favored. This is in excellent agreement with the experimentally observed selectivity patterns (Table 5.1) and with the results of the deuterium labeling experiments. The equilibrium between the intermediates **7**, **8a** and **8b** has been proven by the hydrogen scrambling in the nitrile products.

Similarly, in the presence of AlCl$_3$ (Figure 5.11(c)), the additional mechanistic details provide a deeper insight into the molecular-level effect of the Lewis acid co-catalyst. DFT calculations show that in this case the coordination of both linear and branched nitrile product to the Ni complex is rather unstable. Indeed, the repulsion caused by the presence of the AlCl$_3$ moiety does not allow a strong interaction between the -CN group of the coordinated nitrile and the Ni center ((**9a**)$_{Al}$ and (**9b**)$_{Al}$, Figure 5.12). Instead, a less favorable monodentate Ni···C$_{CN}$ coordination interaction is realized. In agreement with the above discussion, due to the weaker binding of AlCl$_3$ to the nitrile **2**, the free energy of the overall catalytic reactions becomes less negative, although at the qualitative level this does not cause any substantial change in the thermodynamics of the overall catalytic process (Figure 5.11(c)).

More importantly, addition of AlCl$_3$ results in substantial qualitative changes in the computed energetics of the reductive elimination step ((**8a,b**)$_{Al}$→ (**9a,b**)$_{Al}$, Figure 5.11(c)). The reaction pathway leading to the formation of the linear product is both

kinetically and thermodynamically favored in this case. The computed free energy change (ΔG^{solv}, Figure 5.12) for the reaction $(\mathbf{8a})_{Al} \rightarrow (\mathbf{9a})_{Al}$ in toluene is lower by 23 kJ mol^{-1} as compared to the one for the formation of the branched isomer $((\mathbf{8b})_{Al} \rightarrow (\mathbf{9b})_{Al})$. Furthermore, the activation free energy for the former reaction is lower by 10 kJ mol^{-1}. The stabilizing Ni$\cdots$C$_\pi$ contacts in $(\mathbf{TSb})_{Al}$ are somewhat longer as compared to those observed in $\mathbf{TSb}$ (Figure 5.12). Although the similar elongation of the Ni–C bond is also observed in the transition state $(\mathbf{TSa})_{Al}$, its destabilizing effect is apparently well compensated by the enhanced interaction within the newly formed C−CN bond (Figure 5.12).

This reverse energy trends upon Lewis acid coordination is associated with the above noted effect of the selective additional stabilization of the η^3–benzyl intermediate $(\mathbf{8b})_{Al}$. This leads to the generation of a steady state in the catalytic cycle. An enhanced selective stabilization of this species slows down the respective reaction path $(\mathbf{8b})_{Al} \rightarrow (\mathbf{9b})_{Al}$, while the competitive path $(\mathbf{8a})_{Al} \rightarrow (\mathbf{9a})_{Al}$ *via* the σ−alkyl intermediate is affected to a lesser extent. In contrast to the above-considered Lewis acid free hydrocyanation reaction, the reverse reactions are thermodynamically favored and show very low activation free energies (Figure 5.11(c)). Indeed, similar to the initial HCN oxidative addition step, coordination to the AlCl$_3$ Lewis acid also facilitates the corresponding reaction with the nitrile product. It is important to note that the oxidative addition of the branched product in $(\mathbf{9b})_{Al}$ is both thermodynamically and kinetically preferred. This suggests that the decomposition rate of the branched intermediate product $(\mathbf{9b})_{Al}$ takes place with a significantly higher rate than that of $(\mathbf{9a})_{Al}$. This would further hamper the reaction path towards the formation of the branched nitrile $\mathbf{2b}$. All these effects substantially facilitate the route *via* the formation of the less stable linear intermediate $(\mathbf{8a})_{Al}$. Taking the reversible nature of the reactions $\mathbf{7} \rightarrow \mathbf{8}$ into account,[7] the calculated free energy diagrams (Figure 5.11(c)) show that the catalytic hydrocyanation of styrene would ultimately lead to the predominant formation of the linear product $\mathbf{2a}$ in the presence of the AlCl$_3$ co-catalyst. This perfectly agrees with the experimental results (Table 5.1).

The fact that no C-CN cleavage occurs during the Ni–catalyzed phenylpropionitrile isomerization reaction is furthermore in line with the very high computed free energies

for the substitution of the COD ligand with the nitriles **2** coordinated to AlCl$_3$. Indeed, the corresponding ΔG^{solv} values of the reaction **5** + (**2a,b**)$_{Al}$ → (**9a,b**)$_{Al}$ + COD are equal to +85 and +74 kJ mol^{-1}, respectively, for the formation of (**9a**)$_{Al}$ and (**9b**)$_{Al}$.

Thus, AlCl$_3$ has a dual role in the catalytic hydrocyanation of styrene. First, the addition of the Lewis acid co-catalyst facilitates the initiation of the catalytic cycle *via* oxidative addition of HCN. Moreover, it favors the catalytic path leading to the elimination of the linear product. The latter is mainly an indirect result of the exceptional stabilization of the η^3-benzyl-complex by the Lewis acid, along with a weaker binding of AlCl$_3$ to the nitrile products, resulting in the reverse stability of the intermediate reaction products. Both these effects alter substantially the energetics of the reductive elimination step as compared to the Lewis acid–free reaction.

5.6. Screening of reaction conditions and Lewis acids in styrene hydrocyanation

5.6.1. Styrene hydrocyanation at different temperature and reaction time

In order to validate the DFT calculation, the hydrocyanation reactions with and without AlCl$_3$ were repeated using BIPPP as ligand and were terminated after 1h (Table 5.3, Entries 1 and 2). The promotion of the oxidative addition by the Lewis acid is supported by the observed high reaction rate after 1 h, compared to the Lewis acid free reaction. Both reactions were also carried out at 60°C (Table 5.3, Entries 3 and 4). At lower temperature, the conversion decreases and the selectivity changes in favor of the branched product. Apparently, the reaction becomes slower and the route *via* formation of the most thermodynamically stable η^3-benzyl-intermediate is preferred over the less stable σ-alkyl intermediate. The absence of a temperature dependence of the reaction selectivities without addition of the Lewis acid co-catalyst is in excellent agreement with the equal stabilities of the respective isomers predicted by DFT calculations.

Table 5.3. Hydrocyanation of styrene (neat HCN added in one portion) using BIPPP as ligand.

Entry	Temp (°C)	Time (h)	Lewis acid	Conversion (%) [a]	Selectivity (%) [b]	l/b [c]
1	90	1	/	33	100	<1/99
2	90	1	$AlCl_3$	88	72	83/17
3	60	16	/	93	100	<1/99
4	60	16	$AlCl_3$	76	74	45/55

Conditions: 0.033 mmol Ni(cod)$_2$, Ni: Lewis acid: L: S: HCN = 1: 1.05: 1.2: 20: 25, 1 mL toluene. [a] Conversions are based on the substrate and were determined by GC using n-decane as internal standard. [b] Selectivity = yield of nitriles/conversion. Styrene oligomers are identified as by-products. [c] Linear/Branched ratio.

5.6.2. Comparison with other Lewis acids

To investigate further the role of Lewis acids in the hydrocyanation of styrene and its effect on the regioselectivity of the reaction we considered the application of other co-catalysts, such as $FeCl_3$, BPh_3, and CuCN (Table 5.4). Similar to the previous case, formation of the linear nitrile product was observed in the presence of the Lewis acid. The use of $FeCl_3$ results in a comparable linear/branched ratio, but the selectivity towards the nitrile products is rather low, due to the enhancement of polymerization reactions (Table 5.4, Entry 1). In the case of CuCN the branched nitrile is predominantly obtained (Table 5.4, Entry 3) and BPh_3 represents an intermediate situation, where the linear to branched ratio is 59/41 (Table 5.4, Entry 2). One of the most commonly used Lewis acids, $ZnCl_2$, could not be applied in the reaction because of its insolubility in apolar solvents. The reaction performed in THF or dioxane leads to fast polymerization of the substrate. $B(C_6F_5)_3$ is soluble in toluene and therefore, it was also tested in the reaction as Lewis acid. Unfortunately, the promotion of the competitive styrene polymerization was higher than the co-catalyst activity in hydrocyanation and only polystyrene was obtained.

Table 5.4. Hydrocyanation of styrene (neat HCN added in one portion) using different Lewis acids.

Entry	Lewis acid	Conversion (%)[a]	Selectivity (%)[b]	l/b[c]
1	FeCl$_3$	64.7	31.3	70/30
2	BPh$_3$	58	69	59/41
3	CuCN	74	88	13/87

Conditions: 0.033 mmol Ni(cod)$_2$, Ni: Lewis acid: L: S: HCN = 1: 1.05: 1.2: 20: 25, 90°C, 16 h, 1 mL toluene. [a] Conversions are based on the substrate and were determined by GC using n-decane as internal standard. [b] Selectivity = yield of nitriles/conversion. Styrene oligomers are identified as by-products. [c] Linear/ Branched ratio.

5.6.3. DFT calculations on styrene hydrocyanation in the presence of CuCN as Lewis acid

Taking into account the above discussion on the role of the Lewis acid on the regioselectivity in the styrene hydrocyanation, it is expected that the difference between AlCl$_3$ and CuCN is mainly due to the less pronounced selective stabilization of the η^3–benzyl intermediate **8b,** upon the interaction with the CuCN Lewis acid and different relative stabilities of the intermediate reaction products (**9a,b**)$_{Cu.}$ The DFT calculations (Figure 5.11(d)) clearly support this assumption. Similar to AlCl$_3$, CuCN affects all elementary reaction steps to almost the same extent except for the intermediate (**8b**)$_{Cu}$ and the elimination products. The coordination of CuCN to the cyanide group results in a uniform shift of the relative energies by ~180 kJ mol^{-1} compared to ~130 kJ mol^{-1} in the case of AlCl$_3$. Although the computed reaction (ΔG^{solv}) and activation free energies ($\Delta G^{\#,solv}$) in this case are close for the competing reaction paths (Figure 5.12), a clear preference for the route towards the formation of the branched product is observed. The stronger binding of CuCN to the nitrile products substantially stabilizes the intermediate products (**9a,b**)$_{Cu}$ and prevents their decomposition over the Ni catalyst *via* oxidative addition. Moreover, the somewhat stronger binding of the CuCN co-catalyst in the intermediate shifts the equilibrium of the process towards the formation of the branched nitrile. These effects allow the catalytic reaction to proceed preferentially *via* the route involving the formation of the η^3–benzyl intermediate **8b** and consequently mainly lead to the elimination of the branched product **2b**. However, in line with the experimental

findings, the minor differences in the energetics of the competing paths do not allow entire selectivity towards **2b**.

5.7. Conclusions

High conversion and nitro regioselectivity could be reached in the Ni-catalyzed hydrocyanation of styrene applying phosphite ligands. At high catalyst loading a dramatic shift in regioselectivity from more than 90% branched to almost 90% linear nitrile product was observed by applying $AlCl_3$ as a Lewis acid co-catalyst. Experiments using deuterated styrene as substrate gave new insights into the mechanism of the reaction. The scrambling of the hydrogen (the deuterium labeling experiments have been performed adding HCN to the deuterated substrate) in the nitrile products and in the unreacted styrene showed the formation of η^3-benzyl and σ-alkyl intermediate during the catalytic cycle and a fast equilibrium between the two species with the styrene substrate. Furthermore, no C-CN bond cleavage was observed for the nitrile products during the isomerization experiments, suggesting the irreversibility of the elimination step.

DFT calculations provided a molecular-level picture of the catalytic process considered and allowed an in depth rationalization of the experimental observations. It was found that the conventional thermodynamic cycle could not be used for the correct description of the Ni-catalyzed hydrocyanation reaction, because it lacked important mechanistic details. Formation of the molecular complex by coordination of a nitrile product to the Ni-catalyst, as an intermediate product of the reductive elimination step, is essential for the overall catalytic performance.

Selectivity patterns were controlled by the relative stabilities of the η^3-benzyl and σ-alkyl intermediates and the intermediate products of their decomposition. The degree of stabilization of these species in the presence of the Lewis acid co-catalyst was not uniform. This determined the qualitative shifts in the energetics of the competing reaction paths and altered the regioselectivity of the hydrocyanation reaction.

Thus, it was concluded that the selectivity towards the linear product 3-phenylpropionitrile in the presence of $AlCl_3$ is due to the higher stability of the

intermediate η^3-benzyl complex. The selective stabilization of this intermediate in the presence of the Lewis acid leads to the formation of a "steady state" for the η^3-benzyl intermediate and indirectly promotes the formation of the linear product 3-phenylpropionitrile *via* the σ-alkyl intermediate. This assumption was supported by DFT calculations as well as by experimental data concerning the conversion and selectivity in styrene hydrocyanation at different reaction times and temperatures. Different Lewis acids, such as $FeCl_3$, BPh_3, and $CuCN$ were applied in the reaction, leading to lower selectivity and activity compared to $AlCl_3$. This deeper understanding of the mechanism of the hydrocyanation reaction might lead to improved catalysts in the future also for the hydrocyanation of simple alkenes.

5.8. Experimental section

General considerations.

Chemicals were purchased from Aldrich, Acros, and Merck and used as received. Styrene was filtered over neutral alumina and distilled over CaH_2 prior to use and was stored at -30°C. All preparations were carried out under argon atmosphere using standard Schlenk techniques. DPEphos,[17] Sixantphos,[17] Thixantphos,[17] BIPPP,[2] Ni(cod)$_2$,[18] and HCN[19] were synthesized according to literature procedures. NMR spectra were recorded on a Mercury 400 and a Varian Unity Inova 500 spectrometer (^{1}H, ^{13}C{^{1}H}, ^{31}P{^{1}H}).

Caution! HCN is a highly toxic, volatile liquid (bp 27°C) that is also susceptible to explosive polymerization in the presence of base catalysts. It should be handled only in a well-ventilated fume hood by teams of at least two technically qualified persons who have received appropriate medical training for treating HCN poisoning. Sensible precautions include having available proper first aid equipment as well as HCN monitors. Uninhibited HCN should be stored at a temperature lower than its melting point (-13°C). Excess of HCN may be disposed by addition to aqueous sodium hypochlorite, which converts the cyanide to cyanate.

Coordination of styrene to AlCl$_3$ (1d).

Styrene (50 μL) and AlCl$_3$ (120 mg) were dissolved in 1 mL of benzene-d_6. The solution was stirred for 2 hours and analyzed by NMR spectroscopy. ^{1}H NMR (400 MHz, C$_6$D$_6$, 25°C, TMS) δ: 7.21-7.17 (m, 2H), 7.08-6.98 (m, 3H), 6.53 (dd, 1H), 5.56 (dd, 1H), 5.03 ppm (dd, 1H); ^{13}C NMR (500 MHz, C$_6$D$_6$, 25°C, TMS) δ: 137.58, 136.95, 128.39, 126.19, 113.27 ppm.

Coordination of 2-phenylpropionitrile to AlCl$_3$ (2b).

2-Phenylpropionitrile (50 μL) and AlCl$_3$ (120 mg) were dissolved in 1 mL of benzene-d_6. The solution was stirred for 2 hours and analyzed by NMR spectroscopy. ^{1}H NMR (400 MHz, C$_6$D$_6$, 25°C, TMS) δ: 7.50-7.47 (m, 3H), 7.46-7.34 (m, 2H), 4.49-4.47 (m, 1H), 1.91-1.90 ppm (m, 3H); ^{13}C NMR (400 MHz, C$_6$D$_6$, 25°C, TMS) δ: 149.5, 131.6, 130.2, 129.9, 126.9, 123.9, 99.8, 31.6, 19.7 ppm.

Coordination of (BIPPP) to AlCl$_3$ (7).

BIPPP (16 mg, 0.018 mmol) and AlCl$_3$ (2.4 mg) were dissolved in 1 mL of toluene-d_8. The solution was stirred for 2 hours and analyzed by NMR spectroscopy. ^{1}H NMR (400 MHz, C$_6$D$_5$CD$_3$, 25°C, TMS) δ: 7.51-6.87 (m, 7H), 3.94-2.94 (m, 1H), 1.40-0.89 ppm (m, 6H); ^{31}P NMR (162 MHz, C$_6$D$_5$CD$_3$, 25°C, H$_3$PO$_4$) δ: 161.1 ppm (s).

Coordination of [Ni(cod)(BIPPP)] to AlCl$_3$ (8).

Ni(cod)$_2$ (5 mg, 0.018 mmol) and BIPPP (16 mg, 0.018 mmol) were dissolved in 1 mL of toluene-d_8. AlCl$_3$ (2.4 mg) was added and the solution was stirred for 2 hours and analyzed by NMR spectroscopy. ^{31}P NMR (400 MHz, C$_6$D$_5$CD$_3$, 25°C, H$_3$PO$_4$) δ: 146.0 (s, [Ni(cod) BIPPP]), 126. 0 ppm (d, J=19.4 Hz).

General procedure for the hydrocyanation experiments.

A solution of the ligand (1.2 equiv.) in 1 mL of solvent was added to Ni(cod)$_2$ (9.0 mg, 0.033 mmol). Styrene (20 equiv.) was added by an Eppendorf pipette, followed by 50 μL of *n*-decane as internal standard and AlCl$_3$ (1.05 equiv.). The solution was transferred into a 15 mL Schlenk tube equipped with a Teflon coated stirring bar.

Method A: An excess of HCN was added via an Eppendorf pipette and the Schlenk tube was warmed to 90°C in an oil bath. The mixture was stirred for 16 h.

Method B: A round-bottom Schlenk flask was filled with 1 mL of solvent and an excess of HCN (13 μmol/min), which was collected in a 5 mL syringe and added to the reaction mixture by syringe pump during 3 h (closed system). The mixture was stirred for another 2 h.

The reaction product was cooled to 0°C and flushed with a gentle stream of argon for 1 minute to remove traces of HCN. Samples were analyzed by GC, using *n*-decane as internal standard. All the reactions were carried out at least in duplo, showing variability for conversion and selectivity of ±2% and ±1%, respectively.

Computational details.

Density functional theory with the B3LYP[20] hybrid exchange-correlation functional was used for the quantum chemical calculations. Full geometry optimizations and saddle-

point searches were all performed using the Gaussian 03 program.[21] The full-electron 6-31+G(p) basis set was used for nickel ion, whereas all atoms of the styrene molecule, HCN and Lewis acids (AlCl$_3$ and CuCN) were described by the 6-311+G(d,p) basis set. Phosphorous and oxygen atoms from the ligand **4** were treated by the 6-311G(d,p) basis set. The modest Dunning/Huzinaga valence double-zeta[22] basis set was used for the remaining C and H atoms of the ligand **4**. The use of such a basis set combination allowed of a high-level quantum chemical description of the reaction center along with the realistic representation of the ligand system at *ab initio* level. Our preliminary calculations show that the excessive simplification of the molecular models or the theoretical methodology used for the description of the ligand systems or substrate leads to results inconsistent with the experimental observations. No symmetry restrictions were used in the calculations.

The nature of the stationary points was evaluated from the analytically computed harmonic modes. No imaginary frequencies were found for the optimized structures corresponding to local minima on the potential energy surface. All of the transition states showed a single imaginary frequency corresponding to the eigenvector along the reaction path. The assignment of the transition state structure to a particular reaction path was tested by perturbing the structure along the reaction path eigenvector in both directions of products and the reagents with subsequent geometry optimization. All of the energies computed within DFT used for the estimation of the reaction (ΔG^{solv}) and activation free energies ($\Delta G^{\#,solv}$) provided in the text (unless indicated otherwise) were corrected for the presence of solvent using the polarizable continuum model within the conductor reaction field (COSMO) approach developed by Klamt *et al.* [23] as implemented in the Gaussian 03 program package using the standard parameters for toluene as solvent. Electronic DFT-computed energies provided in the text were all corrected for the zero-point vibrations. The corresponding energy changes are denoted as ΔE^{ZPE}. Atomic charges were computed using the Natural Bond Orbital (NBO) method as implemented in the Gaussian 03 program package.

5.9. References and Notes

1. Pollak, P.; Romeder, G.; Hagedorn, F.; Gelbke, H. in *Nitriles. Ullman's encyclopedia of industrial chemistry, 5*[th] *copl. Rev. ed., Vol. A17*, Wiley-VCH, Weinheim, **1985**, pp. 363-376.

2. Wilting, J.; Janssen, M.; Müller, C.; Lutz, M.; Spek, A. L.; Vogt, D. *Adv. Synth. Catal.* **2006**, *349*, 350.

3. a) Casalnuovo, A. L.; RajanBabu, T. V.; Ayers, T. A.; Warren, T. H. *J. Am. Chem. Soc.* **1994**, *116,* 9869; b) RajanBabu, T. V.; Casalnuovo, A. L. *J. Am. Chem. Soc.* **1996**, *118,* 6325.

4. Goertz, W.; Keim, W.; Vogt, D.; Englert, U.; Boele, M. D. K.; van de Veen, L. A.; Kamer, P. C. J.; van Leeuwen, P. W. N. M. *J. Chem. Soc., Dalton Trans.* **1998**, 2981.

5. a) Bini, L.; Müller, C.; Wilting, J.; von Chrzanowski, L.; Spek, A. L.; Vogt, D. *J. Am. Chem. Soc.* **2007**, *129*, 12622; b) Göthlich, A. P. V.; Tensfeldt, M.; Rothfuss, H.; Tauchert, M. E.; Haap, D.; Rominger, F.; Hofmann, P. *Organometallics* **2008**, *27*, 2189.

6. De Greef, M. and Breit, B. *Angew. Chem.Int. Ed.* **2009**, *48*, 551.

7. Tolman, C. A.; Seidel, W. C.; Druliner, J. D.; Domaille, P. J. *Organometallics* **1984**, *3*, 33.

8. a) Taylor, B. W.; Swift, H. E. *J. Catal.* **1972,** *26*, 254; b) Druliner, J. D. *Organometallics* **1984**, *3*, 205; c) McKinney, R. J.; Nugent, W. A. *Organometallics* **1989**, *8*, 2871; d) Goerz, W.; Kamer, P. C. J.; van Leeuwen, P. W. N. M.; Vogt, D. *Chem. Commun.* **1997**, 1521.

9. Wilting, J.; Janssen, M.; Müller, C.; Vogt, D. *J. Am. Chem. Soc.* **2006**, *128,* 11374.

10. Tolman, C. A. *J. Am. Chem. Soc.* **1970**, *92,* 6777.

11. a) Acosta-Ramirez, A.; Munõz-Hernandez, M.; Jones, W. D.; Garcia, J. J. *J. Organomet. Chem.* **2006**, *691*, 3895; b) Swartz, B. D.; Reinartz, N. M.; Brennessel, W. W.; Garcia, J. J.; Jones, W. D. *J. Am. Chem. Soc.* **2008**, 130*,* 8548.

12. The reactions reported in Table 1 were performed by addition of neat HCN in one portion. That is only possible with a high catalyst loading. In fact, an excess of HCN destroys the Ni-catalyst forming [Ni(CN)$_2$] compounds. To use a low catalyst loading, the reaction was performed under slow HCN addition (Table 2).

13. (a) Jordan, D. O.; Mathieson, A. R. *Nature* **1951**, *167*, 523;(b) Jordan, D. O.; Mathieson, A. R. *J. Am. Chem. Soc.* **1952**, 611.

14. Vriezen, W. H. N.; Jellinek, F. *Chem. Phys. Lett.* **1967**, *1*, 284.

15. Pearson, R. G. *Coord. Chem. Rev.* **1990**, *100*, 403.

16. Huang, J.; Haar, C. M.; Nolan, S. P.; Marcone, J. E.; Moloy, K. G. *Organometallics* **1999**, *18*, 297.

17. Kranenburg, M.; van der Burgt, Y. E. M.; Kamer, P. C. J.; van Leeuwen, P. W. N. M. *Organometallics* **1995**, *14*, 3081.

18. Schunn, R. A. *Inorg. Synth.* **1974**, *15*, 5.

19. Slotta, K. H. *Ber. Dtsch. Chem. Ges.* **1934**, *67B*, 1028.

20. a) Becke, A. D. *Phys. Rev.* **1988**, *A38*, 3098; b) Becke, A. D. *J. Chem. Phys.* **1993**, *98*, 1372; c) Becke, A. D. *J. Chem. Phys.* **1993**, *98*, 5648.

21. Frisch, M. J.; Trucks, G. W.; Schlegel, H. B.; Scuseria, G. E.; Robb, M. A.; Cheeseman, J. R.; Montgomery, J. A. Jr.; Vreven, T.; Kudin, K. N.; Burant, J. C.; Millam, J. M.; Iyengar, S. S.; Tomasi, J.; Barone, V.; Mennucci, B.; Cossi, M.; Scalmani, G.; Rega, N.; Petersson, G. A.; Nakatsuji, H.; Hada, M.; Ehara, M.; Toyota, K.; Fukuda, R.; Hasegawa, J.; Ishida, M.; Nakajima, T.; Honda, Y.; Kitao, O.; Nakai, H.; Klene, M.; Li, X.; Knox, J. E.; Hratchian, H. P.; Cross, J. B.; Bakken, V.; Adamo, C.; Jaramillo, J.; Gomperts, R.; Stratmann, R. E.; Yazyev, O.; Austin, A. J.; Cammi, R.; Pomelli, C.; Ochterski, J. W.; Ayala, P. Y.; Morokuma, K.; Voth, G. A.; Salvador, P.; Dannenberg, J. J.; Zakrzewski, V. G.; Dapprich, S.; Daniels, A. D.; Strain, M. C.; Farkas, O.; Malick, D. K.; Rabuck, A. D.; Raghavachari, K.; Foresman, J. B.; Ortiz, J. V.; Cui, Q.; Baboul, A. G.; Clifford, S.; Cioslowski, J.; Stefanov, B. B.; Liu, G.; Liashenko, A.; Piskorz, P.; Komaromi, I.; Martin, R. L.; Fox, D. J.; Keith, T.; Al-Laham, M. A.; Peng, C. Y.; Nanayakkara, A.; Challacombe, M.; Gill, P. M. W.; Johnson, B.; Chen, W.; Wong, M. W.; Gonzalez, C.; Pople, J. A. Gaussian 03, revision B.05, Gaussian, Inc.: Pittsburgh PA, **2003**.

22. Dunning Jr., T. H.; Hay, P. J. in *Modern Theoretical Chemistry*, Ed. H. F. Schaefer III, Vol. 3 (Plenum, New York, **1976**) 1-28.

23. Eckert, F.; Klamt, A. *AIChE J.* **2002**, *48*, 369; Barone, V.; Cossi, M. *J. Phys. Chem. A* **1998**, *112*, 1995.

Chapter **6**

Hydrocyanation of 1-Octene: an Open Challenge

So far, the hydrocyanation of monoalkenes has not attracted much attention. The reason is mainly the lower conversion generally observed for these substrates compared to the hydrocyanation of dienes and vinylarenes. The role of the Lewis acid in the mechanism of this reaction is still not completely clear, in particular its effect in the increase of the reactivity and regioselectivity towards linear nitriles. A conversion of 89% in the hydrocyanation of 1-octene has been achieved, applying a binaphthol-based diphosphite (BIPPP) as ligand and AlCl₃ as the Lewis acid. The mechanism of the reaction was investigated via deuterium labeling experiments and DFT calculations.
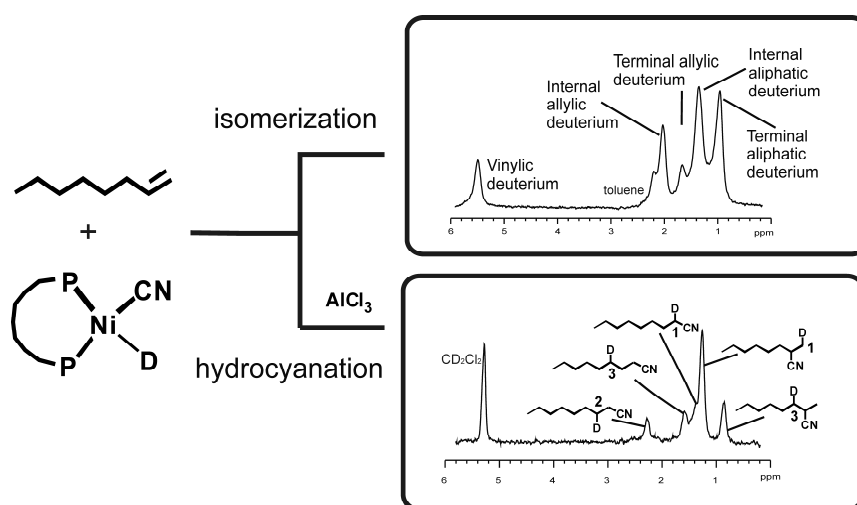
6.1. Introduction

Although alkyl nitriles are valuable intermediates in the bulk and fine chemical industry for the synthesis of amides, amines, carboxylic acids, and esters,[1] only a few examples for their direct catalytic preparation can be found in the literature. Arthur and Pratt[2] published on the first homogeneously catalyzed hydrocyanation of linear alkenes in 1954 (Scheme 6.1). $Co_2(CO)_8$, in combination with PPh_3, was used for the hydrocyanation of non-activated monoalkenes, as well as of conjugated dienes. The addition of HCN was accomplished within 5-7 hours at 130°C. The conversion decreased dramatically when the chain length of the monoalkene was increased from 1-butene to 1-octene (65% vs 13%).

The hydrocyanation of 1-hexene to a mixture of heptanenitrile and 2-methylhexanenitrile, using Lewis acid-promoted Ni(0) phosphite complexes, was studied by Taylor and Swift.[3] The Lewis acid significantly enhances the reaction rate and has an effect on the linear:branched product ratio. The nature of the solvent also has an effect on both the selectivity to normal nitriles and the reaction rate. Unfortunately, it was not possible to find a clear relation between the character of the Lewis acid or the solvent and their effects on the reaction.

Using *n*-octenes as starting materials, Keim *et al.*[4] have found that, independently of the position of the double bond, the anti-Markovnikov product 1-cyanooctane is formed with 80% regioselectivity. The isomerization and β-elimination rates are much faster than the hydrocyanation rate. Therefore, the regioselectivity of the reaction is dependent on the equilibrium between the isomers, reached *via* the isomerization reaction before the slower hydrocyanation step. In order to avoid fast deactivation of the catalyst, due to the addition of a second molecule of HCN to the Ni center and formation of inactive dicyano complexes, monodentate phosphite ligands were employed in large excess (Ni:L=1:15). The hydrocyanation of 1-alkenes and ω-unsaturated fatty acid esters was accomplished also by applying chelating diphosphines, with a ligand to metal ratio of 1.05:1.[5] The use of diphosphines with a large bite angle induces yields that are comparable to those obtained with the monodentate phosphite system. The yields reported in the Ni-catalyzed
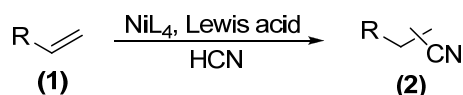
Scheme 6.1. Hydrocyanation of non-activated monoalkenes.

hydrocyanation of 1-octene were approximately 50%, applying a substrate to ligand ratio of 20:1.

Consequently, it is still an open challenge to perform the hydrocyanation reaction of non-activated monoalkenes, keeping in mind that the aliphatic nitrile products are valuable intermediates. A deeper understanding of the role of the Lewis acid and the species involved in the catalytic cycle is crucial in order to improve the reaction rate, to achieve higher conversions, and to control the regioselectivity. Therefore, mono- and diphosphite ligands in combination with several Lewis acids have been applied in the hydrocyanation of monoalkenes. Moreover, deuterium labeling experiments and DFT calculations have been performed to investigate the mechanism of the reaction.

6.2. Hydrocyanation of 1-Octene

6.2.1. The hydrocyanation of 1-octene applying the monodentate phosphite ligand P(OPh)₃

1-Octene was chosen as a model substrate, in order to investigate the hydrocyanation of non-activated monoalkenes. In fact, it is an industrially important α-olefin[6] and has been already reported as substrate in the hydrocyanation reaction.[4,5]

The hydrocyanation of 1-octene was performed with the monophosphite ligand P(OPh)₃ in the presence of different Lewis acids. A more moderate excess of monodentate ligand compared to the literature example[4] (L:Ni=5:1) was applied. As
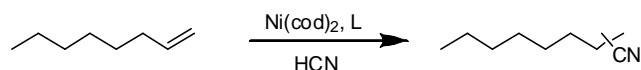
Scheme 6.2. Hydrocyanation of 1-octene.

explained before, the loss of catalytic activity can be attributed to the addition of a second molecule of HCN to the nickel complex, leading to inactive dicyano species (Scheme 6.3). An excess of ligand consequently competes with HCN in the binding to free coordination sites at the metal center.

The addition of AlCl$_3$ to the catalyst system led to a conversion of 21% and the linear mononitrile was the only product detected by GC analysis (Table 6.1, Entry 1). Keim *et al.*[4] reported on the hydrocyanation of 1-octene using P(OPh)$_3$ and AlEtCl$_2$ as Lewis acid under similar reaction condition, obtaining high activities. In the literature example a larger excess of phosphite was applied and the Lewis acid was added as stock solution in acetonitrile. Under the chosen conditions, conversions of 15% and selectivities of 73% towards the linear nitrile were obtained (Table 6.1, Entry 2). GC-analysis showed large amounts of degradation products of the ligand, which were observed only with AlEtCl$_2$ as Lewis acid. It can be concluded that the aluminum alkyl compound reacts with the ligand and a larger excess of the latter prevents the degradation of the catalyst. BPh$_3$ did not lead to the formation of any nitrile products, while its more soluble analogue B(C$_6$F$_5$)$_3$ led to 11% of conversion and a large distribution of isomers in the product mixture (Table 6.1, Entries 3 and 4). The presence of 3- and 4-cyanooctane is not observed using other

$$\text{NiL}_4 \xrightleftharpoons{\text{HCN}} \text{NiL}_3\text{HCN} + \text{L} \xrightleftharpoons{\text{HCN}} \text{NiL}_2(\text{CN})_2 + \text{H}_2 + \text{L}$$
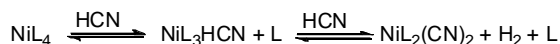
Scheme 6.3. Formation of nickel dicyano complexes.[4]

Table 6.1. Hydrocyanation of 1-octene using P(OPh)$_3$ as ligand in the presence of different Lewis acids.

Entry	Lewis acid	Conversion[a] (%)	Isomers (%)
1	AlCl$_3$	21	1-CN > 99
2	AlEtCl$_2$	15	1-CN:2-CN = 73:27
3	BPh$_3$	/	/
4	B(C$_6$F$_5$)$_3$	11	1-CN:2-CN:3-CN:4-CN = 74:15:5.5:5.5
5	CuCN	22	1-CN:2-CN = 89:11
6	/	2	1-CN > 99

Conditions: 0.033 mmol Ni(cod)$_2$, Ni:Lewis acid:L:S:HCN = 1:1.05:5:20:25, T = 90°C, 16 h, 1 mL toluene. [a] Conversions are based on the substrate and were determined by GC using n-decane as internal standard.

Lewis acids. Curiously, boron-based Lewis acids have already been reported for similar catalytic systems, giving the most regioselective catalyst systems in the hydrocyanation reaction.[7] The highest activity was obtained using CuCN, but with a lower regioselectivity compared to $AlCl_3$ (22% of conversion and 89% of linear product, Table 6.1, Entry 5). Only traces of the linear nitrile were detected after the hydrocyanation reaction in the absence of any Lewis acid (Table 6.1, Entry 6).

This series of experiments performed showed that the Lewis acid is necessary for the activity of the catalyst in this reaction and the best performing one in terms of activity and regioselectivity is apparently $AlCl_3$.

6.2.2. The hydrocyanation of 1-octene applying the bidentate phosphite ligand BIPPP

More recently bidentate phosphite ligands have been reported in the patent literature[8] to form the most efficient system in the Ni-catalyzed hydrocyanation of butadiene and 3-pentenenitrile, as well as in the isomerization of 2-methyl-3-butenenitrile (the three steps of the DuPont adiponitrile process).[9] Binaphthol-based diphosphites in combination with $Ni(cod)_2$ showed very good activity also in hydrocyanation of styrene.[10] The rigid backbone of these ligands is believed to stabilize the active tetrahedral Ni(0) complex and to suppress the formation of square-planar dicyano Ni(II) complexes. Therefore, the binaphthyl-isopropylphenyl-diphosphite ligand BIPPP (Figure 6.1) was applied in the hydrocyanation of 1-octene. The reaction was performed under the same conditions as in the previous case using the monodentate ligand $P(OPh)_3$. Since the catalyst is more stable and due to the chelating properties of the ligand, the L:Ni ratio was lowered to 1.2:1.

Figure 6.1. Binaphthyl phosphite ligand (**BIPPP**).

Table 6.2. Hydrocyanation of 1-octene using BIPPP as ligand and different Lewis acids.

Entry	Lewis acid	Conversion[a] (%)	Isomers (%)
1	$AlCl_3$	89	1-CN:2-CN = 78:22
2	BPh_3	16	1-CN:2-CN:3-CN = 76:20:4
3	/	2	1-CN $>$ 99
4	$FeCl_3$	11	1-CN $>$ 99
5	$Yb(OTf)_3$	18	1-CN $>$ 99

Conditions: 0.033 mmol $Ni(cod)_2$, Ni:Lewis acid:L:S:HCN = 1:1.05:1.2:20:25, T = 90°C, 16 h, 1 mL toluene. [a] Conversions are based on the substrate and were determined by GC using n-decane as internal standard.

The hydrocyanation reaction was carried out using the best performing Lewis acid $AlCl_3$ for the monophosphite ligands. Interestingly, the conversion of 89% obtained is the highest ever reported for this reaction. The selectivity toward the linear nitrile product was 78% (Table 6.2, Entry 1). The use of BPh_3 in combination with the bidentate ligand led to a conversion of 16% and the formation of all possible nitrile isomers: 1-, 2-, 3- and 4-cyanooctane (Table 6.2, Entry 2). Only traces of the linear nitrile product were obtained in the hydrocyanation of 1-octene in the absence of a Lewis acid (Table 6.2, Entry 3). $FeCl_3$ and $Yb(OTf)_3$ were also tested, leading exclusively to the linear product. The conversions with 11% and 18%, respectively were much lower compared to the application of $AlCl_3$ (Table 6.2, Entries 4 and 5).

Using BIPPP as ligand, $AlCl_3$ was confirmed to be the most suitable Lewis acid for this reaction.

6.3. Application of different monoalkene substrates: the polarity of the reaction medium

The optimized reaction conditions were further applied in the hydrocyanation of different monoalkenes; i.e. using BIPPP as ligand and $AlCl_3$ as Lewis acid. The hydrocyanation of 1-hexene reproduced the result obtained with 1-octene (88% conversion; Table 6.3, Entry 2), but the higher alkenes were less efficiently converted.

Table 6.3. Hydrocyanation of monoalkenes using BIPPP as ligand and AlCl$_3$ as Lewis acid.

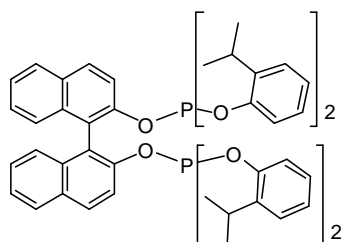| Entry	Substrate	Lewis acid	Conversion[a] (%)	Isomers (%)
1	1-butene	AlCl$_3$	20	1-CN:2-CN = 75:25
2	1-hexene	AlCl$_3$	88	/
3	1-dodecene	AlCl$_3$	20	/
4[b]	1-octene (40 eq)	AlCl$_3$	14	1-CN:2-CN:3-CN = 41:44:15
5[c]	1-octene (40 eq)	AlCl$_3$ (2 eq)	11	1-CN:2-CN:3-CN = 82:14:4

Conditions: 0.033 mmol Ni(cod)$_2$, Ni:Lewis acid:L:S:HCN = 1:1.05:1.2:20:25, T = 90°C, 16 h, 1 mL toluene. [a] Conversions are based on the substrate and were determined by GC using n-decane as internal standard. [b] Ni:S = 1:40. [c] Ni: Lewis acid: S = 1:2.1:40.

The low reactivity of 1-butene might be attributed to the gaseous nature of the compound (Table 6.3, Entry 1). In the case of 1-dodecene a difference in the solubility of the Lewis acid was observed and the conversion of the substrate to the nitrile products was only 20%. To confirm a negative influence of the long chain alkene on the polarity of the reaction medium, the hydrocyanation of 1-octene was performed using a two-fold concentration of the alkene. The conversion decreased dramatically from 89% (Table 6.2, Entry 1) to 14% (Table 6.3, Entry 4). With 41% also the regioselectivity towards the linear nitrile was rather low. 2-Cyanooctane and 3-cyanooctane were formed in 44% and 15% yield respectively. A two-fold addition of AlCl$_3$ in the latter reaction was beneficial for the regioselectivity, which increased again to 82%. However, with 11% the conversion was still very low (Table 6.3, Entry 5).

Solvent effects in the hydrocyanation reaction have been reported several times. Taylor and Swift proposed the influence of dielectric effects in the hydrocyanation of 1-hexene.[3] The higher activity of the Ni-catalyst in polar solvents has been observed in the hydrocyanation of butadiene[11] and in the isomerization of 3-methyl-2-butenenitrile.[12] Aromatic and apolar solvents, respectively increase the regio- and the enantio-selectivity in 1-hexene[3] and styrene hydrocyanation[13]. The solubility of the Lewis acid in the reaction medium also plays a role, as it coordinates to the catalyst. The results presented above are in line with these previous reports and underline that influencing the polarity of the reaction mixture can also affect the reaction.

Table 6.4. Hydrocyanation of 1-octene using BIPPP as ligand and AlCl$_3$ as Lewis acid in polar solvents.

Entry	Solvent	Conversion[a] (%)	Isomers (%)
1	THF	20	1-CN:2-CN:3-CN = 93:5:2
2	dioxane	18	1-CN:2-CN = 77:23

Conditions: 0.033 mmol Ni(cod)$_2$, Ni:Lewis acid:L:S:HCN = 1:1.05:1.2 :20:25, 90°C, 16 h, 1 mL toluene. [a] Conversions are based on the substrate and were determined by GC using n-decane as internal standard.

Therefore, polar solvents that have shown to be beneficial in the hydrocyanation of other substrates were used.[11,12] The hydrocyanation of 1-octene in THF and dioxane led to good selectivities of up to 93% of the linear product (Table 6.4, Entries 1 and 2). Unfortunately, with about 20% the conversion was rather low. Aromatic solvents such as toluene seem to enhance the activity in the hydrocyanation of 1-octene.

6.4. Deuterium labeling experiments

In order to investigate the mechanism of the reaction, deuterium labeling experiments were performed using DCN[14] as reactant. The deuterocyanation of 1-octene was carried out applying BIPPP as ligand and AlCl$_3$ as Lewis acid. The conversion was 72% and the product distribution determined by GC-analysis was 1-CN:2-CN:3-CN = 69:17:4. The lower conversion compared to the experiments performed using HCN is most probably due to an isotope effect.
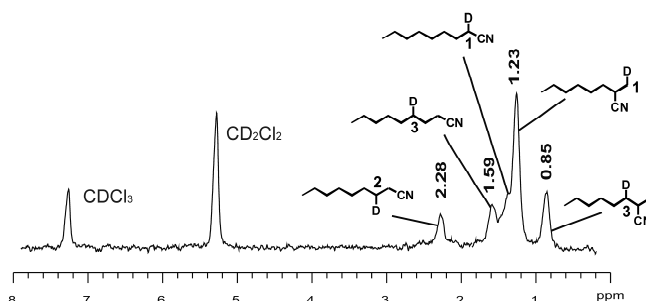
Figure 6.2. ^{2}H NMR of the 1-octene hydrocyanation crude mixture in the presence of AlCl$_3$ (CH$_2$Cl$_2$).

Moreover, the reaction was analyzed by ^{2}H NMR spectroscopy. Extensive deuterium scrambling was observed for the 1-CN and 2-CN product: deuterium was present in 1- (δ = 1.23 ppm), 2- (δ = 2.28 ppm) and 3-position (δ = 0.85 and 1.59 ppm) (Figure 6.2). The 3-CN species could not be detected due to the low concentration. CDCl$_3$ was added as internal standard to the NMR tube.

During the deuterocyanation reaction, DCN undergoes oxidative addition to the Ni(0) species and the catalyst (**3a**) is formed (Figure 6.3). 1-Octene coordinates to the metal center and after migratory insertion of the alkene, σ-alkyl-Ni species are formed. Markovnikov-addition of the Ni-D over the double bond leads to the branched σ-alkyl species (**4**) with deuterium in 1-position. If the addition occurs in an anti-Markovnikov fashion, the linear σ-alkyl species (**5**) is generated with deuterium in 2-position. These two σ-alkyl-Ni species can undergo reductive elimination generating the nitrile product or they undergo β-(H/D)-elimination leading to alkene isomerization. The ^{2}H NMR spectrum shows that the deuterium incorporation occurs mainly in the 1-position.
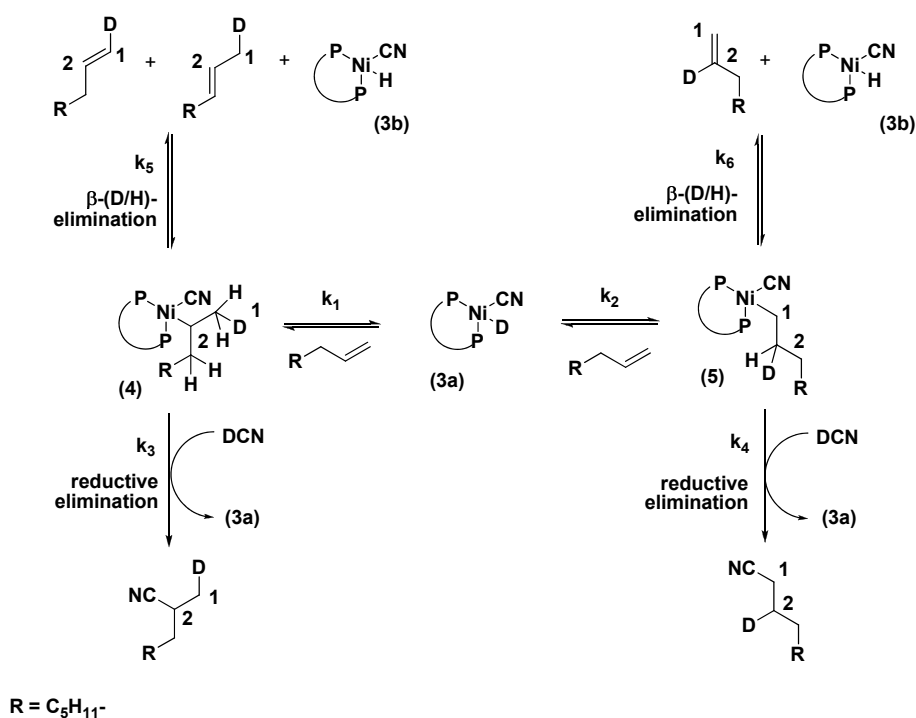
Figure 6.3. The mechanism of the β-(H,D)-elimination versus the hydrocyanation reaction.

163

Therefore, the formation of the branched σ-alkyl intermediate (**4**) must be preferred ($k_1>k_2$). This is in line with the reaction pattern found for Ni-H species also in other reactions, e.g. in the propene dimerization in the Dimersol process.[15] Once that the deuterium is inserted in the terminal position of the alkene, the 2-CN product can be formed *via* reductive elimination. Concurrently, the addition of DCN to the metal center can regenerate the catalyst (**3a**). However, the branched nitrile is not the major product of the deuterocyanation reaction, but the linear nitrile formed *via* reductive elimination from the linear σ-alkyl intermediate (**5**) ($k_4>k_3$). For complex (**4**) the β-(D/H)-elimination must be favored over the reductive elimination ($k_1,k_5>k_3$) and 1- or 2-octene are the preferred products. The formation of 2-octene implies the regeneration of the complex (**3b**), in which the deuterium is substituted by hydrogen. Moreover, the double bond isomerization process takes place. If 1-octene is the product of the β-(D/H)-elimination, the catalyst (**3b**) is still preferentially regenerated since the breaking of the C-H bond in terminal position compared to the C-D bond is favored by statistics and by the isotope effect. The deuterium inserted in terminal position of the alkene after migratory insertion to the nickel center to form the intermediate (**4**) will be most probably present in the new 1- and 2-octene generated *via* β-(D/H)-elimination. The two new alkenes can further undergo migratory insertion and the catalyst (**3b**) is active in hydrocyanation and isomerization of the alkenes without deuterium addition. The β-(D/H)-elimination from the intermediate (**5**) will also preferentially generate species (**3b**) due to the isotope effect. In this case deuterium will be incorporated in 2-position of 1-octene.

In conclusion the presence of the deuterium mostly in 1-position proves the favored formation of the branched σ-alkyl intermediate (**4**). On the other hand, the reductive elimination to form the nitrile product is preferred for the linear σ-alkyl intermediate (**5**), since the linear nitrile is the major product. Thus, in order to improve the activity of the hydrocyanation, this latter reaction step has to be enhanced. Furthermore, it was clearly proven that the reductive elimination is the step controlling the regioselectivity in the hydrocyanation reaction.
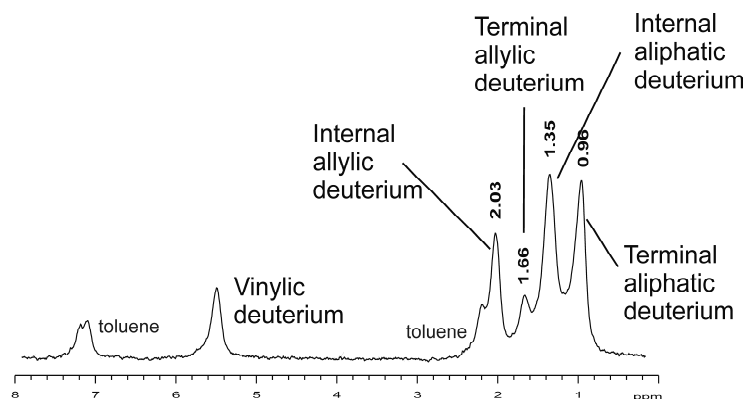
Figure 6.4. ^{2}H NMR of the 1-octene deuterocyanation crude mixture in the absence of Lewis acid.

As control experiment, the deuterocyanation of 1-octene was repeated in the absence of a Lewis acid. The addition of DCN to the double bond did not take place. The mixture of unreacted octenes was analyzed by GC, showing 2% 1-octene, 29% 2-octene, 59% 3-octene, and 10% 4-octene and thus, extensive isomerization.

The crude reaction mixture was also analyzed by ^{2}H NMR spectroscopy, using toluene as internal standard. The deuterium addition was detected in all positions of the octenes skeleton (Figure 6.4). Deuterium scrambling is shown in the double bonds, as well as in the aliphatic chain. The high intensity of the resonance at δ = 1.35 and 0.96 ppm, related to the deuterium in internal and terminal aliphatic position and therefore not in proximity of the double bond, suggests that the isomerization took place over the entire alkene chain. The resonances at δ = 0.96 and 1.66 ppm represent the deuterium in 1-position. The insertion in this position does not seem to be largely preferred, as in the previous situation. Clearly, the presence of the Lewis acid is crucial for the reductive elimination of the nitriles. Furthermore, the Lewis acid must favor the reductive elimination of the nitrile from the linear σ-alkyl species. Over all this leads to the preferred formation of the linear nitrile and to a less extensive isomerization of the alkene.

6.5. DFT calculations

Side reactions and, in particular, the deactivation of the catalyst *via* formation of [Ni(CN)$_2$L$_n$] species were considered to explain the low conversion in the hydrocyanation of monoalkenes in the absence of a Lewis acid. These catalytically inactive species contain a square-planar metal-center and their formation is particularly favored once the Ni complex possesses this particular configuration. DFT calculations for the hydrocyanation of styrene (Chapter 5) have shown that the Ni-complexes obtained after the oxidative addition of HCN have also a square-planar coordination geometry around the metal center.[16]

In order to investigate this aspect of the reaction mechanism, preliminary calculations were performed using the rather small ligand P(OMe)$_3$ (cone angle 107°)[17] and 1-butene as substrate. The catalytic cycle is depicted in Figure 6.5. The complex [Ni(cod)L$_2$] (**6**) was chosen as the zero level for the free energy. The first step, the oxidative addition of HCN is slightly unfavored (**6**→**7**). As already reported[16], the addition of a Lewis acid would strongly facilitate the latter step, making the reaction highly exothermic. The coordination of the alkene to the Ni center (**8**) and the migratory insertion (**9**) are thermodynamically favored (ΔG = 27 and 28 kJ mol^{-1}). The reductive elimination of the nitrile product and the regeneration of the Ni(0) catalyst are the rate determining step of the reaction. These findings are in line with the extensive deuterium scrambling observed in the deuterium labeling experiments. In fact, the formation of the σ-alkyl intermediate and the β-(H/D)-elimination of the alkene occur several times before the reductive elimination takes place.

DFT calculations confirmed that the dicyano Ni(II) complexes are very stable, in particular in the *trans* configuration (-171 kJ mol^{-1} for the *cis* complex (**10**) and -210 kJ mol^{-1} for the *trans* complex (**11**); Figure 6.5). The addition of a second HCN molecule to form the inactive dicyano complexes is more difficult in the presence of AlCl$_3$ or CuCN. The coordination of the Lewis acid to the nickel cyanide intermediate most likely causes electrostatic repulsion effects and steric hindrance that avoid the second HCN addition and facilitate the formation of the nitrile products versus the dicyano complexes.

The activation free energies $\Delta G^{\#}$ for the reductive elimination have been computed without a Lewis acid and in the presence of AlCl$_3$ and CuCN. The results are 66, 51 and 52 kJ mol^{-1}, respectively. The differences between the situation in the absence of a Lewis acid and the reaction in the presence of the co-catalyst are not consistent with the experimental results. In fact, an energy gap of 15 kJ mol^{-1} does not explain the fact that the hydrocyanation of monoalkenes takes place only in the presence of a Lewis acid. The stabilization of the complex versus the formation of dicyano species seems to be the prevalent effect of the co-catalyst coordination, and the key for understanding its role in the reaction mechanism.
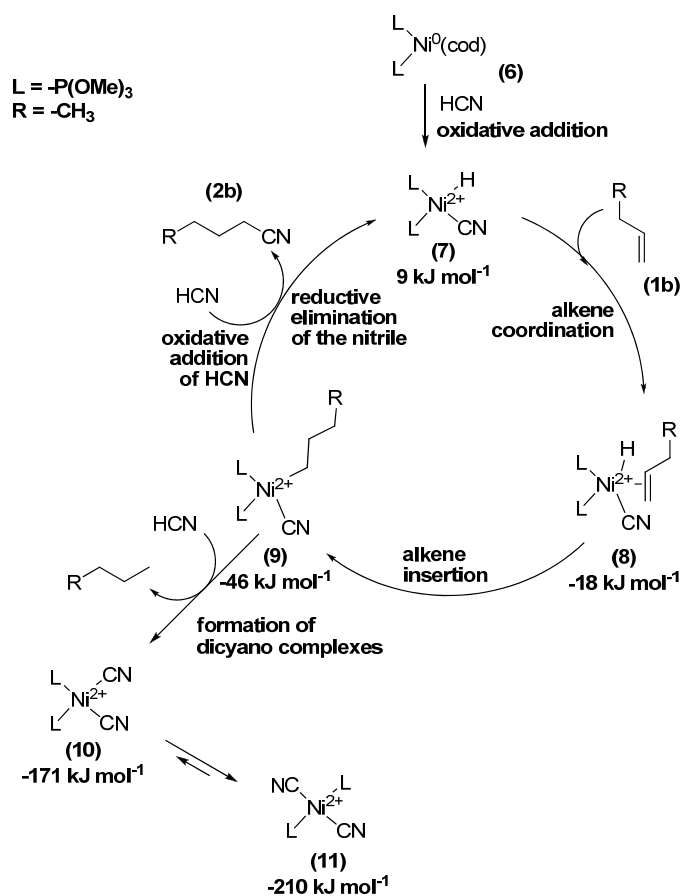
Figure 6.5. Catalytic cycle for the hydrocyanation of 1-butene. The free energies computed for the different intermediates are indicated.

6.6. Conclusions

The hydrocyanation of 1-octene and other monoalkenes has been addressed in this chapter. The influence of several Lewis acids and solvents has been investigated. The best results were observed using $AlCl_3$ as Lewis acid and toluene as solvent. For the first time a diphosphite ligand (**BIPPP**) has been applied in this reaction, obtaining the highest conversion ever reported (89%).

Deuterium labeling experiments elucidated the competition between isomerization and hydrocyanation. The double bond isomerization takes place *via* reversible migratory insertion of the alkene into the Ni-D/H bond and β-(H/D)-elimination from the σ-alkyl-Ni species. The Markovnikov addition of the deuterium in the terminal position is largely preferred in the presence of the Lewis acid. An extensive deuterium scrambling further proved that this reversible process is much faster than the irreversible reductive elimination to form the nitrile products. However, the major product of the hydrocyanation is always the terminal nitrile, generated from an anti-Markovnikov addition of HCN or DCN. Therefore, the reductive elimination is the regioselective step of the reaction.

A first theoretical approach to the hydrocyanation of monoalkenes suggests that the formation of the inactive dicyano complexes of the type $[Ni(CN)_2L_n]$ is disfavored by the co-catalyst coordination. The presence of $AlCl_3$ or CuCN in close proximity to the nickel center in the nickel cyanide intermediate most likely causes steric hindrance and electrostatic repulsion, disfavoring the addition of a second HCN molecule. This contribution of the Lewis acid could be an explanation for its crucial role in the hydrocyanation of 1-alkenes.

Higher level calculations of the active catalytic system in the future are expected to lead to a deeper understanding of the reaction's activity and selectivity.

6.7. Experimental section

General considerations

Chemicals were purchased from Aldrich, Acros or Merck and used as received. Toluene and 1-octene were distilled over CaH_2 prior to use. All preparations were carried out under argon atmosphere using standard Schlenk techniques. BIPPP,[10] Ni(cod)$_2$,[18] and HCN[14] were synthesized according to literature procedures. NMR spectra were recorded on a Varian Unity Inova 500 (^{2}H{^{1}H}).

Caution! HCN is a highly toxic, volatile liquid (bp 27°C) that is also susceptible to explosive polymerization in the presence of base catalysts. It should be handled only in a well-ventilated fume hood by teams of at least two technically qualified persons who have received appropriate medical training for treating HCN poisoning. Sensible precautions include having available proper first aid equipment as well as HCN monitors. Inhibitor-free HCN should be stored at a temperature lower than its melting point (-13°C). Excess of HCN may be disposed by addition to aqueous sodium hypochlorite, which converts the cyanide to cyanate.

General procedure for the hydrocyanation experiments

A solution of ligand BIPPP (35 mg, 0.039 mmol) in 1 mL of solvent was added to Ni(cod)$_2$ (9.0 mg, 0.033 mmol). 1-Octene (105 μL, 20 equiv.) was added by an Eppendorf pipette, followed by 50 μL of *n*-decane as internal standard. The solution was transferred into a 15 mL Schlenk tube equipped with a Teflon coated stirring bar. An excess of HCN was added *via* Eppendorf pipette and the Schlenk tube was warmed to 90°C in an oil bath. The mixture was stirred for 16h. The reaction product was cooled to 0°C and flushed with a gentle stream of argon for 1 minute to remove traces of HCN. Samples were analyzed by GC, using *n*-decane as internal standard. All reactions were carried out in duplo, showing a variability for conversion and selectivity of ±2 % and ±1 %, respectively.

Computational details

The quantum chemical calculations were performed within density functional theory using the Gaussian 03 program.[19] The LanL2DZ[20] basis set was used for Nickel atoms, while all other atoms were treated with the standard 6-31G (d, p) basis set.[21] No symmetry restrictions were used in the calculations. Earlier, this combination of the basis set and the density functional was successfully applied for the investigation of various molecular properties of different compounds.[22,23]

6.8 References and notes

1. Beller, M.; Seayad, J.; Tillack, A.; Jiao, H. *Angew. Chem Int. Ed.* **2004**, *43*, 3368.

2. (a) Arthur, P., Jr.; Pratt, B. C. Hydrocyanation of conjugated diolefinic compounds. US 2,571,099, **1951.** *Chem. Abstr.* **1952***, 46*, 3068; (b) Arthur, P.; Jr., England, D.C.; Pratt, B.C.; Whitman, G. M. *J. Am. Chem. Soc.* **1954**, *76*, 5364-536.

3. Taylor, B. W.; Swift, H. E. *J. Catal.* **1972,** *26* (2), 254-260.

4. Keim, W.; Behr, J. P.; Weisser, *J. Erdol Kohle, Erdgas, Petrolchrm.* **1982**, *35* (9), 436.

5. Keim, W.; Behr, J. P.; Lühr, H.-O.; Weisser, *J. Catal.,* **1982**, *78*, 209-216.

6. Lappin, G. R.; Sauer, J. D. in *Alpha Olefins Application Handbook*; CRC Press; **1989**.

7. (a) Tolman, C. A.; Seidel, W. C.; Druliner, J. D.; Domaille, P. J. *Organometallics* **1984**, *3*, 33; (b) Tolman, C. A.; McKinney, R. J.; Seidel, W. C.; Druliner, J. D.; Stevens, W. R. *Adv. Catal.* **1985**, *33*, 1-46.

8. Foo, T.; Garner, J. M.; Tam, WO 99/06357, **1999**. *Chem. Abstr.* **1999***, 130*, 169815.

9. Huthmacher, K.; Krill, S. in *Applied Homogeneous Catalysis with Organometallic Compounds,* 2nd ed.; Cornils, B., Hermann, W. A., Eds.; Wiley-VCH: Weinheim, **2002**; Vol. 1 pp 465-486; (b) Tolman, C. A. *Chem. Rev.* **1977**, *77*, 313-348.

10. Wilting, J.; Janssen, M.; Müller, C.; Lutz, M.; Spek, A. L.; Vogt, D. *Adv. Synth. Catal.* **2006**, *349*, 350-356.

11. Bini, L.; Müller, C.; Wilting, J.; von Chrzanowski, L.; Spek, A. L.; Vogt, D. *J. Am. Chem.Soc.* **2006**, *128,* 11374.

12. Swartz, B. D.; Reinartz, N. M.; Brennessel, W. W.; Garcia J. J., Jones, W. D. *J. Am. Chem.Soc.* **2008**, *130,* 8548-8554.

13. Casalnuovo, A. L.; RajanBabu, T. V.; Ayers, T. A.; Warren, T. H. *J. Am. Chem. Soc,* **1994**, *116,* 9869-9882.

14. Slotta, K. H. *Ber. Dtsch. Chem. Ges.*, **1934**, *67B*, 1028-1030.

15. (a) Henrici-Olivé, G.; Olivé, S. *Top. Curr. Chem.*, **1967**, *67*, 107; (b) Bogdanovic, B. *Adv. Organomet. Chem.*, **1969**, *17*, 105.

16. Bini, L.; Pidko, E. A.; Müller, C., van Santen, R.; Vogt, D. *Chem. Eur. J.,* accepted for publication

17. a) Tolman, C. A. *J. Am. Chem. Soc.*, **1970**, *92,* 2953; b) van Leeuwen, P. W. N. M. in *Homogeneous Catalysis Understanding the Art*; Kluwer Academic Publishers; Dordrecht, The Netherlands, **2004**; pp 10-20.

18. Schunn, R. A. *Inorg. Synth.* **1974**, *15*, 5-9.

19. Frisch, M. J.; Trucks, G. W.; Schlegel, H. B.; Scuseria, G. E.; Robb, M. A.; Cheeseman, J. R.; Montgomery, J. A., Jr.; Vreven, T.; Kudin, K. N.; Burant, J. C.; Millam, J. M.; Iyengar, S. S.; Tomasi, J.; Barone, V.; Mennucci, B.; Cossi, M.; Scalmani, G.; Rega, N.; Petersson, G. A.; Nakatsuji, H.; Hada, M.; Ehara, M.; Toyota, K.; Fukuda, R.; Hasegawa, J.; Ishida, M.; Nakajima, T.; Honda, Y.;

Kitao, O.; Nakai, H.; Klene, M.; Li, X.; Knox, J. E.; Hratchian, H. P.; Cross, J. B.; Bakken, V.; Adamo, C.; Jaramillo, J.; Gomperts, R.; Stratmann, R. E.; Yazyev, O.; Austin, A. J.; Cammi, R.; Pomelli, C.; Ochterski, J. W.; Ayala, P. Y.; Morokuma, K.; Voth, G. A.; Salvador, P.; Dannenberg, J. J.; Zakrzewski, V. G.; Dapprich, S.; Daniels, A. D.; Strain, M. C.; Farkas, O.; Malick, D. K.; Rabuck, A. D.; Raghavachari, K.; Foresman, J. B.; Ortiz, J. V.; Cui, Q.; Baboul, A. G.; Clifford, S.; Cioslowski, J.; Stefanov, B. B.; Liu, G.; Liashenko, A.; Piskorz, P.; Komaromi, I.; Martin, R. L.; Fox, D. J.; Keith, T.; Al-Laham, M. A.; Peng, C. Y.; Nanayakkara, A.; Challacombe, M.; Gill, P. M. W.; Johnson, B.; Chen, W.; Wong, M. W.; Gonzalez, C.; Pople, J. A. Gaussian 03, revision B.05; Gaussian, Inc.: Pittsburgh PA, 2003.

20. Hay, P. J.; Wadt, W.R. *J. Chem. Phys.* **1985**, *82*, 270; Hay, P. J.; Wadt, W.R. *J. Chem. Phys.* **1985**, *82*, 284; Hay, P. J.; Wadt, W.R. *J. Chem. Phys.* **1985**, *82*, 299.

21. Becke, A.D. *Phys. Rev.* **1988**, *A38*, 3098; Becke, A.D. *J. Chem. Phys.* **1993**, *98*, 1372; Becke, A.D. *J. Chem. Phys.* **1993**, *98*, 5648.

22. Bren, V.A.; Dubonosov, A.D.; Minkin, V.I.; Tsukanov, A.V.; Gribanova, T.N.; Shepelenko, E.N.; Revinsky, Y.V.; Rybalkin, V.P. *J. Phys. Org. Chem.* **2007**, *20*, 917.

23. Liu, T.; Zhang, H.-X.; Shu, X.; Xia, B.-H. *Dalton Trans.* **2007**, 1922.

Summary

Mechanistic Insights into the Hydrocyanation Reaction

The hydrocyanation of an alkene is a catalytic carbon-carbon bond formation reaction and the obtained nitriles can be converted into a variety of valuable products. The investigation of this reaction has mainly focused on the DuPont adiponitrile (AdN) process. This process is so far the only example of a large scale industrial application of an alkene hydrocyanation. Adiponitrile is produced from butadiene in 3 steps: the Ni-catalyzed hydrocyanation of butadiene leads to a mixture of 2-methyl-3-butenenitrile (2M3BN) and 3-pentenenitrile (3PN), obtained in varying ratio (typically 2:3) depending on the ligand employed. In a second step, the branched 2M3BN is isomerized to the desired linear 3PN in the presence of similar Ni-catalysts. The last step is the hydrocyanation of 3PN to AdN. The catalyst performance in this process still needs to be improved in terms of activity, especially for the hydrocyanation of 3PN, and, in selectivity for both hydrocyanation steps. Many investigations are also focusing on the hydrocyanation of vinylarenes. Several ligands have been applied in this reaction and their influence on activity, regio- and enantioselectivity has been considered.

An overview on the hydrocyanation of alkenes is given in **Chapter 1**. The chemistry behind this reaction is discussed prevalently from a mechanistic point of view. The reactivity of different classes of substrates is underlined. Mainly examples of the Ni-catalyzed hydrocyanation are reported, along with a brief overview on catalysis based on other metals.

In **Chapter 2**, a new route for the synthesis of the triptycene-based diphosphine ligand **Tript(PPh₂)₂** is described, giving the desired compound in good yield. The corresponding Pt(II)- and Ni(0)-complexes are characterized. In butadiene hydrocyanation the [Ni(cod)(**Tript(PPh₂)₂**)] pre-catalyst leads to unprecedented high selectivities for the linear product 3PN, combining concurrently high activity for both,

hydrocyanation and isomerization reaction. The double activity of the catalyst enables to reduce the synthesis of 3PN to a one-step procedure consisting of a hydrocyanation followed by an isomerization reaction. This new catalyst could be the key towards process intensification in the future.

Chapter 3 describes for the first time an *in situ* FT-IR spectroscopic study of the isomerization of 2M3BN towards 3PN. The spectra were analyzed comprehensively to obtain conversion profiles from the different band dynamics. Each band was transformed to its second derivative to enhance peak resolution. Calculated spectra of the substrate and the products support the peak assignment. An average conversion profile was calculated from different bands of the substrate and the product, applying a "*quasi*-multivariate analysis" technique to correlate different band dynamics. This approach was validated using advanced chemometrics. Furthermore, these profiles obtained by IR spectroscopic analysis of the formation of 3PN and the consumption of 2M3BN showed a zero order kinetic.

The application of new tetraphenol-based diphosphite ligands (TP) in the hydrocyanation reaction is described in **Chapter 4**. Very high activities were observed in the hydrocyanation of 3-pentenenitrile. Surprisingly, these systems are neither active in the hydrocyanation of butadiene nor do they show any isomerization of 2M3BN. This peculiar behavior of the [Ni(**TP**)] catalysts was investigated by means of NMR and IR spectroscopy, considering the formation of σ-alkyl and π-allyl intermediates. The σ-alkyl species formation seems to be prevalent with the **TP** ligands, while the formation of π-allyl species is disfavored. Since the hydrocyanation of 3PN proceeds *via* σ-alkyl intermediates and the first two steps of the DuPont process *via* the π-allyl species, these results provide an explanation for the observed catalytic activity. Moreover, the coordination of $ZnCl_2$ to the [Ni(2M3BN)(**TP2**)] complex was studied by IR spectroscopy. The comparison with a binaphthol-based diphosphite (**BIPPP**) ligand, often applied in hydrocyanation reactions, is also presented in relation to the coordination and catalytic activity.

Chapter 5 reports on the hydrocyanation of styrene. According to present knowledge, this reaction leads predominantly to the branched product 2-phenylpropionitrile (98%). A dramatic inversion of the regioselectivity upon addition of a Lewis acid is observed. Up to 83% of the linear product 3-phenylpropionitrile was obtained applying phosphite ligands in the presence of $AlCl_3$. The mechanism of the Ni-catalyzed reaction and the influence of additional Lewis acids have been elucidated by means of deuterium labeling experiments, NMR studies, and DFT calculations. It was concluded that the selectivity towards the linear product 3-phenylpropionitrile in the presence of $AlCl_3$ is due to the higher stability of the intermediate η^3-benzyl complex. The selective stabilization of this intermediate in the presence of the Lewis acid leads to the formation of a "steady state" for the η^3-benzyl intermediate and indirectly promotes the formation of the linear product 3-phenylpropionitrile *via* the σ-alkyl intermediate. Furthermore, the influence of different Lewis acids, such as CuCN, could be predicted *via* DFT calculations.

Chapter 6 deals with the hydrocyanation of simple monoalkenes. So far, this reaction did not attract much attention, due to the lower conversion generally obtained as compared to the hydrocyanation of 1,3-dienes and vinylarenes. Yet, this reaction leads to aliphatic nitriles, which are potentially valuable intermediates for both bulk and fine-chemical industry. The role of the Lewis acid in the mechanism of the reaction is still not completely clear; in particular its exact role in the increase of the reactivity and regioselectivity towards linear nitriles. A conversion of 89% in the hydrocyanation of 1-octene is reported, applying a binaphthol-based diphosphite (**BIPPP**) as ligand and $AlCl_3$ as Lewis acid. The competition between β-(H,D)-elimination and hydrocyanation in the reaction mechanism has been investigated by deuterium labeling experiments. Furthermore, preliminary DFT calculations have been performed to study the deactivation of the Ni-catalyst by formation of dicyano species.

176

Samenvatting

De hydrocyanering van een alkeen is een katalytische reactie waarin een koolstof-koolstof-binding wordt gevormd en de verkregen nitrillen kunnen worden omgezet naar diverse waardevolle producten. Het onderzoek naar deze reactie heeft zich voornamelijk geconcentreerd op het DuPont adiponitril (AdN) proces. Dit proces is tot op heden het enige voorbeeld van een industriële toepassing op grote schaal van de hydrocyanering van een alkeen. Adiponitril wordt gemaakt van butadieen in een drie staps-procedure: De nikkelgekatalyseerde hydrocyanering van butadieen leidt tot een mengsel van 2-methyl-3-buteennitril (2M3BN) en 3-penteennitril (3PN), verkregen in veschillende verhoudingen (typisch 2:3), afhankelijk van het toegepaste ligand. In een tweede stap wordt het vertakte 2M3BN geïsomeriseerd naar het gewenste lineaire 3PN in aanwezigheid van een vergelijkbare nikkel-katalysator. De laatste stap is de hydrocyanering van 3PN naar AdN. Voor de prestatie van de katalysator in dit proces is er nog volop ruimte voor verbetering met betrekking tot activiteit, vooral voor de hydrocyanering van 3PN, en selectiviteit voor beide hydrocyaneringsstappen. Vele onderzoeken zijn ook gericht op de hydrocyanering van vinylarenen. Verscheidene liganden zijn toegepast in deze reactie om hun invloed op activiteit, regio- en enantioselectiviteit te bestuderen.

Een overzicht van de hydrocyanering van alkenen wordt beschreven in **Hoofdstuk 1**. De chemie die ten grondslag ligt aan deze reactie wordt voornamelijk behandeld met betrekking tot hun mechanismen. De reactiviteit van verschillende klassen substraten wordt benadrukt. Voornamelijk worden er voorbeelden gerapporteerd van de nikkelgekatalyseerde hydrocyanering, maar ook wordt er een kort overzicht gegeven van de hydrocyaneringsreactie gekatalyseerd door andere metalen.

In **Hoofdstuk 2** is een nieuwe route beschreven voor de synthese van het op triptyceen gebaseerde difosfine ligand **Tript(PPh$_2$)$_2$**, dat het gewenste product levert met een goede opbrengst. De corresponderende Pt(II)- en Ni(0)-complexen zijn

gekarakteriseerd. De hydrocyanering van butadieen met de [Ni(cod)(**Tript(PPh₂)₂**)] pre-katalysator leidt tot een ongekend hoge selectiviteit voor het lineaire product 3PN, vanwege een hoge activitieit in zowel de hydrocyanering als de isomerisatie-reactie. De tweevoudige activiteit van de katalysator maakt het mogelijk de synthese van 3PN te reduceren naar een één staps-procedure, waarbij hydrocyanering en isomerisatie hand in hand gaan. Deze nieuwe katalysator kan de doorbraak zijn voor procesintensivering in de toekomst.

Hoofdstuk 3 beschrijft voor de eerste keer een *in situ* FTIR spectroscopische studie van de isomerisatie van 2M3BN naar 3PN. De spectra zijn uitvoerig geanalyseerd om conversieprofielen te verkrijgen van de verschillende veranderingen in piekintensiteiten. De spectra zijn getransformeerd naar hun tweede afgeleide om de piekresolutie te vergroten. Berekende spectra van het substraat en producten ondersteunen de piekaanduidingen. Een gemiddeld conversieprofiel is berekend uit verschillende banden van het substraat en het product, waarbij een "*quasi*-multivariate" analysetechniek is toegepast om de verschillende piekveranderingen te correleren. Deze aanpak is gevalideerd gebruikmakende van geavanceerde chemometrie. Verder bleek uit deze profielen verkregen met spectroscopische IR-analyse, dat de vorming van 3PN en de consumptie van 2M3BN een nulde orde kinetiek volgt.

De toepassing van nieuwe op tetrafenol gebaseerde difosfiet liganden (TP) in de hydrocyaneringsreactie is beschreven in **Hoofdstuk 4**. Zeer hoge activiteiten zijn waargenomen in de hydrocyanering van 3PN. Het was verrassend dat deze systemen inactief zijn in zowel de hydrocyanering van butadieen als in de isomerisatie van 2M3BN. Dit opzienbarende gedrag van de [Ni(**TP**)] katalysator is onderzocht met NMR- en IR-spectroscopie, waarbij specifiek gelet is op de vorming van σ-alkyl- en π-allyl-intermediairen. De vorming van het σ-alkyl-intermediair lijkt de voorkeur te hebben ten opzichte van de vorming van het π-allyl-intermediair bij gebruik van de **TP** liganden. Aangezien de hydrocyanering van 3PN *via* een σ-alkyl-intermediair verloopt en de eerste twee stappen van het DuPont-proces *via* de π-allyl-intermediairen, geven deze resultaten een verklaring voor de waargenomen katalytische activiteit. Verder is de coördinatie van

ZnCl$_2$ aan het [Ni(2M3BN)(**TP2**)]-complex bestudeerd met behulp van IR spectroscopie. De vergelijking met een op binaphthol gebaseerd difosfiet (**BIPPP**) ligand, dat vaker wordt toegepast in hydrocyanerings-reacties, wordt ook gepresenteerd in relatie tot de coördinatie en katalytische activiteit.

Hoofdstuk 5 behandelt de hydrocyanering van styreen. Volgens de huidige inzichten geeft deze reactie voornamelijk het vertakte produkt 2-fenylpropionitril (98%). Een dramatische omkering van de regioselectiviteit is waargenomen, wanneer een Lewis-zuur wordt toegevoegd. Tot 83% van het lineaire product 3-fenylpropionitril wordt verkregen met fosfiet-liganden in de aanwezigheid van AlCl$_3$. Het mechanisme van de gekatalyseerde reactie en de invloed van de toegevoegde Lewis-zuren zijn opgehelderd met behulp van deuterium-labeling-experimenten, NMR-studies en DFT-berekeningen. Hieruit is geconcludeerd dat de selectiviteit naar het lineair product 3PN in de aanwezigheid van AlCl$_3$ veroorzaakt wordt door de hogere stabiliteit van het intermediair η^3-benzyl-complex. De selectieve stabilisatie van dit intermediair in de aanwezigheid van het Lewis-zuur leidt tot de vorming van een "steady state" voor het η^3-benzyl intermediair en stimuleert indirect de vorming van het lineaire product 3-fenylpropionitril *via* het σ-alkyl-intermediair. Verder is het mogelijk gebleken de invloed van de verschillende Lewis-zuren, zoals CuCN, te voorspellen met behulp van DFT-berekeningen.

Hoofdstuk 6 beschrijft de hydrocyanering van simpele monoalkenen. Tot dusver heeft deze reactie relatief weinig aandacht gekregen, vanwege het feit dat deze normaliter resulteert in lage conversie in vergelijking tot de hydrocyanering van 1,3-diënen en vinylarenen. Desalniettemin geeft deze reactie alifatische nitrillen, die in potentie waardevolle intermediairen kunnen zijn voor zowel de bulk- als fijnchemische industrie. De rol van het Lewis-zuur in het reactiemechanisme is nog steeds niet volledig begrepen; vooral wat betreft de exacte rol in de verhoogde reactiviteit en regioselectiviteit naar lineaire nitrillen. Een conversie van 89% in de hydrocyanering van 1-octeen is gerapporteerd, waarbij een op binaphthol gebaseerd difosfiet (**BIPPP**) als ligand en AlCl$_3$ als Lewis-zuur is toegepast. De competitie tussen β-(H,D)-eliminatie en hydrocyanering

in het reactiemechanisme is onderzocht met behulp van deuterium-labeling-experimenten. Verder zijn er eerste DFT-berekeningen uitgevoerd om de deactivering van de nikkel-katalysator door de vorming van dicyano-complexen te bestuderen.

Sommario

L'idrocianazione di un alchene è una reazione catalitica per la formazione di legami carbonio-carbonio e i nitrili ottenuti possono essere convertiti in un vasto numero di prodotti commerciali. Lo studio di questa reazione si è focalizzato soprattutto sul processo DuPont per l'adiponitrile (AdN). Questo processo è a oggi il solo esempio di applicazione industriale in larga scala dell'idrocianazione di alcheni. L'adiponitrile è prodotto a partire dal butadiene in tre passaggi: l'idrocianazione del butadiene mediata da un catalizzatore al nichel porta a una miscela di 2-metil-3-butenenitrile (2M3BN) e 3-pentenenitrile (3PN), ottenuti in proporzioni diverse (tipicamente 2:3) dipendenti dal ligante impiegato. Nel secondo passaggio, 2M3BN che è un nitrile ramificato viene isomerizzato a 3PN, un nitrile lineare e il prodotto desiderato della reazione in presenza di un catalizzatore al nichel simile a quello precedentemente impiegato. L'ultimo passaggio è l'idrocianazione del 3PN a AdN. La prestazione del catalizzatore in questo processo ha ancora bisogno di essere migliorata, in termini di attività, specialmente nell'idrocianazione del 3PN, e di selettività in entrambi i passaggi di idrocianazione. Molti studi si sono concentrati anche sull'idrocianazione dei vinilareni. Diversi liganti sono stati applicati in questa reazione e la loro influenza sull'attività, la regio- e l'enantioselettività sono state investigate.

Una panoramica sull'idrocianazione degli alcheni è proposta nel **Capitolo 1**. la chimica di questa reazione è descritta prevalentemente da un punto di vista meccanicistico. La reattività delle diverse classi di substrati è sottolineata. Sono soprattutto riportati esempi dell'idrocianazione catalizzata via nichel, insieme a una breve trattazione della stessa reazione mediata da altri metalli.

Nel **Capitolo 2** è descritta una nuova procedura per la sintesi della difosfina **Tript(PPh$_2$)$_2$** con una struttura basata sulla molecola triptosina e usata come ligante. La difosfina è stata ottenuta con buone rese. I complessi corrispondenti formati con Pt(II) e Ni(0) come metalli sono stati caratterizzati. Nell'idrocianazione del butadiene il

precatalizzatore [Ni(cod)(**Tript(PPh₂)₂**)] porta a una alta selettività senza precedenti per il prodotto lineare 3PN, combinando contemporaneamente alta attività per entrambi, la reazione di idrocianazione e di isomerizzazione. La doppia attività del catalizzatore rende possibile ridurre la sintesi del 3PN a un solo passaggio di idrocianazione e isomerizzazione nello stesso tempo. Il nuovo catalizzatore potrebbe essere nel futuro la chiave verso l'intensificazione del processo.

Capitolo 3 descrive per la prima volta uno studio spettroscopico in situ della isomerizzazione di 2M3BN a 3PN, utilizzando FT-IR. Gli spettri sono stati analizzati comprensivamente per ottenere i profili per la conversione della reazione dalle differenti dinamiche delle bande infrarosse. Ogni banda è stata trasformata nella sua seconda derivata per intensificare la risoluzione dei picchi. Spettri infrarossi del substrato e dei prodotti sono stati calcolati usando DFT per supportare l'assegnamento delle bande. Una media dei profili per la conversione è stato calcolata considerando diverse bande appartenenti al substrato e al prodotto, utilizzando un'analisi "quasi" multivariata per correlare le diverse dinamiche delle bande infrarosse. Questo approccio è stato validato applicando tecniche avanzate di chemometrica. In aggiunta è stato osservato che i profili ottenuti via analisi spettroscopica (IR) della formazione di 3PN e del consumo di 2M3BN mostrano una cinetica di ordine zero.

Nel **Capitolo 4** è riportata l'applicazione come liganti nella reazione di idrocianazione di nuove difosfiti con uno scheletro basato sulla molecola tetrafenolo (TP). Un'attività molto alta è stata osservata nell'idrocianazione del 3PN. Sorprendentemente questi sistemi catalitici non sono attivi nella idrocianazione del butadiene o nell'isomerizzazione del 2M3BN. Questo comportamento peculiare del catalizzatore [Ni(**TP**)] è stato investigato facendo uso di tecniche spettroscopiche, quali NMR o IR, considerando la formazione di intermedi σ-alchilici e π-allilici. La formazione dei composti σ-alchilici sembra essere la prevalente con i leganti **TP**, mentre la formazione dei π-allilici è sfavorita. Poiché l'idrocianazione del 3PN procede via intermedi σ-alchilici e i primi due passaggi del processo DuPont via intermedi π-allilici, questi risultati provvedono ad una possibile spiegazione per l'attività catalitica osservata.

Inoltre la coordinazione dello $ZnCl_2$ con il complesso [Ni(2M3BN)(**TP2**)] è stata studiata per mezzo della spettroscopia infrarossa. Il paragone con una difosfite basata sulla molecola binaftolo (**BIPPP**) e usata sempre come ligante viene presentato in relazione al tipo di coordinazione e all'attività catalitica del corrispondente catalizzatore al nichel.

Il **Capitolo 5** riporta l'idrocianazione dello stirene. Finora questa reazione ha sempre portato all'ottenimento del prodotto ramificato 2-fenil-propionitrile (98%). Un'inversione totale della regioselettività è stata ora osservata mediante l'addizione di un acido di Lewis. E' stato ottenuto fino all'83% del prodotto lineare 3-fenilproprionitrile con l'applicazione di fosfiti come liganti in presenza di $AlCl_3$. Il meccanismo di questa reazione catalizzata da complessi al nichel e l'influenza dell'addizione dell'acido di Lewis sono state elucidate per mezzo di esperimenti con marcatori al deuterio, studi al NMR e calcoli basati su DFT. E' stato concluso che la selettività verso il prodotto lineare 3-fenilpropionitrile in presenza di $AlCl_3$ è dovuta all'alta stabilità del complesso intermedio η^3-benzilico. La stabilizzazione selettiva di questo intermedio alla presenza di acidi di Lewis porta alla formazione di uno "steady state" per l'intermedio η^3-benzilico e indirettamente promuove la formazione del prodotto lineare 3-fenilpropionitrile via intermedi σ-alchilici. Inoltre l'influenza di altri acidi di Lewis, come CuCN, può essere predetta da calcoli basati su DFT.

Il **Capitolo 6** tratta dell'idrocianazione di semplici alcheni. Ad oggi questa reazione non ha attratto molta attenzione, dovuto alle modeste conversioni generalmente ottenute a paragone con l'idrocianazione di 1,3-dieni e vinilareni. Nitrili alifatici sono però ottenuti da questa reazione, cioè prodotti potenzialmente importanti per l'industria. Il ruolo dell'acido di Lewis nel meccanismo della reazione non è stato ancora completamente chiarito; in particolare il contributo nell'aumento della reattività e della regioselettività verso i nitrili lineari. Una conversione del 89% viene riportata per l'idrocianazione dell'1-ottene, utilizzando la difosfite basata sulla molecola binaftolo (**BIPPP**) come ligante e $AlCl_3$ come acido di Lewis. La competizione tra la β-(H,D)-eliminazione e l'idrocianazione nel meccanismo della reazione è stata investigata per mezzo di marcatori

al deuterio. Inoltre calcoli preliminari basati su DFT sono stati analizzati per studiare la inattivazione del catalizzatore al nichel attraverso la formazione di diciano-complessi.

List of Publications

Laura Bini, Christian Müller, Jos Wilting, Lars von Chrzanowski, Anthony L. Spek, and Dieter Vogt, "High selective hydrocyanation of butadiene toward 3-pentenenitrile", *J. Am. Chem. Soc.,* **2007**, *129(42)*, 12622-3.

Johannes W. de Boer, Wesley R. Browne, Syuzanna R. Harutyunyan, Laura Bini, Theodora D. Tiemersma-Wegman, Paul L. Alsters, Ronald Hage and Ben L. Feringa, "Manganese catalysed asymmetric cis-dihydroxylation with H_2O_2" *Chem. Comm.,* **2008**, *129(42)*, 3747-3749.

Laura Bini, Evgeny A. Pidko, Christian Müller, Rutger A. van Santen, and Dieter Vogt, "Lewis acid-controlled regioselectivity in styrene hydrocyanation", *Chem. Eur. J.,* accepted for publication.

Laura Bini, Erwin Houben, Evgeny A. Pidko, Christian Müller and Dieter Vogt, "Nickel-Catalyzed Isomerization of 2-Methyl-3-Butenenitrile to 3-Pentenenitrile. A Kinetic Study Using *in situ* FTIR-ATR Spectroscopy", submitted for publication.

Michèle Janssen, Laura Bini, Bart Hamers, Christian Müller, Maxime Siegler, Anthony Spek, and Dieter Vogt, "Tetraphenol-based diphosphite ligands in the rhodium catalyzed hydroformylation of octenes", under review from the industrial partner.

Laura Bini, Michèle Janssen, Bart Hamers, Christian Müller, and Dieter Vogt, "Hydrocyanation of 3-pentenenitrile with tetraphenol-based ligands: formation of η^3-allyl and σ-alkyl intermediates.", under review from the industrial partner.

Curriculum Vitae

Laura Bini was born in Lucca, a small town in Tuscany, Italy on October 16, 1980. After she finished high school in her hometown in 1999, she started her studies in Chemistry at the University of Pisa. She was introduced to the field of catalysis during her Master project under the supervision of Prof. Dr. Mauro Pineschi. The project concerned copper-mediated asymmetric addition of organometallic reagents to double bonds of heterocyclic compounds.

Upon graduation cum laude in Chemistry in May 2004 she began an internship for DSM Research in Geleen, The Netherlands. She was involved in asymmetric epoxidation of olefins using hydrogen peroxide in the presence of manganese catalysts. During this time, she also completed a second degree (cum laude) on industrial applications of microwave-assisted drug extraction from plants and soil under the supervision of Prof. Dr. Luisa Pistelli.

In July 2005, she started her PhD in the Eindhoven University of Technology in the group of Prof. Dr. Dieter Vogt. Her research here mainly involved mechanistic aspects of the nickel-catalyzed hydrocyanation reaction. The most important results of the research are described in this thesis.

Recently, she has been awarded with a Humboldt Research Fellowship for a postdoctoral project, which will start in November 2009 at the RWTH Aachen in the group of Prof. Dr, Jun Okuda.

Acknowledgements

A thesis is never a one-person work. Many people helped me with my research, to improve my skills or to overcome difficult moments that several times occurred in these four years. I am now glad to acknowledge them for anything they did for me.

I would like to start thanking my promoter and co-promoter Dieter Vogt and Christian Müller. Dieter thanks to choose me as one of your PhD students and to welcome me in your group. Your enthusiasm and your energy have always been very inspiring and you taught me, among thousand of other things, how to enjoy my work! Christian, you have always been a very good example for all of us and you gave me precious suggestions to find my way after the PhD. I will always remember your support. Erik, Ik kan jouw sympathie echt waarderen en zoals je me altijd laat herinneren dat ik een vrouw ben, ook met de labjas aan. I am also very grateful to the promotion committee for their willingness to correct the manuscript and for the very insightful comments.

I was fortunate to have many industrial collaborations during the course of this project. I would like to thank Dr. Langstein from Bayer Materials Sciences and Dr. Buchholz, Dr. Franke, Dr. Christiansen and Dr. Hess from Evonik Oxeno. Especially the work with Evonik has been very successful and enjoyable.

Michéle, we hebben het afgelopen anderhalf jaar samengewerkt en ik ben heel blij de kans te hebben gehad om jou beter te leren kennen, zowel in het werk als persoonlijk. Je bent een hele lieve meid en een zeer slimme onderzoekster. Ik heb veel van je en met je geleerd. The contradictory and often irritating personality of Evgeny hides an intelligent man, a caring father and husband, an attentive friend. I am happy that you have shown me to be also all these other things. Katharina has been my office mate for almost four years. Although sharing our space every day has been often very difficult, you are the one that I will always miss the most. Aan mijn ultrastrikte en superhardwerkende zuurkast-buur Bart wil ik een speciaal bedankje geven voor al zijn kleine tips en al zijn opmerkingen op presentaties, rapporten, nieuwe ideeën… Daniel, you left already two years ago, but I treasure your support during the first period of my PhD, when nothing worked and I felt the surrounding very hostile. I hope we will find the time to go out

dancing again. Veel erkenning gaat naar Jos, die mij in het begin heeft geholpen met het onderzoek en ook van tijd tot tijd gedurende de daaropvolgende jaren. Probeer te onthouden dat het leven gewoon mooi is en geef ons een glimlach. Ik wens alle anderen, Jarno, Andreas en Gijsbert het allerbeste bij het voltooien van hun AIO en voor Patrick en Leandra met hun nieuwe baan. Ton, Wout en Hendawy bedankt voor jullie hulp in het lab en jullie vriendelijkheid. Veel dank aan de secretaresses Marion en Elize voor de dagelijkse zorg voor ons.

Some people have been in the group shortly, but they still left memories behind. Erik, bedankt voor je raad om te solliciteren voor een AIO in deze groep. Jarl, ik heb met jou de beste strijdjes van mijn leven gehad. I was sorry, Mabel, that I did not have the time to know you better. I liked always to talk with you. Grazie Maria per avermi accolta nella tua casa, quando sono arrivata ad Eindhoven.

Many students and PhDs did join the group for a few weeks or months: Matthijs, Tiina, Andy, Laura, Patrick, Christine, Carolina, Julie. In particular, Ariadna, Silvia, Ismael and William have shared the office with me and we have had many nice chats together. Good luck for your future!

I wish all the best also to the other colleagues from the SKA: Gilbere, Arijan, Freek, Maarten, Tiny, the Moodley's, Bouke, Cristina, Joost, Emile, Gabriela, Ramona. Adelaida, grazie per le chiacchierate-sfoghi!

Ik ben ontzettend blij met het ontwerp van mijn kaft. Renée en Nico, bedankt voor alle gezellige avondjes die hiermee gepaard gingen.

Cosa dire di Irene! A parte tutto il supporto psicologico cha va dalle ore a chiacchierare, cominciando 1000 discorsi e non portandone nessuno alla fine, allo shopping terapeutico... A parte tutto il sostegno che hai sempre dato alle mie scelte, anche non condivise… Grazie soprattutto per l'aiuto con la tesi e con la proposal per la Humboldt. Ho imparato tanto su come spiegare i miei risultati e su come creare una storia chiara e interessante dal guazzabuglio delle mie idee. So che é costato tanto tempo e impegno e non ti ringrazierò mai abbastanza.

A Olga e Alessio un grazie sentito per tutto il supporto tecnico con il template, l'uso di Corel Draw, la scelta del printing service. Impagabile anche la revisione dei PDFs! Ma

soprattutto grazie di ripetermi di non fissarmi troppo sul lavoro e di cercare di rilassarmi un po'! Lo so, tendo a esagerare!

Per parlare di Lucy e Barbarina mi piace citare la mitica Samantha. Sono favolose e il fatto che le mie amiche sono favolose rende favolosa pure me! Ringraziarle di qualcosa di specifico sarebbe riduttivo, basti dire che dai tempi dell'università so che loro ci sono e questo mi fa sentire molto meglio.

Gli zii Piero e Giovanni sono sempre stati come due secondi babbi per me e mio fratello, grazie per tutto quello che ci avete insegnato! Grazie per farmi sentire a casa ogni volta che vengo in Italia! Grazie per farvi tutta questa strada solo per vedere il giorno della mia promozione!

Tutte le volte che penso a Giulia, mi ricordo un po' di come ero io alla sua età! Vedere l'apertura verso gli altri e la capacità di mostrare affetto che hai, Giulia, mi ha insegnato tanto negli ultimi anni. E' con stima e orgoglio che ti vedo raggiungere tutti gli obbiettivi che ti prefiggi e diventare sempre più capace e sicura di te.

Al mio fratellino va un grazie molto speciale. Quando ho deciso di restare in Olanda sei stato il primo a capire e sostenere la mia scelta. Il tempo che passi con me e Erwin tutte le volte che puoi e l'interesse che hai per quello che faccio mi hanno aiutato ad andare avanti tutti questi anni lontano da casa. Grazie! Spero che ti diverta a fare il paraninfo, di sicuro sarai bellissimo!

Veel dank gaat uit naar mijn Nederlandse familie, Riny, Thuur en Armand. Ik heb nog steeds het gevoel dat mijn baan onduidelijk is gebleven voor jullie, maar jullie hebben altijd mijn succesjes toegejuicht en mij als doorzetter erkent in het reizen van Maastricht naar Eindhoven.

A mamma e a babbo devo tutto quello che sono oggi. Grazie mamma per telefonarmi tutti i giorni e per farmi sentire così importante e sempre parte della famiglia. Babbo, sapere che sei fiero di me é la cosa più importante che abbia mai ottenuto nella vita.

Erwin, mijn maatje, mijn beste reviewer, mijn paranimf, mijn liefde. Je hebt alles in dit boek helemaal gelezen en hebt me geholpen bij het schrijven van de meest moeilijke stukken. Je hebt altijd naar mijn ideeën geluisterd, met mij mijn projecten doorgesproken, me altijd gerustgesteld bij een obstakel, me altijd gesteund bij een uitdaging. Dit boek is

ook van jou, en ik ben zo enorm blij dit moment met jou te kunnen delen. Zoals vele momenten die nog zullen volgen.

Grazie a tutti!

Laura